RUHR-UNIVERSITÄT BOCHUM

Qasim Abdulkarem Jassim Al-Obaidi

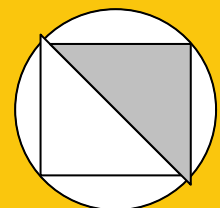Hydro-Mechanical Behaviour of Collapsible Soils

Bochum 2014   Heft 54

Ruhr-Universität Bochum

Schriftenreihe Grundbau, Boden- und Felsmechanik

Heft 54

Hydro-Mechanical Behaviour of Collapsible Soils

Dissertation

as a requirement of the degree of
Doktor-Ingenieur (Dr.- Ing.)

at the Faculty of
Civil and Environmental Engineering
Ruhr-Universität Bochum

submitted by
Qasim Abdulkarem Jassim Al-Obaidi
from Baghdad, Iraq

Reviewers

Prof. Dr.-Ing. habil. Tom Schanz

Prof. Dr.-Ing. habil. Achim Hettler

Prof. Dr. Hussein Hameed Karim

Bochum-Germany, August 2014

This work is dedicated to

My homeland (Iraq)

My family and friends

Vorwort des Herausgebers

Die vorliegende Promotionsarbeit von Herrn Qasim Al-Obaidi beschäftigt sich mit einer Untergruppe der sogenannten problematischen Böden. Charakteristische Eigenschaft dieser Böden im vorliegenden Fall ist ihre Volumenverringerung bei Bewässerung. Dieses Phänomen wird als Kollaps bezeichnet und ist seit längerer Zeit in der Wissenschaft bekannt.

Kollapsible Böden haben vor allen Dingen eine Bedeutung in ariden Gebieten, wo auf Grund der Diagenese dieser Böden, die Neigung zu deren Kollaps hervorgerufen wird. Ursache dieses Kollapses ist die besondere Mikrostruktur dieser Böden. An den Korn- zu Korn- bzw. Partikel- zu Partikelkontakten, kommt es zur Brückenbildung, welche die Struktur des Bodens zunächst begünstigt. Diese Brücken können aus Gips oder Zement oder anderen ähnlichen Bindemitteln sein. Bei Bewässerung dieser Böden z.B. durch Infiltration von Niederschlag, weichen diese Brücken quasi auf und es entsteht eine metastabile Struktur. Diese Struktur leistet bei mechanischer Beanspruchung einen geringeren Widerstand als die ursprünglich verkittete Struktur. Es kommt zu einem spröden Materialversagen, verbunden mit ausgeprägtem Kompressionsverhalten. Derartige kollapsible Böden treten auch in Deutschland auf. Ein herausragendes Beispiel hierfür ist der im ostdeutschen Raum anzutreffende Lössboden, z.B. im Freistaat Sachsen.

In den Ländern, in denen kollapsible Böden vorherrschen, ist festzustellen, dass die experimentelle Versuchstechnik in der Regel relativ einfach ist. So wird beim Herbeiführen des Kollapses oft der Boden in einem Schritt dem Wasserzutritt bzw. Lösungszutritt ausgesetzt. In der Realität ist jedoch dieser Bewässerungsvorgang ein allmählicher.

In der vorliegenden Arbeit hat Herr Al-Obaidi deswegen eine Versuchstechnik entwickelt, die es erlaubt, die im Boden vorhandenen Kapillarspannungen schrittweise abzubauen und dadurch den Kollaps zeitlich zu skalieren. Diese Vorgehensweise entspricht einer erheblichen Verbesserung der realitätsnahen Qualität der durchgeführten Experimente und ist in dieser Form international einzigartig. Durch eine Gegenüberstellung des konventionellen Vorgehens mit der hier vorgeschlagenen Motivation gelingt eine sehr gute Einordnung der bisher erzielten Ergebnisse.

Univ. Prof. Dr.-Ing. habil. Tom Schanz

Bochum, im Sommer 2014

Acknowledgement

Abstract

Collapsible soils present significant geotechnical and structural engineering challenges through worldwide. These soils suffer volume changes and collapse deformation upon wetting. The collapse potential resulted from complete wetting of soil layer may not be achieved in the field, due to the inability to reach full saturation state through a single-step wetting. Therefore, the multi-step wetting procedure is more convenient due to the slowly rising of ground water by capillary forces, especially in the low rainfall regions.

This work investigates the behaviour of the collapsible soils, studies the effect of suction and other relevant factors on the collapsibility characteristics and the hydro-mechanical properties, and provides geotechnical data and parameters useful for the numerical analysis and foundations design.

Three types of collapsible soils have been experimented in this study; sandy gypseous soil from Iraq, silty loess soil from Germany and a mixture of 70% artificial gypsum with 30% Silber sand. A series of Oedometer collapse tests were carried out using two procedures; single-step wetting (single and double Oedometer test) and multi-steps wetting (suction decreases under constant net vertical stress). Moreover, a combination of the axis-translation technique and the vapor equilibrium technique were deployed in order to cover a wide range of entire soil suction. The hydro-mechanical properties were investigated through the soil-water characteristics curve, permeability coefficient under both saturated and unsaturated states, and the behaviour of gypseous soil during leaching processes. Furthermore, factors influencing the collapse potential, suction effect on the volume change behaviour, ESEM-EDX analysis at different states of the soil samples, variations of the pore-water pressure and volumetric water content in soil-column test were analyzed and discussed in this thesis.

The results indicate that the selected soil samples exhibit a significant collapse volume change in response to single and multi steps wetting under constant net vertical stress. The collapse potential is stress path dependent and is a function of net vertical stress, initial void ratio, suction and degree of saturation. The critical collapse occurred mainly with the influence of matric suction zone, and the risk of collapse is aggravated due to the effect of leaching phenomenon on the gypseous soil.

Zusammenfassung

Kollapsfähige Böden sind in der Geotechnik und in der Bautechnik weltweit sehr bedeutsam, da sie bei Befeuchtung z.B. durch einen ansteigenden Grundwasserspiegel oder Niederschläge plötzliche Volumenänderungen erfahren können. Klassisch wird das Kollapspotenzial durch Bewässerung einer kompaktierten Bodenprobe in einem Schritt bis zur Sättigung ermittelt. In der Realität wird eine vollständige Sättigung in einem Schritt jedoch nicht erreicht. In dieser Arbeit wurde das Kollapsverhalten verschiedener Böden unter schrittweiser Bewässerung untersucht. Die Arbeit liefert geotechnische Daten und Parameter, welche für numerische Analysen und die Bemessung von Grundbauwerken genutzt werden können.

Es wurde ein experimentelles Programm mit drei verschiedenen kollapsfähigen Böden bearbeitet. Es wurde eine Reihe von Einzel- und Doppeloedometerversuchen nach der klassischen Methode, d.h. mittels Bewässerung mit Fluid in einem Schritt bis zur Sättigung durchgeführt, sowie Versuche mittels schrittweiser Sättigung durch Verminderung der Saugspannung bei konstanter Nettospannung. Zur Saugspannungskontrolle wurden die Achsentranslationstechnik und Exikkatormethode verwendet. Zusätzlich zu den kleinmaßstäblichen Elementversuchen wurden Säulenversuche durchgeführt, um den zeitlichen Verlauf von Wassergehalt und Sättigung unter kontrollierter Saugspannung zu bestimmen. Die hydromechanischen Eigenschaften wurden von der experimentell bestimmten Saugspannungs-Sättigungs-Beziehung und den gemessenen gesättigten und teilgesättigten Durchlässigkeit-skoeffizienten abgeleitet. Desweiteren wurde die Struktur der Böden zu verschiedenen Versuchszeitpunkten untersucht.

Die Ergebnisse zeigen, dass die Bodenproben sowohl in den klassischen Versuchen als auch in den saugspannungskontrollierten Versuchen eine erhebliche Volumenverminderung (Kollaps) als Reaktion auf die Bewässerung bei konstanter Nettospannung aufwiesen. Das Kollapspotenzial ist stark spannungspfadabhängig und ist eine Funktion der Nettovertikalspannung, der Anfangsporenzahl, der Saugspannung und dem Sättigungsgrad. Der kritische Kollaps tritt überwiegend im Bereich der Matrixsaugspannungen auf. Bei gipshaltigen Böden erhöht sich das Risiko eines Kollapses aufgrund von Auswaschungen.

Contents

List of Figures

List of Tables

List of Symbols

$\Delta \epsilon$ Difference in volumetric strain before and after wetting

χ Bishop's effective stress parameter

χ' Gypsum content

ϵ_{800} Volumatric strain at vertical stress of 800 kPa

$\gamma_{d-initial}$ Initial dry density

λ Pore-size distribution index

π Osmotic suction

ψ Suction

ψ_o Initial suction

ψ_r Residual suction

ψ_{final} Final suction

σ Total normal stress

σ' Effective vertical stress

σ_n Net normal stress

σ_v Vertical stress

σ_{vm} Maximum preconsolidation pressure

θ Volumetric water content

θ_s Saturated volumetric water content

A Cross-sectional area

C_C Coefficient of concavity

C_c Compression index

C_r Swell or rebound index

C_U Coefficient of uniformity

CP Collapse potential according to Jennings and Knight (1975)

e_f Final void ratio

e_o Initial void ratio

e_t Void ratio at any time during inundation under same vertical stress

Gs Specific gravity

h_f Final height of the soil sample

h_o Initial height of the soil sample

h_t Height of the soil sample at any time during inundation under same vertical stress

I_c Collapse potential according to ASTM D533303

I_e Collapse index

I_{cl} Collapse potential due to leaching phenomenon

k Coefficient of permeability

K_r Solution rate constant

K_w Coefficient of permeability at unsaturated condition

LL Liquid limit

PI Plasticity index

PL Plastic limit

q Flow rate

S_r Degree of water saturation

Sr_e Effective degree of saturation

Sr_o Initial degree of saturation

$Sr_{opt.}$ Optimum degree of saturation

u_a Air pressure

u_w Water pressure

V_a Volume of air

V_c Volume of contractile skin

V_o Initial volume of an unsaturated soil element

V_v Volume of soil voids

V_w Volume of water

w Gravimetric water content

1. Introduction

1.1. Background and motivations

Many researches deal with the investigation on the main reasons for foundation failure problems. They found that there are mainly two often cited unsaturated soil problems confronting the geotechnical and foundation engineers. These are collapsible and expansive soil behavior, and they are associated with wetting-induced volume change (Fookes & Parry, 1994; Bell & Culshaw, 2001).

In general, a partial or full wetting of the moisture-sensitive unsaturated soil deposit causes either collapsing in most gypseous and loess soil or swelling in many types of clay soils. Therefore, a major consideration for a technical professional dealing with unsaturated soils is related to the effect of wetting on engineering performance. This soil behaviour leads to great challenges in foundations design during and after the construction of engineering structures (Barden et al., 1969; Fredlund & Rahardjo, 1993; Houston, 1995; Al-Mufty, 1997).

In other words, when any soil is wetted it may decrease/increase in volume or experience no significant volume change. The amount and type of volume change depend on the soil type and geological composition, soil structure, the initial soil density, the imposed stress state and the degree of wetting. Soils that exhibit significant compression or shrink/swell response to moisture content changes are often referred to as moisture-sensitive soils (Feda, 1995; Houston, 1995; Houston et al., 2001; Ng & Menzies, 2007).

In general, collapsible soils are moisture-sensitive and considered as one of the problematic and widely distributed soils in the world especially in arid or semi arid regions. Moreover, they are characterized by low values of dry unit weight and natural water content. Engineering projects constructed on collapsible soils suffered from a considerable deformation and large settlements when these soils are saturated after construction. Predicting collapse potential is important to the design of many engineering structures (ASTMD5333, 2003).

In arid or semi arid regions having low rainfall intensity, the wetting process of subsurface

layers is normally due to gradually rising of ground water by capillary forces. This fact should be taken in consideration when estimating the volume change behaviour of collapsible metastable-structured soil. Collapse potential by full wetting of soil layer may not be achieved in the field due to the inability to reach a complete saturation of the sandy or clayey soil deposit by single step wetting. Therefore, it is important to investigate the effect of progressive wetting on the soil sample of the expected collapse settlement as well as evaluate the relationship between the critical values of collapse potential corresponding to the magnitude of applied suction.

1.2. Research objectives and scope

The main objectives of this work are to provide a better understanding regarding the behaviour of collapsible soils, investigate the effect of suction, inundation vertical stress, initial dry density and initial degree of saturation on the collapsibility characteristics and hydro-mechanical properties. Provide valuable geotechnical data and parameters necessary for the numerical simulations and foundation design. Three types of unsaturated collapsible soils are considered. These are natural sandy gypseous with gypsum content of more than 70% from Iraq, artificial sandy gypsified with gypsum content of 70% composed by mixing sand and pure Calcium sulphate $CaSO_4.2H_2O$ and the third type is silt loess soil from Germany.

In general the experimental works can be categorised into four main parts:

A. Basic physical, chemical properties, Environmental Scanning Electron Microscope (ESEM) and Energy-dispersive X-ray spectroscopy (EDX) measurements.

B. Volume change behaviour without suction control (i.e. consolidation, single and double Oedometer collapse test).

C. Volume change behaviour under suction control (i.e. constant net vertical stress-suction control) for wetting and drying path.

D. Investigation of hydro-mechanical characteristics such as: permeability coefficient at saturated and unsaturated conditions, leaching phenomenon and soil-water characteristics curve.

E. Soil-column test (i.e. monitoring of pore-water pressure and volumetric water content).

The detailed scope of the work is listed as follow:

1. Providing a comprehensive and detailed state-of-the-art review which addresses the issue of collapsible soils for the period of more than a half century ago. The literature review covers background on soil microstructure, theories and conclusions that explain

the problem of collapsible soils.

2. Investigation of the reasons that lead to large volume change and sudden collapse of the soil layers and the main factors affecting the collapse mechanism.

3. Determination of basic geotechnical properties that include physical and chemical properties, gypsum and sulfate content of the tested soils, and characterisation for the mechanism of collapse by analyzing the Environmental Scanning Electron Microscope (ESEM) and Energy-dispersive X-ray spectroscopy (EDX) measurements of unsaturated soil after inundation and leaching with water.

4. Evaluation of the collapse potential of different soils under different initial condition of soil specimen such as dry density, degree of saturation and inundation vertical stress. These are achieved by using single and double Oedometer collapse test method without suction control. Moreover, the effect of soil structure, wetting time and dissolved gypsum on the collapsibility characteristics were intensively investigated.

5. Measurements of total volume changes, degree of collapse and degree of saturation were investigated at multi step suction values (i.e. progressively decrease the suction from initial to zero value) following a wetting stress path under a constant net normal vertical stress. In addition, the volume change resulting from drying stress path (i.e. multi steps suction increases) was also investigated. Furthermore, definition of the collapse phases during wetting process and determination of the critical value of the collapse corresponding to applied suction and net normal vertical stress are also included.

6. Estimation the coefficient of permeability at saturated and unsaturated soil condition and perform the leaching process by water flow after the collapsing stage.

7. Investigation the variation of pore-water pressure and volumetric water content resulting from reduction of matric suction in soil-column test using tensiometer and TDR sensors.

1.3. Organization of the thesis

The thesis consists of six chapters in addition to two appendixes. A brief description of each chapter is presented below:

Chapter 1 presents a background and the motivation, research objective and scope, and the organization of the thesis.

Chapter 2 provides an overview of the behaviour of collapsible soils and focuses on many topics such as formation, types and distribution, physical-chemical characteristics, structure and collapse mechanisms. In addition, it identifies collapsible soils and methods

to calculate the collapse potential. In order to investigate the collapse deformation in the framework of unsaturated soil mechanics, this chapter describes the concept of suction, effective stress, the two independent stress state variables, volume change and the measurement of soil suction. The literature explains various aspects of the soil-water characteristics curve (SWCC) including the general concept, the determination method and hysteresis in addition to determining the permeability coefficient in unsaturated soil. Soil stabilisation and improvement techniques are also summarised.

Chapter 3 explains the site investigations, types of the selected soil samples and their basic properties and characterisation that are used in this research. Moreover, this chapter discusses the gypsum content determination and the elementary characteristics (ESEM and EDX analysis in addition to the detailed description for the experimental program including initial conditions of soil samples and stress path followed for the tests.

Chapter 4 introduces the equipments used (i.e. function and description), techniques (i.e. theories and applications) and methodology (i.e. specimen condition and test procedure).

Chapter 5 presents the analysis and discussion of the laboratory tests results. This chapter is categorised into two main parts:

The first part explains the results of volume change behaviour without suction control such as consolidation tests and collapse tests (i.e. single Oedometer test and double Oedometer test) using conventional Oedometer device.

The second part presents the volume change behaviour under suction control such as constant net stress-suction decreases (wetting-collapse) tests and constant net stress-suction increases (drying) tests using UPC-Barcelona cell and UPC-Isochoric cell in addition to the results of permeability-leaching tests and soil-water characteristics curves determinations using axis-translation technique and vapor equilibrium technique. Moreover, elementary characteristics using (ESEM-EDX) analysis, soil-column test and soil improvement and foundation options procedure are also included as part of explanation and discussion.

Chapter 6 presents the conclusions that can be drawn from this work and recommendations and suggestions for future works.

Appendix A explains the techniques of suction application and measurements, Appendix B presents the calibration of the equipments used and Appendix C presents the elementary characteristics (ESEM-EDX) analysis.

2. Literature review

2.1. Introduction

This chapter provides an overview of the behaviour of collapsible soils and focuses on many topics such as formation, types and distribution, physical-chemical characteristics, structure and collapse mechanisms. In addition, it identifies collapsible soils and methods to calculate the collapse potential. In order to investigate the collapse deformation in the framework of unsaturated soil mechanics, this chapter describes the concept of suction, effective stress, the two independent stress state variables, volume change and the measurement of soil suction. The literature explains various aspects of the soil-water characteristics curve (SWCC) including the general concept, the determination method and hysteresis in addition to determining the permeability coefficient in unsaturated soil. Soil stabilisation and improvement techniques are also summarised.

2.2. Overview of collapse problem in soil

Collapsible soils present severe geotechnical and structural engineering challenges around the world. They can be formed either naturally or through human activities. However, a substantial precondition is that an open metastable structure or open porous fabric is developed through different bonding mechanisms. Bonds among the soil particles can be created via capillary forces (e.g. suction) and/or by cementing fine materials (e.g. clay or salts). Moreover, when the vertical stresses (e.g. by loading or wetting processes) exceed the yield strength of these bonding materials, collapse suddenly occurs (Dudly, 1970; Lutenegger & Saber, 1988; Jefferson & Rogers, 2012).

Collapsible soils in their natural moisture content can support a heavy load with only a small amount of compression or deformation, but when wetting occurs, they undergo a significant reduction in volume (Dudly, 1970; Clemence & Finbarr, 1981; Das, 1990). Wetting soil layers may occur from different water sources and can result in the danger of

collapse, although the effect of wetting or the degree of saturation yields varying degrees of the collapse potential (Houston et al., 2001; Jefferson & Rogers, 2012).

Collapsibility of the soil could be investigated through direct response to wetting/loading tests using laboratory and field methods. The volume change and the degree of wetting that will take place are considered as major challenges facing collapsible soils (Jefferson & Rogers, 2012). Collapse due to volume changes that occur are more sudden than those experienced through consolidation processes and occur typically in non-plastic or of very low plasticity soils at initially dry state (Houston et al., 2001).

Furthermore, the volume changes of collapsing soils and expansive soils take place in a diametrically opposed manner. In both collapsing and expansive soils, the initial pore-water pressures are negative. Also volume changes result from an increase in negative pore-water pressure. Subjecting the collapsing soil to an additional load is not an essential condition for collapse; collapse can commonly occur when the soil has access to water. The water causes an increase in pore-water pressure, which is associated with a significant decrease in volume (Fredlund & Rahardjo, 1993). However, the shear resistance of soil particles before collapse suffices to support the soil structure at a given porosity or void ratio under the existence of a stress state. When the interparticular shear resistance is exceeded or decreased, the soil mass is compressed to a new equilibrium due to the change in the equilibrium between the void ratio and the stress state (Lefebvre, 1995).

Consequently, collapsible soils are considered to be problematic soils which directly affected by the wetting process. The wetting process triggers large deformations, differential settlement and a sudden collapse in engineering structures. Moreover the wetting of soil can be caused by different water sources such as landscape irrigation, broken water or sewer pipes, run-off or poor drainage control, ground water recharge, or water content changes through capillary rise.

Many parts of the world such as Russia, Middle East, China, Europe and North and South America suffer from the presence of moisture sensitive soils. Therefore, it is necessary to understand the process of collapse and assess whether the problems associated with collapsible soils can be avoided or mitigated.

2.3. Definitions

Many definitions of the collapsible soils can be found in the literature; therefore it is important to illustrate them to understand this kind of soil behaviour. Collapsible soils can be defined as follows:

"A metastable structured soil, an increase in pore-water pressure results in swelling for an unsaturated stable soil, whereas an increase in pore-water pressure may cause a volume decrease for unsaturated metastable-structured soil"(Barden et al., 1969, 1973).

"Any unsaturated soil that goes through a radical rearrangement of particles and great loss of volume upon wetting with or without additional loading"(Dudly, 1970; Jennings & Knight, 1975; Clemence & Finbarr, 1981; Lawton et al., 1991; Terzaghi et al., 1996; ASTMD5333, 2003).

"A soil that exhibits a volume decrease as a result of reduction in matric suction. Collapsing soils have an open type of structure with large void spaces which give rise to a metastable structure"(Fredlund & Rahardjo, 1993; Houston et al., 2001).

"One in which the major structural units are initially arranged in an open metastable packing through a suite of different bonding mechanisms. Upon wetting, the cementation bonds are weakened and the initially loose fabric collapses and densifies, often resulting in dramatic and damaging settlement"(Jefferson & Smalley, 1995; Lefebvre, 1995; Lu & Likos, 2004; Jefferson & Rogers, 2012).

2.4. Occurrence and formations

Collapsible soils can be found in arid and semi-arid regions where evaporation rates exceed rainfall. Arid-region deposits are often associated with collapsible soils including alluvium, colluvium and loess. Naturally occurring collapsible soils are typically formed from debris flow (e.g. alluvial fan materials) such as wind-blown sediments (e.g. loess), cemented high salt content metastable soils (e.g. sabkha), and tropical residual soil. Moreover, non-engineered or poor compaction with low moisture content or waste materials may produce artificially collapsible soil. However, most common collapsible soils are relatively stiff and strong at dry states even with low densities (Madhyannapu et al., 2006; Jefferson & Rogers, 2012).

Naturally formed collapsible soils are typically lightly to heavily cemented as a result of various salts, oxides, dried clay and soil suction. They exist in a loose, metastable or poor fabric states with relatively low density and moisture content (Fredlund, 1996; Ng & Menzies, 2007).

2.5. Types of collapsible soils

Collapsible soils can be found worldwide either naturally (e.g. loess or gypseous deposits) or as the result of human activities (e.g. poorly compacted soil).Dudly (1970); Rogers (1995); Al-Mufty (1997); Houston et al. (2001); Jefferson & Rogers (2012) represented different types of collapsible soils in their studies. In this study, two of the main types of collapsible soils are utilised and they are described in the following subsections.

2.5.1. Gypseous soil

2.5.1.1. Introduction

Gypseous soil presents a high collapse potential as a result of its metastable structure. It has low dry density and moisture content in its natural state due to the presence of cementation bonds and an open gypsum structure, particularly at unsaturated states or in arid or semi-arid regions. Moreover, large deformations, rapid settlement and a high decrease in the void ratio of a metastable soil structure can occur. Large volume changes and sudden collapses take place when the soil is inundated under constant vertical stress. Soil deformation occurs as a result of the dissolution of the cemented gypsum bonds, which causes a pronounced increase in the compressibility of the soil. The leaching phenomenon facilitates additional softening as well as large and complex deformations in gypseous soil due to the movement of underground water (Al-Mufty, 1997).

Gypseous soils are widely distributed through the world. Van Alphen & Romero (1971) estimated that these soils cover roughly 850,000 km^2 of the earth's surface, while (Nafie, 1989) estimated the area to be approximately 724,000 km^2. However, according to the United Nations Food and Agriculture Organisation (FAO, 1990), the extent of gypseous soils covers 1.0-1.5 million km^2 of the world area (see Figure 2.1). Major areas where gypseous soils are located include the Middle East (e.g. Iraq and Saudi Arabia), the southern regions of the former USSR (e.g. Siberia, Georgia and Transcaucasia), Northwest and East Africa (e.g. Libya, Algeria, Somalia and Ethiopia), Southern Europe (e.g. Spain) and in the drier regions of USA from California to Texas. Buringh (1960); Barzanji (1986); Nafie (1989); Nashat (1990); Al-Mufty (1997); Al-Obaidi (2003) reported that gypseous soils are widely distributed in Iraq, especially in the west, northwest and southwest regions and covers about 20-30% of Iraq's total area. The gypsum content in the soil is very high in some regions and could account for more than 60% of the total dry mass of the soil sample.
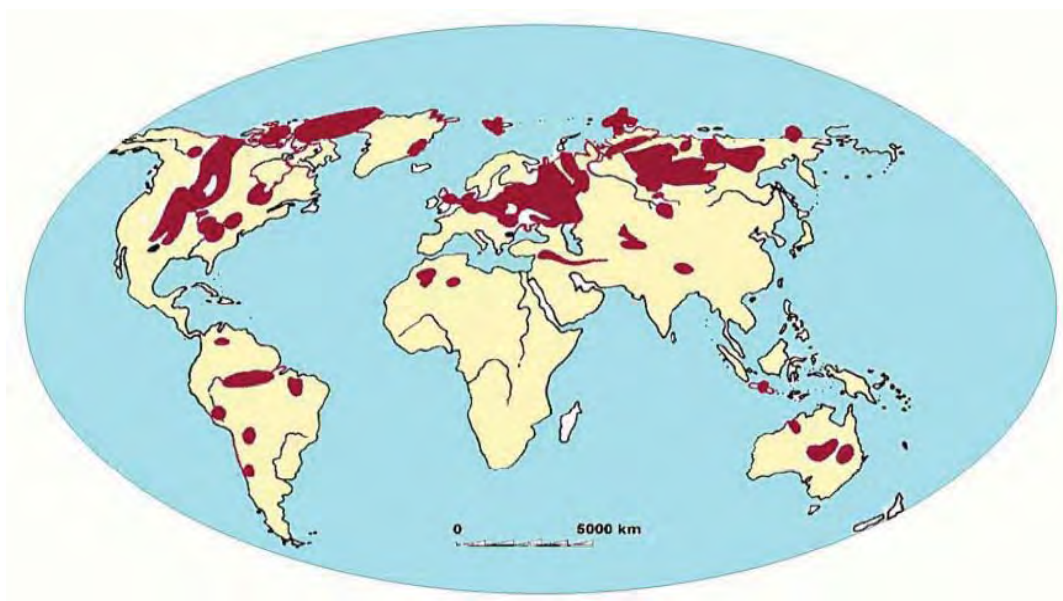
Figure 2.1.: Distribution of gypseous soils in the world (FAO, 1990).

2.5.1.2. Definitions

According to Seleam (2006), the term "gypsiferous soil" used by Van Alphen & Romero (1971) refers to soils containing more than 2% gypsum, while Saaed & Khorshid (1989) defined gypsiferous soil as soil that contains more than 6% gypsum. In Iraq, Smith & Robertson (1962) and (FAO, 1990) discovered that 3-10% of gypsum does not significantly interfere with soil characteristics such as structure, consistency and water holding capacity, while the gypsum crystals tend to break down the continuity of the soil mass in soil containing 10-25% gypsum. In civil engineering a soil can be defined as a gypseous soil when the gypsum content suffices to change the properties of the soil (Nashat, 1990). The term "gypseous soil" and "gypsiferous soil" are synonymous terms. The term gypsified soil refers to natural soils to which a predefined percent of gypsum is added. Many investigators use this type of soil to study the effect of gypsum on soil properties and behaviour. Sometimes it is considered a soil stabiliser, especially for road construction. Reid (2012) described the gypsum in UK as a widespread occurrence in soils and rocks, white crystals and powder. This gypsum is slightly soluble at neutral pH and soluble in acid. Moreover, Barzanji (1973) classified soils according to gypsum content, as shown in Table 2.1.

Table 2.1.: Classification of gypseous soils (Barzanji, 1973).

Gypsum content,%	Classification
0-0.3	Non- gypsiferous
0.3-3	Very- slightly gypsiferous
3-10	Slightly gypsiferous
10-25	Moderately gypsiferous
25-50	Highly gypsiferous
> 50	Gypsiferous soil to be described by the other fraction such as sandy gypsiferous soils

2.5.1.3. Gypsum formation in the soil

The weathering of rocks that contain different types of minerals commonly forms gypsum. Its chemical composition can be written as $CaSO_4.2H_2O$. The mineral has several varieties, including selenite (e.g. yields broad colourless folia), alabaster (e.g. fine grained, usually massive) and satin spar (e.g. fibrous gypsum) (Pirsson & Knopf, 1958; Klein & Hurlbut, 1985). Large amounts of hydration water molecules are lost if gypsum is heated to 170^oC, forming plaster of Paris (e.g. Bassanite, $CaSO_4.0.5H_2O$), but if heating continues to more than 200^oC, anhydrite starts to form when the hydration water completely evapourates. Anhydrite ($CaSO_4$) is heavier than gypsum, having a specific gravity of Gs=2.96, while gypsum has Gs=2.32. The physical and mechanical properties of the soil are directly affected if a large amount of gypsum is present (Nashat, 1990; Al-Mufty, 1997). Under natural conditions, the weathering of sulphides normally leads to the production of gypsum $CaSO_4.2H_2O$, which has limited solubility under neutral pH conditions. This is the normal form of sulphate in near-surface soils. Gypsum can occur in a wide variety of forms, from large clear crystals in undisturbed strata to fine, white, powdery crystals growing on exposed surfaces of reactive clays or mudstones. If carbonate minerals such as calcite are present, the acid will react with them to produce gypsum and carbon dioxide, as can be seen in Equation 2.1 (Reid, 2012).

$$CaCO_3+H_2SO_4+H_2O \rightarrow CaSO_4.2H_2O+CO_2 \qquad\qquad (2.1)$$
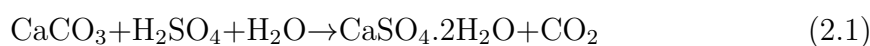
Al-Mufty (1997) stated that gypsum in soils and rocks could originate in either pedogentically or geogentically.

Pedogentic origins include the formation of secondary gypsum in the soil due to the accumulation of gypsum particles within the soil (Barzanji, 1973). There are two important requirements to form gypsum in the soil deposits. These are an external source of gypsum and a sufficiently arid climate (high temperatures of more than 20°C, and low rainfalls of less than 450 mm annual). The secondary gypsum in a soil can be formed by one or more of the following actions: Dissolution from primary rocks, ground water evaporation, windblown gypsum and cat-ion exchange.

Geogenetic origins include forms of processes which are of digenetic type (i.e. gypsum formed in place). These can be summarized as: the weathering of igneous rocks, sea water evaporation, the chemical origins of gypsum and the dolomisation of calcite. Taylor & Cripps (1984) presented a detailed description of the chemical reactions during gypsum formation.

2.5.1.4. Cementation

Cements are crystals that grow into existing pore spaces, which may or may not totally occlude the available pore space. Berner (1980) explained the rate of cement growth, formation and mathematical formulations. However, cementing bonds between soil particles can be formed in soil structure as a result of originally redistributing gypsum through dissolution-precipitation cycles. Otherwise, cementing gypsum normally originates from outside the soil. Thus, gypsum easily and rapidly develops between the soil particles via the flow of water when the permeability of the soil is relatively high (Al-Mufty, 1997).

2.5.1.5. Solubility and rate of solution

According to James & Kirkpatrick (1980), the solubility of a substance can be defined as "the amount which can be dissolved in a given quantity of water (solvent) at equilibrium". Also, the rate of solution is defined as "the speed with which it achieves this equilibrium concentration". Moreover, the rate of solution of many substances is determined by the transport rate of the soluble components across the boundary layer attached to the dissolving solid.

Freeze & Cherry (1979); James & Kirkpatrick (1980); Nashat (1990); Al-Mufty (1997) reported that the solubility of gypsum in pure water is a function of temperature and the presence of other salts. The solubility ranges between 2.0 g/l at 20°C to 2.5 g/l at 10°C.

James & Lupton (1978) showed that the solution rate of gypsum depends on many factors such as:

-Temperature, which increases with the increase of temperature

-Flow of water and flow velocity, which increases as the flow velocity increases

-Rock type, which varies according to the origin and type of gypseous soil rock

-Sodium chloride (NaCl) concentration in the water, which increases when NaCl concentrations in water increase

-Area, which increases as the area of gypsum exposed to the flowing water increases

-Concentration of calcium sulphate, which inversely dependent upon the sub-saturation concentration of calcium sulphate and

-Time, whereby the solubility of gypsum increases with time.

Razouki et al. (1994) concluded that increasing the applied pressure leads to an increase in the rate of gypsum dissolution in water. While the rate of total soluble salts is high for lower values of permeability, it is low for high values of permeability. In addition, Al-Farouk et al. (2009) concluded that the type of water flowing through the soil mass and the porosity of soil have a significant effect on the axial strain and gypsum dissolution.

2.5.1.6. Leaching

The term "leaching" can be generally defined according to Al-Zgry (1993) as "the process by which liquids percolate whether naturally or artificially through a porous material resulting in the dissolving and washing of soluble constituents out of the percolated material". In the practice of soil mechanics, Brenner et al. (1981) defined leaching in soil as "a process which removes materials in solution (e.g. salts) and cementation agent from a section in the soil profile". Gypseous soils undergo several changes in their characteristics due to a continuous loss in their mass and due to the alteration in properties of the material constituents during leaching (Al-Mufty, 1997; Al-Busoda, 1999; Al-Obaidi, 2003).

The dissolution of gypsum within the soil mass under wetting and loading conditions leads to one or a combination of following three processes: a collapse in the soil structure as a result of the immediate softening and bonding destruction of gypsum particles from inundation, consolidation after rearrangement of the soil structure at the end of the collapse process and the leaching process due to a continuous flow of water through the soil mass (Al-Ani & Seleam, 1993; Al-Jumaily, 1994; Al-Farouk et al., 2009).

The processes of leaching take place in soil deposits as a result of water movement due to ground water fluctuations, surface water percolation, the breakage of sewage pipes and irrigation channels Al-Obaidi (2003). In the laboratory, leaching has been conducted us-

ing a hydraulic gradient or by diffusion (Al-Abdullah, 1995).

Several studies deal with the effect of the leaching phenomenon on the geotechnical be-
haviour of soil deposits. Some of these studies investigate volume change and collapsibility
characteristics by carrying out a field collapse-leaching test, such as tests on gypseous soil
in Russia (Mikheav & Petrukhin, 1973; Mikheev et al., 1977; Petrukhin & Boldyrev, 1978)
as well as tests on gypseous soil in Iraq (Al-Sharrad, 2003). Other studies carried out labo-
ratory collapse-leaching tests on Iraqi gypseous soils using different laboratory equipment,
such as the Rowe cell apparatus (Seleam, 1988; Nashat, 1990; Al-Abdullah, 1995), the
triaxial cell apparatus (Al-Busoda, 1999; Al-Neami, 2000), the Oedometer permeability-
leaching cell (Torrance, 1974; Al-Busoda, 1999; Al-Obaidi, 2003) and the modified large
cell apparatus (Al-Kashab, 1981; Al-Obaidi, 2003; Al-Sharrad, 2007).

Al-Obaidi (2003) investigated the effect of the leaching phenomenon on the collapsibility
characteristics of gypseous soil by conducting collapse-leaching tests on different sizes of
soil mass. In this test, two types of cell were used: an Oedometer permeability-leaching
cell (7 cm in diameter and 1.9 cm in height) and a modified soil leaching apparatus (15
cm in diameter and 15, 7.5 and 4 cm in height). These tests were conducted under dif-
ferent conditions such as vertical stress, time, flow direction and the diameter to height
ratio D/H of soil sample. The study concluded that the accumulative leaching strain and
dissolved gypsum increase over time, while the permeability coefficient (k) decreases with
the increase in time, leaching strain and dissolved gypsum, see Figure 2.2. Al-Sharrad
(2007) and Namiq & Nashat (2011) also obtained similar results.
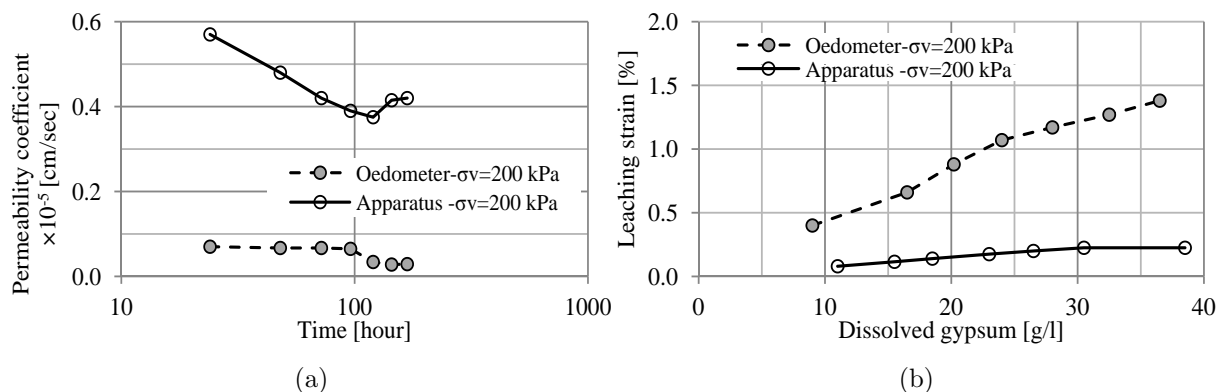
Figure 2.2.: Results of permeability-leaching test for sandy gypseous soil
(soil=SP,σ_v=200kPa,i=16, χ'=60%), Al-Ramadi city, west of Iraq (Al-Obaidi, 2003).

2.5.2. Loess soil

2.5.2.1. Introduction

Loess is one of the most widespread formations of the ice age. It was proposed that loess soil covers about 10% of the earth's surface (Pecsi, 1990). Loess is formed by silt-sized (e.g. typically 20-30μ) primary quartz particles that are created by high-energy earth-surface processes such as glacial grinding or cold climate weathering (Rogers et al., 1994). Moreover, when floods occur, loess soil may be moved from its source through rivers. After that, the quartz silt grains are deposited on flood plains as a result of subsequent flooding (Smalley et al., 2007). On the other hand, when loess soil dries out in arid climates, the particles are separated and transported by high winds until they are deposited in a new area. Cementing materials are often added after deposition or dissolved and reprecipitated at particle contacts (Houston et al., 2001).

Figure 2.3 explains loess soil distribution map showing [1] loess and [2] loess-like soils. [A] materials with the addition of the extent of the last glacial maximum and [B] present dust deposition areas, as cited and modified by (Pecsi, 1990; Rousseau et al., 2001; Haase et al., 2007; Smalley et al., 2011).

Loess soils were produced during the Quaternary Glacial period in Europe and the resulting dust accumulation ranged from the maritime areas of northwest Europe (France, Belgium, Germany), over central Europe to the Ukraine and the Russian plains which are characterised by a continental climate (Grahmann, 1932; Osopov & Sokolov, 1995; Frechen et al., 2003; Delage et al., 2005; Haase et al., 2007).

Wagner (2011) described the loess belt in Germany as follows:

In Germany, the northern boundary of the loess belt runs north of the Rhenish Massif, the Harz Mountains and the Ore Mountains and separates the loess and loess-like sediments from cover sands and drift sands (Eissmann, 2002; Haase et al., 2007). Five main loess regions adjoin to the northern boundary. These are from west to east the lower Rhine area, southern parts of the Weser-Aller catchment (southern Lower Saxony and Northern Hesse), and the loess region northeast of the Harz Mountains (e.g. Saxony-Anhalt) and the loess region north of the Ore Mountains (e.g. Saxony). Moreover, loess soils are distributed in many regions in Asia such as North China (Derbyshire et al., 1995; Lin, 1995), Thailand, see Phien-wej et al. (1992) and North Africa, such as Algeria, see Nouaouria et al. (2008). The open structure of loess soils causes subsequent collapse deformations when these soils are wetted and/or loaded during hydro-compaction or hydro-consolidation processes (Waltham, 1988).
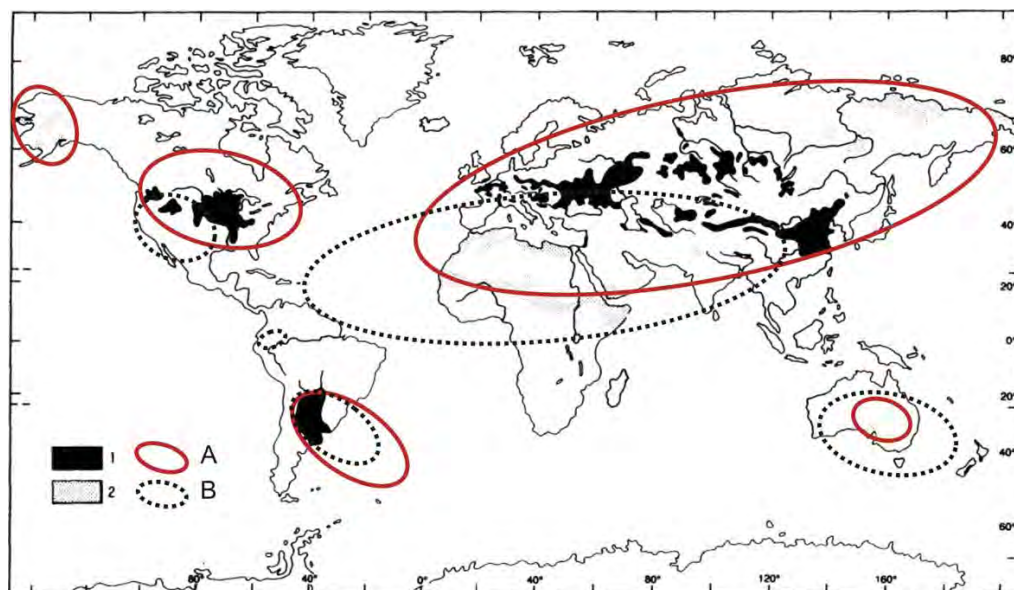
Figure 2.3.: Loess soil distribution map through the world, Legend 1.Loess, 2.Loess-like Sediments,A.Main glacial dust area,B.Main present dust area (Pecsi, 1990).

2.5.2.2. Definitions

According to Barden et al. (1973) loess soils can be defined as "an Aeolian Quaternary deposit of predominately silt-sized particles ranging between 20-60 mm with clays, carbonates and capillary water acting as bonding materials at particle junctions".

Terzaghi et al. (1996) described loess soils as "uniform, cohesive, wind-blown sediment, and is commonly light brown with particles size ranges between 0.01 and 0.05 mm". However, Terzaghi et al. (1996) defined modified loess as "a loess generated because of secondary processes including temporary immersion, erosion and subsequent deposition, chemical changes involving the destruction of the bond between the particles, or chemical decomposition of the more perishable constituents such as feldspar".

Jackson et al. (2005) and others defined Alluvium and Colluvium loess deposits as:

-Alluvium "is loose, unconsolidated soil or sediments, which has been eroded, reshaped by water in some form, and redeposited in a non-marine setting. Alluvium is typically made up of a fine particles of silt and clay and larger particles of sand and gravel".

-Colluvium "is a general name for loose, unconsolidated sediments that have been deposited at the base of hill slopes by either rain-wash, sheet wash, slow continuous down slope, or a variable combination of these processes".

2.5.2.3. Criteria and microstructure

Pecsi (1990, 1995) listed many criteria that can be applied to define and describe typical loess. Smalley et al. (2011) summarised these criteria as follows:

-Loess is a homogeneous, porous, pale yellow subaerial deposit. It is predominantly coarse silt (10-50μ), and the silt percentage ranges between 40-70% by weight, while clay and sand percentages range between 5-25% by weight. Among clay minerals illite or montmorillonite dominates, while in smaller amounts kaolinite, vermiculite, or chlorite is also frequently present. However, quartz grains are predominant with an average percentage ranging between 60-70%. In addition, loess contains feldspar, calcite and dolomite in lesser amounts. Carbonate content varies, ranging between 1-20% depending on environmental conditions.

-Loess deposits are usually unstratified, but loess sequences often contain intercalated palaeosols or loam or sand beds. The loess grains are partly cemented and partly aggregated.

-Loess as a mineral matter that commonly accumulates as a result of frequent transport and sorting in nature. Also small grains continue to move until they are stabilised by steppe vegetation due to the effect of rainwater run-off, snowmelt and other processes on the slop.

-The compressive strength of loess is 1.5 kg/cm^2 under dry conditions; even steep loess walls are stable. Large collapses occur upon inundation, and the walls are easily eroded and hollow formations occur due to surface water flow.

Delage et al. (2005) studied the microstructure and collapse behaviour of widespread Aeolian loess deposits in Northern France. Microscan SEM observations indicated they had a porous microstructure with a heterogeneous scattering of clay aggregations that filled the intergrain pores and work as a linking agent between the grains in some areas. In areas with no clay, sharp-edge angular silt grains approximately 15-30μ in diameter has been observed with large intergrain pores. These pores were located in the areas with no clay probably significantly contributed to a decrease in collapse volume. Mercury intrusion porosimetry identified the changes in intergrain pores that occur during collapse and showned that the smaller pores inside the clay aggregations were not affected. The collapse structure was apparently more organised with a well-graded pore size distribution curve.

On the other hand, Munoz-Casteblanco et al. (2011a) explained that collapse due to wetting normally occurs as a result of the densification of the areas where the grains are clean with large pores around them. The zones in which the porosity is filled by clay

aggregation are typically more resistant and locally less sensitive to collapse.

Munoz-Casteblanco et al. (2011*b*) pointed out what occurs when loess contains a significant amount of calcium carbonate. Some layers of loess are characterised by a significant calcareous content, a higher porosity and a low plasticity. These features lead to a metastable structure that is strengthened by suction when the soil is partially saturated. Subsequent soil saturation may thus induce a loss of stability of the structure with relatively large volumetric deformations due to the collapse of the open structure of the soil.

2.6. Factors controlling collapse mechanism

To study the behaviour of the collapse mechanism, three main factors can be categorised: cementation and the degree of bonding, microstructure and stress path, and types of collapse.

Many researchers studied and discussed the main factors controlling the behaviour of collapse mechanisms in detail. Such studies were conducted by the following scientists:Knight (1960); Larionov (1965); Barden et al. (1969); Dudly (1970); Barden et al. (1973); Clemence & Finbarr (1981); Lawton et al. (1989, 1992); Rogers & Smalley (1993); Feda (1995); Klukanova & Frankovska (1995); Pererira & Fredlund (2000); Charles & Skinner (2001); Charles & Watts (2001); Houston et al. (2001); Delage et al. (2005). In the following sections, some of this literature is summarised.

2.6.1. Cementation and the degree of bonding

Collapse behaviour in cemented soils is a function of cementation type and the degree of bonding. In contrast, in uncemented and unsaturated soil, collapse simply occurs if the capillary forces are destroyed. Although the bond strength among soil grains generated from cementing and suction can be characterised in similar ways, upon inundation the suction will decay and disappear, whereas chemical bonding is likely to be less affected by a change in suction. In addition, salt and clay bonds connecting the soil particles will tend to be removed or softened after inundation, and collapse occurs (Jefferson & Rogers, 2012).

Furthermore, in uncemented soils, where collapse is related to the destruction of capillary (matric suction) forces, the volume change associated with collapse is confined to the wetted zone (Fredlund & Gan, 1995).

Klukanova & Frankovska (1995) and Milodowski et al. (2012) indicated that collapse oc-
curs in cemented loess soils throughout the three stages after inundation. Jefferson &
Rogers (2012) summarised these stages as follows:

-Stage 1 Clay bridges or buttresses are dispersed or disrupted between loosely packed silt
grains, leading to an initially rapid collapse of the inter-ped matrix.

-Stage 2 The load is taken up via contact between adjacent compact silt peds, which
rearrange into closer packing.

-Stage 3 As loading increases, progressive ped deformation and shearing occur and result
in further collapse.

Rogers (1995) concluded that there are two important factors affecting the collapse mech-
anism. The first one is particle shape: a soil laid down in a loosely packed structure can
maintain its structure, either until cementation can withstand the forces involved or until
a trigger causes collapse. The second factor is particle attraction, whether by cementa-
tion, chemical or physical attraction or negative pore water pressures (e.g. suctions).

Jefferson & Rogers (2012) pointed out that the collapse in cemented soil structure with
relatively large voids commonly occurs when the soil grains are weakened by adding wa-
ter and/or an additional load, allowing particles to slide over one other, which results in
collapse.

There are three main bonding mechanisms present in collapsible soils (Dudly, 1970; Bar-
den et al., 1973; Clemence & Finbarr, 1981; Rogers, 1995), namely:

(i) Under capillary or matric suction forces, soil consists of sand-sand with meniscus water
or sand-sand with a fine silt binder (see Figure 2.4a, b).

(ii) Knight (1960) indicated the clay forms a randomly flocculated structure when clay
and silt particles have coarser particle contacts, providing a buttress to the bulky grains
(see Figure 2.4c). The majority of collapsing soils, however, involve the action of clay
plates in the bonds between the bulky sand and silt grains. When the clay is formed
by authigenesis, it could result in a parallel plate onion skin effect around the quartz
particles (see Figure 2.4d). Alternatively, when the clay is suspended in the pore-water,
gradual evaporation causes the clay plates to retreat with the water into the menisci at
interparticle contacts.

(iii) In certain collapsing soils the important bonding effect may be due to chemical ce-
menting agents such as iron oxide, calcium carbonate, etc., which are often the main agent
in loessial soils (see Figure 2.4e).

Considering the above-mentioned bonding agents, Lefebvre (1995) observed that either
simple capillary suctions and clay buttresses or chemical cementing can introduce and
generate bridges between the solid grains in metastable open fabrics of collapsible soils.
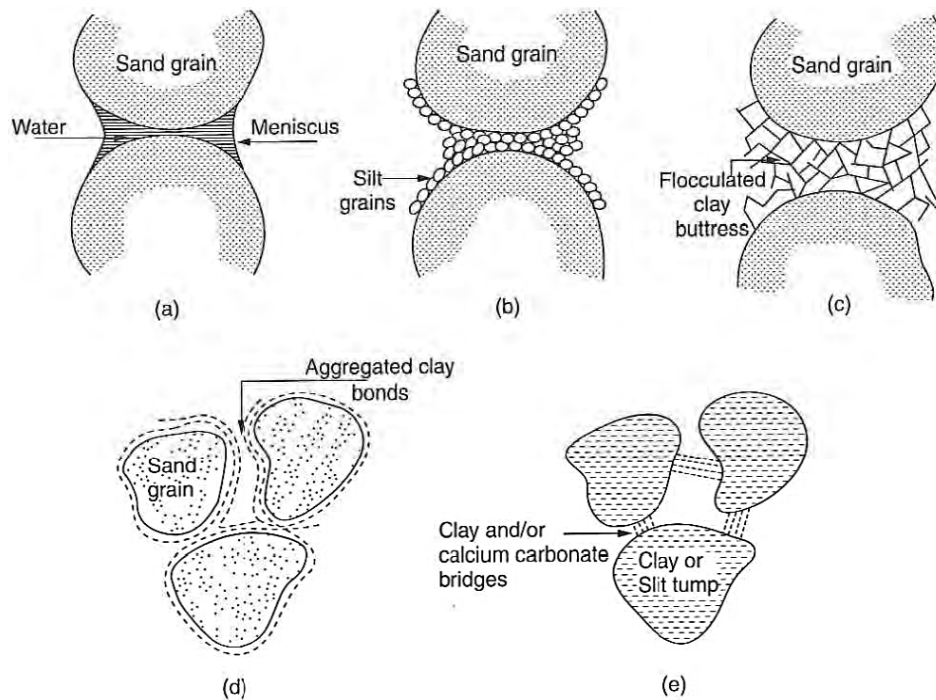
Figure 2.4.: Typical bonding arrangments formed in collpsible soils, as cited in (Jefferson & Rogers, 2012)

.

Although one type may dominate, complex interaction is possible in some cases. On the other hand, Lefebvre (1995) concluded that the water can weaken nearly any bond strength.

However, whatever the physical basis of the bond strength is, all types are weakened by the addition of water. In the case of capillary suction the drop in chemical cementing it might be very slow. The additional resistance of the soil skeleton is generally related to different types of bonds between particles. These bonds may result from dissolution-precipitation of cementing agents or may be formed by amorphous or clayey minerals cementing the particle contacts.

2.6.2. Microstructure and stress path

The metastable structure of collapsible soil is greatly affected by the stress path and by the degree of saturation of the soil sample. Barden et al. (1973) explained the impact of the stress path as follows:
The collapse phenomenon was apparently a contradiction of the principle of effective stress

which underlies all soil mechanics theory, since wetting increases pore pressure, decrease effective stress and hence is expected to cause heave rather than settlement. However, more detailed consideration of the mechanism indicated that the collapse was due to local shear failure between soil grains or peds, and hence is compatible with the principle of effective stress. The collapse process in partly saturated soil is better considered in terms of two separate components of effective stress, the applied stress and the suction, following the approach of Bishop & Blight (1963).These two components develop intergranular stress by different mechanisms, thus the applied stress develops shear stresses and hence potential instability at intergranular contacts, while the suction is strictly a normal stress and hence increases the stability at intergranular contacts.

Barden et al. (1969) and Rogers (1995) pointed out that appreciable collapse required the following conditions:

1. An open, potentially unstable, partly saturated structure

2. Sufficiently applied stress components to develop a metastable condition

3. Sufficient soil suction (or other bonding "cementing" agent) to stabilise intergranular contacts, whose reduction upon wetting will lead to collapse and

4. High void ratios, high porosity and low dry density.

Lefebvre (1995) illustrated the main factors related to the collapse mechanism in partly saturated soil as follows:

1. For collapse to occur, the soil structure needs to be at an initially loose state.

2. Relatively small deformations upon loading can occur if the soil skeleton resistance resulting from interparticle bonds is not exceeded.

3. When the soil skeleton resistance is fully mobilised by the applied loading, a small increase in load can result in large deformations or collapse.

4. The soil skeleton can support any loading below its critical pressure without any significant deformation at a dry state; otherwise large deformations and collapse into a denser state can occur without the application of an additional load due to the softening of interparticle bonds. Pererira & Fredlund (2000) made similar observations while conducting research on compacted soils.

According to Bell & Culshaw (2001), porous textures of collapsible soils consist of low dry densities and high void ratios with sufficient void space in their natural state to hold their liquid limit moisture at saturation. Moreover, collapsible soils possess high apparent strength, but they are susceptible to large reductions in void ratios upon inundation. In other words, the metastable texture collapses as the bonds between the grains break down when the soil is wetted. Hence, the collapse process represents a rearrangement of soil particles into a denser state of packing. When the soil is saturated, collapse rapidly

occurs. Otherwise, longer periods are required when such soil contains additional clay.

Delage et al. (2005) concluded that the collapsibility of loess soil in northern France appears to be significantly sensitive to changes in water content. Collapse deformation decreased as the initial water content increased. They also observed that collapse could be considered a plastic deformation in the elasto-plastic framework provided by the Barcelona group (i.e. the BBM model).

In the elasto-plastic constitutive modelling approach for collapsible soils, Alonso et al. (1990); Chiu & Ng (2003) developed several theoretical models. These models extended the Modified Cam Clay model, applied the principles to unsaturated soils, and introduced the loading collapse (LC) surface to define yielding due to either external loading (e.g. total stress) or saturation (e.g. zero suction) (Ng & Menzies, 2007).

Pererira & Fredlund (2000) indicated the following key features about the collapse behaviour of compacted soils:

-Collapse is expected for any type of dry compacted soil with optimum water content.

-Capillary soil action commonly generates high micro forces of shear strength through bonding.

-A gradual increase in compressibility corresponds to a gradual decrease in the shear strength of collapsible soils upon wetting.

-Soil collapse progresses with increasing degrees of saturation; however, above a critical degree of saturation, no further collapse occurs.

-Collapse is associated with localised shear failure.

-Horizontal stresses increase as a result of collapse when the soil inundation is under a constant load and anisotropic Oedometer conditions.

-In triaxial collapse tests for a given mean normal total stress, the value of axial collapse increases and radial collapse decreases with increased stress ratios.

2.6.3. Types of collapse

Collapsible behaviour in soil structure can be considered a combination of deformation and stability phenomena and can be described from a physical point of view using the micromechanics theory of soil structure. Thus, a typical collapsible structure is postulated as an open macroporous (e.g. silty and/or sandy) skeleton with contact bonds ensuring its local stability.

Feda (1995) indicated that, two levels of analysis are available to describe the failure mechanism of collapsible soils. These levels are the micromechanical approach and the macromechanical approach, both of which should be followed when classifying both local

and total collapse behaviour.

Under loading and when the stress and wetting conditions are changed, the soil structure becomes metastable; afterwards, collapsing begins and the soil structure attempts to regain equilibrium under a new set of stresses and degrees of saturation. The collapse may be only localised or it may result in a total collapse.

According to Feda (1995) a localised collapse is "a smaller extent being confined to weak regions of the soil structure. Its outcome is the homogenisation of the soil structure, i.e. from the thermodynamical standpoint, an increase of entropy". However, total collapse is "a complete failure of the system which cannot find equilibrium without completely rebuilding its structure".

In Figure 2.5, collapses are classified both micromechanically (collapse by debonding, grain crushing, fabric transition and softening-hardening) and macromechanically (collapse by loading, wetting, creep, radial softening and excess pore water pressure).

Figure 2.5.: Classification of the mechanisms of collapses (Feda, 1995).

2.7. Collapse potential identification and test methods

The one-dimensional response-to-wetting test, which is performed using conventional consolidation equipment represents the frequently used laboratory collapse test for determining the collapse potential of the soil (Houston et al., 2001). In Oedometer-collapse test, two procedures are commonly followed; single Oedometer (SOT) and double Oedometer (DOT) methods. The typical output of this test can be represented as in Figure 2.6.

(a)

(b)
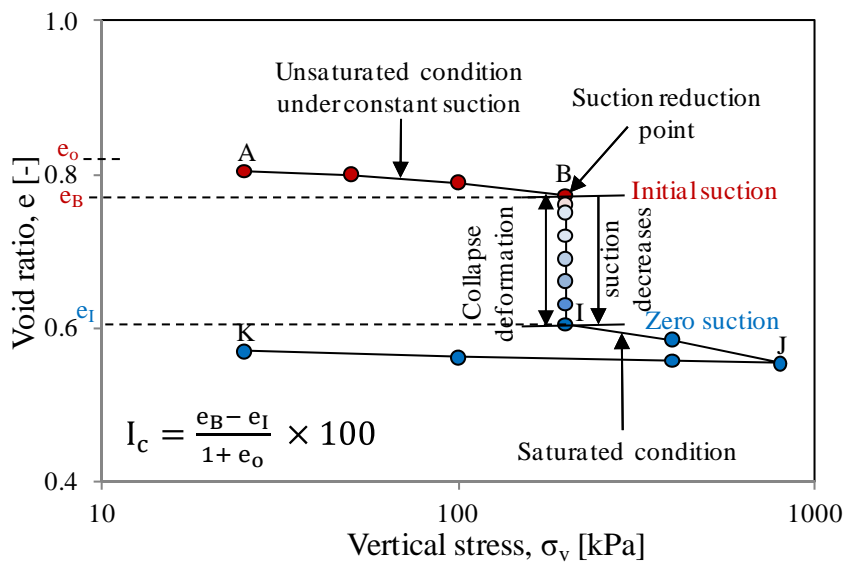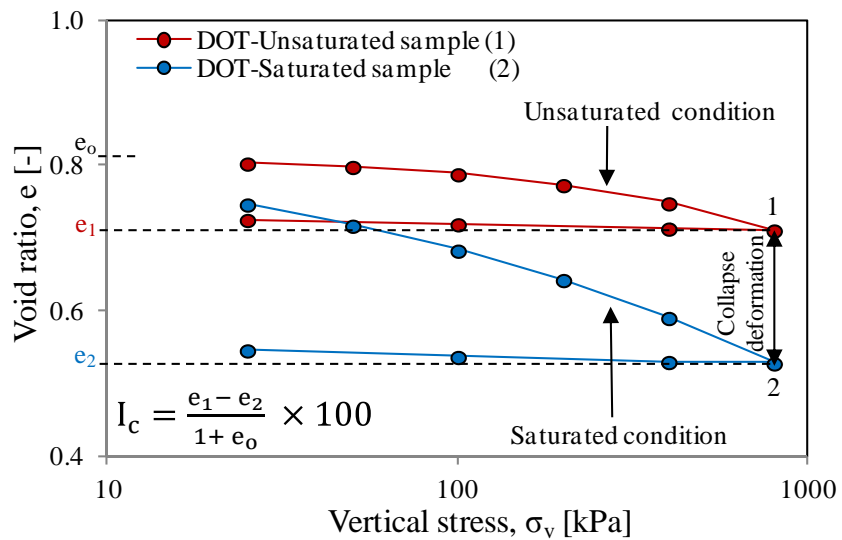
Figure 2.6.: Typical Oedometer-collapse test result: (a) Double Oedometer test (DOT) and (b) Single Oedometer test (SOT).

The actual collapse potential is determined using the double Oedometer test (DOT) method suggested by Jennings & Knight (1957). In this method, two identical samples are prepared and tested individually in Oedometer device. One sample is tested at its natural moisture content, while the other is tested under saturated conditions. The same load sequence is used in both cases. The difference between the two stress-strain curves represents the amount of collapse deformation that occurs depending on the stress level as shown in Figure 2.6a .

Jennings & Knight (1975) suggested a procedure to describe the collapse potential of a soil which is mostly a qualitative evaluation. This procedure was subsequently modified by Houston et al. (1998) and standardised by the American Society for Testing and Materials (ASTM) under code number ASTMD5333 (2003).

Figure 2.6b illustrates a typical response in which a seating stress of 5 kPa was used to establish an initial state. Any compression under this stress was attributed to sample disturbance. The initial compression curve (points A-B) represents the response of the soil at its in situ water content. Pressure was applied until the stress on the sample was equal to (or greater than) that expected in the field or up to 200 kPa as suggested by Jennings & Knight (1975) and as standardised by ASTMD5333 (2003).

At point B, the specimen was flooded to reach saturation and left for 24 hours (ASTMD5333, 2003). The duration of the load increment following inundation lasted overnight or until primary consolidation was completed (ASTMD2435, 1996). The difference between the strains before and after inundation with water (points B-I) represents the amount of collapse deformation at the specified stress level, after which further loading is undertaken corresponding to points (I-J). The path (J-K) represents the unloading stage of the soil specimen.

According to ASTMD5333 (2003), the following definitions are outlined:

-*Collapse*: indicates a decrease in the height of confined soil following wetting at a constant applied vertical stress.

-*Collapse index* (I_e): refers to the percent-relative magnitude of collapse determined and calculated at 200 kPa.

-*Collapse potential* (I_c) denotes the percent-relative magnitude of collapse determined at any stress level as follows:

$$I_c = [\frac{d_f - d_o}{h_o} - \frac{d_i - d_o}{h_o}] \times 100 = [\frac{d_f - d_i}{h_o}] \times 100 \qquad (2.2)$$

where: d_o= the dial reading at seating stress, mm, d_i= the dial reading at the appropriate stress level before wetting, mm, d_f= the dial reading at the appropriate stress level after wetting, mm, h_o= the initial specimen height, mm, $\frac{d_f-d_o}{h_o}$= the strain at the appropriate stress level after wetting, and $\frac{d_i-d_o}{h_o}$= the strain at the appropriate stress level before wetting.

Or, since the test is conducted as a one-dimensional test, Equation (2.2) may be rewritten as:

$$I_c = \frac{\Delta h}{h_o} \times 100 \qquad (2.3)$$

where: Δh= the change in specimen height resulting from wetting, mm, h_o= the initial specimen height, mm.

Equation (2.2) may be rewritten in terms of void ratio as follow:

$$I_c = \frac{e_B - e_I}{1 + e_o} \times 100 \qquad (2.4)$$

where: I_c= the collapse potential, e_B,e_1= the void ratio at the appropriate stress level before wetting, e_I,e_2= the void ratio at the appropriate stress level after wetting, e_o= the initial void ratio.

Based on the Oedometer-collapse test, the collapse potential can be assessed and used to indicate the problem severity of collapse. Table 2.2 provides details presented by Jennings & Knight (1975) and ASTMD5333 (2003), showing a slight difference between the two references in the collapse potential range corresponding to problem severity.

Table 2.2.: The severity of the collapse potential.

Jennings and Knight, 1975		ASTM (D5333-2003) standard	
I_c,(%) at σ_v=200 kPa	Severity of problem	I_c,(%) at σ_v=200 kPa	Degree of collapse
0-1	No problem	0	None
1-5	Moderate trouble	0.1-2.0	Slight
5-10	Trouble	2.1-6.0	Moderate
10-20	Severe trouble	6.1-10.0	Moderately severe
> 20	Very severe trouble	> 10.0	Severe

2.8. Collapsible soils in unsaturated soil framework

2.8.1. Introduction

In recent decades most researchers agree that the collapsible soils are always unsaturated. Large collapse deformation and volume changes occur as a result of a reduction in matric suction. Wetting processes resulting from a reduction in applied matric suction under constant net stress are considered one of the major causes of collapse. Some of the literature dealing with collapse behaviour includes: Tadepalli & Fredlund (1991); Rahardjo & Fredlund (1992); Tadepalli et al. (1992a,b); Fredlund & Rahardjo (1993); Fredlund & Gan (1995); Pereira & Fredlund (1997); Pererira & Fredlund (2000); Rao & Revanasiddappa (2000); Houston et al. (2001); Rao & Revanasiddappa (2003); Jotisankasa (2005); Pereira et al. (2005); Aziz et al. (2006); Sun et al. (2007); Al-Badran (2011); Nelson et al. (2011).

2.8.2. Unsaturated soil and concept of suction

Classically unsaturated soil is considered to have three phases: solid, water and air. However, in recent decades, the existence of a fourth phase, namely, the air-water interface, also called the contractile skin, was recognised. When the air phase is continuous, the contractile skin interacts with the soil particles and influences the mechanical behaviour of the soil (Fredlund & Morgenstern, 1977; Fredlund & Rahardjo, 1993). The mass and volume of each phase can be schematically represented in a phase diagram as shown in Figure 2.7.
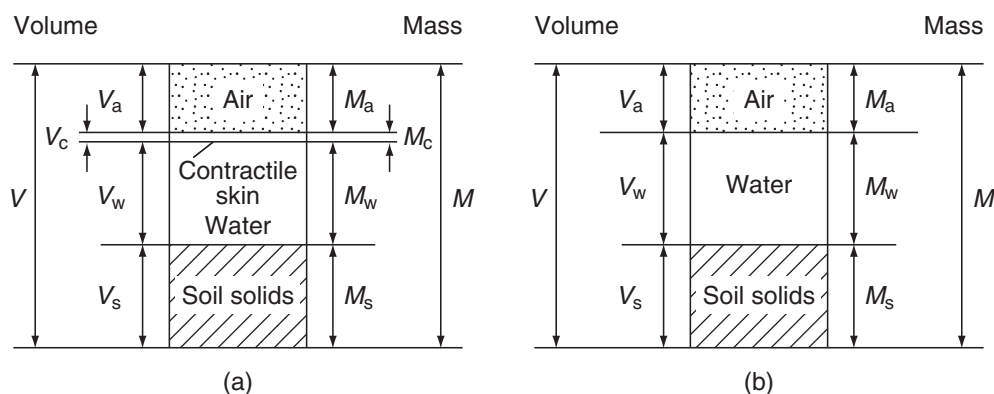
Figure 2.7.: Phase diagrams for unsaturated soil,(a) a rigorous four-phase unsaturated soil system and (b) a simplified three-phase diagram (Fredlund & Rahardjo, 1993).

The concept of soil suction is associated with unsaturated soil mechanics. Soil suction is a general term that may be used when referring to matric suction, osmotic suction or total suction.

According to Aitchison (1964); Fredlund & Rahardjo (1993); Fredlund et al. (2012), total, matric and osmotic suctions can be defined as follows:

-Matric suction (or the capillary component of free energy): "is the equivalent suction derived from the measurement of the partial pressure of water vapour in equilibrium with soil-water relative to the partial pressure of water vapour in equilibrium with a solution identical in composition with the soil water".

-Osmotic suction (or the solute component of free energy): "is the equivalent suction derived from the measurement of the partial pressure of water vapour in equilibrium with a solution identical in composition with the soil water relative to the partial pressure of water vapour in equilibrium with free pure water".

-Total suction (or the free energy of soil water): "is the equivalent suction derived from the measurement of the partial pressure of water vapour in equilibrium with the soil water relative to the partial pressure of water vapour in equilibrium with free pure water".

Fredlund & Rahardjo (1993) explained that, considering the above-mentioned definitions, total suction corresponds to the free energy of the soil water, while matric suction and osmotic suction are the components of free energy. Thus, they formulate it in an equation form as follows:

$$\psi = (u_a - u_w) + \pi \tag{2.5}$$

where: ψ=total suction, $(u_a - u_w)$ = matric suction, u_a = pore-air pressure, u_w = pore-water pressure and π = osmotic suction.

Considering the general concept of suction and the soil water potential in expansive soil (e.g., bentonite), the matric component of soil suction comes from hydration forces and capillary component effects. Therefore, in expansive soils, the matric suction is the sum of hydration forces and capillary forces (Agus, 2005; Arifin, 2008; Arfin & Schanz, 2009; Al-Badran, 2011).

2.8.3. Stress state variables

According to Fredlund & Rahardjo (1993), stress state variables can be defined as: "the non-material variables required for the characterisation of the stress condition. The me-

chanical behaviour of a soil (i.e. the volume change and shear strength behaviour) can
be described in terms of the state of stress in the soil". In unsaturated soil mechanics,
two approaches are utilised to describe stress state variables, namely the effective stress
approach (Bishop, 1959) and the two independent state variables approach (Fredlund &
Morgenstern, 1977).

2.8.3.1. Effective stress concept

For saturated soil, Terzaghi (1936) formulated the effective stress equation as follows:

$$\sigma' = (\sigma - u_w) \tag{2.6}$$

where: σ'=effective normal stress, σ=total normal stress and u_w=pore-water pressure.
For unsaturated soil, Bishop (1959) proposed the most frequently used effective stress
formulation for unsaturated soils, which is commonly referred to as Bishop's effective
stress equation for unsaturated soils and is represented by the following formula:

$$\sigma' = (\sigma - u_a) + \chi(u_a - u_w) \tag{2.7}$$

where: σ'= effective normal stress, u_a = pore- air pressure and χ = a soil parameter
related to degree of saturation and ranging from 0 (for saturated soils) to 1.0 (for dry
soils).
Several studies investigated and briefly discussed the relationship between Bishop's ef-
fective stress parameter χ and degree of saturation, type of test and stress path. Such
studies were done by Bishop & Henkel (1962); Morgenstern (1979); Fredlund & Rahardjo
(1993); Khalili et al. (2004). It was pointed out that the χ value is not only function of
soil the degree of saturation but also is related to the soil structure, stress and suction
paths to which the soil was subjected.
Khalili & Khabbaz (1998) showed that by plotting the values of χ against the ratio of
matric suction over the air entry value (e.g. suction ratio), a unique relationship may be
obtained for most soils as depicted in Figure 2.8.

Khalili et al. (2004) investigated the effective stress concept in unsaturated collapsible
soil. They outlined the following points:
-The dual impact of suction is proved through its impact on the effective stress and the
preconsolidation pressure or the yield stress of the soil. This effect can be clearly observed
during the collapse phenomenon when the preconsolidation pressure shifts with suction
upon wetting.
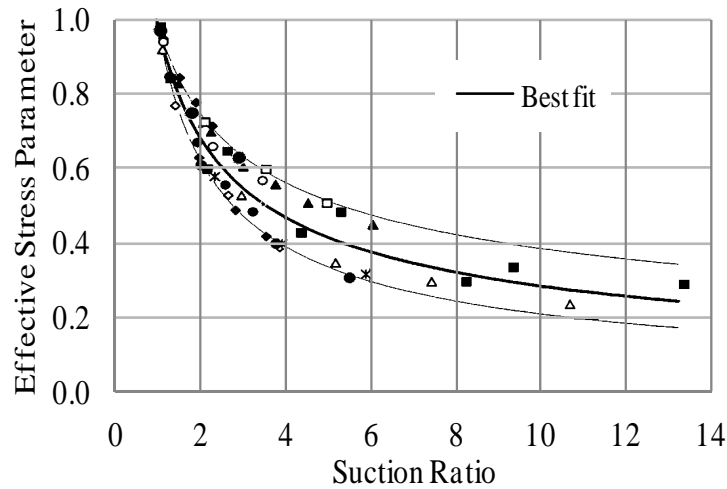
Figure 2.8.: Effective stress parameters versus suction ratio χ (Khalili & Khabbaz, 1998).

-For collapsible unsaturated soils, when the suction varies, the preconsolidation pressure commonly increases at a rate greater than the increase in the rate of effective stress (Loret & Khalili, 2000). For noncollapsible unsaturated soils, the opposite behaviour is observed. Moreover, upon inundation of collapsible soils, plastic volumetric contractions are observed, while upon desaturation, the soil response enters the elastic region. Thus, the elastic coefficient of compressibility must be used when analysing the volume change of such soils (Fleureau et al., 1993).

-The stress path of unsaturated soil has been considered in the effective stress principle according to Bishop (1959) equation (see Equation 2.7) during the constant net vertical stress-suction control procedure. The stress paths involving a change in the net stress (i.e. constant suction) need not be considered. This is because a change in the net stress is equal to a change in the effective stress and the effective stress principle is normally valid.

-Upon inundation, the suction in the soil specimen is reduced to zero resulting in collapse and a tendency for elastic dilatancy. Moreover, the specimen undergoes plastic volumetric contraction at constant effective stress and collapses onto the new state boundary.

2.8.3.2. Two-Independent stress state variable approach

Coleman (1962) and Matyas & Radhakrishna (1968) were the first researchers who used the term of "state parameters" to describe volume change behaviour in unsaturated soils. Fredlund & Morgenstern (1977) provided theoretical analysis of stress state variables for unsaturated soils based on multi-phase continuum mechanics by assessing the contractile

skin as the fourth phase of the soil. The analysis proposed that the state of stress in unsaturated soils can be described in terms of two independent stress variables, namely matric suction $(u_a - u_w)$ and net stress $(\sigma - u_a)$. Many researchers subsequently adopted the two-independent stress state variable approach, including Alonso et al. (1999); Cui et al. (2002); Agus (2005); Lu & Likos (2006).

Based on the theoretical analysis of Fredlund & Morgenstern (1977) and Fredlund & Gan (1995) the volume change formulation of unsaturated collapsible soil was proposed as follows:

The compressibility form of the constitutive equation for one-dimensional soil structure volume change in saturated soil is written as:

$$\frac{dV_v}{V_o} = m_v d(\sigma_y - u_w) \tag{2.8}$$

where: $dV_v =$ the change in the total volume, $V_o =$ the initial total volume, $m_v =$ the coefficient of volume change, $d(\sigma_y - u_w) =$ the change in effective stress, $\sigma_y =$ the total stress at yielding condition and $u_w =$ the pore water pressure.

In equation (2.8), the deformation state variable, $\frac{dV_v}{V_o}$, is related to the stress state variable, i.e., $(\sigma_y - u_w)$, by a soil property, (m_v), known as the coefficient of volume change. The stress state variable, $((\sigma_y - u_w)$, is known as effective stress when dealing with saturated soils.

Equation (2.8) can be similarly extended to describe the deformation of unsaturated soil by relating the deformation state variable, $\frac{dV_v}{V_o}$, to the two stress state variables, i.e., $(\sigma_y - u_w)$ and $(u_a - u_w)$. The resulting compressibility form of the constitutive relationship for the one-dimensional volume change of the soil structure in unsaturated soil is written as:

$$\frac{dV_v}{V_o} = m_1^s d(\sigma_y - u_a) + m_2^s d(u_a - u_w) \tag{2.9}$$

where: $m_1^s =$ the coefficient of volume change with respect to a change in net normal stress $d(\sigma_y - u_a)$ and $m_2^s =$ the coefficient of volume change with respect to a change in matric suction $d(u_a - u_w)$.

Similarly, an independent, water phase volume change equation can be written for an unsaturated soil,

$$\frac{dV_w}{V_o} = m_1^w d(\sigma_y - u_a) + m_2^w d(u_a - u_w) \tag{2.10}$$

where: dV_w = the change in volume of water, m_1^w = the coefficient of water volume change with respect to a change in net normal stress $d(\sigma_y - u_a)$, m_2^w = the coefficient of water volume change with respect to a change in matric suction $d(u_a - u_w)$ and u_a = the pore air pressure.

For air volume change in the soil, an equation can also be written by follow the similar procedure above.

2.8.4. Volume change of unsaturated collapsible soils

2.8.4.1. Introduction

When soils exhibit a reduction in total volume during inundation or matric suction reduction at a constant vertical net stress, this is called collapsible soils of metastable structure. For stable soil structure, an increase in pore-water pressure results a swelling behaviour, whereas for metastable structure, an increase in pore-water pressure results collapse behaviour (Barden et al., 1969). Fredlund (1996) introduced a three-dimensional constitutive surface for stable and metastable unsaturated soils. The surface is plotted in three-dimensional space of the void ratio-matric suction-net vertical normal stress as shown in Figure 2.9.

For stable structure of unsaturated soils, wetting processes induced by reduction of matric suction caused swelling phenomenon, see Figure 2.9a. While for a metastable structured, reduction of matric suction caused a collapsing phenomenon due to reduction in the void ratio, see Figure 2.9b.

2.8.4.2. Volume change tests under suction control

Many types of volume change tests under suction control were conducted for unsaturated soils. Several studies such as those conducted by Tadepalli & Fredlund (1991); Pererira & Fredlund (2000); Pereira et al. (2005); Sun et al. (2007) indicated that the same methodology is also valid for unsaturated collapsible soils.

The stress path and the initial condition of volume change tests for unsaturated soils depend on the expected output results regarding the initial conditions of the soil specimen. Volume change tests under suction control can be categorised into two main types: the
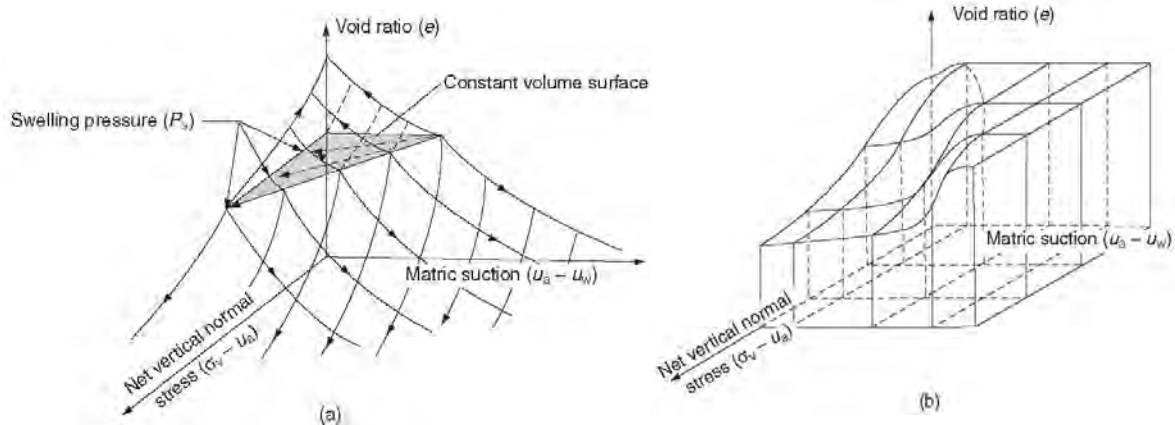
Figure 2.9.: Three dimensional constitutive surfaces of unsaturated soil:(a) Stable structured (i.e. swell) and (b) Metastable structured (i.e. collapse) (Fredlund, 1996).

constant net vertical stress-suction controlled test and the constant suction-net vertical stress controlled test. Due to the experimental tests schedule in this study, this section will focus on the literature review and general aspects of constant net vertical stress-suction controlled test.

The constant net vertical stress-suction controlled test can be conducted using Oedometer or triaxial-suction control cells. The stress path and the value of applied stress state variables $(\sigma - u_a)$ and $(u_a - u_w)$ depend on the value of initial suction and the initial conditions of the soil sample. There are two procedures that can be followed when using this test. First, the drying path occurs by increasing the suction value incrementally from initially low values (i.e. several kilopascals or near zero) to high values. This behaviour can be represented in nature by sunny, warm weather after heavy rain where the soil deposits transform from a partially or fully saturated state to an unsaturated state. Second, the wetting path occurs by decreasing the suction value incrementally from initially high values (e.g. several hundreds or thousands kilopascal) to low values. This behaviour of volume change can be observed in semi arid or arid regions when unsaturated soil deposits are inundated by heavy rain or by ground water fluctuations (i.e. collapse behaviour).

Tadepalli (1990); Tadepalli & Fredlund (1991); Tadepalli et al. (1992b) conducted collapse tests using an Oedometer specially designed with controlled matric suction. Their results indicated a unique relationship between the change in matric suction and the total volume change during collapse. Figure 2.10 shows that soil volume changes progressively as the matric suction decreases, and the volume change ceases when the matric suction drops to zero throughout the entire soil specimen.
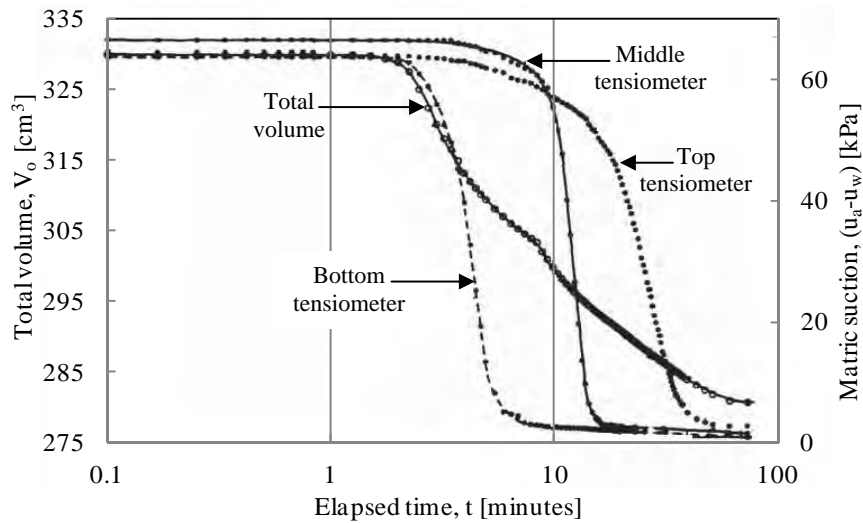
Figure 2.10.: Matric suction and total volume changes versus time during inundation of collapsible soil (Tadepalli & Fredlund, 1991).

Pererira & Fredlund (2000) suggested that collapsing soil shows three distinct phases of deformation during the wetting process as shown in Figure 2.11a (stress path of 100 kPa). These phases are:

-Pre-collapse phase: Collapse deformation in this phase commonly occurs at high matric suction ranges. Inconsiderable volumetric deformation and compressibility of collapsing soil occurs in correspondence to a relatively large decrease in matric suction. This behaviour can be attributed to the elastic compression of the soil structure caused by cementing and/or microforces via matric suction.

-Collapse phase: Collapse deformation in this phase commonly occurs at intermediate matric suction ranges. Considerable volumetric deformation and compressibility of collapsing soil occur as a result of a reduction in matric suction. This behaviour can be attributed to the combination of the rearrangement of soil structure resulting from severing cementing bonds as well as from the local shear behaviour between soil particles and soft cementing bonds. Moreover, the collapse settlement ends as soon as the soil structure reaches a new equilibrium under the new matric suction value.

-Post-collapse phase: Collapse deformation in this phase occurs at low matric suction ranges. Neither additional volumetric deformations nor negligible compressibility for the collapsing soil is observed corresponding to further reductions in matric suction. At this stage, the collapsing soil is fully saturated except for a limited number of trapped air bubbles. The small deformation associated with this phase can be attributed to secondary compression of the soil mass.
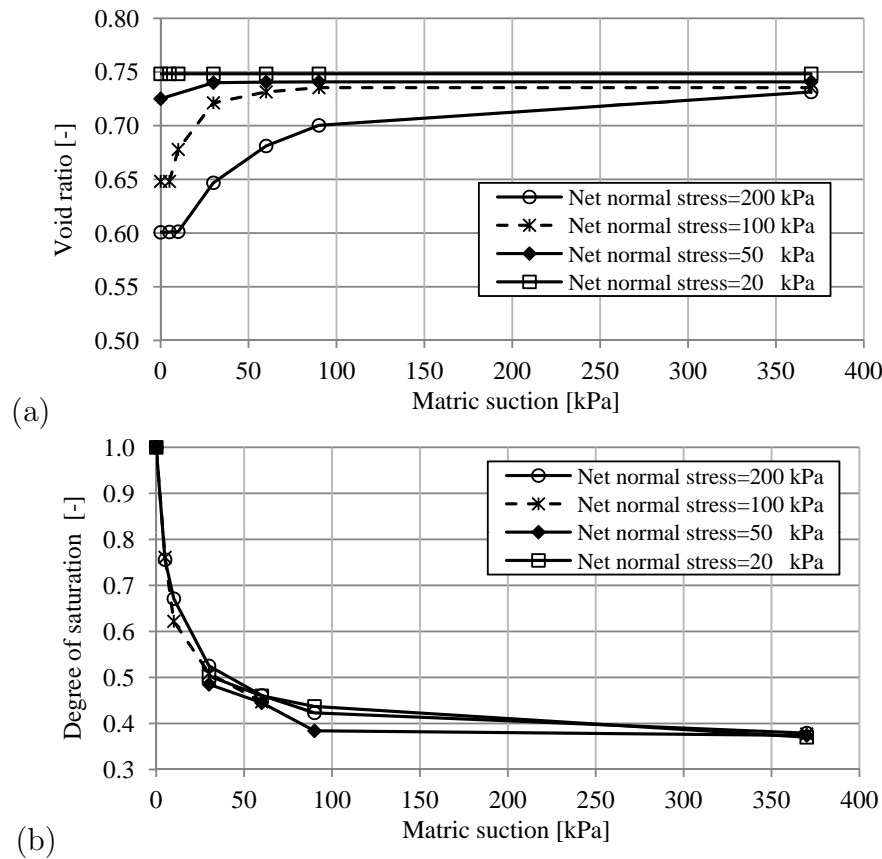
Figure 2.11.: Volume change behaviour for "Alka-Seltzer dam" collapse soil of (SM-ML, e_o=0.754 and w_o=10.5%) from Brazil (Pererira & Fredlund, 2000).

Pererira & Fredlund (2000) and Pereira et al. (2005) conducted further investigations on volume change behaviour of collapsible soils. They concluded that irrespective of the variation in collapses resulting from net vertical stress, the metastable soil structure seemedto show the same increases in degrees of saturation when the matric suction was reduced to zero (see Figure 2.11b). They also observed that the collapse potential of the soil sample is achieved before full saturation of the sample. In other words, the soil sample may be able to achieve total collapse at low porosity when full saturation is reached. The small increase in the degree of saturation causes low response to further decreases in matric suction.

On the other hand, Ng et al. (1998) observed that the collapse potential was a function of initial matric suction (i.e. initial moisture content). In other words, unsaturated soil with high initial suction tends to indicate larger amounts of collapse deformation than other soil with low initial suction compacted at the same range of relative compaction (see Figure 2.12).
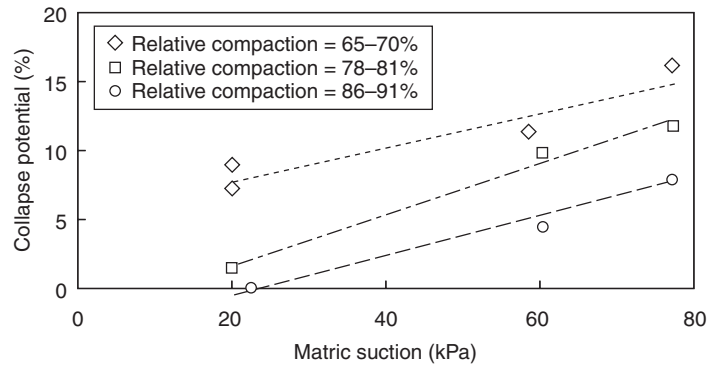
Figure 2.12.: Collapse potential relationships with initial matric suction (Ng et al., 1998).

Houston et al. (2001) studied the effect of full and partial wetting processes on the volume change behaviour of typical silty collapsible soil. They explained how the conventional Oedometer-collapse test procedure provides the soil with free access to water, resulting in full wetting, while partial wetting of unsaturated soil deposits in the field occur gradually by downward infiltration or ground water fluctuation, especially in arid or semi-arid regions. Therefore, full collapse potential would not be expected in partially wetted layers (see Figure 2.13).

Aziz et al. (2006) investigated the volume change behaviour of unsaturated residual soil under suction and net vertical stress control. The results show that there is an apparent unique relationship between the void ratio, matric suction and net stress. This relationship can be observed when collapse deformation occurs as a result of a reduction in matric suction under constant net vertical stress. Furthermore, when the matric suction is reduced, a reduction in the void ratio is observed due to the damaging of capillary forces.
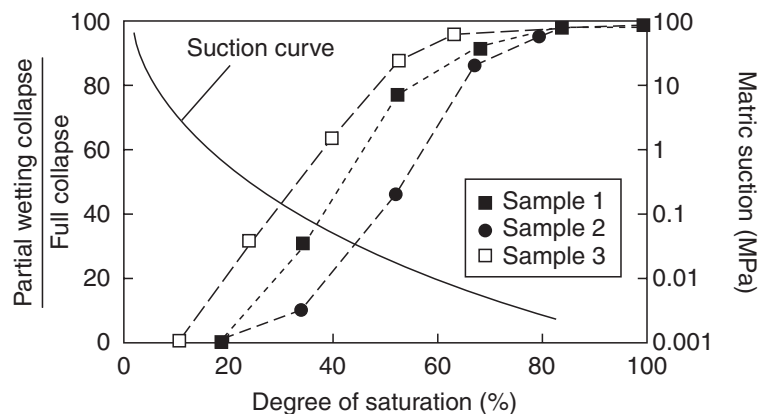
Figure 2.13.: Collapse due to partial wetting curves for silt soils (Houston et al., 2001).

Sun et al. (2007) studied volume changes and hydraulic characteristics of unsaturated collapsible soil called Pearl clay of LL=49%, PI=22% and Gs=2.71 using controlled-suction triaxial tests with varying initial dry densities and suction. They stated that the collapse volumetric strain is a function of the mean net vertical stress and the initial void ratio. Furthermore, they observed that a large collapse potential is achieved mainly in low suction ranges (i.e. 20-100 kPa). Pererira & Fredlund (2000) also observed the same behaviour.

Al-Badran (2011) investigated the volume change behaviour of a compacted mixture of 30% bentonite-70% sand and 100% bentonite under slurry and unsaturated loose conditions by using a suction-controlled Oedometer apparatus. The tests results demonstrated that wetting processes under constant net normal stress under initially loose conditions result in three different phases of collapse deformation after a reduction in suction (i.e. wetting process). He continued, by stating that the volume change is significantly influenced by the location of void ratios before the wetting process with respect to the saturated normal consolidation line (NCL) of the net vertical stress versus the void ratio relationship (see Figure 2.14).
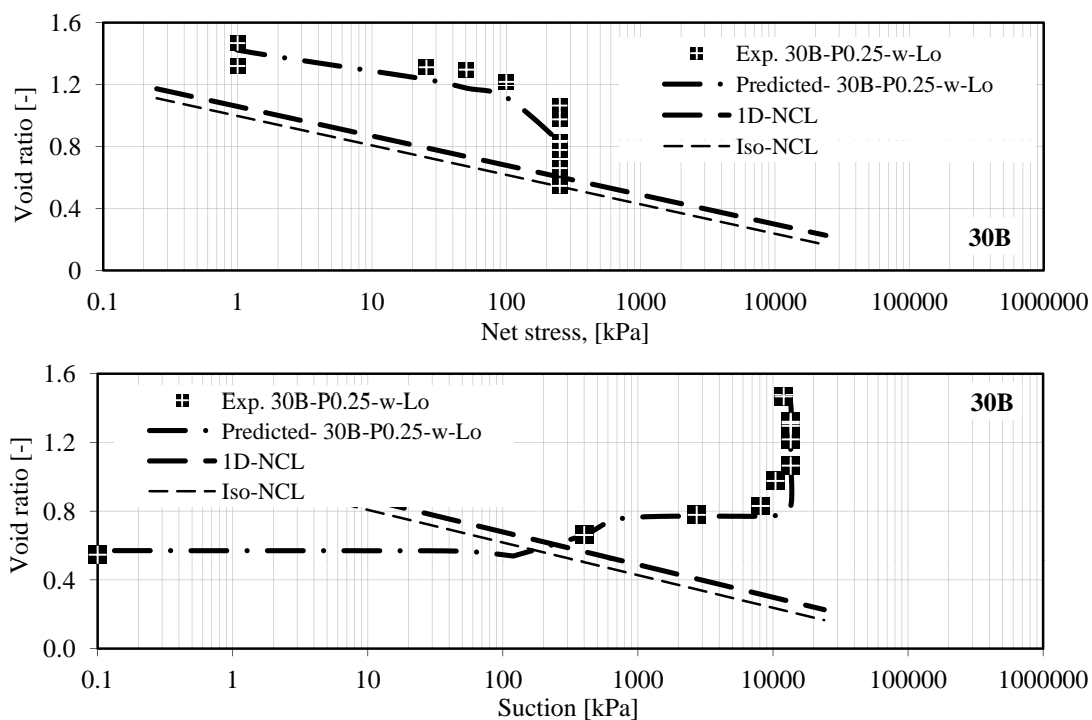
Figure 2.14.: Experimental and model predictions of suction control-wetting test under constant net stress=250 kPa for (30% bentonite-70% sand) soil (Al-Badran, 2011).

2.9. Measurements of soil suction

Measurements of soil suction are considered as a great challenge in geotechnical engineering practice especially when measuring low values of total suction.

Several devices and techniques recently proposed for measuring matric suction, osmotic suction and total suction. Agus (2005) and Fredlund et al. (2012) are summarised these techniques as listed in Table 2.3.

Table 2.3.: Devices for measuring soil suction and its components (Agus, 2005),(Fredlund et al., 2012).

Device name	Suction component	Range, kPa	Comments
Psychrometers (Peltier type)	Total	100 to≈ 8000	Constant temperature environment required
Filter paper	Direct matric,Indirect total	0-1500,2000-10000	May measure matric suction when in good contact with moist soil
Tensiometers	Negative pore-water pressures or matric suction when pore-air pressure is atmospheric	0-90	Difficulties with cavitations and air diffusion through ceramic cup
Null-type pressure plate(axis translation)	Matric	0-1500	Range of measurement is a function of the air-entry value of ceramic disk
Thermal conductivity sensors	Matric	10 to ≈ 1500	Indirect measurement using variable-pore-size ceramic sensor
Time domain Reflectometry(TDR)	Matric	Entire range	Indirect measurement
Pore fluid squeezer	Osmotic	Entire range	Used in conjunction with psychrometer or electrical conductivity measurement
Chilled-mirror hygrometer	Total	3000-300000	Depends on relative humidity measurement of the soil

Based on Table 2.3 it is clear that there is no unique technique or device which covers the entire range of suction measurements of unsaturated soils. Therefore, in order to measure wide range of suction, a combination of two or more techniques may be used. More details about the suction measurement techniques are discussed in several literatures such as: Fredlund & Rahardjo (1993); Agus (2005); Ng & Menzies (2007); Fredlund et al. (2012). The suction measurement techniques and equipment which is relevant to this study are briefly illustrated in appendix A.

2.10. Soil-Water Characteristics Curve (SWCC)

2.10.1. Introduction

To study and solve the air and water flow problem and to analyse seepage, shear strength and volume change behaviour involving unsaturated and saturated soils, the soil water characteristics curve (SWCC) is required. The SWCC illustrates the relationship between the mass and/or volume of water in a soil and the energy state of the water phase.

The SWCC can be simply defined as the relationship between the amount of water in a soil and soil suction (Fredlund & Rahardjo, 1993; Fredlund, 2000; Fredlund et al., 2012). Many studies have been carried out regarding the properties, measurement, analysis and application of the SWCC. They include research conducted by Fredlund & Xing (1994); Leong et al. (2004); Agus (2005); ASTMD6836 (2008); Vanapalli et al. (2008); Lins (2009); Al-Badran (2011); Fredlund et al. (2012).

2.10.2. Determination of SWCC: techniques and test procedure

In order to determine the SWCC, the amount of water in the soil sample with respect to the applied suction is required. The amount of water in the soil sample can be represented in different forms such as: gravimetric water content (recommended with small volume change specimens, e.g. sand), volumetric water content (recommended with large volume change specimens, e.g. clay), the degree of saturation and water volume.

A combination of two methods is utilised to determine the SWCC because there is no unique technique or device that can cover the entire range of unsaturated soil suction values.

Several types of equipment and test procedures have been used to determine the SWCC. The most common laboratory technique is the axis translation technique (ATT), which

utilises high-air-entry ceramic disks in a pressure plate device. This method can cover matric suctions reaching 1500 kPa (i.e. to the air-entry value of the ceramic disk). However, when a high range of suction is required, a controlled relative humidity environment (i.e. vapour equilibrium technique, or VET) is used to apply total suction. This technique provides a total suction up to more than 250,000 kPa depending on the type and concentration of salt used (Agus, 2005; Lins, 2009; Al-Badran, 2011; Fredlund et al., 2012).

In general, the SWCC consists of two main parts (i.e. the drying path and the wetting path). To determine the drying path, the applied suction is increased incrementally on the initially fully saturated sample under zero net vertical stress (i.e. unconfined, such as using the pressure plate apparatus), or under any specific net vertical stress (i.e. isotropic, or one-dimensional compression, such as using a Oedometer-suction controlled cell). The volume and the amount of water in the saturated sample are slightly decreased as the suction increases until the air-entry value suction is reached ψ_{aev} (i.e. the saturation zone). Then, as the suction increases, the volume and the amount of water significantly decrease along a drying path (i.e. transition zone) until the residual suction ψ_{res} is reached. After that, the increases in applied suction cause relatively no change in the volume or amount of water of the soil sample (i.e. the residual zone). Usually, the drying path is completed at oven-dried condition of the soil specimen.
The wetting path is a process in which the water content of the soil increases incrementally with a decrease in the applied suction on an initially oven-dried sample (Figure 2.15).

The SWCC results for unsaturated soils are normally plotted from a low suction value (e.g. 0.1 kPa) to the maximum value of 10^6 kPa (Croney & Coleman, 1961; Fredlund & Rahardjo, 1993; Fredlund et al., 2012).
Figure 2.15 shows the typical drying and wetting paths of the SWCC. From this figure, three stages of desaturation can be observed: the boundary effect stage, the transition stage (i.e. both primary and secondary) and the residual stage. The air-entry value separates the boundary effect stage and the transition stage. The soil type, mineralogy, stress histories, the initial state and the method of specimen preparation have a considerable effect on the datasets and behaviour of the SWCC. Moreover, to establish reliable analysis for the SWCC, best fit for the datasets is required (Fredlund & Xing, 1994; Fredlund et al., 2012).
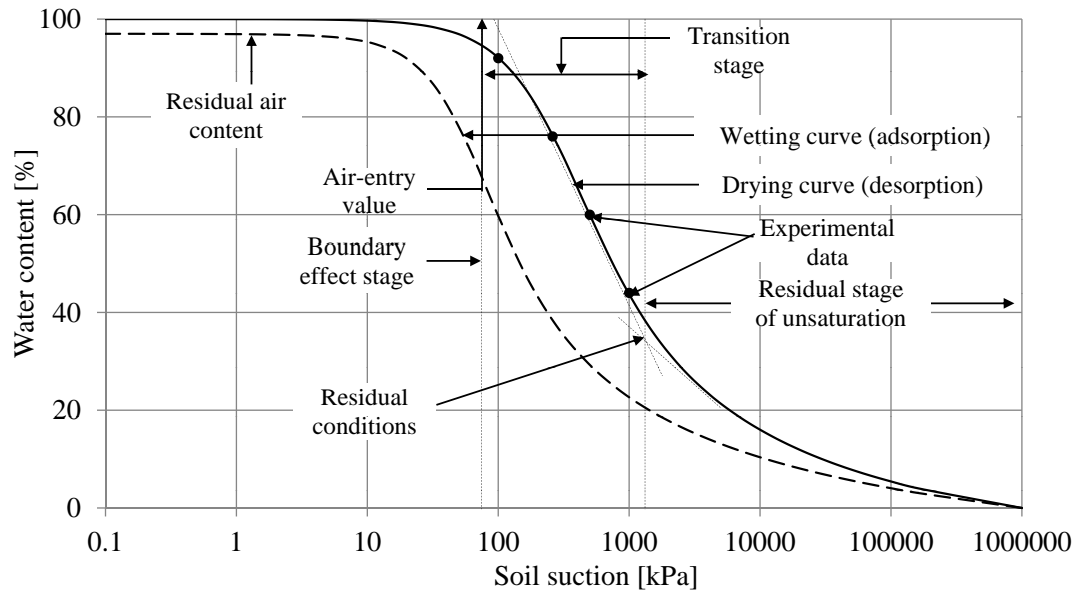
Figure 2.15.: Definition of variables associated with a typical SWCC (Fredlund et al., 2012).

2.10.3. Hysteresis in SWCC

Klausner (1991); Feng & Fredlund (1999); Pham et al. (2002, 2003, 2005); Tami et al. (2004) investigated hysteresis associated with the SWCC. These researchers concluded that the desorption (i.e. drying) and adsorption (i.e. wetting) curves of the SWCC are significantly different due to hysteresis.

The hysteresis loop denotes that there is no single or unique SWCC, and the wetting and drying paths are defined by extreme limits of the water content versus the soil suction relationship as shown in Figure 2.16 (Fredlund et al., 2012). Moreover, Fredlund et al. (2012) indicated that "there are an infinite number of intermediate drying and wetting scanning curves that bridge between the wetting and drying curves" (see Figure ??). Pham et al. (2002, 2003) used many data sets of different soil types reported in the literatures for theoretical analyzing of hysteresis phenomenon in SWCC. The data analysis shows that the amount of hysteresis can be primarily estimated from the difference in water content between the hysteresis loops at the inflection points.

Hysteresis (i.e. the distance between the drying and wetting curves) also differs depending on the soil type. Moreover, the results indicate that the bounding drying curve and the bounding wetting curve seem to be parallel on a semilog diagram. This finding corroborates the simplified model proposed by Feng & Fredlund (1999).
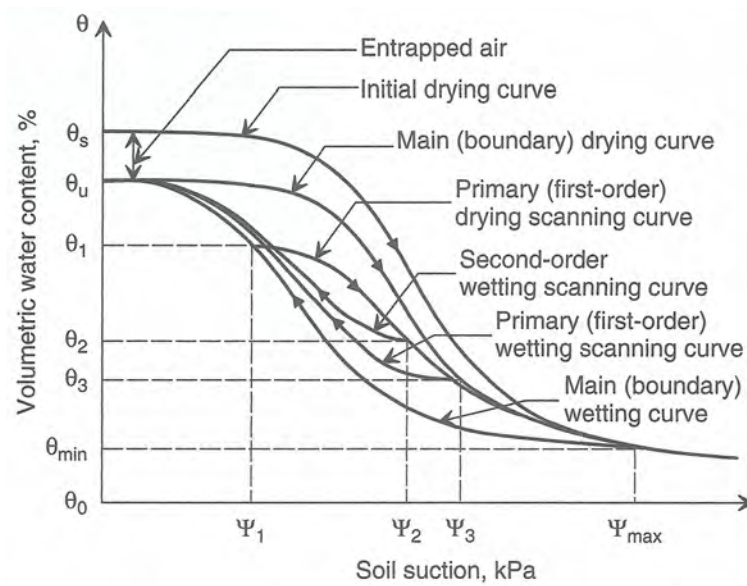
Figure 2.16.: Bounding and scanning curves used to define the drying and wetting of unsaturated soil (Pham et al., 2003).

2.11. Permeability coefficient of unsaturated soils

In saturated soil, the permeability coefficient of soil samples can be determined by direct experimental measurements (i.e. the constant head test or the falling head test) using Darcy's low to analyse the flow through the soil media as follows:

$$k = \frac{q}{iA} \tag{2.11}$$

where: $k=$ the permeability coefficient for saturated soil, $q =$ the flow rate, $A=$ the cross-sectional area of the specimen normal to the direction of flow, i= hydraulic gradient.

In unsaturated soil, determining the permeability coefficient is quite difficult and time consuming. Brooks & Corey (1964); Van Genuchten (1980); Fredlund & Xing (1994); Leong & Rahardjo (1997) proposed statistical models for geotechnical engineering applications. In this section the model devised by Brooks & Corey (1964) is presented as one of the earliest approaches for modelling the SWCC.

Brooks & Corey (1964) proposed an empirical model to estimate the permeability coefficient based on the SWCC of the soil. The model parameters are defined in Figure 2.17, and the empirical model consists of two parts:

-The permeability below the air-entry value of the soil is equal to the saturated coefficient

of permeability:

$$k_w = k \quad for \quad u_a - u_w \leqslant (u_a - u_w)_b \tag{2.12}$$

-The permeability above the air-entry value of the soil: the Brooks & Corey (1964) model can be written as:

$$k_w = k \left\{ \frac{(u_a - u_w)_b}{(u_a - u_w)} \right\}^{2+3\lambda} \quad for \quad u_a - u_w > (u_a - u_w)_b \tag{2.13}$$

where: k_w = unsaturated coefficient of permeability, k = saturated coefficient of permeability, $(u_a - u_w)$ = matric suction, $(u_a - u_w)_b$ = air-entry value, λ = pore-size distribution index defined as the negative slope of the effective degree of saturation and equal to:

$$\lambda = \left[\frac{\Delta log S_e}{\Delta log(u_a - u_w)} \right], s_e = \left[\frac{\Delta S - S_r}{1 - S_r} \right]$$

where: s_e= effective degree of saturation and s_r= residual degree of saturation.
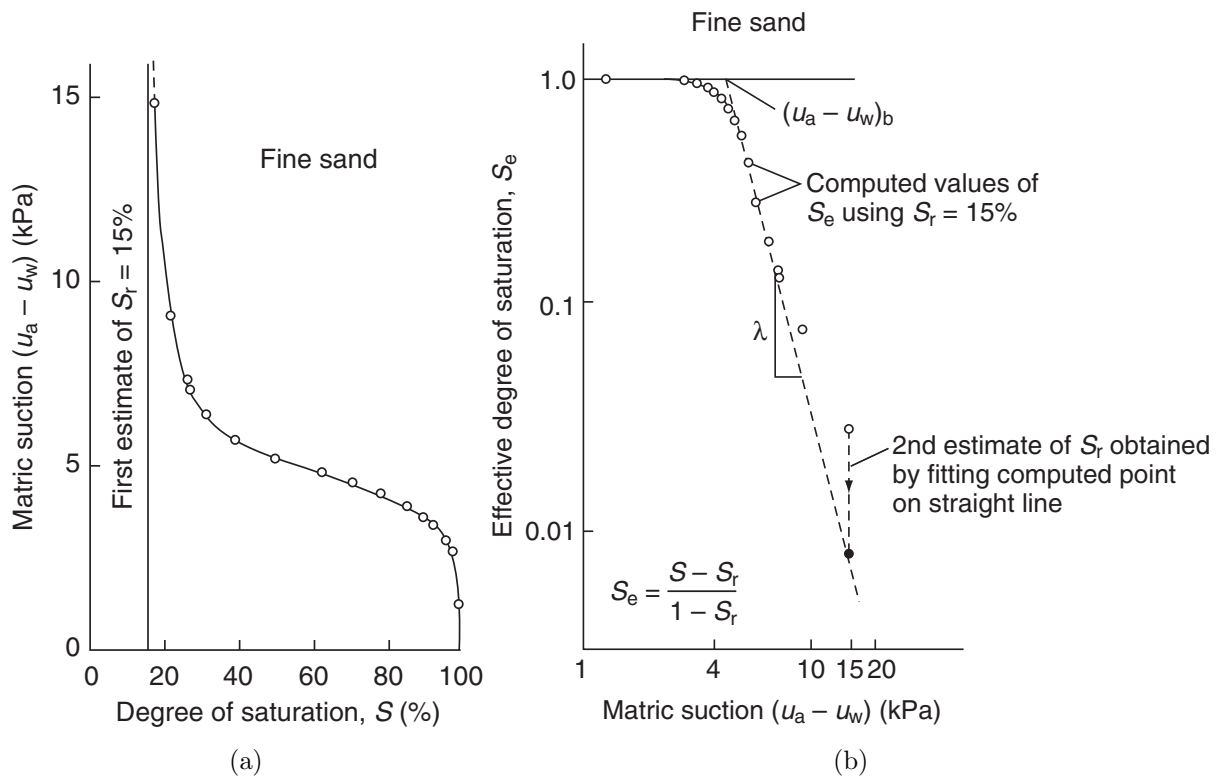
Figure 2.17.: Permeability coefficient parameters for unsaturated soil (Brooks & Corey (1964) as cited in Ng & Menzies (2007)).

2.12. Stabilization and improvement

Many attempts have been made to improve the geotechnical properties of collapsible soils, and several researchers have been searching for the most suitable methods to stabilise soil.

Terzaghi et al. (1996) defined ground improvement as follows: It includes "any procedures undertaken to increase the strength, decrease the permeability or compressibility, or otherwise render the physical properties of soil more suitable for engineering use. The improvement is accomplished in most instances by drainage, compaction or preloading". They added that "the most suitable depends principally on the type of soil to be improved and on whether the soil is being placed as a fill or is to be treated in its present location".

Das (1984) showed that the improvement of soil is usually carried out to accomplish any of the following goals:

-Reduce the settlement of structures

-Improve the shear strength of soil and thus increase the bearing capacity of shallow foundations

-Prevent possible slope failure of embankments and earth dams and

-Reduce the shrinkage and swelling characteristics of soils.

Houston et al. (2001) pointed out that there are different types of improvement techniques, and choosing the most appropriate one depends on the following factors:

-When a collapsibility problem is discovered in the soil, whether during investigation, construction or after the construction

-The type of applied stress, whether it is an overburden or a structural load

-The depth of improvement, usually depending on the depth of the collapsible soil layer

-The sources of wetting and

-Mitigation costs.

Soil stabilisation and property improvement were summarised and described by several authors such as:Clemence & Finbarr (1981); Bowles (1984); Rollins & Rogers (1994); Lefebvre (1995); Terzaghi et al. (1996); Pengelly et al. (1997); Houston et al. (2001); Al-Obaidi (2003); Jefferson et al. (2005); Rollings & Kim (2011).

Houston et al. (2001); Jefferson et al. (2005) provided an overview of the most frequent improvement techniques that can be used to treat collapsible soils and reduce/remove its collapse potential. Jefferson & Rogers (2012) outlined these techniques as shown in Table 2.4.

Table 2.4.: Methods of treating collapsible loess ground (Jefferson et al., 2005) and as cited in (Jefferson & Rogers, 2012).

Depth (m)	Treatment method	Comments
0-1.5	Surface compaction via vibratory rollers, light tampers	Economical., but requires careful site control, e.g. limits on water content
	Pre-wetting(inundation)	Can effectively treat thicker deposits but needs large volumes of water and time
	Vibrofloatation	Needs careful site control
1.5-10	Vibrocompaction (stone columns, concrete columns, encased stone columns)	Cheaper than conventional piles but requires careful site control and assessment. If uncased, stone columns may fail with loss of lateral support on collapse
	Dynamic compaction; rapid impact compaction	Simple and easily understood but requires care with water content and vibrations produced
	Explosions	Safety issues need to be addressed
	Compaction pile	Needs careful site control
	Grouting	Flexible but may adversely affect the environment
	Ponding/inundation/pre-wetting	Difficult to control effective of compression produced
	Soil mixing lime/cement	Convenient and gains strength with time. Various environmental and safety aspects, and the chemical controls on reactions need to be assessed
	Heat treatment	Expensive
	Chemical methods	Flexible; relatively expensive
> 10	As for 1.5-10 m, some techniques may have a limited effect	(See above)
	Pile foundations	High bearing capacity but expensive

However, Grigoryan (1997) reported that the bearing capacity of piles installed in collapsible soils can be lost and excessive settlements can be recorded due to the effect of

negative skin friction that occurs immediately after wetting. In addition, the presence of a collapsible layer may adversely affect the performance of piles during the life of a building.(Bally, 1988; Popescu, 1992; Chen et al., 2008; Kakoli, 2011) provided further details on the general behaviour of piles in collapsible soils.

Many experimental studies in Iraq illustrated how collapsible soil, especially gypseous soil, has been successfully treated, and the collapse potential has been reduced to an acceptable amount. Most of these studies have assessed the effects of chemicals, oil derivatives and fine materials as additives to gypseous soil using the re-compaction method. Such studies include Seleam (1988)(Kerosene; Gas oil); Al-Busoda (1999)(Calcium chloride); Al-Abdullah et al. (2000)(Bentonite); Hassan (2000) (Emulsified asphalt); Al-Obaidi (2003) (Powder of glass sand; Powder of ceramic); Fattah et al. (2012) (Dynamic compaction) and Karim et al. (2012).

2.13. Summary

Collapsible soils are considered to be problematic soils that are directly affected by the wetting process regardless of the water source. The main property of collapsible soils is a metastable structure along with a high void ratio and low density. Moreover, these soils show a major collapse potential and a significant reduction in compressibility and shear resistance upon the wetting process and the leaching phenomenon.

The reduction in the volume of the soil mass results from the destruction of the cementation bonds, as in case of gypseous soil, and due to the softening and rearrangement of the soil fabric to a denser state, as in case of loess soil. The common procedure for measuring the collapse potential is using single step wetting (i.e. single and double-Oedometer collapse tests). In nature, the single step wetting process may not occur. Therefore the incremental wetting procedure under constant net vertical stress-suction controlled tests is more satisfy with field conditions.

Furthermore, to investigate and solve the flow problem in unsaturated soils, the relationship between the amount of water in a soil and soil suction in terms of the soil water characteristics curve (SWCC) is required. To cover the entire suction range of soil, a combination of two techniques should be used to determine the SWCC.

Several treatment techniques have been proposed to improve collapsible soil behaviour, such as layer recompaction, grouting, chemical additives, prewetting and the use of deep piles.

However, based on the literature review, there is still a lack of knowledge and open ques-

tions concerning the behaviour of collapsible soils. In the following chapters, this study addresses the following research questions:

-What is the effect of wide range variation in suction on the collapse potential of collapsible soils, especially natural and artificial gypseous soil?

-What is the hydro-mechanical behaviour of collapsible soils, especially in terms of the SWCC and the unsaturated coefficient of permeability?

-How do the mineralogy, microstructure and collapsibility of unsaturated soil mass during multi-steps wetting-suction degreases and leaching states?

-How do the distribution of the water content and the variation in suction behave, and where is the critical collapse zone in a large-scale soil sample?

-Which factors affect the selection of suitable soil improvements techniques?

3. Material characterization and experimental program

3.1. Introduction

This chapter covers the site investigation, types of the selected soil samples which are used in this research and their basic characteristics. The physical and chemical properties of the selected soils are summarized in order to provide an overview of their specifications and for better understanding when analyze and discuss of the advanced tests results. The detailed description of the experimental program is also included. The initial conditions of soil samples and the stress paths that were followed for the advance tests are also an aim for this chapter.

3.2. Site investigation and soil used

In order to enable a good understanding for the behaviour of the collapsible soils, three types of these soils were used in the experimental program of this work. Two of these soils are samples of natural occurrences, e.g. Gypseous soil (GI) and Loess soil (LG). The third sample is mixture of the 70% artificial gypsum-30% Silber sand (70G30S).

3.2.1. Gypseous soil (GI)

According to the map of gypseous soil distribution in the world reported by the United Nations, Food and Agriculture Organization (FAO, 1990) as shown in Figure 2.1,the major areas of gypseous soils in the Middle East can be found in Iraq. However, large parts of Iraqi areas are covered with gypseous soil especially west, northwest and southwest regions. According to the exploratory soil map of Iraq reported by Buringh (1960) as shown in

Figure 3.1, and regarding to the geotechnical studies carried out by Seleam (1988); Al-Obaidi (2003); Al-Sharrad (2003); Al-Kaabi (2007), a highly gypseous soil deposits can be found near Al-Ramadi city in Al-Anbar governorate. This region is mixed gypsiferous desert land with gypsum content of more than 60% as mentioned in the legend no.17 of Figure 3.1.
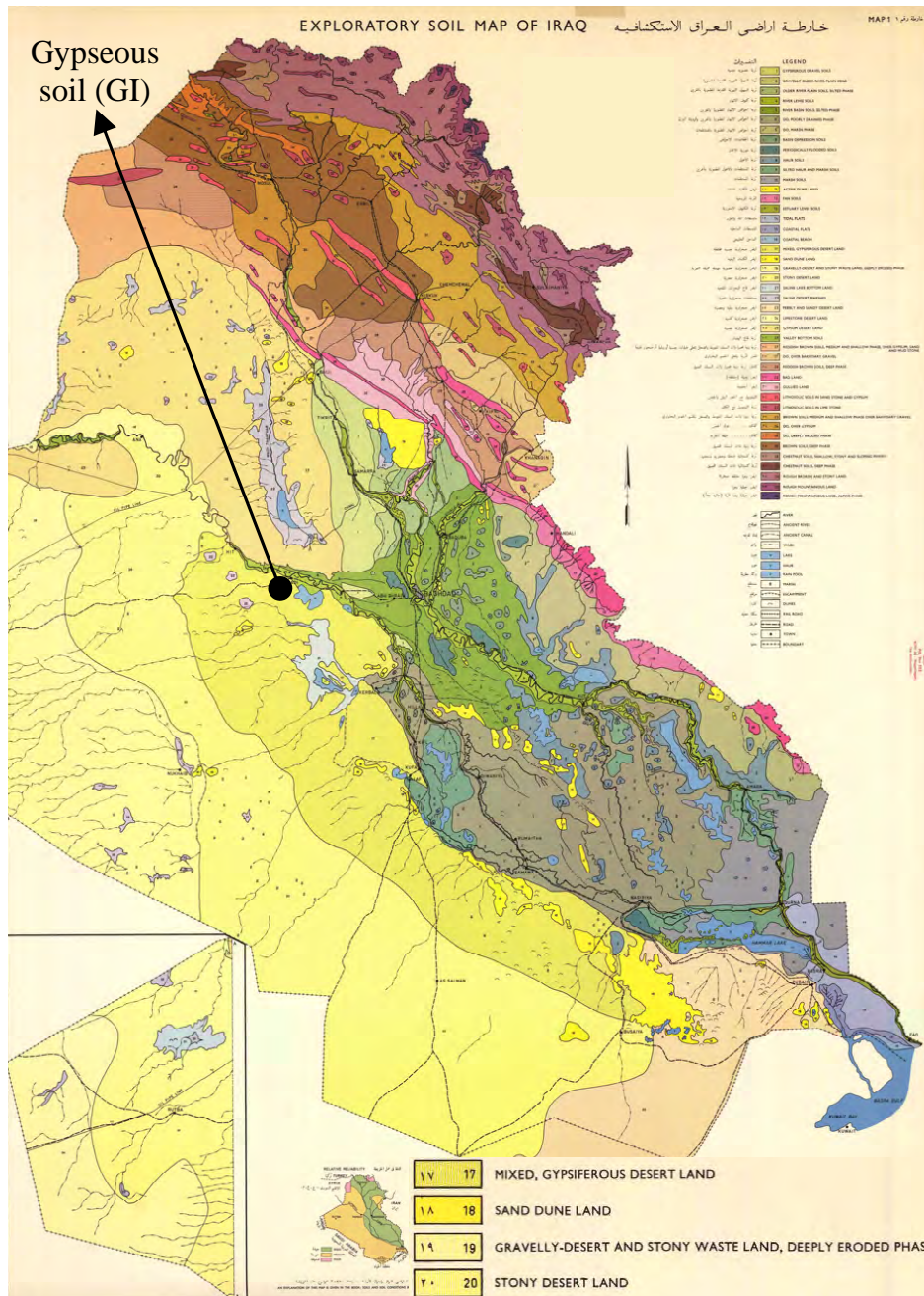
Figure 3.1.: Exploratory soil map of Iraq reported by Buringh and published by Ministry of Agriculture, Baghdad, Iraq 1957.

Moreover, it is considered as a semi arid to arid region with very high temperature and low rains in all seasons. The investigated site is chosen in the west of Euphrates River, six kilometers northwest of Al-Ramadi city especially close to Al-Anbar University (i.e. 33° N, 43° E; 135 km west of Baghdad). The reasons for selecting this site are due to the observation of cracks in many buildings which have been constructed on highly gypseous soils layers, and because of the perceived risk for the possibility of formation the caverns under the foundation of these building as a result of the leaching process of gypsum by ground water fluctuation, surface water percolation and broken of sewage water pipes.

As a general description of the soil layer, it consists of medium to stiff, light to reddish brown sitly sand with high gypsum content. The investigated depth is 1 m below the natural ground surface. The ground water table is at depth of more than 1.5 m from the natural surface. It is worth mentioned that the gypsum is encountered in the form of agglomerations and sometimes in the form of crystals or white particles. Also gypsum is observed as bonding material among the soil particles.

Field measurements found that the investigated soil layer has a low density with very low moisture content which could reach to zero. Due the difficulties in obtaining undisturbed soil samples, disturbed soil samples are extracted then packed in double nylon bags and transported to the soil and rocks laboratory of the Ruhr Universität Bochum, Germany, for testing.

The symbol GI will be used in this research when referring to gypseous soil, where: G referring to gypseous and I referring to Iraq.

3.2.2. Loess soil (LG)

According to the loess soil distribution map in the world reported by Pecsi (1990) and cited in Smalley et al. (2011) (Figure 2.3), and the loess soil distribution map in Europe reported by Haase et al. (2007), in addition to the geotechnical investigation carried out by Wagner (2011), it is obviously noted that large parts of Germany consist of loess deposits of thickness ranging between 2 to 20 m. Moreover, according to soil/rock distribution map of Germany (i.e. BAG5000, 2008BGR) in Figure 3.2 and based on the estimations of the soil information system (i.e. 1:1.000.000, BÜK 1000 Vers. 1.0, Digitales Archiv FISBo BGR) published by Federal Institute for Geosciences and Natural Resources (BGR) in Germany, the loess soil covers an area of about 56.000 Km^2 representing 15.5% of the total area of Germany.

Saxony region including the city of Dresden (selected site) contains wide area of loess soil and is considered as a non-arid region with low temperature and high rains in all seasons.
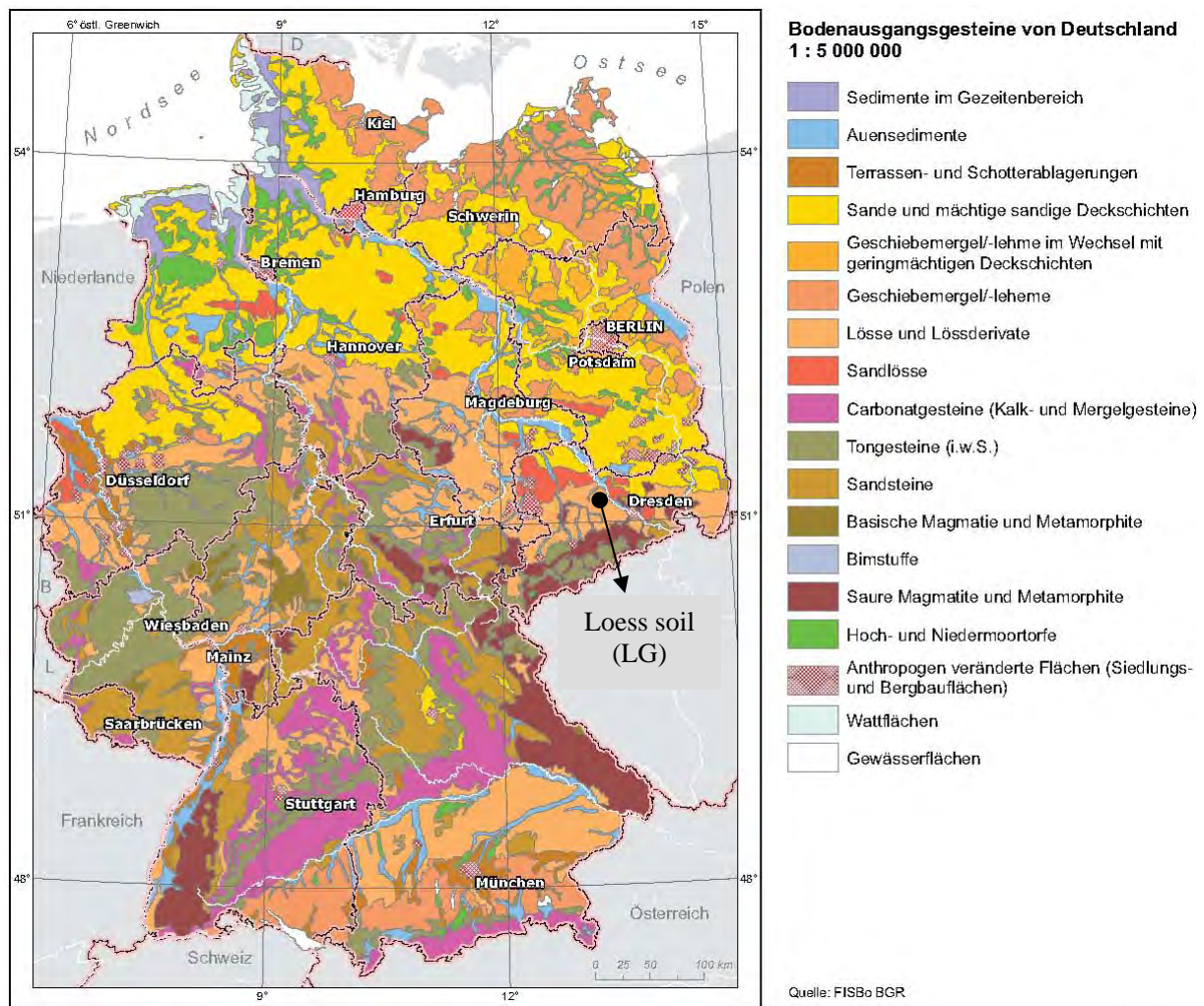
Figure 3.2.: Soil/Rock distribution map of Germany, (all rights reserved to Federal Institute for Geosciences and Natural Resources (BGR, 2008) in Germany).

The investigated site is chosen in the northwest of Dresden city especially close to 01623 Leuben-Schleinitz, OT Graupzip, Ziegelwerk Huber (i.e. 51° N, 13° E; 225 km south of Berlin).

This site has been selected due to the rich information available about the presence of loess soil in site area, in addition to some industrial factories located there where the collapse deformation of loess soil represents a big challenge.

This soil layer consists of medium to stiff, dark to reddish brown clayey Silt soil with organic materials appear as black spots with some roots of plant. The ground water table is located at less than 1.0 m from the natural ground surface.

Disturbed and undisturbed soil samples are extracted from 0.5 m depth below the ground

surface. Then, the samples are packed in double nylon bags and transported to the soil and rocks laboratory of the Ruhr Universität Bochum, Germany for testing.

Field measurements found that the soil layer has a high density with high moisture content that could reach up to 20%. The symbol LG will be used in this research to refer to Loess soil, where: L referring to loess and G referring to Germany.

3.2.3. Artificial gypsum-Silber sand mixture (70G30S)

The mixture of the 70% artificial gypsum-30% Silber sand 70G30S is used in order to investigate the difference in the geotechnical behaviour between the naturally and artificially occurrence of gypsum as a cementing material within soil structure.

Artificially pure gypsum $CaSO_4.2H_2O$ (produced by Alfa Aesar GmbHCo.KGA Johanson Matthey Company, Germany) of 70% dry weight is added to 30% dry weight of Silber sand passing sieve size of 1.0 mm. The two materials were carefully mixed at dry state.

In this research, recompacted soil samples were used for all the tests. Dry density was varied regarding to the initial conditions and stress path and the moisture content was the hygroscopic value.

3.3. Basic characteristics of the investigated soils

The basic characteristics of the investigated soils include the determination of the physical properties, chemical and elementary characteristics (ESEM-EDX) analysis.

3.3.1. Physical properties

Physical properties like water content, specific gravity, particle size distribution, Atterberg's limits (liquid limit and plastic limit), field density, relative density and compaction properties were investigated.

The summary of physical tests results is shown in Table 3.1. The following sections discuss their determination techniques.

Table 3.1.: Summary of physical soil properties

Property	Gypseous soil	Loess soil	Mixed soil	Silber sand
Natural water content (%)	0.25	20	-	-
Hygroscopic water content (%)	0.25	2.5	0.25	-
Atterberg's limits				
LL(%)	-	28.2	-	-
PL(%)	-	16.8	-	-
PI(%)	-	11.4	-	-
Specific gravity(Gs)				
With water	2.37	2.63	2.41	2.65
With kerosene	2.35	-	2.4	-
In place dry density(g/cm^3)	1.3	1.6	-	-
Standard compaction test				
Maximum dry density(g/cm^3)	1.7	1.74	1.69	1.58
Optimum water content(%)	8.0	16.4	12.85	17.8
Relative density(%)	82	-	-	-
$e_{max.}(-)$	1.28	-	-	0.901
$e_{min.}(-)$	0.69	-	-	0.556
$e_{field}(-)$	0.81	0.64	-	-
Particle size analysis				
(DIN18123-1996-with water)				
$d_{10}(mm)$	0.019	-	0.018	0.15
$d_{30}(mm)$	0.037	0.0085	0.032	0.18
$d_{60}(mm)$	0.22	0.035	0.35	0.3
$C_U(-)$	11.58	-	19.4	2.0
$C_C(-)$	0.33	-	0.16	0.72
Passing sieve (0.125mm) (dry, kerosene, water)(%)	33.3,39.3,43.3	97,-,99	21.6,43.2,74.1	3,-,-
Passing sieve (0.075mm) (dry, kerosene, water)(%)	18.1,22.1,33.2	90,-,98	7.4,35.5,71.8	-
Classification	clayey sandy SILT	clayey SILT	sandy clayey SILT	fine SAND
Gypsum content(%)	70	0	70	0

3.3.1.1. Water content

The water content was determined by oven drying according to method described in ASTMD2216 (2010) standard. In this study, a standard drying temperature of 105°C was used for LG soil, while a drying temperature of 45°C was used for both GI and 70G30S soils. The reason behind using drying temperature of 45°C is to reduce the degree of dehydration of gypsum in those materials containing calcium sulfate as $CaSO_4.2H_2O$ or to reduce decomposition in highly/fibrous organic soils. Porta (1998); Al-Mufty & Nashat (2000); Al-Obaidi (2003) and others recommended that the drying temperature of gypseous soil should not exceeded 40-50°C to avoid gypsum transformation. Hygroscopic water content was considered as the initial water content for all soil samples.

3.3.1.2. Specific gravity (Gs)

The specific gravity was determined according to method described in ASTMD854 (2010) standard. Distilled water is normally used for specific gravity determination, but Kerosene is recommended instead of distilled water when the soil specimens contain a significant fraction of organic matter or gypsum material (Head, 1980; Seleam, 1988; Al-Obaidi, 2003; ASTMD854, 2010).
In this study, distilled water was used for specific gravity determination of LG soil. For GI and 70G30S soils both of distilled water and Kerosene were separately used. No significant difference in the values of specific gravity was observed when using distilled water or Kerosene for both specimens.

3.3.1.3. Particle size analysis

Many researches in the literature indicate that there are considerable difficulties and significant challenges in the determination of particle size distribution and soil classification of gypseous soil when standard test methods are used. Actually there are two problems associated with the determination of the particle size distribution. The first is the gypsum being semi-soluble and dissolved in water when the soil is washed on sieve during the preparation for the hydrometer test. In the hydrometer test, after sieve washing, the rest part of gypsum might be dissolved during the test itself causing an error in the density of soil water mixture. Also the dissolved gypsum may acts as a flocculating agent around the silt and clay particles and causes rapid settlement (Hesse, 1976; Vieillefon, 1979; Seleam, 1988; Porta & Herrero, 1990; Poch, 1992; Al-Mufty, 1997; Porta, 1998). Therefore, when

the soil is rich with gypsum the hydrometer analysis becomes meaningless. However, when the soil contains low amount of gypsum (i.e.10%) or when gypsum grains are larger than 0.075 mm with high clay content, the problem arises from gypsum dissolution is decays and can be neglected (Al-Abdullah, 1995; Porta, 1998).

In many cases, treatment of soils is required before hydrometer analysis especially with those of high amount of gypsum content. One treatment method is to remove the gypsum before hydrometer analysis by washing the soil with distilled water or with other liquid (Taha, 1979; Al-Kashab, 1981; Rivers et al., 1982; Stern et al., 1989). The removal of gypsum leads to meaningless results and being unrelated to the actual physical behaviour of the soil as gypsum is an actual component of it (Porta, 1998). Some other types of treatments have been used such as treating the soil with hot dilute HCl (Nashat, 1990), blockage of gypsum dissolution which consisting of coating gypsum particles with a thin layer of $BaSO_4$ after treatment of the sample with $BaCl_2$, and increasing the amount of dispersing agent (Poch, 1992). In fact, any type of gypseous soil treatment may result in an over or under estimation for the grain size distribution. Therefore, Horta (1980) suggested that dry sieve analysis would be significant only at a level of 0.075 mm sieve.

In the present study, the particle size analysis for GI, 70G30S, LG and Silber sand soil were investigated according to DIN18123 (1996) and ASTMD422 (1963) standards. The results are shown in Figure 3.3 and summarized in Table 3.1.

For GI and 70G30S soils, the particle size analysis was carried out by using three methods: dry sieving, washing with water then sedimentation using hydrometer and washing with Kerosene. The test results showed that the finer percentage (i.e. passing sieve size 0.125 mm according to DIN18123 (1996) standard and passing sieve size 0.075 mm according to ASTMD422 (1963) standard) increases at washing. This is due to two reasons, the first is that the fine particles of gypsum (especially for GI soil) were originally coalesced and crystallized around the silt and clay particles, forming larger grains which cannot pass through a small sieve openings. The second is that the dry fine particles of gypsum (especially for 70G30S soil) try to close the opening size of sieves due to its high surface area. Furthermore, for both soils containing gypsum material and according to both standards, the finer percentage by washing with water was larger than the finer percentage by washing with Kerosene. This is because the gypsum particles are able to disintegrate, dissolve and suspend in water faster than their ability in Kerosene. On the other hand, non reliable hydrometer analysis is obtained because the high value of dissolved gypsum acts as a flocculating agent around the silt and clay particles causing rapid settlement, see Figures 3.3a, 3.3b and 3.4. For LG soil the standard particle size analysis was carried out without any problem, see Figure 3.3c and 3.4.

(a)

(b)

(c)
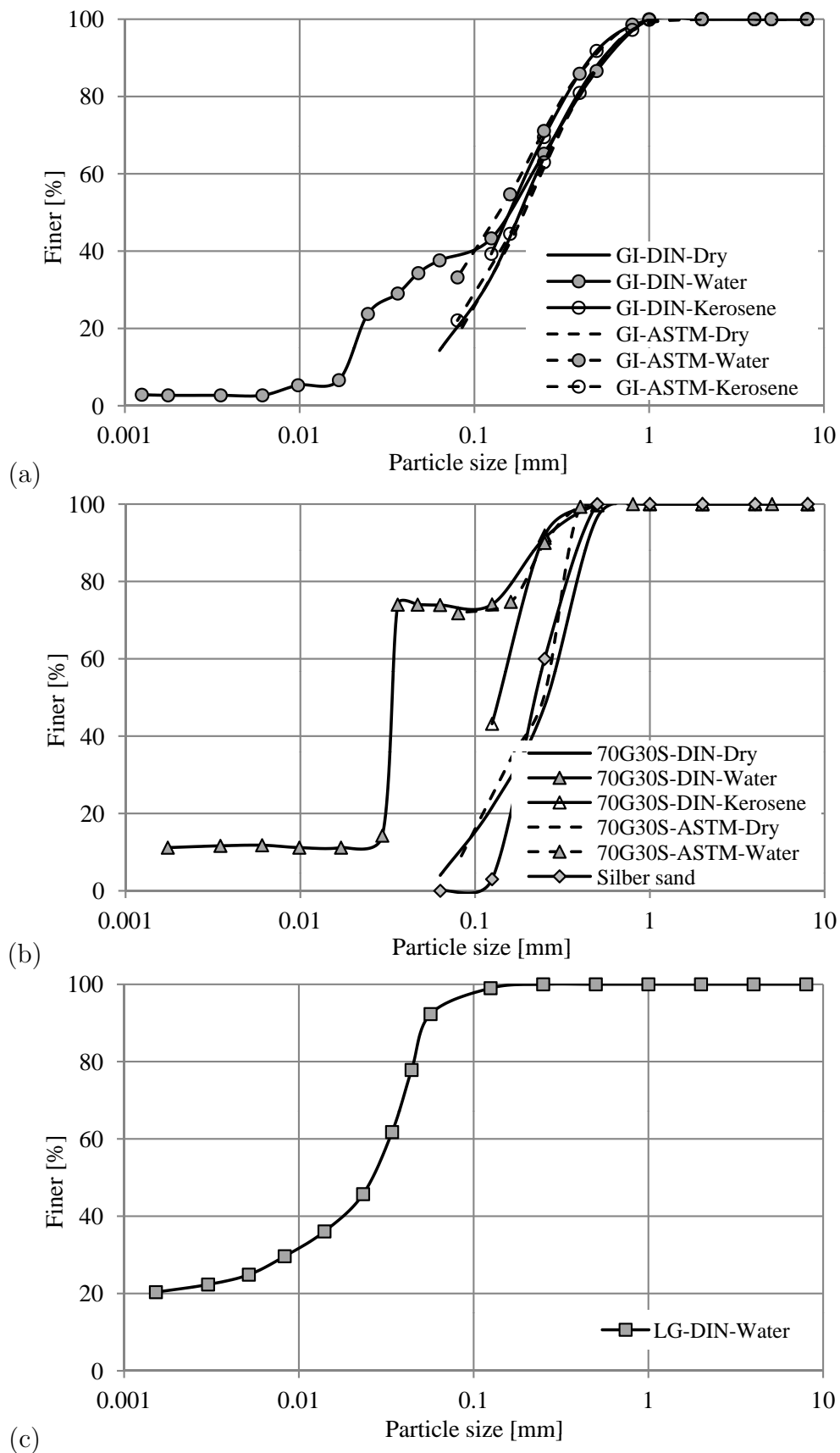
Figure 3.3.: Particle size distributions for: (a) GI, (b) 70G30S and (c) LG soils.
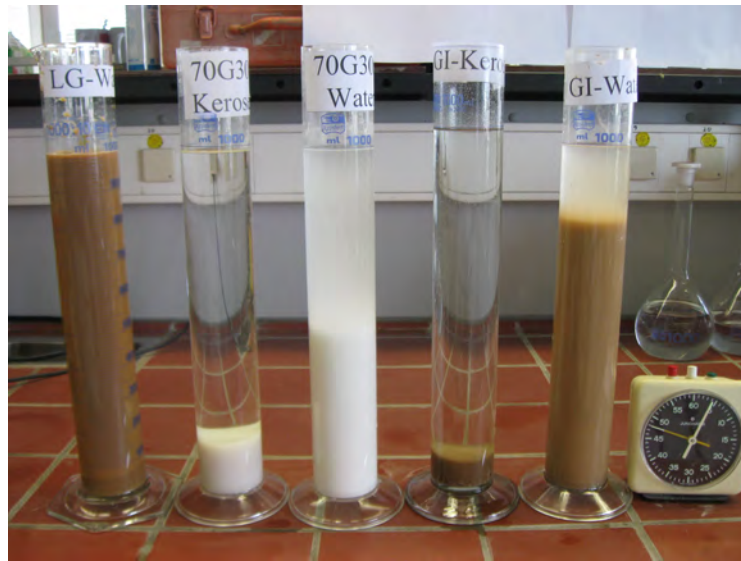
Figure 3.4.: Sedimentation of soil particles in water and Kerosene within four minutes after mixing.

3.3.1.4. Atterberg's limits (liquid limit and plastic limit)

The Atterberg's limits were determined according to the method described in ASTMD4318 (2010) standard. In this study, loess soil (LG) showed sufficient plastic behaviour, while non plastic behaviour is observed for both gypseous soil (GI) and mixed soil of artificial gypsum-Silber sand (70G30S), see Table 3.1. It is worth to mention that for highly gypseous soils, the Atterbergâs limits become insignificant or non-existent especially with low clay content. This is because as gypsum content increases the soil becomes friable and alkaline causing extreme changes in plasticity characteristics of soil

3.3.1.5. Density and compaction properties

Field density for both loess and gypseous soils were determined according to ASTMD2937 (2000) standard, while the relative density test was carried out on the gypseous soil sample according to DIN18126 (1996) standard. The standard compaction test for the three types of selected soil samples were carried out according to the Proctor method described in ASTMD1557 (2012) standard. The results of density and compaction properties are shown in Figure 3.5 and Table 3.1.
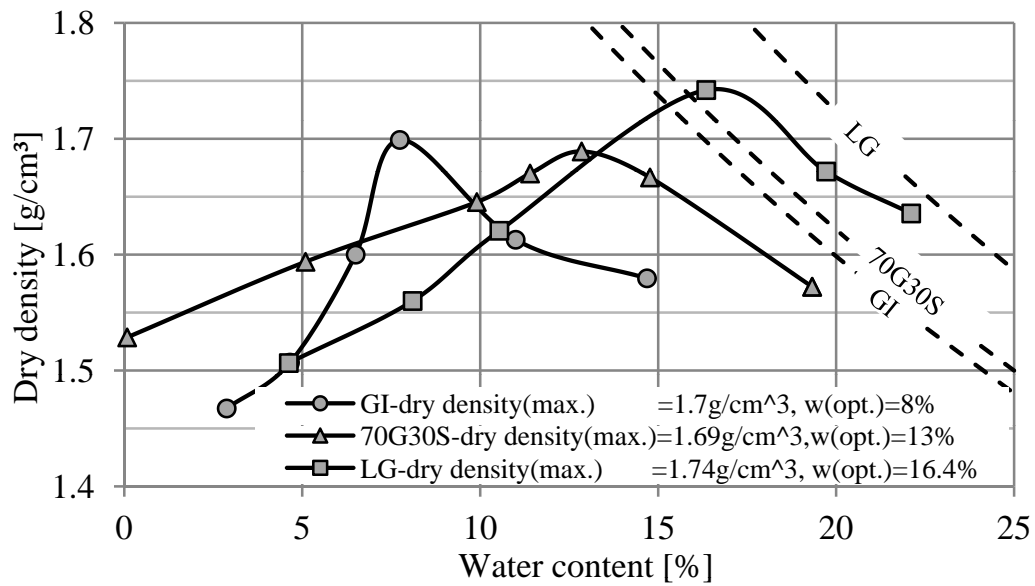
Figure 3.5.: Standard Proctor compaction curve for GI, 70G30S and LG soils.

3.3.2. Chemical and elementary characteristics

3.3.2.1. Chemical compositions

The chemical compositions analysis for gypseous soil (GI) and loess soil (LG) were carried out in the Chemical Department laboratory, Ruhr Universität Bochum, Germany as shown in Table 3.2. The data of chemical compositions for mixted soil of artificial gypsum-Silber sand 70G30S are obtained separately for pure gypsum $CaSO_4.2H_2O$ and Silber sand from the manufacturing companies provided these materials as shown in Table 3.3.

Table 3.2.: Chemical analysis for gypseous soil (GI) and loess soil (LG).

Soil type	Na (mg/l)	K (mg/l)	Mg (mg/l)	Ca (mg/l)	Cl (mg/l)	Nitrate (mg/l)	Sulfate (mg/l)	S (mg/l)
Gypseous	15.6	5.7	6.7	689	42.4	47.1	1780	20.3
Loess	14.3	1.6	3.3	17.2	0.2	< 0.1	5.9	0.02

Table 3.3.: Chemical analysis for Silber sand and Calcium sulfate.

Silber Sand[1]	SiO_2	Fe_2O_3	Al_2O_3	Ti_{O2}	Loss on Ignition
	99%	0.05%	0.3%	0.08%	0.2%
Calcium sulfate[2]	Assay	Iron	Fluoride	Solubility in water at 100°C	Loss on drying
	100.3%	< 100ppm	< 30ppm	2.22 (g/l)	20.6%

(1)Source: Quarzwerke GmbH in Frechen.www.Quazwerke.com
(2)Source: Alfa Aesar GmbHCo.KG A Johanson Matthey Company.www.alfa.com

3.3.2.2. Gypsum content determination

Gypsum in soil can be uniformly distributed, isolated in the soil structure or crystallized in different forms. The chemical composition of gypsum in soil is commonly in hydration form $CaSO_4.2H_2O$ when the temperature does not exceed 50°C. Several methods of gypsum identification and determination have been developed, each one with its own limitations. A simple review for most of these methods is given in Bower & Huss (1948); Hesse (1976); Porta et al. (1986); ISRIC (1987); Skarie et al. (1987); Abbas (1995); Porta (1998). The summary of the most important methods is:

1. Wet chemical method: In this method all the gypsum of the sample must be dissolved in water. Due to its low solubility in water 2.6 g/l at 25°C a low soil-water ratio will be required. When all the gypsum of the sample has been dissolved, it is possible to analyze SO_4^{-2} content or Ca^{+2} content to calculate the original amount of gypsum in the sample (Porta, 1998).

2. Thermogravimetric method: This method is based on the loss of weight as a result of heating the highly gypseous soil. The lost of weight is due to the dehydratation of gypsum (Poch, 1992). This method has been developed by Al-Mufty & Nashat (2000). They explained that gypsum content can be easily estimated by oven drying of the soil specimen at 45°C temperature until the specimen weight becomes constant, the weight is recorded. Then, the same specimen is dried at 105°C temperature and the weight is recorded again. The gypsum content can be calculated as follow:

$$\chi'(\%) = \left[\frac{W_{45^oC} - W_{105^oC}}{W_{45^oC}}\right] \times C \times 100 \qquad (3.1)$$

where: χ' = gypsum content(%), W_{45^oC} = weight of dried soil specimen at 45^oC, W_{105^oC} = weight of dried soil specimen at 105^oC and C= Constant,4.778.

It is important to mention that this method is deployed in this study for gypsum content determination, see Table 3.1.

3. X-ray diffraction techniques: This method can be used for qualitative identification of gypsum on oriented samples. Nevertheless, inaccurate gypsum content determination was obtained when using this method due to the preferred orientation of gypsum crystallites (Khan & Webster, 1968; Porta, 1975, 1998).

3.3.2.3. Elementary characteristics (ESEM-EDX) analysis

The environmental scanning electron microscopy (ESEM) analysis in combination with an energy dispersive X-ray analyzer (EDX), has been used to study the elementary characteristics and micro-fabrics of soils with gypsum, as well as for chemical analysis.
The energy dispersive X-ray analyzer (EDX) provides a quantification and identification of particular elements and their relative proportions. The specimen size is very small (i.e. less than 3 mm in diameter or as powder), therefore, the environment of the specimen can be varied through a range of pressure, temperature, gas composition, initial water content, initial suction and humidity (Herrero, 1987; Poch, 1992; Porta, 1998).
The ESEM-EDX analysis of the selected soil specimens were carried out in the Department of Analytical Chemistry and Center for Electrochemistry laboratory, Ruhr Universität Bochum, Germany. Environmental scanning electron microscope device type Quanta 3D FEG from FEI^{TM} was used as in Figure 3.6.
The soil specimens of gypseous soil (GI), mixed soil of artificial gypsum-Silber sand (70G30S) and loess soil (LG) were tested at initial dry density and at oven dry state. The ESEM-EDX analysis and the effect of inundation and leaching processes on the microstructure and fabric of the selected soils are given in chapter five and appendix C.
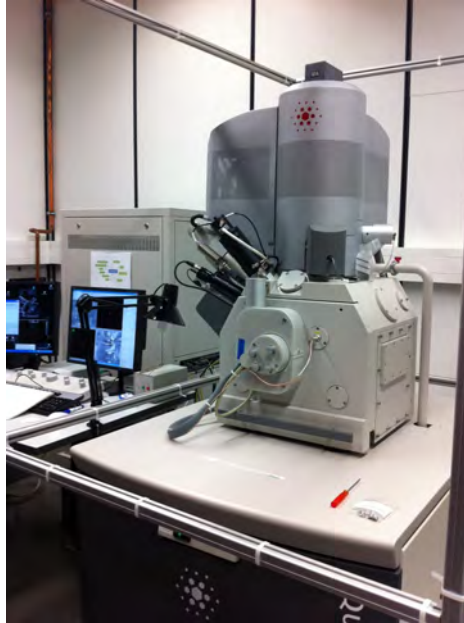
Figure 3.6.: ESEM-EDX analysis device type (Quanta 3D FEG) from FEI^{TM}.

3.4. Experimental program

In order to investigate the collapse behaviour of the three different unsaturated soils, the experimental program is divided into three main categories: (i) Basic characteristics, (ii) Volume change behaviour and (iii) Hydro-mechanical investigation. The summary of the experimental program is explained as a flow chart in Figure 3.7. Moreover, the detailed description of the experimental program is illustrated in following subsections:

3.4.1. Basic characteristics

The basic properties including the determination of physical, chemical and elementary characteristics of the studied soils were described in the section 3.3 above.

3.4.2. Volume change without suction control

3.4.2.1. Consolidation test

The one dimensional consolidation tests were carried out on the three selected soils according to method described in ASTMD2435 (1996) standard.
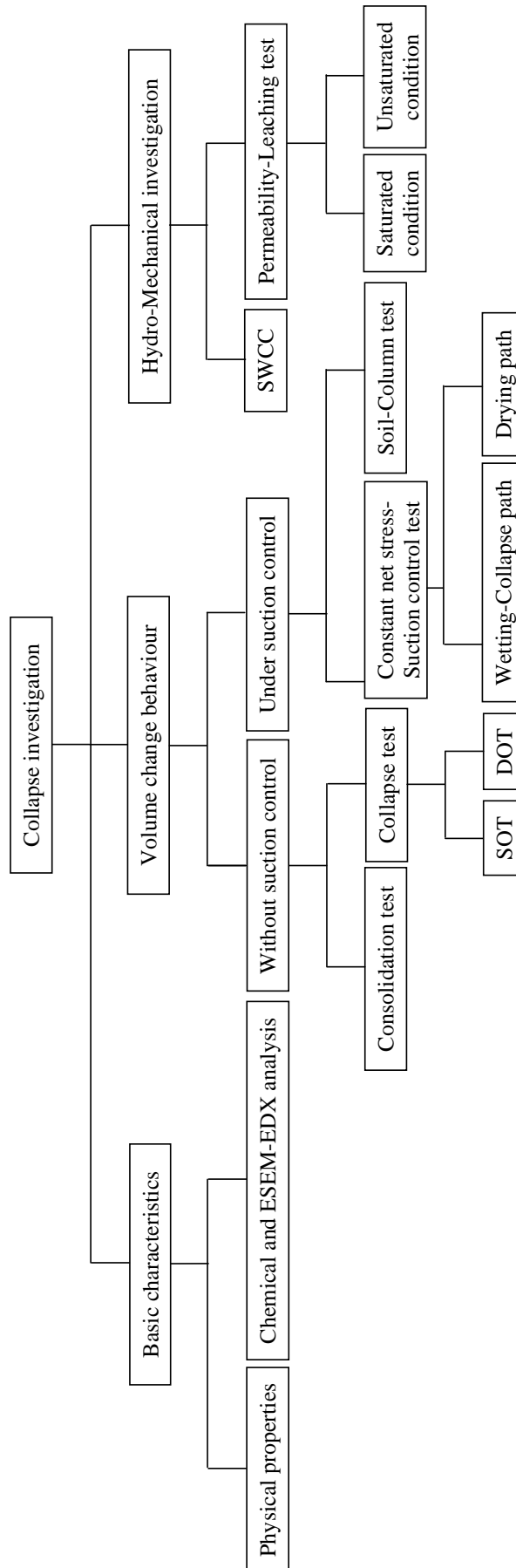
Figure 3.7.: Flow chart of the experimental program.

3.4.2.2. Collapse test

The collapse mechanism and collapse potential of gypseous soil, loess soil and mixed soil were investigated by carrying out a series of collapse tests using the conventional Oedometer device without suction control. Two methods were used to perform this test. The first is the single oedometer test method (SOT), using single step suction decrease (i.e. single step wetting). The collapse potential was determined under different boundary conditions like: value of wetting vertical stress, initial void ratio and initial degree of saturation. The second is the double Oedometer test method (DOT) using two identical soil specimens. The summary of volume change tests without suction control and specimenâs conditions are explained in Table 3.4.

3.4.3. Volume change under suction control

To investigate the volume change and collapse behaviour of unsaturated soils under suction control, a series of constant net stress-control suction (wetting and drying) tests have been carried out. To achieve the full range of entire soil suction, a combination of two techniques has been used. The first one is axis translation technique using UPC-Barcelona cell for suction ranging from zero to 1500 kPa. The second technique is vapor equilibrium technique using modified UPC-Isochoric cell with Oedometer frame for suction range of more than 2000 kPa. The pore water pressure-volumetric water content distribution and critical collapse zone were investigated by using soil-column testing device. However, it is worth mentioned that the experimental program concerning volume change of soil specimen under suction control is greatly restricted by soil type, time consuming to reach the equilibrium and the specifications of the device used.

3.4.3.1. Constant net vertical stress-suction decreases (wetting-collapse) test

Intensive experimental program of constant net stress with multi-step suction decrease (wetting-collapse) test (CNWT) were performed on the three types of unsaturated soils. The test specimen was recompacted in the cell ring at initial suction (i.e. unsaturated state). Each soil specimen was tested separately under a range of constant net stress with decreasing suction from initial value to zero (i.e. saturated state). The initial states for soil specimens and the stress paths for each test are shown in Tables 3.5 and 3.6 respectively.

3.4.3.2. Constant net stress-suction increases (drying) test

In order to investigate the volume change behaviour when the soil gradually transferred from saturated to unsaturated state, constant net stress with multi-step suction increase (drying) test (CNDT) have been done. One test was performed for each soil under constant net stress of 200 kPa. The initial states for soil specimens and the stress paths for each test are shown in Tables 3.5 and 3.7 respectively.

Table 3.4.: Summary of volume change tests without suction control.

Nr.	Soil type	$\gamma_{d-initial}$ [g/cm^3]	$w_{initial}$ [%]	$Sr_{initial}$ [%]	$e_{initial}$	wetting stress [kPa]
1	Gypseous	1.3	0.25	0	0.81	-
2	Gypseous	1.3	0.25	0	0.81	25
3	Gypseous	1.3	0.25	0	0.81	50
4	Gypseous	1.3	0.25	0	0.81	100
5	Gypseous	1.3	0.25	0	0.81	200
6	Gypseous	1.3	0.25	0	0.81	400
7	Gypseous	1.3	0.25	0	0.81	800
8	Gypseous	1.0	0.25	0	1.35	200
9	Gypseous	1.2	0.25	0	0.96	200
10	Gypseous	1.4	0.25	0	0.68	200
11	Gypseous	1.3	6.9	20	0.81	200
12	Gypseous	1.3	13.8	40	0.81	200
13	Gypseous	1.3	20.6	60	0.81	200
14	Gypseous	1.3	0.25	0	0.81	25-800
15	Mixed	1.3	0.25	0	0.85	-
16	Mixed	1.3	0.25	0	0.85	25
17	Mixed	1.3	0.25	0	0.85	50
18	Mixed	1.3	0.25	0	0.85	100
19	Mixed	1.3	0.25	0	0.85	200
20	Mixed	1.3	0.25	0	0.85	400
21	Mixed	1.3	0.25	0	0.85	800
22	Mixed	1.0	0.25	0	1.4	200
23	Mixed	1.2	0.25	0	1.0	200
24	Mixed	1.4	0.25	0	0.7	200
25	Mixed	1.3	6.7	20	0.85	200

26	Mixed	1.3	13.5	40	0.85	200
27	Mixed	1.3	20.3	60	0.85	200
28	Mixed	1.3	0.25	0	0.85	25-800
29	Loess	1.6	2.5	10	0.64	-
30	Loess	1.6	2.5	10	0.64	25
31	Loess	1.6	2.5	10	0.64	50
32	Loess	1.6	2.5	10	0.64	100
33	Loess	1.6	2.5	10	0.64	200
34	Loess	1.6	2.5	10	0.64	400
35	Loess	1.6	2.5	10	0.64	800
36	Loess	1.05	2.5	10	1.51	200
37	Loess	1.39	2.5	10	0.88	200
38	Loess	1.74	2.5	10	0.51	200
39	Loess	1.6	4.8	22	0.64	200
40	Loess	1.6	9.7	30	064	200
41	Loess	1.6	14.6	57	064	200
42	Loess	1.6	2.5	10	0.64	25-800

Table 3.5.: Summary of volume change tests under suction control.

Nr.	Soil type	$\gamma_{d-initial}$ [g/cm^3]	$w_{initial}$ [%]	$Sr_{initial}$ [%]	$e_{initial}$	Net stress [kPa]
1	Gypseous	1.3	0.25	0	0.81	50
2	Gypseous	1.3	0.25	0	0.81	100
3	Gypseous	1.3	0.25	0	0.81	200
4	Gypseous	1.3	0.25	0	0.81	400
5	Gypseous	1.3	0.25	0	0.81	800
6	Gypseous	1.3	34	100	0.81	200
7	Mixed	1.3	0.25	0	0.81	200
8	Mixed	1.3	34	100	0.81	200
9	Loess	1.6	2.5	10	0.64	50
10	Loess	1.6	2.5	10	0.64	100
11	Loess	1.6	2.5	10	0.64	200
12	Loess	1.6	2.5	10	0.64	400
13	Loess	1.6	2.5	10	0.64	800
14	Loess	1.6	24	100	0.64	200

Table 3.6.: Stress path of constant net stress-(wetting-collapse) test.

	Technique	VET**			ATT						
Net stress [kPa]	PWP[kPa]	0	0	0	10	10	10	10	10	10	10
	Suction[kPa]	58000	16500	6100	800	400	200	100	50	25	0
50	GI	√	√	√	√	√	√	-	√	-	√
	LG	√	√	√	√	√	√	-	√	-	√
100	GI	√	√	√	√	√	√	-	√	-	√
	LG	√	√	√	√	√	√	-	√	-	√
200	GI	√	√	√	√	√	√	-	√	-	√
	(70G30S)	√	√	√	√	√	√	-	√	-	√
	LG	√	√	√	√	√	√	-	√	-	√
400	GI	√	√	√	700*	√	√	-	√	-	√
	LG	√	√	√	√	√	√	-	√	-	√
800	GI	√	√	√	-*	-*	√	√	√	√	√
	LG	√	√	√	-*	-*	√	√	√	√	√

*Limitation of air pressure system. **Average value of vapour suction.*

Table 3.7.: Stress path of constant net stress-(drying) test.

	Technique	ATT					VET**		
Net stress [kPa]	PWP[kPa]	10	10	10	10	10	0	0	0
	Suction[kPa]	0	50	200	400	800	6100	16500	58000
200	GI	√	√	√	√	√	√	√	√
	(70G30S)	√	√	√	√	√	√	√	√
	LG	√	√	√	√	√	√	√	√

Average value of vapour suction.

3.4.3.3. Soil-Column test

Soil column testing device was used to perform the controlled matric suction-pore-water pressure-volumetric water content measurements for gypseous soil GI. The main goal of this test is to investigate the pore-water pressure-volumetric water content distribution and critical collapse zone through a big soil sample with volume size of more than 10000 cm^3. Moreover, the collapse deformation due to the wetting (i.e. suction decreases) is also recorded. The initial condition of the soil sample and the followed stress path is shown in Table 3.8.

Table 3.8.: Stress path and initial condition of soil-column test.

Stress path	Suction decreases-Wetting		
Pore-water pressure, [kPa]	10	10	10
Matric suction,[kPa]	20	10	0
Setting load, [kPa]	2.3		
Initial dry density, [g/cm^3]	1.1		
Initial void ratio, [-]	1.14		
Initial average volumetric water content, [%]	6.5		
Initial average suction, [kPa]*	-33.2		

Average measurements of three level Tensiometers.

3.4.4. Total suction

The total suction of soil samples were measured using the chilled-mirror hygrometer which uses a dew-point measurement method according to ASTMD6836 (2008) standard. The total initial suction at hygroscopic water content for GI, 70G30S and LG were 139280 kPa, 198016 kPa and 111311 kPa respectively.

3.4.5. Soil-water characteristics and leaching phenomenon

3.4.5.1. Soil-water characteristics curve determination

The soil-water characteristics curves were determined using a combination of two techniques. The first is axis translation technique using pressure plate device for suction range from zero to 1500 kPa. The second is vapor equilibrium technique using different salts solutions with dissectors for suction range of more than 2000 kPa.

3.4.5.2. Permeability-leaching test

In order to study the effect of water flow on the characteristics of collapsible soils, permeability-leaching tests were carried out using UPC-Barcelona cell in combination with constant water head-leaching set up. The permeability-leaching stage is started after the wetting-collapse stage under the same range of net vertical stress. The leaching stress and the associated hydraulic gradient are shown in the Table 3.9.

Table 3.9.: Stress path of permeability-leaching test.

Net vertical stress, [kPa]	50	100	200	400	800
Hydraulic gradient, [-]	20	20	20	20	20
GI	√	√	√	√	√
LG	-	√	-	-	√*

Using hydraulic gradient equal to (30).

3.5. Summary

In this chapter, a detailed description of soils used and experimental program have been presented. As a summary, three types of collapsible soils were used for the experimental program of this research. These soils are gypseous soil (GI), mixed soil of the 70% artificial gypsum-30% Silber sand (70G30S) and loess soil (LG). The experimental program is divided to three main categories: (i) Basic characteristics, (ii) Volume change behaviour and (iii) Hydro-mechanical investigation as shown in Figure 3.7. The basic characteristics tests include the determination of physical, chemical and elementary (ESEM-EDX) analysis of selected soils. The summary of physical properties is explained in Tables 3.1 and Figures 3.3 and 3.5. Volume change without suction control is investigated by conducted consolidation and collapse tests. The initial properties of the soil specimens are illustrated in Table 3.4. Volume change under suction control is investigated through carrying out constant net stress-suction decrease (wetting-collapse) tests and constant net stress-suction increase (drying) tests. The initial conditions of the soil specimens and stress path are described in Tables 3.5 to 3.7. Also, the initial condition and stress path of the soil-column test for gypseous soil (GI) are summarized in Table 3.8. Moreover, the permeability-leaching tests were conducted under different vertical stress as shown in Table 3.9.

4. Experimental Techniques and Procedures

4.1. Introduction

This chapter describes the experimental techniques, equipments and procedures that were deployed in this study. The techniques, equipments and test procedures of the basic and conventional tests are out of the purpose of this chapter. The description of the experiments and procedures focus on the following: Volume change without suction control by single step wetting (i.e. single and double Oedometer collapse test), volume change under suction control by multi-step wetting (i.e. constant net vertical stress-suction control; wetting and drying test), soil-water characteristics curve determination, permeability-leaching behaviour characteristics, total suction measurements and soil-column investigation. It is worth to mention that some of the experimental techniques and devices concerning the suction measurements and application are not standardized yet. Therefore, these tests were based on procedures proposed in the literatures.

4.2. Experimental techniques

4.2.1. Volume change without suction control

The single and double Oedometer collapse tests were carried out as proposed by Jennings & Knight (1975) and according to ASTMD5333 (2003) standard using standard Oedometer device, see section 2.7. The initial conditions of the soil sample and stress path of the tests were illustrated in Table 3.4. The proposed relationship between the void ratio and vertical stress for the single and double Oedometer collapse tests are presented in Figure 2.6. The collapse potential is calculated according to Equation 2.4.

4.2.2. Techniques of suction application

In order to carry out the volume change experiments under suction control and soil-water characteristics curve (SWCC) test, the axis translation technique (ATT) was used to apply suction range < 1500 kPa while the vapour equilibrium technique (VET) was used to apply suction range > 2000 kPa. The detailed descriptions about these techniques are given in appendix A.1.

4.2.3. Techniques of suction measurements

In order to measure the total suction, matric suction and volumetric water content, the following techniques were used: The chilled-mirror hygrometer technique, time domain reflectometry (TDR) and tensiometer sensors. The detailed descriptions about these techniques are given in appendix A.2.

4.3. Equipments used

4.3.1. Volume change under suction control

4.3.1.1. UPC-Barcelona cell

The Barcelona cell was manufactured and developed in 1999 by the workshop at Universitat Politecnica de Catalunya (UPC), Barcelona, Spain. The main function of this cell is to measure the volume change of soil under wide range of applied suction and net normal stress. Figure 4.1a shows the design drawing of the cell, whilst Figure 4.1b shows the complete measurement set up of the cell with the other stress control parts.

The cell is one dimensional compression Oedometer. The vertical normal stress is uniformly applied on the top of the soil specimen by air pressure through a flexible membrane. The cell can be used for different types of soil ranging from fine grains sand to clay soil. The soil sample might be saturated, unsaturated, compacted or undisturbed sample. The diameter of the specimen ring is 50 mm and the height is 20 mm. The calibration of UPC-Barcelona cell against pressure-deformability is given in appendix B.1.

In this study, the matric suction is applied by axis translation technique (ATT) for suction range < 1500 kPa using UPC-Barcelona cell. The ATT is utilized through a high-air-entry ceramic disk provided in the base plate of the cell below the soil specimen. Different

air-entry values of ceramic disk are available such as 100, 500 and 1500 kPa. The ceramic disk must be saturated and flushed before the test.

The UPC-Barcelona cell is connected with high accuracy burette with a volume of 25 cm^3 and a resolution of 0.05 cm^3 for monitoring of the water content. Also, the cell is connected with one air pressure regulator for application of air- pressure as well as one air-pressure regulator for application of vertical net stress.

(a)

(b)
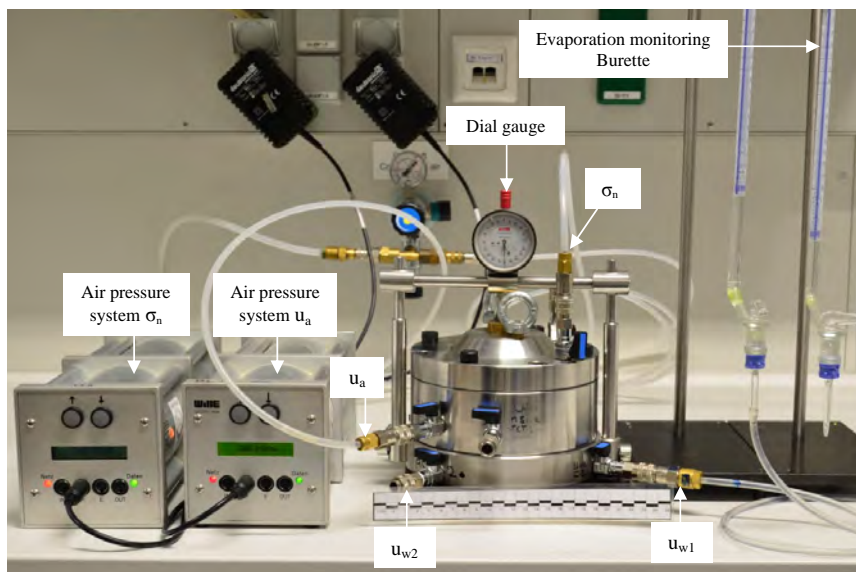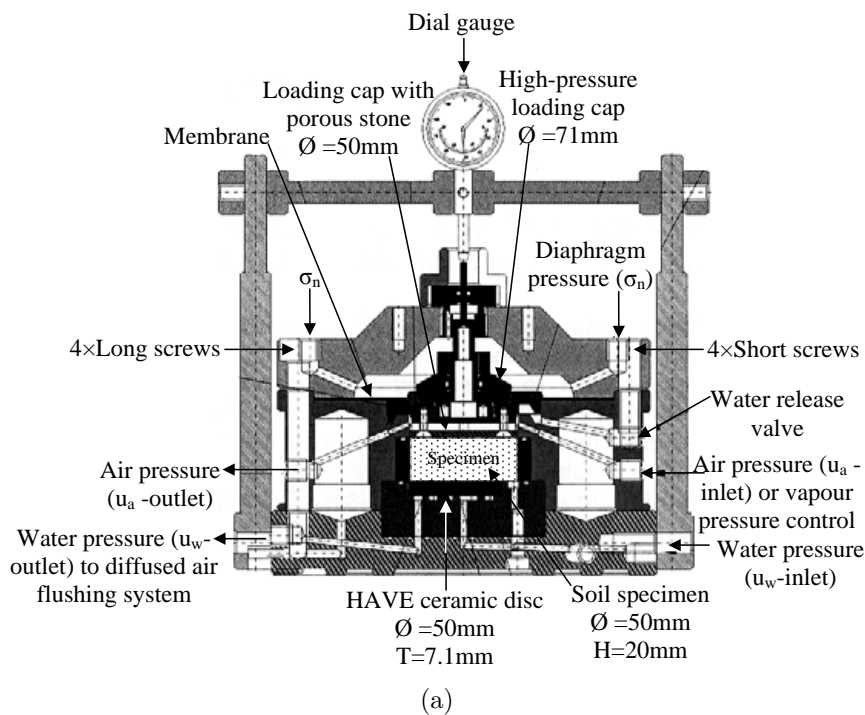
Figure 4.1.: UPC-Barcelona cell: (a) Schematic plot and (b) Cell set up.

4.3.1.2. UPC-Isochoric cell

The Isochoric cell was manufactured and developed by the workshop at Universitat Po-
litecnica de Catalunya (UPC), Barcelona, Spain as shown in Figure 4.2. The basic purpose
of this cell is to measure swelling pressure of the clay soils resulted by wetting processes
at constant volume condition, as used by Villar et al. (2001); Agus (2005); Arifin (2008).
In this cell, suction control is also possible by applying both axis-translation technique
(ATT) and vapour equilibrium technique (VET). Figures 4.2a and b show the design of
the cell and its body. The cell consists of three main parts: an exchangeable pedestal, a
threaded top part with a top cap and the load cell for measuring the swelling pressure.
The diameter of the specimen ring is 50 mm and its height is 20 mm.
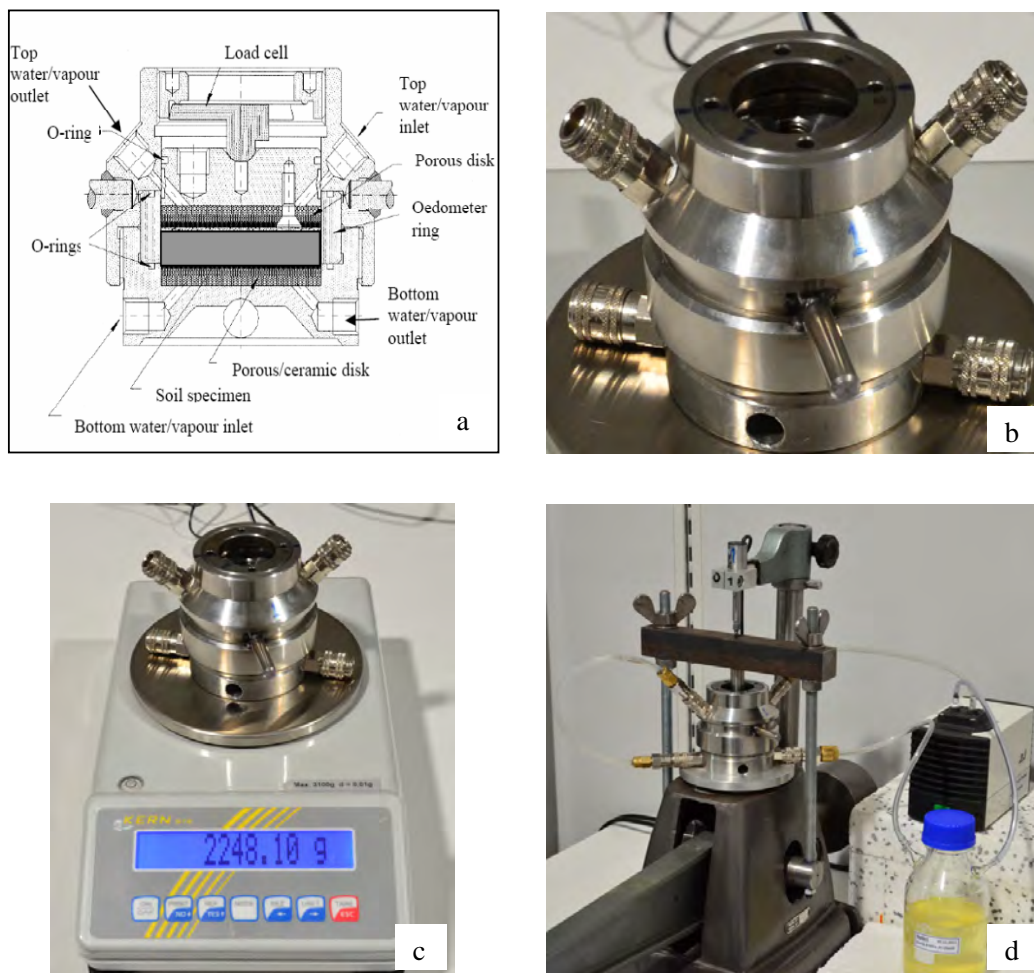
Figure 4.2.: UPC-isochoric cell,(a) schematic of the cell (b)cell body (c) controlling of
water content and (d) modified UPC-Isochoric-Oedometer cell with (VET) technique.

The cell was originally designed for no vertical stress application. Nevertheless, in this study, the UPC-Isochoric cell was modified to utilize with Oedometer frame in order to estimate the soil volume change resulting from suction variation. Special base plate and load piston are used for the sake of setting up the cell body and for vertical stress application, see Figure 4.2d. For this purpose, vapour equilibrium technique (VET) is used to control the high range of total suction (i.e. suction > 2000 kPa) under vertical net stress. The total suction was imposed by circulating the vapour of the salt solution in the flask through the top and the bottom of the soil specimen, using circulation system as shown in Figures 4.2d and 4.3. The changes in the water content of the soil specimen due to total suction variation were controlled by directly weighting the UPC-Isochoric cell body after each step of suction, see Figure 4.2c. Furthermore, the piston movement was prevented and the valves were closed to keep the volume of the specimen constant through the weighting process.

The modification of the UPC-Isochoric cell with Oedometer frame according to the above details was also used by Al-Badran (2011).

Two types of calibration are performed for the modified UPC-Isochoric-Oedometer cell as given in appendix B.2.
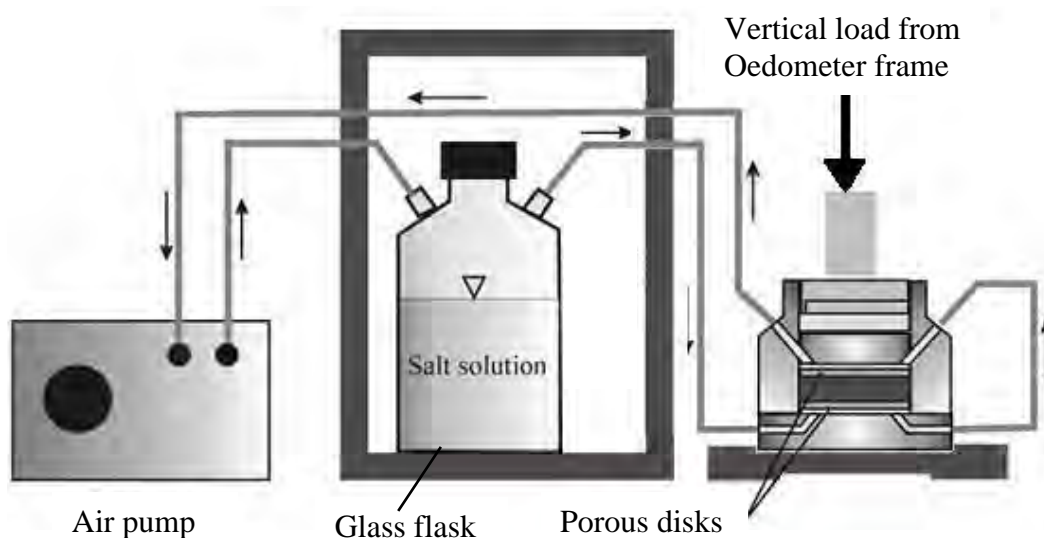
Figure 4.3.: Imposing of total suction to the UPC-Isochoric cell using vapour equilibrium technique with circulation system (Al-Badran, 2011).

4.3.2. Soil-water characteristics curve (SWCC)

4.3.2.1. Pressure plate apparatus

In this study, pressure plate apparatus made by SoilMoisture Company using axis translation technique is used to determine the soil-water characteristics curve for drying and wetting paths. Pressure plate apparatus is used to apply matric suction range < 1500 kPa as shown in Figure 4.4. The soil specimen was prepared in Plexiglas plastic ring of 50 mm in diameter and 15 mm in height.

Three types of saturated and air flushed ceramic disks with different air-entry value (AEV) were used in this test (i.e. 100, 500 and 1500 kPa) depending on the value of applied matric suction.

The pressure plate apparatus is connected with air pressure regulator for applying air-pressure and with high accuracy burette with a volume of 25 cm^3 and a resolution of 0.05 cm^3 for applying water pressure on the soil specimens, see Figure 4.4.

4.3.2.2. Constant relative humidity desiccators

In this study, the constant relative humidity desiccators using VET was utilized for continuing the determination of drying and wetting paths of the SWCC.

Many large and leak-proof desiccators containing different concentrations of salt solutions were used to apply total suction range > 2000 kPa on the soil specimens, as shown in Figure 4.5. The salt solutions were prepared by mixing different types of salts with distilled water separately to create a constant relative humidity and total suction vapour pressure in the desiccators chamber. The relative humidity of the salt solutions was measured at the beginning and the end of the test using the chilled-mirror hygrometer technique (section 4.3.4). The actual total suction was computed from the relative humidity measurements, according to Equation A.1.

The experiment was conducted in a temperature-controlled room with a constant temperature of $22^oC \pm 0.5^oC$.

<center>(a)   (b)</center>
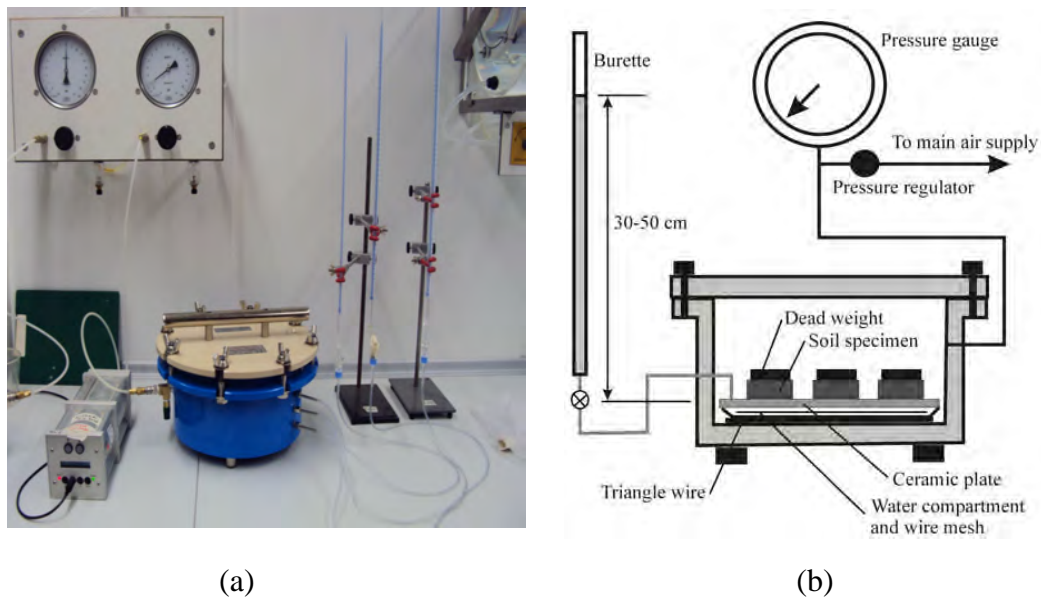
Figure 4.4.: Pressure plate apparatus:(a) device set up (b) schematic plot.

<center>(a)   (b)</center>
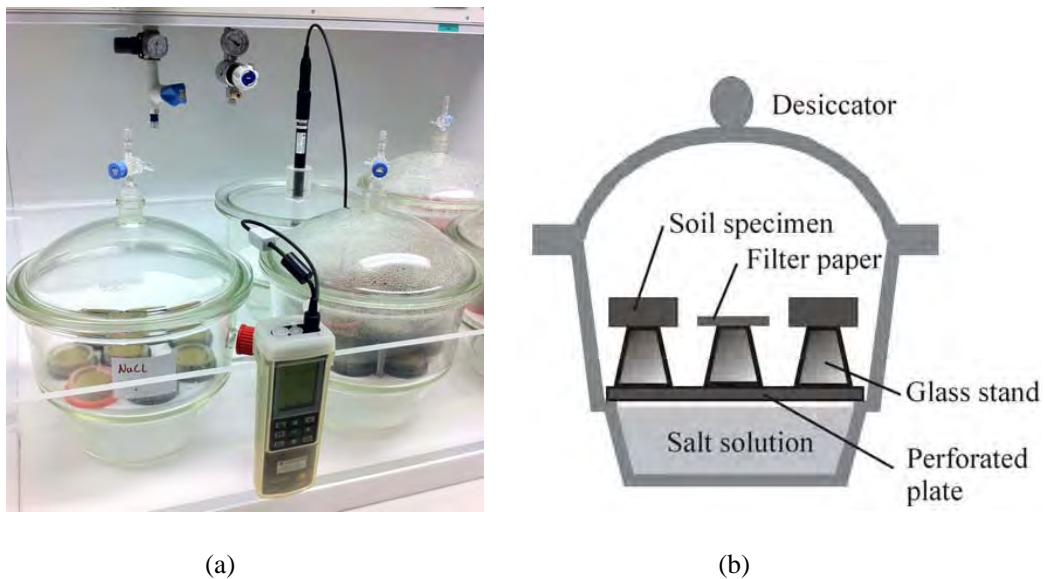
Figure 4.5.: Desiccator of vapour equilibrium technique:(a) test set up,(b) schematic plot.

4.3.3. Permeability-leaching behaviour

In order to determine the coefficient of permeability at saturated condition and to perform the leaching processes on the soil specimen, the constant head-permeability-leaching set

up is used in combination with the UPC-Barcelona cell as shown in Figure 4.6. For this purpose, the porous stone is substituted for the high-air-entry ceramic disk in the base plate of the UPC-Barcelona cell.

The constant head-permeability-leaching set up consists of the following parts: stable stand of 1.2 m height, cylindrical vessel of 3 liters volume, water reservoir of 6 liters volume, high duty water pump and discharge reservoir of 2 liters volume. The discharge reservoir is used to collect the volume of leached water for permeability coefficient and dissolved gypsum determination.

4.3.4. Chilled-mirror hygrometer device

The chilled-mirror hygrometer technique was used to determine and monitor the total suction of soil specimens and for the salt solutions of vapour equilibrium technique (VET). The chilled-mirror hygrometer device used in this study (as shown in Figure A.1) is a water activity meter type 3TE, Decagon Devices, Inc., Pullman, WA. The relative humidity of the specimens was measured and the total suction was calculated using the thermodynamic relationship in Equation A.1.
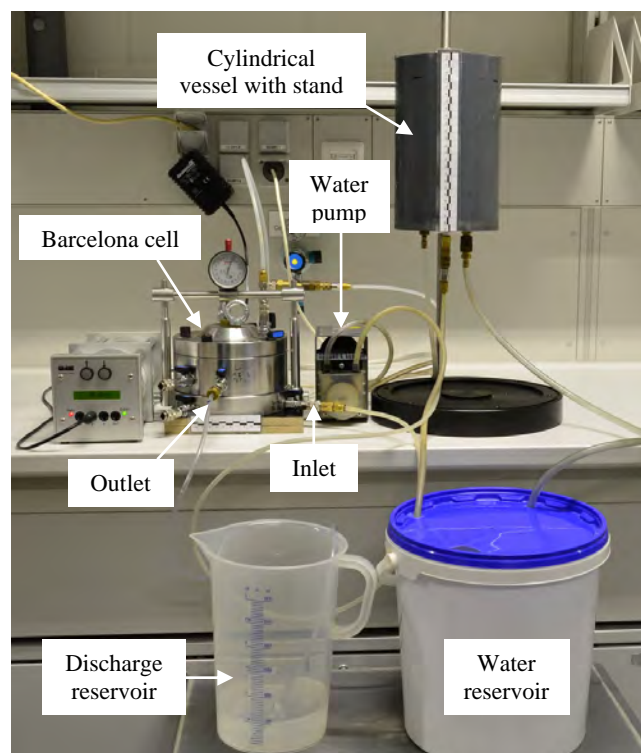
Figure 4.6.: Constant head-permeability-leaching set up.

4.3.5. Soil-Column device

The soil-column device shown in Figure 4.7 is used in order to investigate the transient of the pore-water pressure and the volumetric water content at different elevations of sandy gypseous soil mass. However, the soil-column device was used by Lins (2009) to determine the soil-water characteristics curve of Houston sand using the axis translation technique (ATT) for applying low range of matric suction on the soil sample.

The setup of the soil-column device is mainly consisting of the following parts (see Figures 4.7 and 4.8): cell body, three Time Domain Reflectometry (TDR) sensors with their data logger, three tensiometers with their data logger and two computers to run the two supported software of the TDRs sensors and the tensiometers in addition to saving data. The cell body of the device is manufactured from a Plexiglas cylinder of 282 mm in height, 240 mm in diameter and 5 mm in thickness. The cross sectional plan and photo of the cell body is shown in Figure 4.9. The base part of the cell body contains a ceramic disk of 100 kPa air-entry value, in addition to water reservoir located below the ceramic disk. The water reservoir is connected to the water burette in order to control the water pressure during the test. The Plexiglas cylinder is connected from the top side with loading cap. The loading cap consists of the loading piston to transfer the vertical load, a mechanical dial gauge and/or electronic dial sensor for volume change measurements, pedestal plate to carry the dead load located at the upper end of the piston, and a perforated plate located at the lower part of the piston. The perforated plate directly contacts the top surface of the soil sample, in order to transfer the vertical load from the piston to the soil sample. The air pressure, which is supplied by the air pressure system of the laboratory and controlled by the air pressure controller (Figure 4.7), is connected to the loading cap though two valves (Figure 4.9b). The three parts of the cell body (i.e. Plexiglas cylinder, loading cap and base part) are screwed by three bolts. Two O-rings are used in cell body in order to prevent any air or water leakage. The first O-ring is located between base part and the Plexiglas cylinder, while the second is between the Plexiglas cylinder and the loading cap. The soil sample dimensions used in this study are 240 mm in height and 240 mm in diameter (Figure 4.9a). The TDRs and tensiometers sensors are located at three elevations of the soil sample and in opposite directions. The sensors elevations are 40, 100 and 160 mm for the top surface of the compacted sample.

In this study, the types of the utilized TDRs and tensiometers sensors are different from those used by Lins (2009). Nevertheless, the main functions and properties of the TDRs and tensiometers sensors are described in the following subsections.
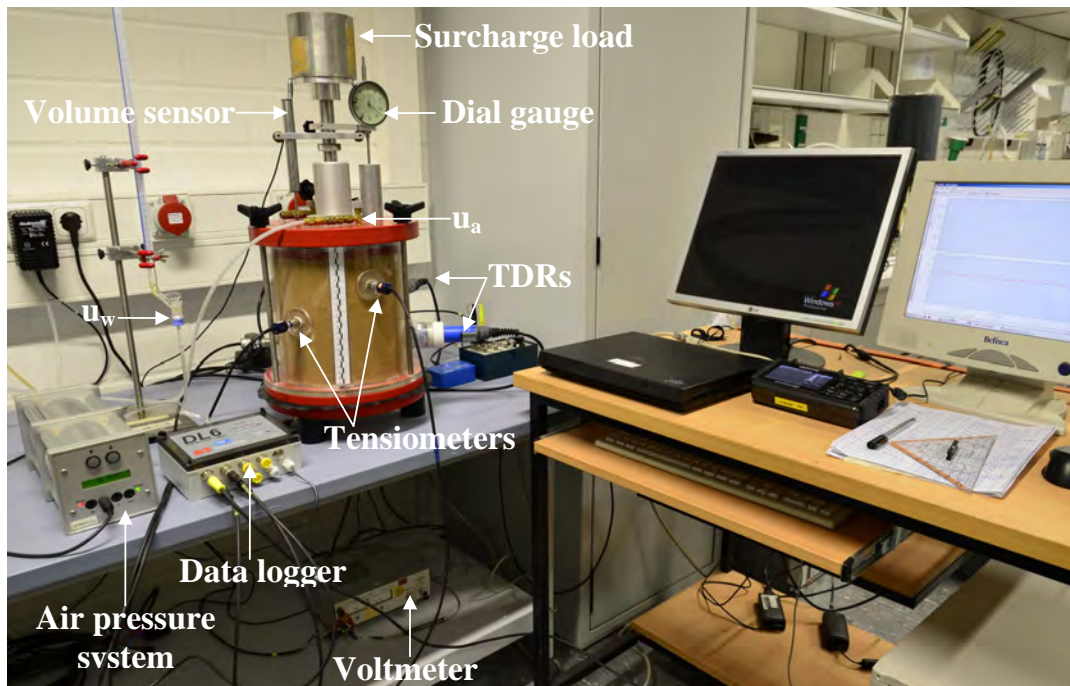
Figure 4.7.: Soil-column device.
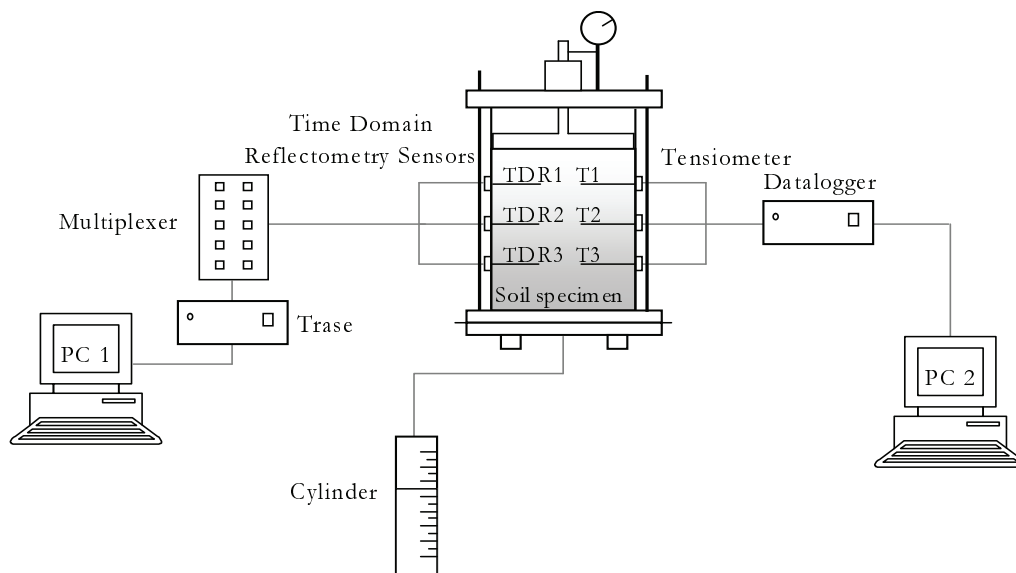
Figure 4.8.: Set up of the soil-column device(Lins, 2009).
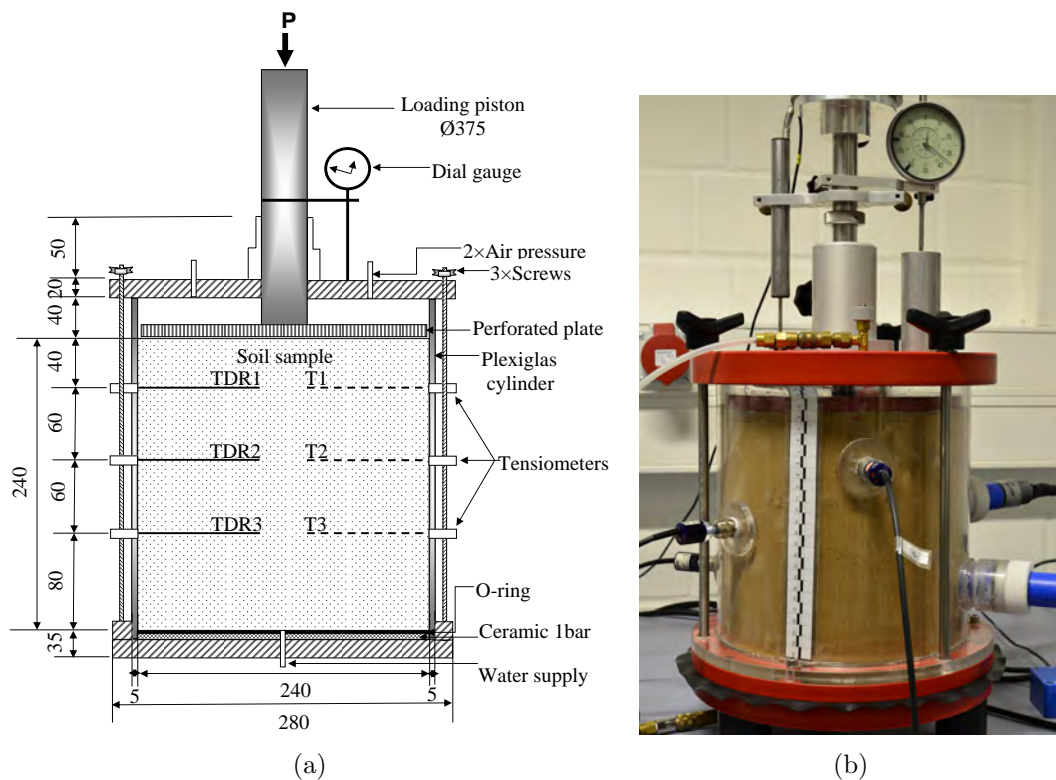
Figure 4.9.: Soil-column device: (a) Schematic plot: not to scale, dimensions in mm and (b) Cell body.

4.3.5.1. Time Domain Reflectometry sensors

The Time Domain Reflectometry (TDR) sensor type (TRIME-PICO32) is used in this investigation as shown in Figure 4.10. The TDR sensor is designed and made by IMKO Micromodul Technik GMBH, Germany.
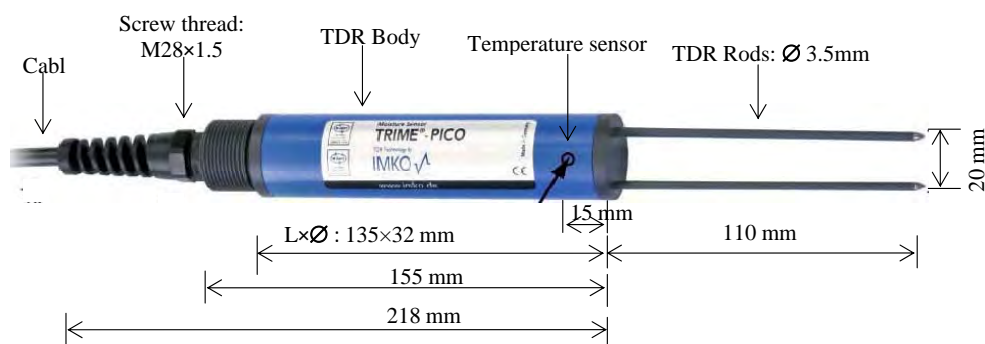
Figure 4.10.: Schematic plot of TDR sensor type TRIME-PICO32.

The main function of this TDR sensor is as a measurement device for continuous and non-destructive determination of volumetric soil moisture and soil temperature. It is originally designed for stationary subterranean field use, as well as laboratory use for soil sample measurements. The basic calibration of TDRs is carried out for a wide range of soil types by IMKO Company, in order to consider a similar relationship between the volumetric water content and the dielectric constant. Therefore, this type of TDR sensor provides measurements for volumetric water content and temperature of the soil sample.

As shown in the schematic plot of the TDR sensor in Figure 4.10, it consists of two parallel rods, TDR body including the temperature sensor and cable. For computing, analyzing and saving the measured data, the TDR sensors are connected to the PICO data logger, then the data logger collect the measurements and send them to the operation software. The software then, enables to scan and collect trial measurements on the connected TDRs sensors in order to check whether the measurements system is working correct or not. The operation software also enables to predefine the dry density of the measured soil sample in addition to the time intervals between the successive measurements. Two types of calibrations are carried out on the three TDRs sensors used in this study as given in appendix B.3.1.

Based on the operation manual provided with the TDR sensor, the main specifications can be outlined as follow:

- Moisture measuring range 0-100 %, measuring accuracy of Moisture range 0-40 %, accuracy $\pm$1-2% and Moisture range 40-70 %, accuracy $\pm$2-3%.

- Soil temperature measuring range -15°C to +50°C, measuring accuracy of $\pm$0.2 ^{o}C.

4.3.5.2. Tensiometer sensors

The tensiometer sensor type (UMS-T5) is used in this investigation as shown in Figure 4.11.
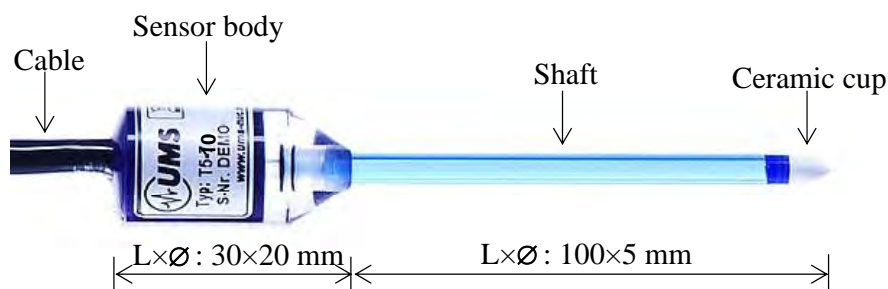
Figure 4.11.: Schematic plot of Tensiometer sensor type UMS-T5-10.

The tensiometer is a miniature pressure transducer tensiometer designed and made by UMS(UmweltUmweltanalytische Mess-Systeme, Germany). The typical applications for this type of tensiometer are:

- Measurement of pore-water pressure of the soil in the laboratory and in the field.

- Measurements of soil-water tension and water potential.

- Miniature soil column studies, e.g. in combination with micro water samplers and soil temperature probes.

- Determination of leachate and capillary water movements.

As shown in the schematic plot of the tensiometer sensor in Figure 4.11, it consists of the sensor body, pressure transducer and water filled shaft including the ceramic cup. The sensor body is made of Acrylic glass and incorporates the pressure transducer and all electronic parts. The corpus is backfilled with resin to hermetically seal the electronics and make the body watertight. The pressure transducer is piezoelectric pressure sensor that measures the soil water tension against the atmospheric pressure. The atmospheric pressure is a conducted through a watertight diaphragm (the white, 2 cm long tube on the cable) and through the cable to the reference side of the pressure sensor. The sensor body including pressure transducer is screwed with the Acrylic glass shaft. The ceramic cup of 0.5 cm^2 active surface areas is made from high porous Al_2O_3 sinter material. It is fixed to the end of glass shaft and must be saturated and filled with degassed water in order to transfer the pore-water pressure of the soil into the tensiometer. The air bubbles refill and removal process is significant to assure a rapid and reliable measurement of the soil water tension. The refill procedure is described in the user manual and it is out of the aim of this chapter. For computing, analyzing and saving the measurements data, the three tensiometer sensors used in this study are connected to the data logger, which connects to the computer. Special operation software is provided with the tensiometer used to collect and display the measurements data on the computer monitor. The calibration was done in order to check the accuracy of the tensiometer measurements as given in appendix B.3.2. The same type of the tensiometer but with shortest shaft was used by Lins (2009) for the same test purpose. It is important to mention that the tensiometer sensors have the following specifications:

- Measuring range of pore-water pressure is -85 kPa to +100 kPa with accuracy ±0.5kPa. It is not suitable for dry soils or for negative pore-water pressure.

- Offset correction for non horizontal installations is 0.1 kPa for each 1 cm length of the glass shaft.

4.4. Tests procedures

4.4.1. Volume change under suction control test

The volume change experiments were carried out on the three unsaturated soils constant net stress-suction control (i.e. wetting and drying) tests. For both test, the initial conditions of the soil samples and the boundary conditions of the test were given in Tables 3.5 to 3.7. While the stress paths were explained in Figure **??**.

4.4.2. Constant net normal stress-suction decreases (wetting-collapse) test

The soil specimen was tested first at unsaturated condition (i.e. initial suction) by UPC-Isochoric cell through applying a vertical load, and then the total suction is decreased stepwise till a value of 6100 kPa. Afterward, the soil specimen is moved to the UPC-Barcelona cell to apply low suction range. The test continued by reloading the soil specimen till reaching the marked net vertical stress under constant suction induced in UPC-Isochoric cell. Then the suction was stepwise decreased under the constant net vertical stress till reaching zero value, see Figure 4.12a.Through the test, the change in the volume and in the water content of the soil specimen were measured. The collapse potential is calculated at the end of each suction level according to Equation 2.4.

4.4.3. Constant net normal stress-suction increases (drying) test

The soil specimen was tested first at saturated condition (i.e. zero suction) by UPC-Barcelona cell. The specimen was loaded till reaching the target net vertical stress, and then the suction was increased under the constant vertical stress. In order to apply high suction range, the same soil specimen was moved to the UPC-Isochoric cell. The test continued by loading the soil specimen till reaching the marked net vertical stress under constant suction induced in UPC-Barcelona cell. Then the total suction stepwise increased under the same previous constant net vertical stress till reaching the initial total suction, see Figure 4.12b.Throughout the test, the changes in the volume and the water content of the soil specimen were measured.
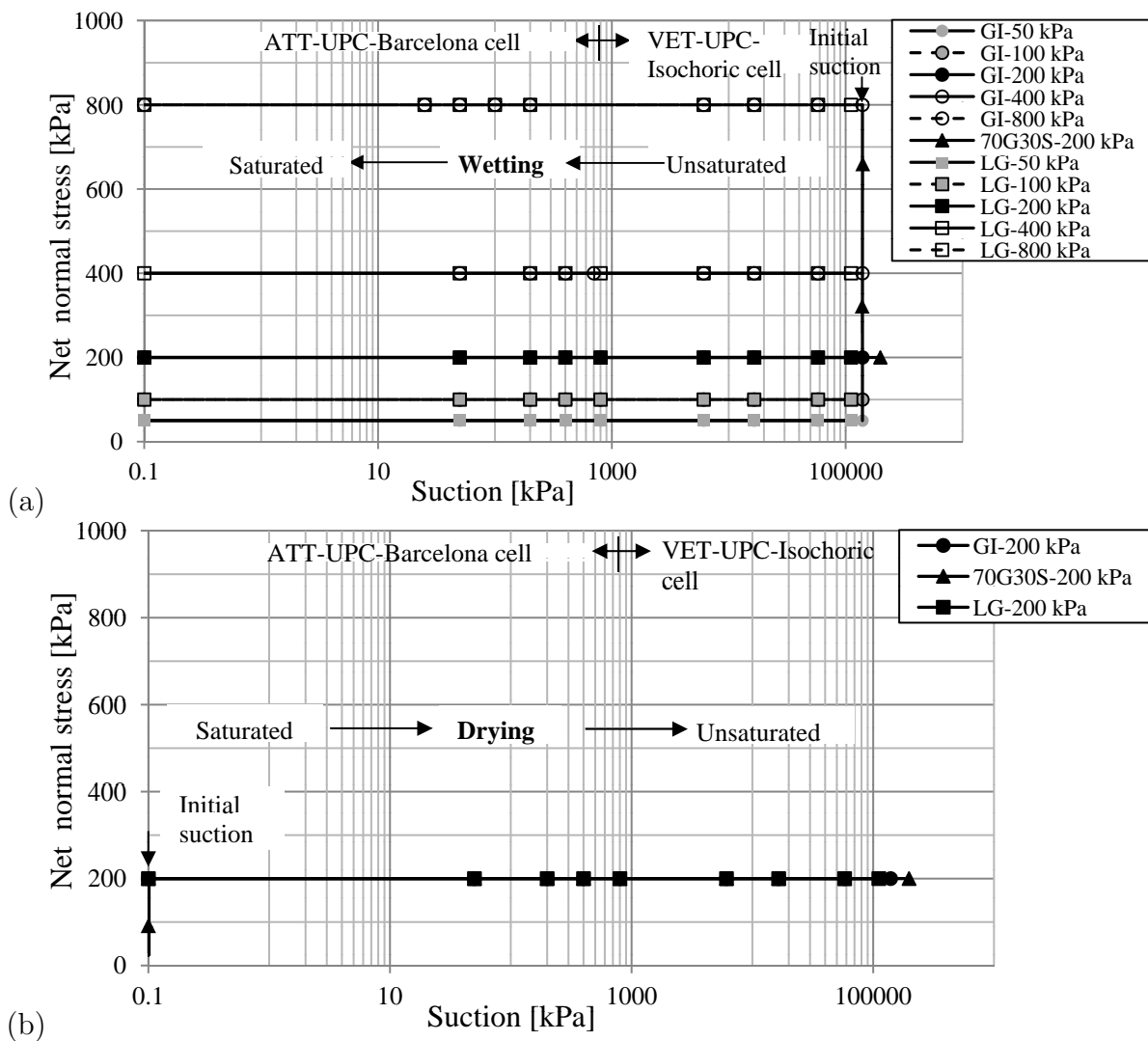
Figure 4.12.: Stress path of constant net normal stress-suction control test: (a) Wetting path and (b)Drying path.

4.4.4. Soil-water characteristics curve (SWCC) determination

In general, the determination of SWCC is based on the measurement the amount of water in the soil specimen corresponding to the value of applied suction for drying and wetting path. The initially saturated specimens followed the drying path (i.e. stepwise increases of applied suction). Then the soil specimens of dry state were subjected to wetting path (i.e. stepwise decreases of applied suction). Figure 4.13 describes the stress path of soil-water characteristics curve measurements for both ATT and VET.
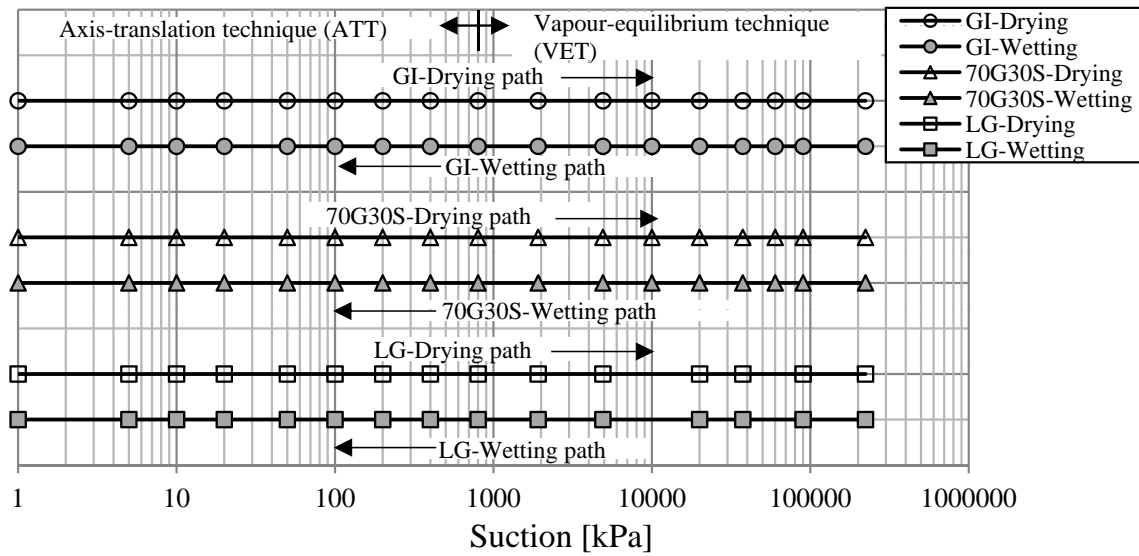
Figure 4.13.: Stress path of the soil-water characteristics curve test.

To control the water content, the weights of the specimens were monitored regularly during the test using a precision balance with an accuracy of 0.0001 g. To control the void ratio and the degree of saturation, the volume of the soil specimens were measured before and after the test, and also at the end of each suction level. The dimension measurements were conducted using digital vernier caliper with accuracy of 0.01 mm. The soil specimen reached to the equilibrium condition when no considerable changes in its water content are recorded under constant suction.

The same techniques and test procedure were also used in the determination of soil-water characteristic curves by different researchers such as Schanz et al. (2004); Agus (2005); Arifin (2008); Lins (2009); Al-Badran (2011).

4.4.5. Permeability-leaching test

The test was conducted on the same soil specimen of the constant net vertical stress-suction decrease (wetting-collapse) test after finishing the collapse stage. The hydraulic gradient and the stress path of the test were illustrated in Table 3.9. The test was started after the soil specimens have reached to equilibrium under vertical stress level. A constant water head was applied to the bottom of the soil sample to remove the air bubbles and reaching fully saturated state. Then, the water was flown through the outlet water line of the cell towards the discharge reservoir. During the test period of 240-360 hours, the volume of the leached water and dissolved gypsum were controlled. In order to determine

the total dissolved gypsum, a sample of leached water was oven dried at 45°C, and the precipitated salts were measured. This method is recommended by ASTMD2216 (2010) standard and used by many researchers such as Al-Mufty (1997); Al-Busoda (1999); Al-Obaidi (2003).

4.4.6. Soil-column test

The soil sample was statically compacted in the cell to an initial void ratio of 1.14 and an initial volumetric content of 6.5%, see Table 3.8. The compaction process is divided into three layers and carried out after the installation of the TDR and tensiometer sensors. A good contact between the sensors and the soil must be satisfied to keep continuous water phase and to get reliable measurements (see Figure 4.14). The test was started by gradually applying the air pressure from the pressure control system to the upper loading cup. Simultaneously the water pressure was applied from the burette to the bottom of the soil sample till it reaches the first stress path level (u_a=30 kPa, u_w=10 kPa, ψ=20 kPa). Then the matric suction was stepwise decreased (i.e. after each equilibrium stage) till zero value following wetting stress path. During the test, the volume change, volumetric water content using TDR sensors and pore-water pressure using tensiometer sensors were monitored.
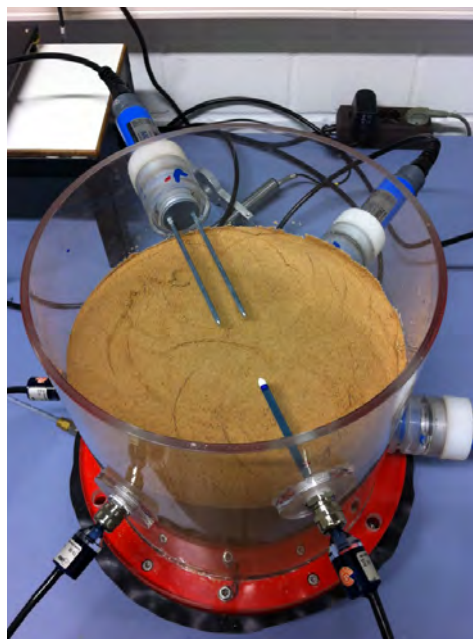
Figure 4.14.: Preparation of soil-column test.

4.4.7. Summary

In the previous sections, description for the techniques, equipment and test procedures used for adopting the experimental program were presented. The test procedure for performing the volume change without suction control by single step wetting (i.e. single and double Oedometer collapse test), volume change under suction control by multi-step wetting (i.e. constant net vertical stress-suction control; wetting and drying test), soil-water characteristics curve determination, permeability-leaching behaviour characteristics, total suction measurements and soil-column investigation were outlined step by step.

In order to cover a wide range of entire soil suction, two of the main techniques were used. The first is to impose low suction range (i.e. suction$<$ 1500 kPa), which is the axis-translation technique. The second is to apply high suction range (i.e. suction$>$ 2000 kPa), which is vapour equilibrium technique. For constant net normal stress-suction control (i.e. wetting and drying tests), the UPC-Barcelona cell was used with ATT for matric suction $<$ 1500 kPa and the UPC-Isochoric cell with VET for total suction$>$ 2000 kPa. Also, the axis translation technique was used with pressure plate apparatus and the vapour equilibrium technique with salt solution desiccators for soil-water characteristics curve determination. For soil-column test, axis-translation technique was also used to apply the matric suction, while the TDR and tensiometer sensors were used for volumetric water content and pore-water pressure measurements respectively. Furthermore, the permeability-leaching test was carried out using UPC-Barcelona cell with porous stone base, in addition to the constant head permeability set up. The chilled-mirror hygrometer device was used to determine and monitor the total suction of the three selected collapsible soils and for the salt solutions of vapour equilibrium technique.

5. Experimental Results and Discussion

5.1. Introduction

This chapter presents and discusses the experimental results of the laboratory test program described in Chapter 3. The aim of these tests is to investigate the effect of suction and other initial conditions on the collapse behaviour for the three types of unsaturated collapsible soils selected for this research. Qualitative analysis is also undertaken in this chapter to calculate the volume change and leaching strain in collapsible soils.

This chapter presents the results of the collapse potential measurement by single step wetting without suction control performed in a standard Oedometer device under different inundation stress, dry density and degree of saturation. Moreover, volume change is illustrated under suction control (i.e. constant net stress with multi-step suction decreases and constant net stress with multi-step suction increases) using both a UPC-Barcelona cell and a UPC-Isochoric cell. In addition, various issues are addressed including the results of the consolidation tests, the soil water characteristic curves, the permeability-leaching tests, elementary characteristics (i.e. ESEM-EDX) analysis, the soil column tests and soil improvement and foundation option.

5.2. Volume change without suction control results

This section presents the results of volume change without suction control performed in a standard Oedometer device for the three collapsible soils.

5.2.1. Consolidation test results

In this subsection, the results of standard consolidation test as void ratio versus logarithms of the vertical stress relationship are shown in Figure 5.1. The initial conditions of the tested samples and compression characteristics are demonstrated in Table 5.1.

(a)

(b)

(c)
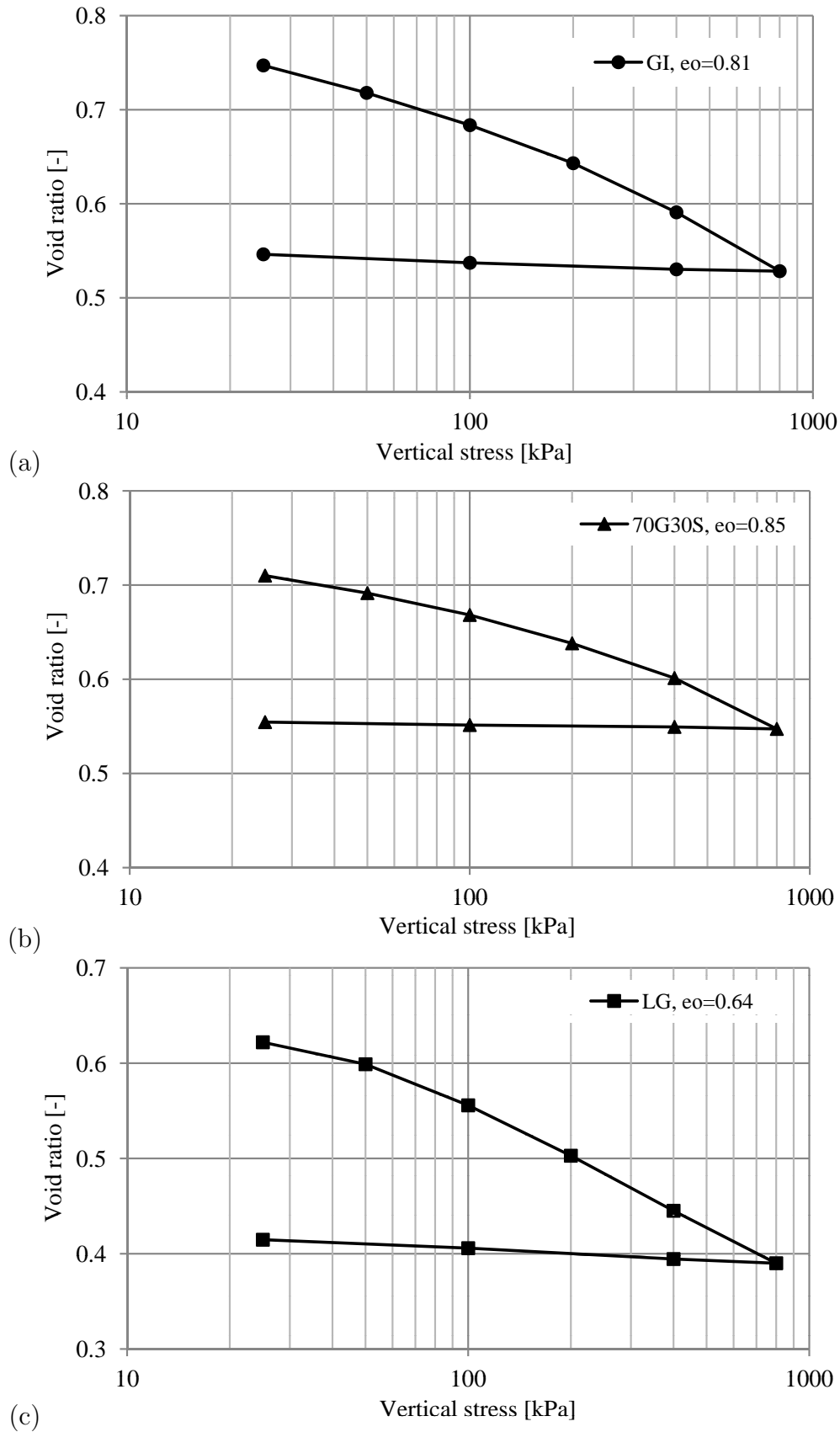
Figure 5.1.: Consolidation test results: (a) GI, (b) 70G30S and (c) LG soils.

Table 5.1.: Initial conditions of soil samples and consolidation test results.

Soil type	D.density [g/cm^3]	e_o	$w_{(Hydroscopic)}$ [%]	χ' [%]	σ_{mv} [kPa]	C_c	C_r	ϵ_{800kPa} [%]
GI	1.3	0.81	0.25	70	176	0.21	0.009	15.5
70G30S	1.3	0.85	0.25	70	165	0.18	0.004	16.2
LG	1.6	0.64	2.5	0	65	0.18	0.017	15.0

It is clearly observed that the trend of compression and recompression curves for the three types of soils was approximately linear. This behaviour can be attributed to the much higher permeability of silty and gypseous soils as compared with clay soil in addition to the rapid settlement which occurs immediately when the load increment is applied.

The typical log time-strain curves for the selected soils at 200 and 800 kPa are shown in Figure 5.2 a, b and c respectively.

For both gypseous and mixed soils, the shape of the first segment of the log-time-strain curve (Figure 5.2a and 5.2b) was relatively flat and several hours was required to reach equilibrium at the primary consolidation stage. However, significant secondary compression was associated with a large amount of settlement, which formed the steep shape of the second segment of the log time-strain curve. This can be attributed to the considerable time required to soften and dissolve the gypsum particles. Soils with high gypsum content may require a couple of weeks until the secondary compression is complete.

In silty loess soil, the reverse applied; graphical analysis showed that the log time-strain curves (Figure 5.2c) concaved upwards from the beginning of the load application. The primary consolidation was finished after less than one minute and the secondary compression reached equilibrium after only several hours.

On the other hand, some challenges arose while calculating the coefficient of consolidation because the 50% consolidation point was difficult to recognise. Therefore, it is recommended to assume that this point lies midway between the beginning and the end of the log time-strain curve. This assumption implies very rapid consolidation, and more explicit results may not be needed (Head & Epps, 2011). These findings were also observed by Hobbs (1986).
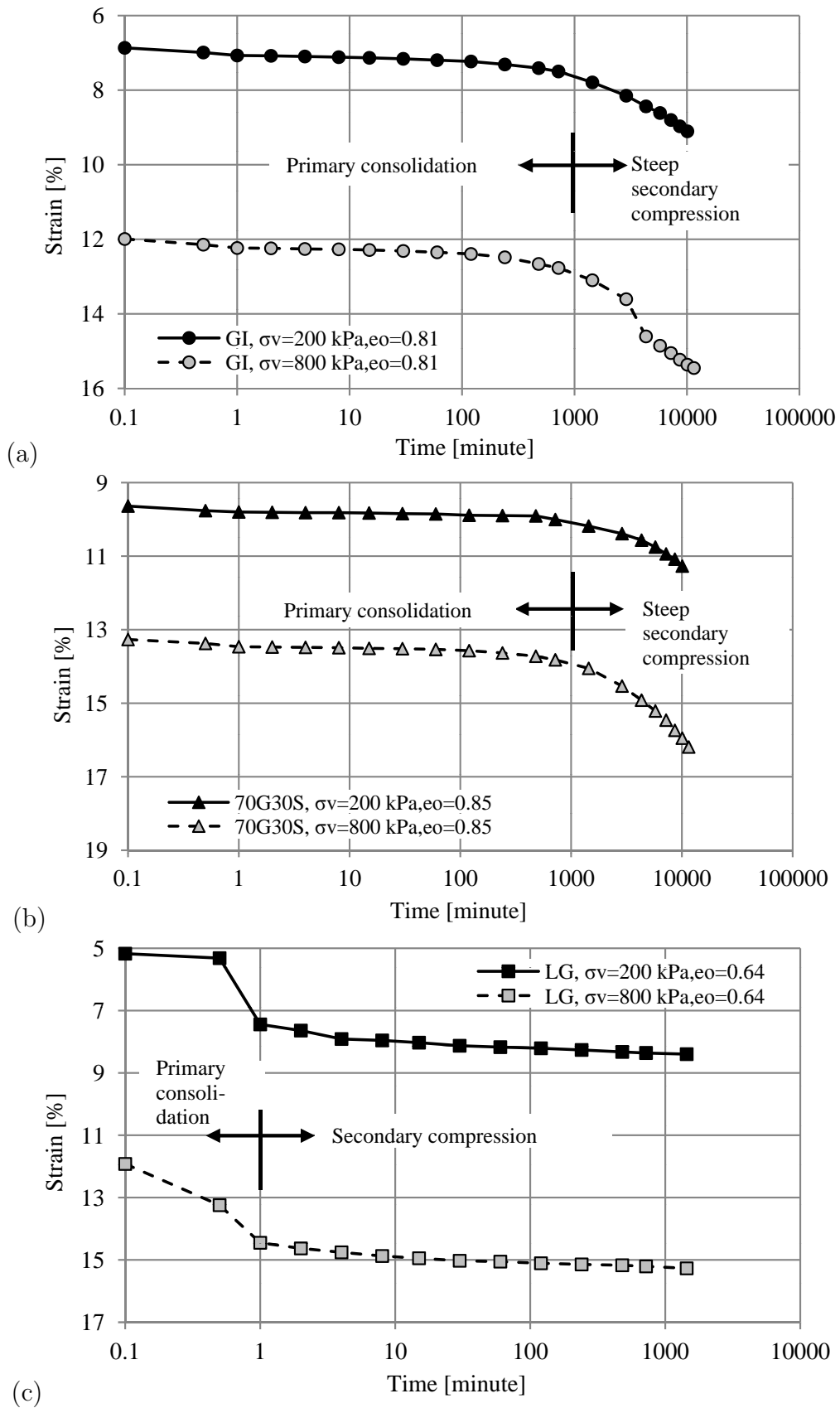
Figure 5.2.: Strain versus time relationship: (a) GI, (b) 70G30S and (c) LG soils.

5.2.2. Collapse test results

Collapse tests following the single step full wetting procedure were performed using a standard Oedometer device. In order to investigate a wide range of collapse behaviour, the collapse test was carried out under different initial conditions of soil samples, such as inundation vertical stress, initial dry density and the initial degree of saturation.

It is important to mention that the collapse test procedure was carried out under the following criteria: stress path of 25, 50, 100, 200, 400 and 800 kPa for loading stage and 400, 100 and 25 kPa for unloading stage.

Based on the consolidation tests results, the load increment duration (LID) was 14 days for both gypseous and mixed soils while it was two days for loess soil. The above-mentioned LID represents the maximum inundation time required for the primary consolidation stage. The plus sign [+] refers to swell volume change, while the minus sign [-] refers to collapse volume change.

5.2.2.1. Effect of inundation vertical stress

- **Single Oedometer-collapse test results (SOT):**

In this subsection, a series of single Oedometer collapse test results are presented. Six identical specimens for each type of collapsible soil were tested under different inundation vertical stresses.

The relationship between void ratio versus vertical stress is shown in Figure 5.3, while Figure 5.4 explains the variation of void ratio with the vertical stress for both unsaturated and saturated specimens of gypseous soil, mixed soil and loess soil respectively. The summary of the test results are given in Table 5.2.

In these figures it can be observed that the response to wetting for all soil types was a collapse volume change. However, the test result for loess soil depicted in Figures 5.3c and 5.4c shows a significant "swelling" volume change that occurred as a response to inundation processes at stresses level lower than the maximum preconsolidation pressure (i.e σ_{vm}= 65 kPa). However, the collapse behaviour was observed when loess soil inundated at vertical stress higher than the maximum preconsolidation pressure. This behaviour can be attributed to the soil sample being subjected to an overconsolidation state when inundation was induced at vertical stresses (σ_v) equal to 25 and 50 kPa.
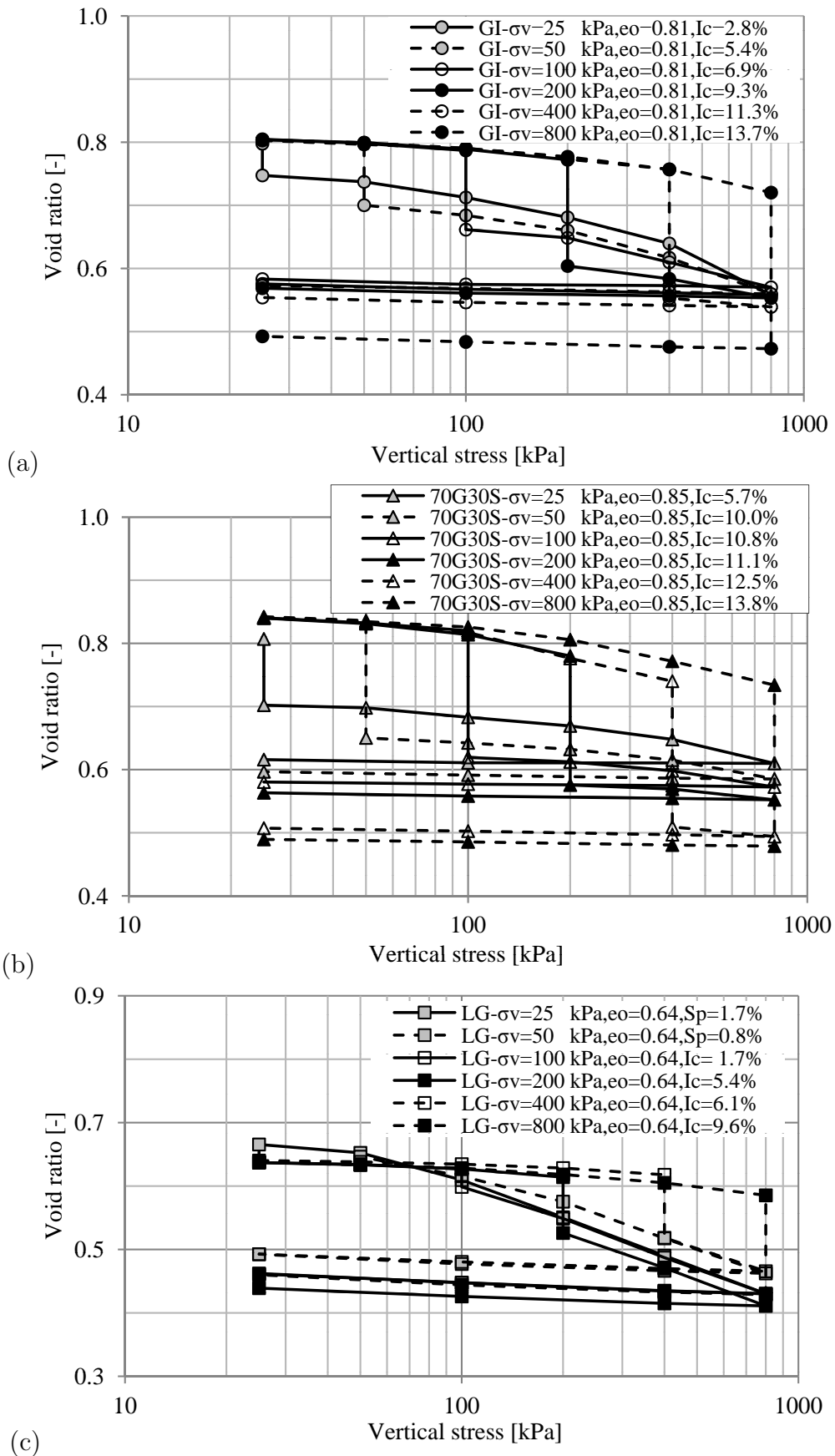
Figure 5.3.: Single Oedometer-collapse test: (a) GI, (b) 70G30S and (c) LG soils.

(a)

(b)

(c)
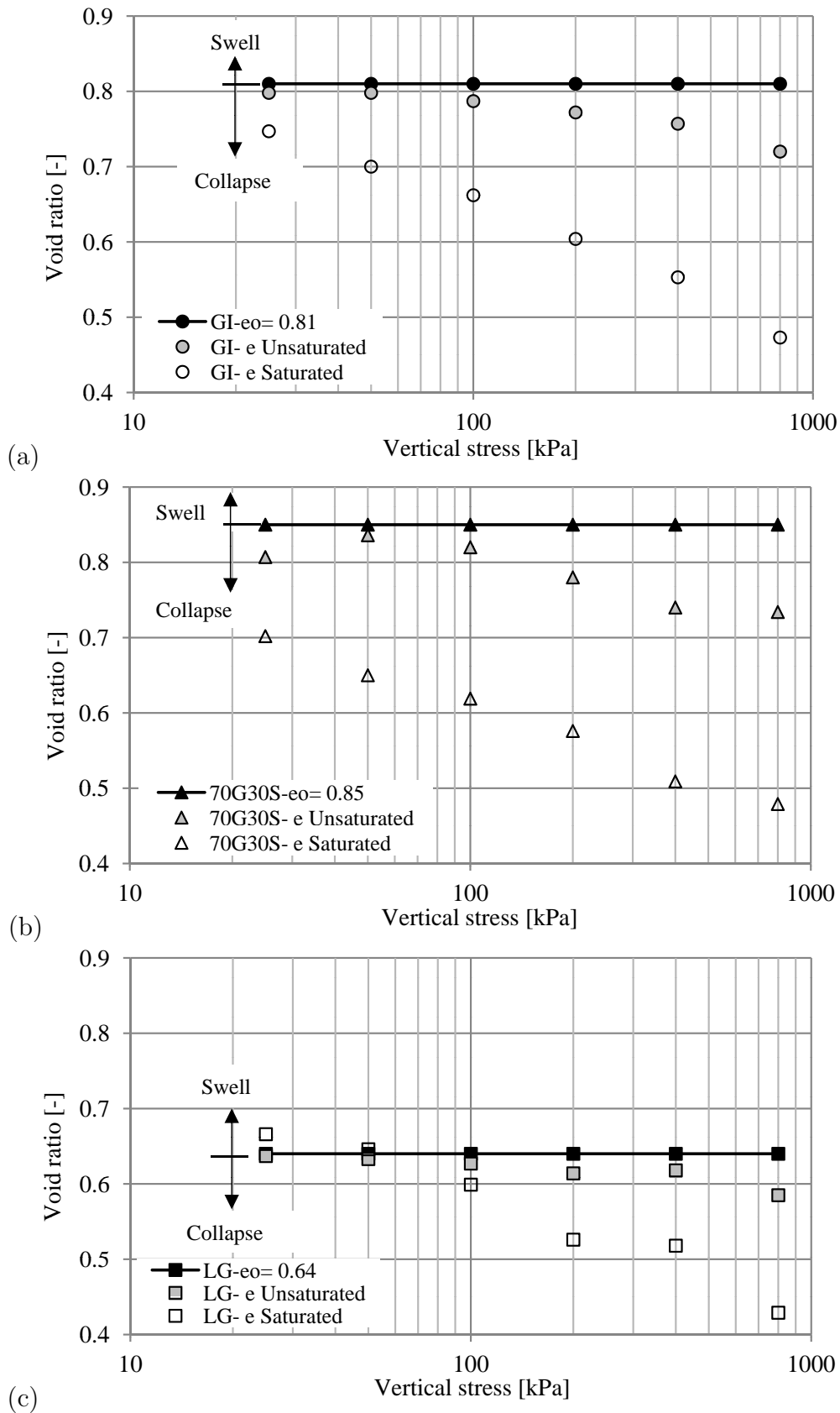
Figure 5.4.: Variation of void ratio with vertical stress: (a) GI, (b) 70G30S and (c) LG soils.

Table 5.2.: The summary of the effect of inundation vertical stress on collapse potential.

Soil type	$e_o/w\%$	Test type		Vertical stress, σ_v[kPa]					
			Time [day]	25	50	100	200	400	800
				Collapse potential, I_c[%]					
GI	0.81/0.25	SOT	7	2.4	4.9	6.3	8.5	10.3	12.6
			14	2.8	5.4	6.9	9.3	11.3	13.7
		DOT	7	3.1	4.5	5.8	7.2	8.7	10.1
70G30S	0.85/0.25	SOT	7	5.2	9.4	10.1	10.2	11.5	12.7
			14	5.7	10.0	10.8	11.1	12.5	13.8
		DOT	7	7.1	7.7	8.3	8.1	7.6	7.9
LG	0.64/2.5	SOT	2	Sp1.7	Sp0.8	1.7	5.4	6.1	9.6
		DOT	1	1.0	2.2	4.4	7.0	9.6	11.8

In other words, the volume of soil mass expanded when free access to water was allowed. Percolated water attempted to expel the air bubbles and quickly filled the voids in the microstructure level at the time of the imposed vertical stress; however, the vertical stress could not restrict the upward movement of soil mass. Considerable collapse settlement was recorded as a result of softening and the rearrangement of soil particles upon inundation at a stress level higher than the preconsolidation pressure. These findings corroborate the results of Lawton et al. (1989).

On the other hand, both naturally gypseous and artificially gypsified soils showed a large number of collapse deformation and sudden volume changes with free access to water, and the void ratio significantly decreased. Moreover, the gap between the void ratio at unsaturated and saturated states steadily increased when the inundation occurred at a high stress level. This behaviour can be attributed to the softening and breaking of gypsum bonds and a reduction in the interparticle contacts. The new shapes of the soil particles attempted to rearrange themselves and densify into a new structure with smaller volume. Seleam (1988); Nashat (1990) and Al-Obaidi (2003) also obtained similar findings.

Furthermore, it is important to mention that in Figure 5.3 the strain of unsaturated curves (i.e. before inundation) occurred due to grain densification whereby the issue of sampling disturbance was not valid. This strain can be ignored since it is not typically used for design purposes. Houston & EI-Ehwany (1991) confirmed this interpretation. Also, the wetting path of the e-$log\sigma_v$ plot is presented as a band form for the three soil

samples wetted at different vertical stresses (see wet sides of the curves in Figure 5.3). The width of this band depended on the value of vertical stress at inundation and on sample heterogeneity. Moreover, during all collapse or compression tests, little unloading strain was observed. This behaviour may be related to the cementation of the bonds, which helps to restrict the volume change during unloading, and/or related to the fact that the sands or silts exhibit negligible elastic strain upon unloading. Houston (1995) and Houston et al. (2001) observed similar behaviour.

Regarding the above-mentioned discussions and depending on the severity classification of the collapse potential mentioned in Table 2.3, the classification of the gypseous soil developed from "trouble" when inundated at vertical stress lower than $\sigma_v < 200$ kPa to "severe trouble" when inundation at $\sigma_v \geq 200$ kPa. Mixed soil was classified as "severe trouble" when inundated at $\sigma_v \geq 50$ kPa. The loess soil classification was modified from "no problem" when inundated occurred at $\sigma_v < 100$ kPa to "trouble" when inundation occurred at $\sigma_v \geq 100$ kPa.

In order investigate the variation in collapse deformation over time a constant vertical stress was applied to the saturated sample for a predefined duration (i.e. a LID of 14 days for GI and 70G30S and a LID of 2 days for LG soils).

Figure 5.5 presents the variation of collapse potential over time, while Figure 5.6 presents the degree of deformation of the soil sample over time. The degree of deformation can be calculated according to Equation 5.1 or Equation 5.2.

$$DD = \frac{h_o - h_t}{h_o - h_f} \times 100 \tag{5.1}$$

$$DD = \frac{e_o - e_t}{e_o - e_f} \times 100 \tag{5.2}$$

where:

$DD=$ the degree of deformation of soil sample [%].

$h_o, e_o=$ the initial height, void ratio of the soil sample before inundation at vertical stress equal to (σ_v).

$h_t, e_t=$ the height, void ratio of the soil sample at any time during inundation at same vertical stress (σ_v).

$h_f, e_f=$ the final height, void ratio of the soil sample at end of inundation at same vertical stress (σ_v).

The collapse potential and the degree of deformation for both gypseous soil and mixed soil increased linearly during inundation time.

(a)

(b)

(c)
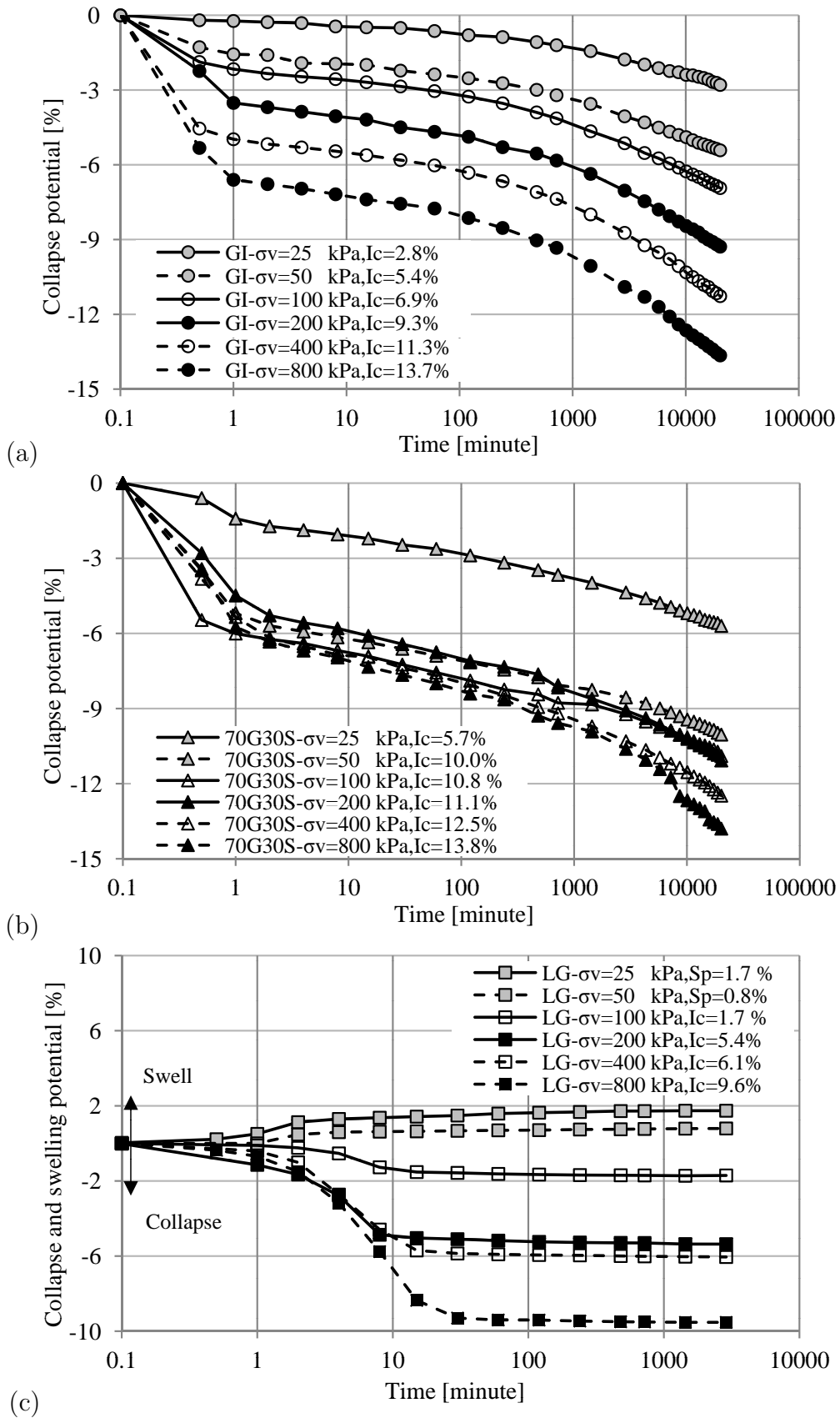
Figure 5.5.: Variation of collapse potential with time: (a) GI, (b) 70G30S and (c) LG soils.
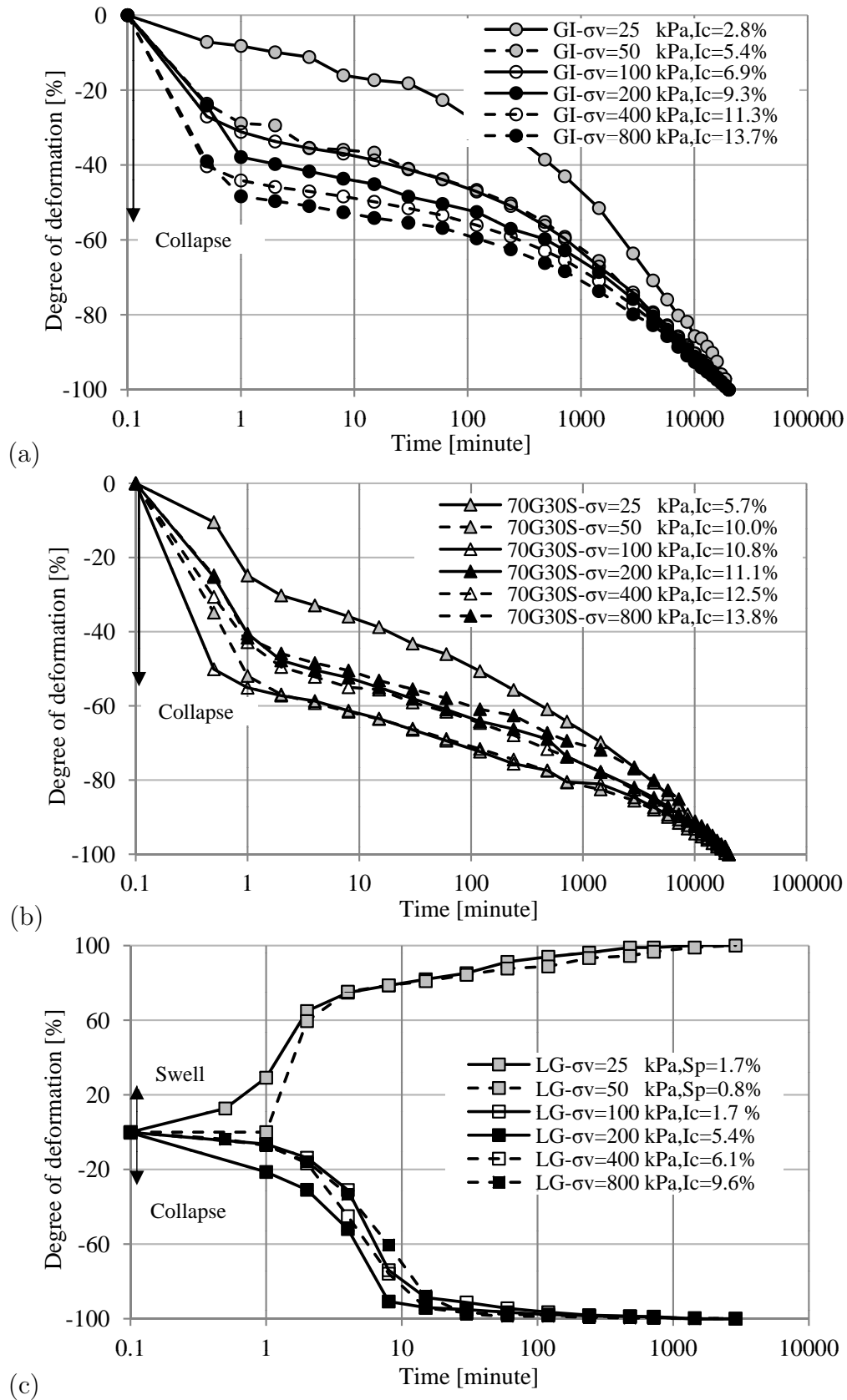
Figure 5.6.: Variation of degree of deformation with time: (a) GI, (b) 70G30S and (c) LG soils.

Gypseous soil showed a uniform a variation in the collapse potential over inundation time with respect to the stress level in the form of wide band, see Figure 5.5a. The same behaviour is observed for mixed soil but in the form of a narrow band, see Figure 5.5b. The reason for this behaviour relates to the type and activity of cementing bonds between soil particles. Natural formation of such bonds in gypseous soil deposits over time due to variations in overburden pressure and climate conditions produced a coherent and homogeneous microstructure. Therefore, the action of boding destruction upon inundation is proportional with the heterogeneity and degree of bonding. Al-Badran (2001) and Fattah et al. (2008) also observed such behaviour see Figure 5.7left. The gypsified mixed soil has the same type of cementing bonds, but the historical formation and homogeneity of soil fabric is absent. Therefore, it can be assumed that the major reason for the variation in the collapse deformation was the progressive strain of soil mass while the load was increased, and the rate of gypsum dissolved with respect to the applied pressure. Such behaviour was not observed for silty loess soil.

Figure 5.5c explains that the loess soil had a relative potential to swell under low vertical stress. A slight collapse over short durations was recorded. It is important to mention that there were three distinct regions of collapse taking place, see Figure 5.5c. Region 1 occurred when the water flowed through the porous stone and entered to the sample. Region 2 happened when the water percolated through the sample, which resulted in a reduction in capillary tension and a softening the bonds or macropeds. Finally, region 3 resulted in some minor or negligible creep when the collapse was complete. Such results completely corroborate the results of Lawton et al. (1992), see Figure 5.7right.

Regarding the foregoing discussion, the degree of deformation for both gypseous and mixed soils reached approximately 60% of the total value after only 10 minutes of inundation, see Figures 5.6a and 5.6b. A creep or secondary compression was recorded after 1440 minutes (24 hours) as a result of the continuous dissolution of gypsum particles over time. Such behaviour was also observed by Seleam (1988); Nashat (1990).

However, the behaviour of loess soil is completely different. The degree of deformation reached approximately 80% of its final value after merely 10 minutes of inundation, see Figure 5.6c. Then the soil reached equilibrium after a new arrangement of particles, and no further deformation was recorded after approximately 120 minutes of inundation. These results confirm the results of Lawton et al. (1992), (Figure 5.7right).

According to the above-mentioned results, in addition to results presented in the literature, the danger of collapse can happen during the first 2-4 hours after inundation, when about 60-80% of the final collapse occurs. In the field, the picture is slightly different because sudden full wetting of the soil deposits does not commonly occur.
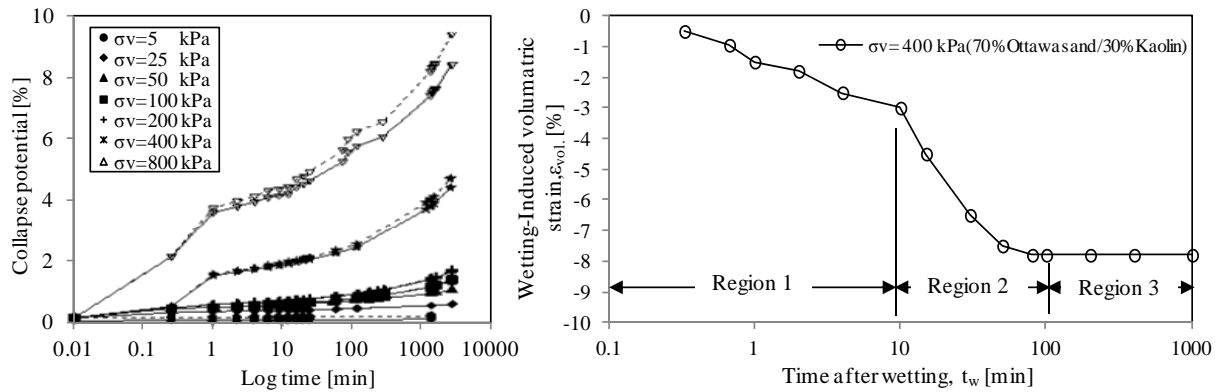
Figure 5.7.: Variation of volume change with time for collapsible soil, (left) gypseous soil (Al-Badran, 2001) and (right) loess soil (Lawton et al., 1992).

- **Double Oedometer-Collapse test results (DOT):**

In this subsection, double Oedometer collapse test results are presented. Two identical samples of each type of collapsible soil were tested. The first sample was loaded and unloaded at an unsaturated state, while the second was loaded and unloaded at a fully saturated state from the beginning of the test. The same SOT loading and unloading sequence was used in both cases. The load increment duration at the unsaturated state was one day for all soils, while it was seven days for GI and 70G30S soils and one day for LG soil at a saturated state.

The relationship between the void ratios versus the vertical stresses is shown in Figure 5.8, while Figures 5.9 and 5.10 compare the collapse potential obtained by the single and double Oedometer collapse test methods. The summary of single and double-Oedometer test results are summarized in Table 5.2.

According to these figures, it can be observed that all soil samples showed a collapse deformation as a result of full saturation at low vertical stress. Progressive development in the volumetric strain of the saturated sample was recorded when the applied load was increased. However, for both gypseous and mixed soils, the values of the collapse potential obtained from the single Oedometer method was relatively greater than those obtained by the double Oedometer method for the same vertical stress level. This behaviour can be explained by the continued existence of all the cementing bonds of gypsum particles in the soil structure until sudden inundation was induced at the specified pressure in SOT. In this instance large and quick deformations occurred as a result of volumetric strain development and the cementing bonds were softened by gypsum dissolution.
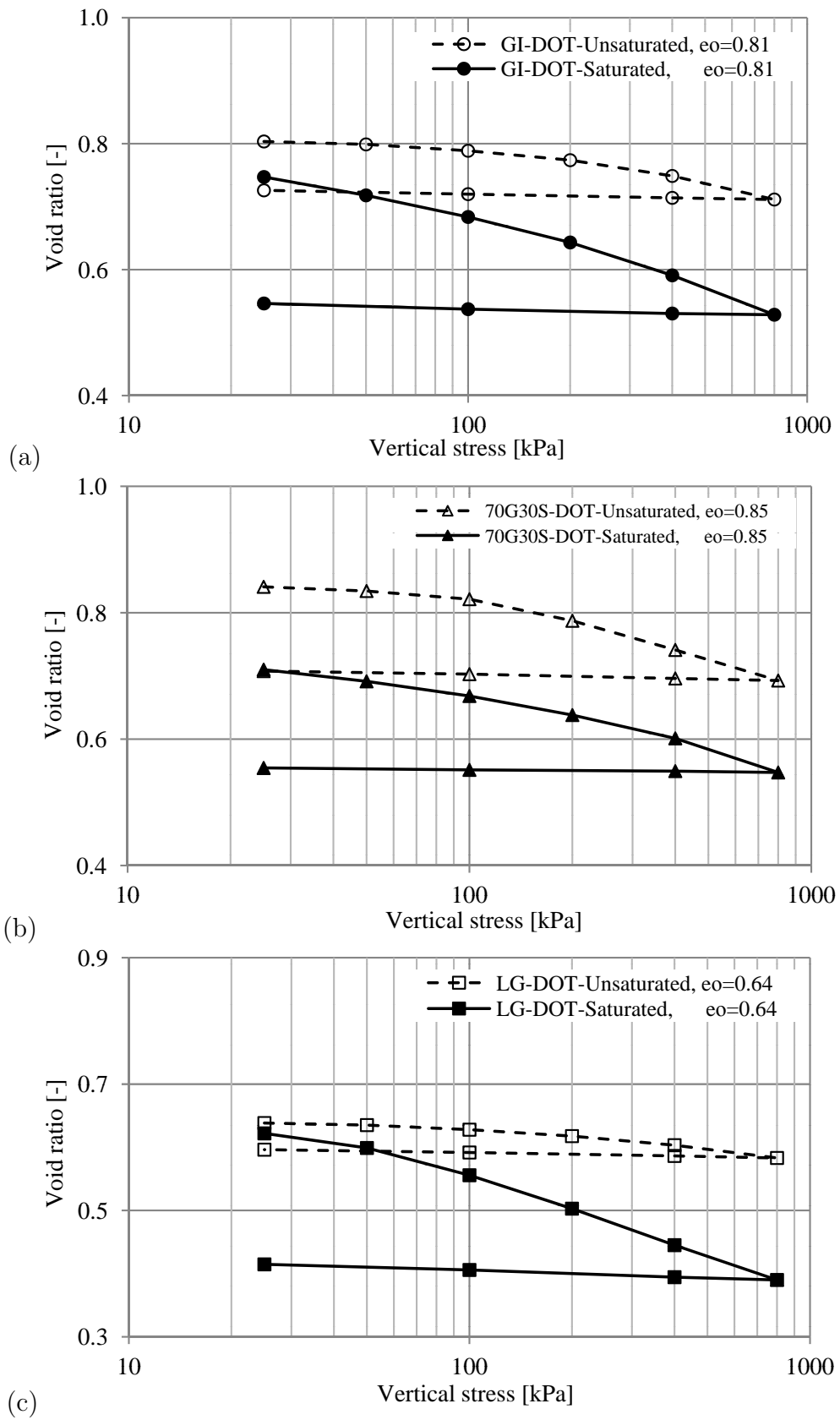
Figure 5.8.: Double Oedometer-collapse test: (a) GI, (b) 70G30S and (c) LG soils.

In the DOT method, the sample had already been stressed and the action of softening and gypsum dissolution had already started before it reached a specified collapse pressure. Furthermore, many studies indicated that the maximum collapse occurs when the inundation stress approaches the preconsolidation stress of the natural state compression curve, after which the increase in the degree of saturation directs the compression curve to the saturated soil curve (Lin & Wang, 1988; Al-Mufty, 2004).

Several collapse tests using SOT and DOT were conducted by different Iraqi researchers and confirmed that the collapse significantly increased with the incremental increases in inundation stress level, particularly after the preconsolidation stress of the natural soil, see Figure 5.9.

On the contrary, the collapse potential of loess soil determined by SOT was relatively smaller than the collapse potential value determined by DOT. This behaviour resulted from the continuous deformation and softening of interparticle bonding in a metastable soil structure, which occurred simultaneously with the rearrangement of this structure to a denser state. Moreover, no swelling was observed for the saturated loess sample test during the DOT even when it was loaded to a vertical stress lower than the maximum preconsolidation pressure. This is because the swelling potential dissipated when the sample was saturated at a seating load before starting the main loading stage, see Figure 5.10. Such results were also observed by Lawton et al. (1989, 1991).
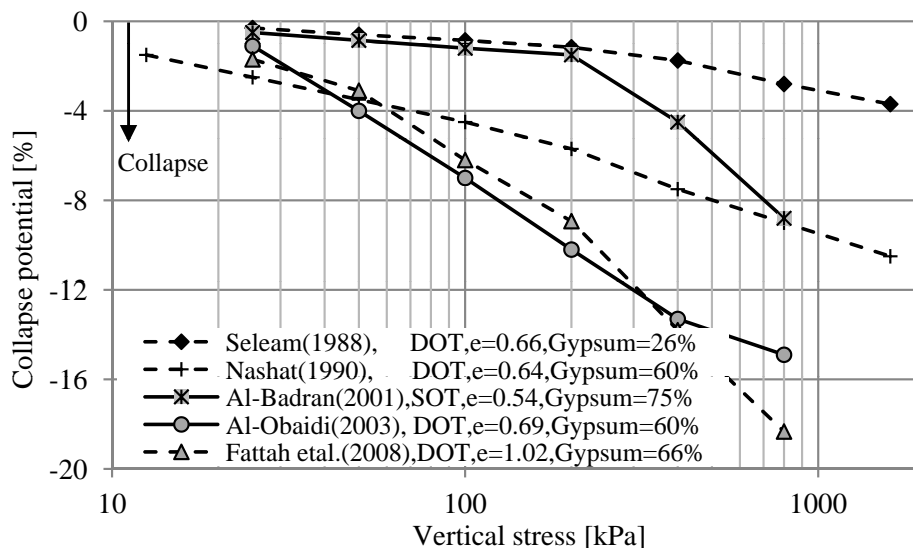
Figure 5.9.: Collapse potential versus inundation vertical stress for different gypseous soils from Iraq, data from (Seleam, 1988; Nashat, 1990; Al-Badran, 2001; Al-Obaidi, 2003; Fattah et al., 2008).
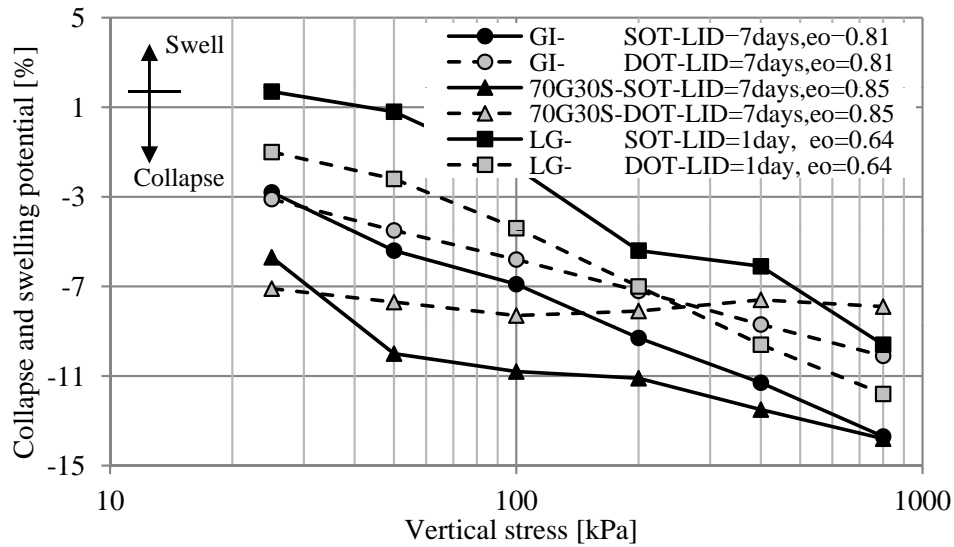
Figure 5.10.: Collapse and swelling potential versus inundation vertical stress for GI, 70G30S and LG soils.

On the other hand, Figure 5.10 shows that for the three selected soils, the collapse potential increased linearly with incremental increases in inundation vertical stress. No critical value of vertical stress was observed to determine the collapse potential.

In general, this behaviour can be attributed to the fact that when higher pressure is applied on looser structural specimens, a denser state of the soil mass is obtained especially under saturated conditions. High applied stress (particularly stress equal to or greater than the maximum preconsolidation pressure) also destroyed and closed all the cavities of the open metastable structural soil. Such results were also obtained by Seleam (1988); Nashat (1990); Fattah et al. (2008), see Figure 5.9.

5.2.2.2. Effect of initial dry density

The effect of initial dry density on the collapse potential is presented in this subsection. Figure 5.11 shows the results of single Oedometer collapse tests carried out under an inundation vertical stress of 200 kPa and at different initial dry densities. Figures 5.12 shows the variation of the initial void ratio with collapse potential for the three selected soils respectively. The summary of tests results are given in Table 5.3. The results indicated that the increases in initial dry density (i.e. decreases of the void ratio) caused gradual decreases in the value of the collapse potential.
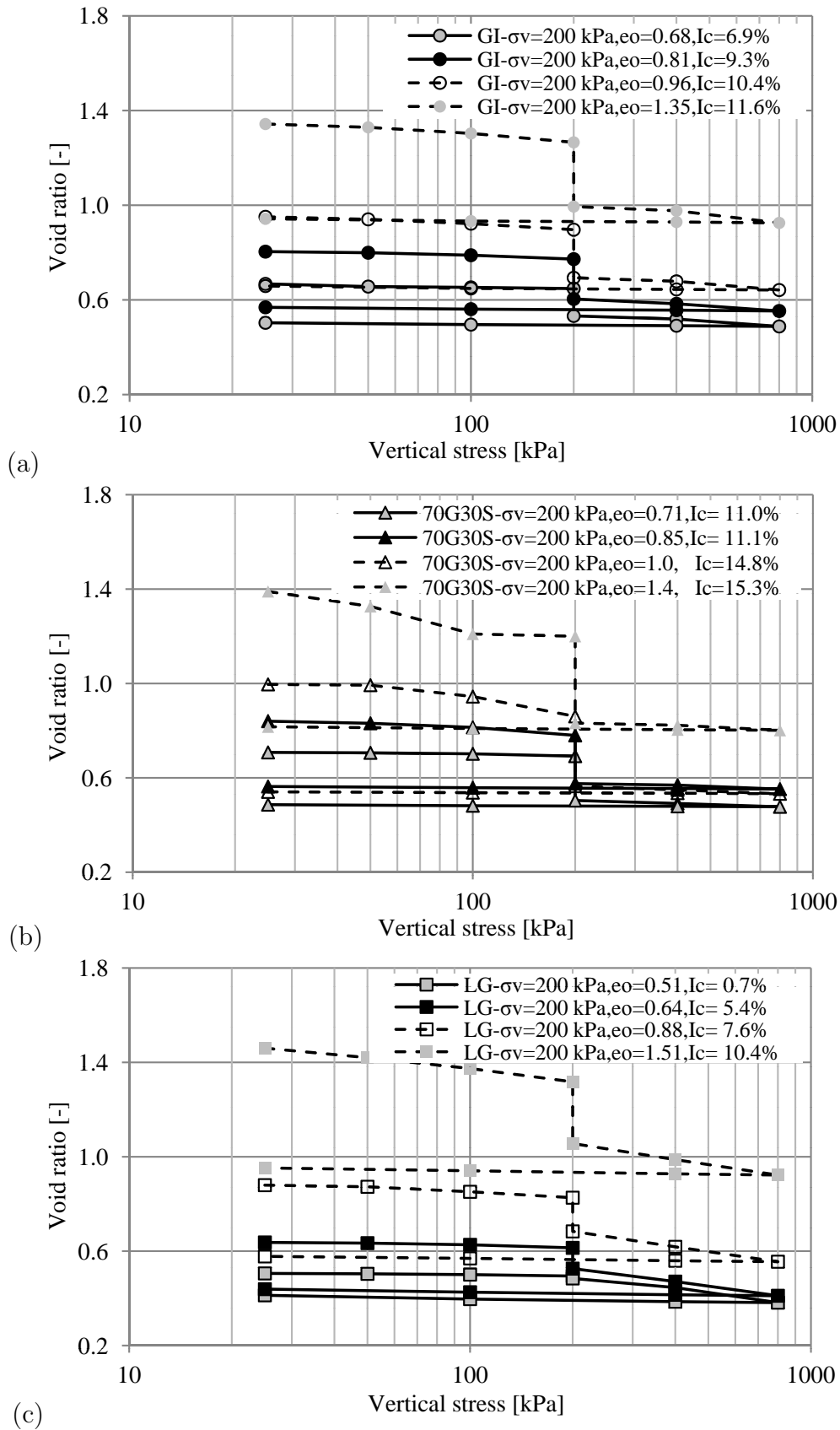
Figure 5.11.: Initial dry density effect on collapse potential: (a) GI, (b) 70G30S and (c) LG soils.
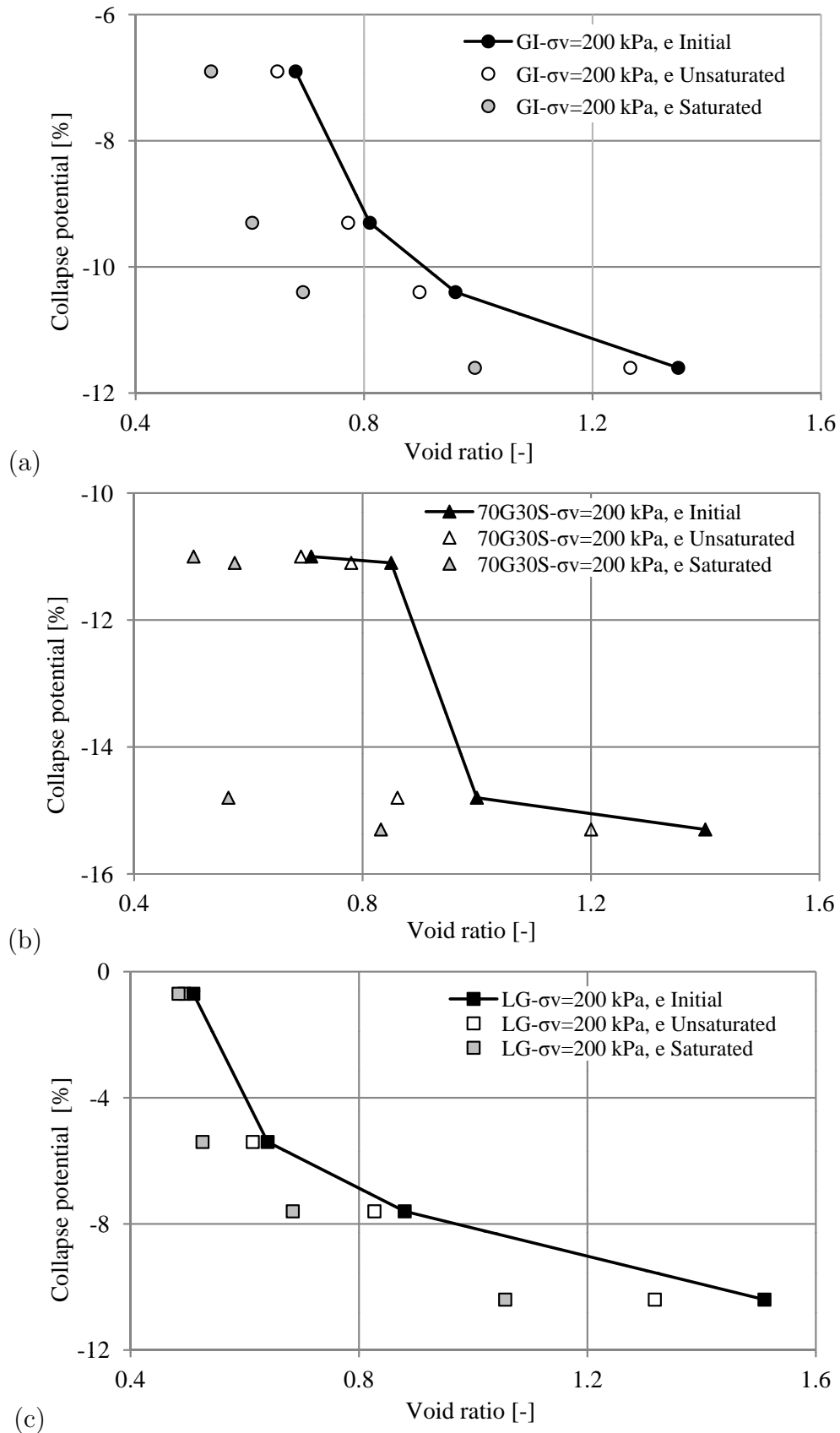
Figure 5.12.: Variation of void ratio with collapse potential: (a) GI, (b) 70G30S and (c) LG soils.

Table 5.3.: The summary of initial dry density effect on collapse potential at $\sigma_v=200$[kPa]

Soil type	GI				70G30S				LG			
e_o[-]	0.68	0.81	0.96	1.35	0.7	0.85	1.0	1.4	0.51	0.64	0.88	1.51
$\gamma_{do}[g/cm^3]$	1.4	1.3	1.2	1.0	1.4	1.3	1.2	1.0	1.74	1.6	1.39	1.05
$w[\%]$	0.25	0.25	0.25	0.25	0.25	0.25	0.25	0.25	2.5	2.5	2.5	2.5
$I_c[\%]$	6.9	9.3	10.4	11.6	11.0	11.1	14.8	15.3	0.7	5.4	7.6	10.4

This resulted from grain densification, cavities and void elimination; a more stable structure was obtained as the compaction effort on soil sample increased. The results presented by Al-Mufty (2004) in Figure 5.13 confirm the obtained results. Upon inundation and after around 2880 minutes, the void ratio sharply decreased over time for both gypseous and mixed soils. After that, secondary compression or creep strain was recorded, see Figures 5.14a and 5.14b. However, at high initial void ratios in loess samples, significant variation in the void ratio during inundation was observed. However, Figure 5.14c explains that a slight to insignificant changes in void ratio were observed for loess samples prepared at initial void ratio of 0.64 and 0.51, respectively. From these results, it can be concluded that initial dry density plays an important role in the estimation of the collapse potential and/or the selection of soil mitigation techniques. Clevenger (1958); Al-Khuzaie (1985); Lawton et al. (1989, 1992); Al-Mufty (1997, 2004) reported similar conclusions.
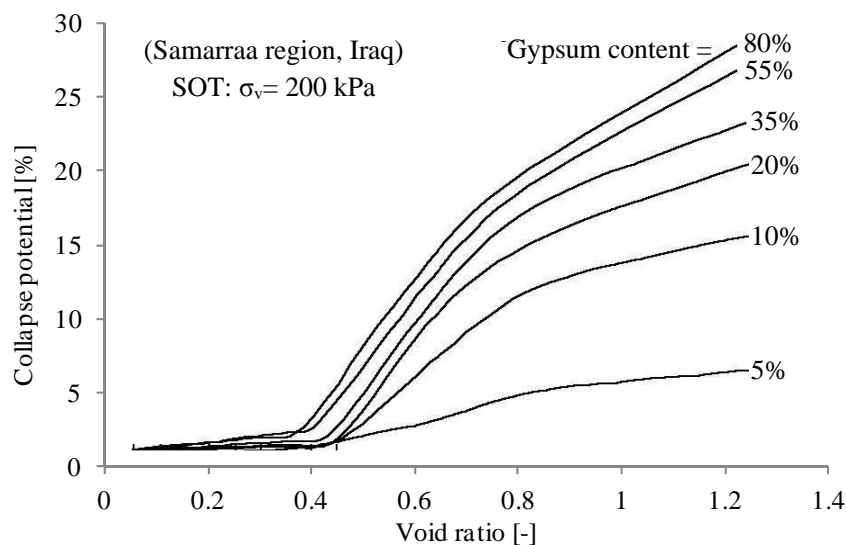
Figure 5.13.: Effect of initial void ratio on collapse potential, Iraq (Al-Mufty, 2004).
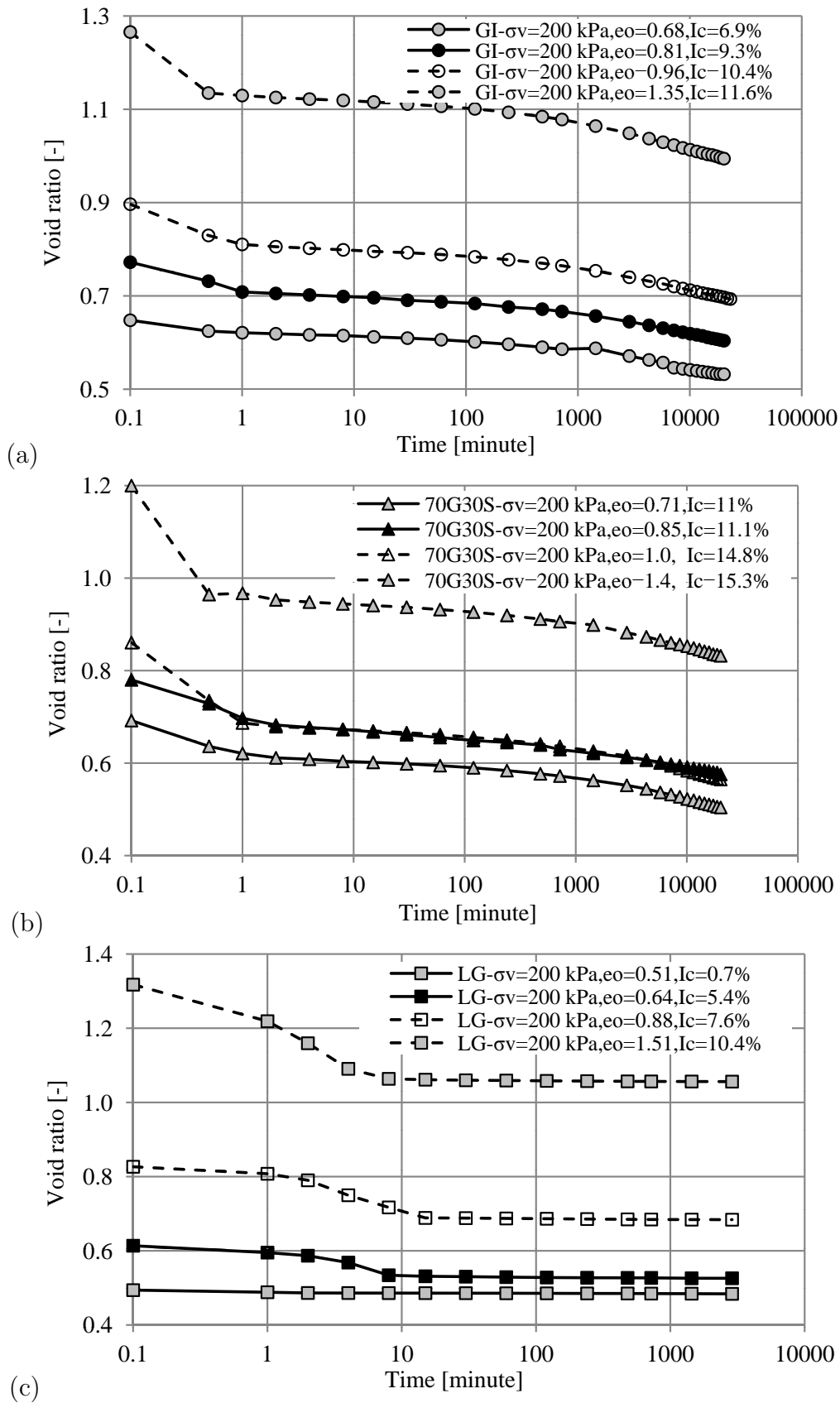
Figure 5.14.: Void ratio versus time for saturated: (a) GI, (b) 70G30S and (c) LG soils.

5.2.2.3. Effect of the initial degree of saturation

The effect of the initial degree of saturation on the collapse potential is presented in this subsection. Figure 5.15 shows the results of single Oedometer collapse tests conducted under an inundation vertical stress of 200 kPa and at various initial degrees of saturation, while Figure 5.16 shows the variation in the collapse potential with the initial degree of saturation for the three selected soils. The summary of test results is given in Table 5.4. In these tests, the concept of the critical degree of saturation and its effect on the collapsibility characteristics was also investigated. The critical degree of saturation can be defined as "It is that degree of saturation after which the sample has behaviour similar the saturated soil" (Jennings & Burland, 1962). While Lawton et al. (1989, 1992) defined the critical degree of saturation as "the initial or prewetting degree of saturation above which negligible collapse potential exists for all expected ranges of relative compaction and overburden pressure, depends on both the dry density and overburden pressure". In general, the increase in the initial degree of saturation causes a noticeable reduction in the collapsibility of all tested samples. In other words, when the soil sample was prepared to a degree of saturation approximately 20% greater than the degree of saturation at hydroscopic water content, the collapse potential reduced to approximately 55% for both gypseous and mixed soil, and to approximately 83% for loess soil, see Table 5.4. Moreover, for both gypseous and mixed soils, the observed critical degree of saturation ranged from 60-70%, while loess soil ranged from 30-40%, see Figure 5.16. This behaviour can be attributed to substantial soil compression that occurred even with a small increase in the degree of saturation. For this reason, the soils show low potential to collapse at a vertical stress of σ_v=200 kPa because most of this potential vanished at low applied vertical stress.

Furthermore, for both gypseous and mixed soils, low initial degrees of saturation could not soften all gypsum bonds between soil particles. Therefore, significant water content and time duration were required in order to completely soften cementing bonds and achieve a new arrangement in the soil structure. The presence of secondary compression (i.e. creep) for these soils led to complex behaviour particularly when the degree of saturation significantly varied (5.17a and 5.17b). This behaviour explains why gypseous soil has a more critical degree of saturation than loess soil. These results corroborate the results obtained by Al-Ani & Seleam (1993). After the critical degree of saturation had been reached, no considerable variation was observed in the void ratio of the saturated curve for the sample prepared at different initial degrees of saturation and loaded up to the same vertical stress, see Figure 5.17c.

(a)

(b)

(c)
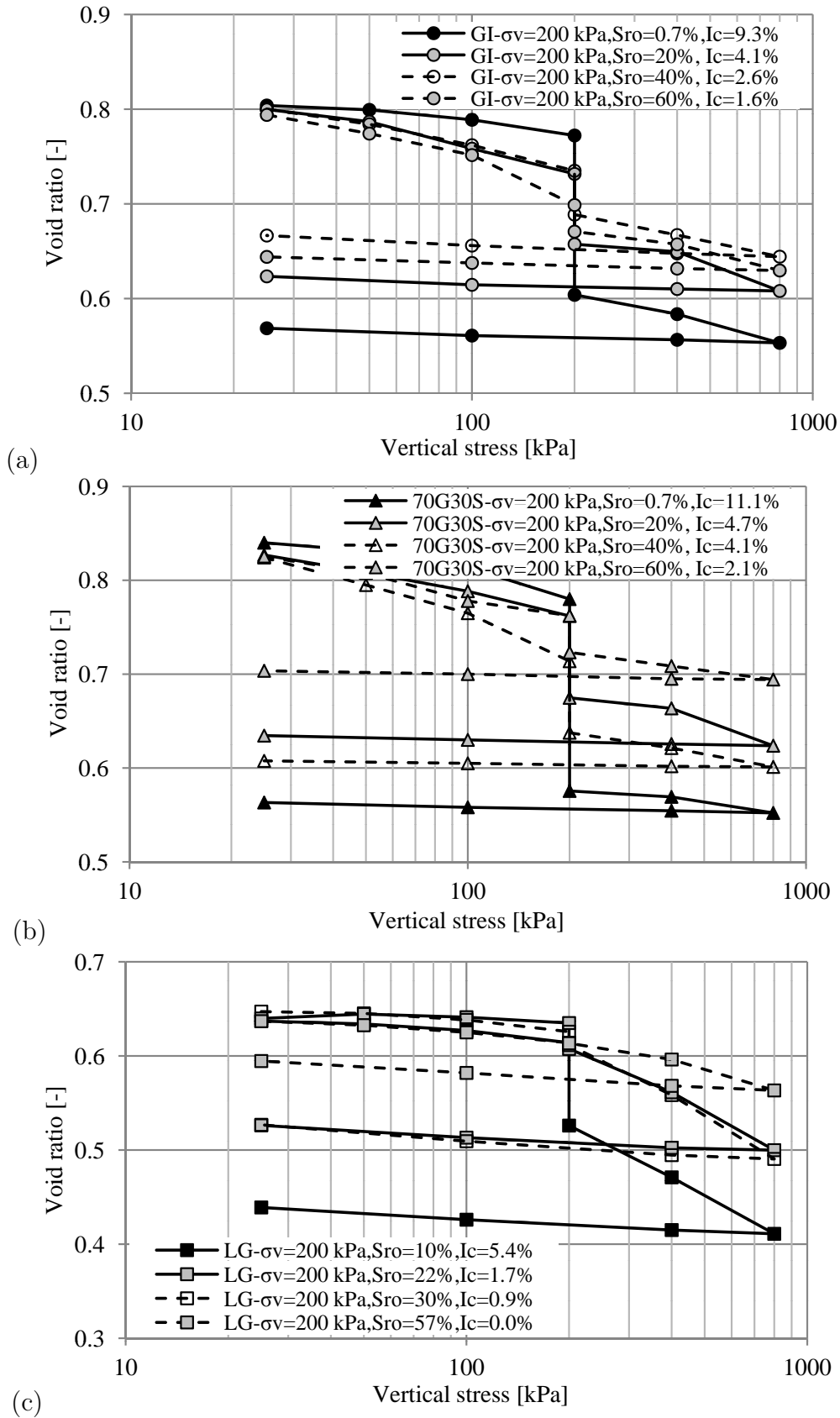
Figure 5.15.: Degree of saturation effect on collapse potential for: (a) GI, (b) 70G30S and (c) LG soils.

Many studies corroborate these results such as (Feda, 1988; Grabowska-Olszewska, 1988; Lawton et al., 1989, 1991, 1992; Nashat, 1990) and Houston et al. (2001) shown in Figure 2.13. It is important to mention that the collapse potential is independent on optimum moisture content (i.e. optimum degree of saturation) of standard compaction curve but its initial degree of saturation dependent, see Figure 5.16 and Table 5.4.

In summary, the inundation vertical stress, initial dry density and the initial degree of saturation are the most important factors affecting the estimation and evaluation of the collapsibility characteristics of unsaturated soils. Hence, the collapse potential significantly increases as inundation vertical stress increases, and decreases when the initial dry density and the initial degree of saturation increase.
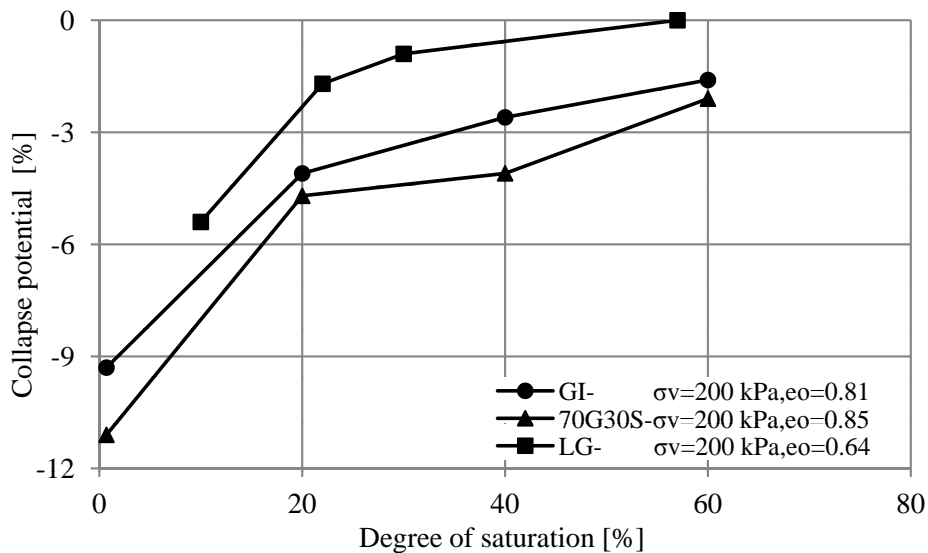
Figure 5.16.: Variation of degree of saturation with collapse potential for: GI, 70G30S and LG soils.

Table 5.4.: Summary of initial degree of saturation effect on the collapse potential.

Soil type	GI				70G30S				LG			
e_o[-]	0.81	0.81	0.81	0.81	0.85	0.85	0.85	0.85	0.64	0.64	0.64	0.64
Sr_o[%]	0.7	20	40	60	0.7	20	40	60	10	22	30	57
$Sr_{opt.}$[%]	49.2	49.2	49.2	49.2	73.4	73.4	73.4	73.4	84.3	84.3	84.3	84.3
w[%]	0.25	6.9	13.8	20.6	0.25	6.7	13.5	20.3	2.5	4.8	9.7	14.6
I_c[%]	9.3	4.1	2.6	1.6	11.1	4.7	4.1	2.1	5.4	1.7	0.9	0.0
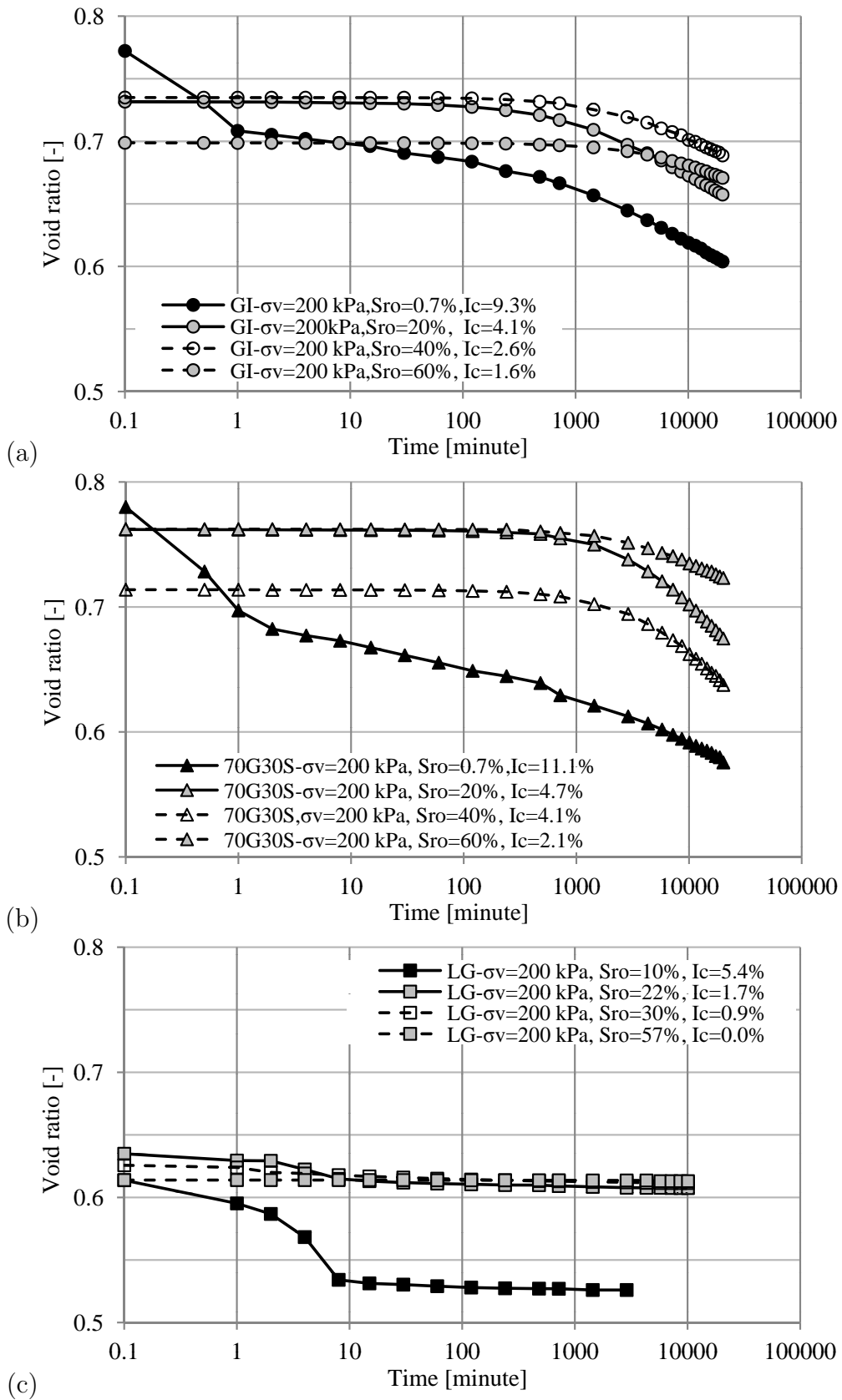
Figure 5.17.: Void ratio versus time for saturated: (a) GI, (b) 70G30S and (c) LG soils.

5.3. Results of volume change under suction control test

In this test, 14 samples were tested for the three selected soils, of which 11 soil samples were utilised for the constant net stress-suction decreases (wetting-collapse) test and three samples were used for the constant net stress-suction increases (drying) test. The initial conditions of the soil samples and the boundary conditions of the test are shown in Tables 3.5 to 3.7 and the stress paths for both tests are explained in Figure 4.12.

5.3.1. Constant net stress-suction decreases (wetting-collapse) test (CNWT)

The test results for the three selected soils are shown in Figures 5.18 to 5.24. Figure 5.18 indicates the relationship between void ratio and net vertical stress. Figures 5.19 to 5.22 demonstrate the variation in the collapse potential, void ratio, gravimetric water content and degree of saturation with applied suction respectively. Figure 5.23 shows the comparison of the collapse and swelling potential obtained by single step wetting and multi-step wetting tests. Figure 5.24 shows the evolution of the collapse potential with the degree of saturation. The summary of test results is presented in Table 5.5.

Figure 5.18 indicates that the gypseous, mixed and loess soils presented low compressibility when loaded under unsaturated conditions (i.e. at their initial suction). Upon gradual wetting the soil by multi-step suction decreases under the same constant net vertical stress, the volume change during suction- equilibrium stage of soil sample is denoted as collapse deformation. The measured collapse potential increased (Figure 5.19) and the values of void ratio decreased (Figure 5.20) progressively as the wetting net vertical stress increased and the applied suction decreased. The increase in the collapse potential and the decrease in the void ratio reached their maximum values at zero suction. However, Figures 5.19c and 5.20c indicate that the loess soil (LG) did not present any collapsing behaviour when the suction was reduced to a stress level equal to or lower than the maximum preconsolidation pressure (i.e. σ_n= 50 and 100 kPa). Furthermore, insignificant swell with relative increases in void ratios was observed at σ_n= 100 kPa when the applied suction ranged between 6100 and 50 kPa.

For GI soil, the collapse potential reached over 60% of its final value when the suction decreased to ψ=800 kPa, where the gravimetric water content (w) and the degree of saturation (Sr) ranged between 1.5-2.5% and 6-8.5% respectively. Likewise the collapse potential exceeded 85% of its final value when the suction was reduced to ψ=50 kPa corresponding to the range of w=3.5-5% and Sr=11-29%.
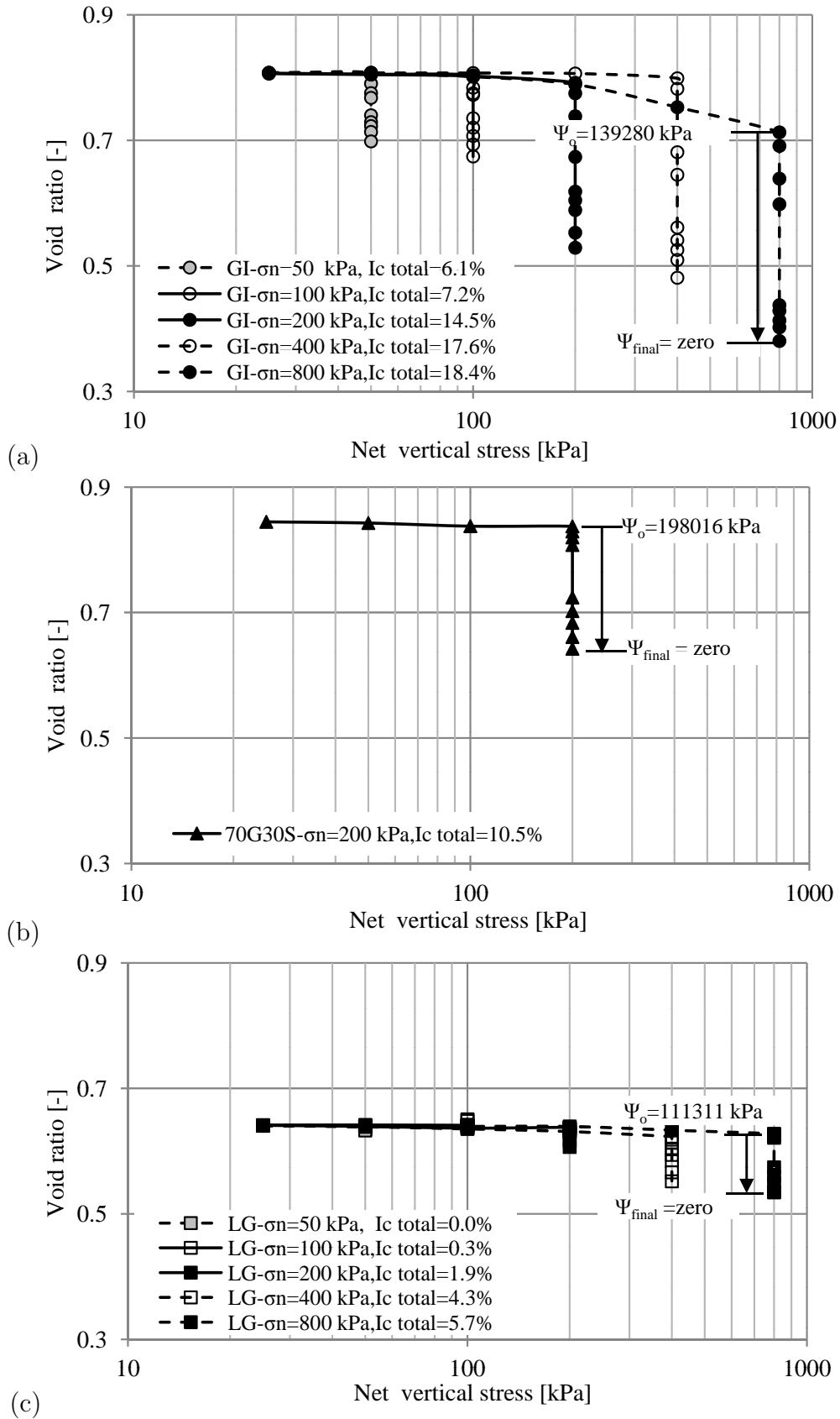
Figure 5.18.: Void ratio versus net vertical stress of CNWT for: (a) GI, (b) 70G30S and (c) LG soils.
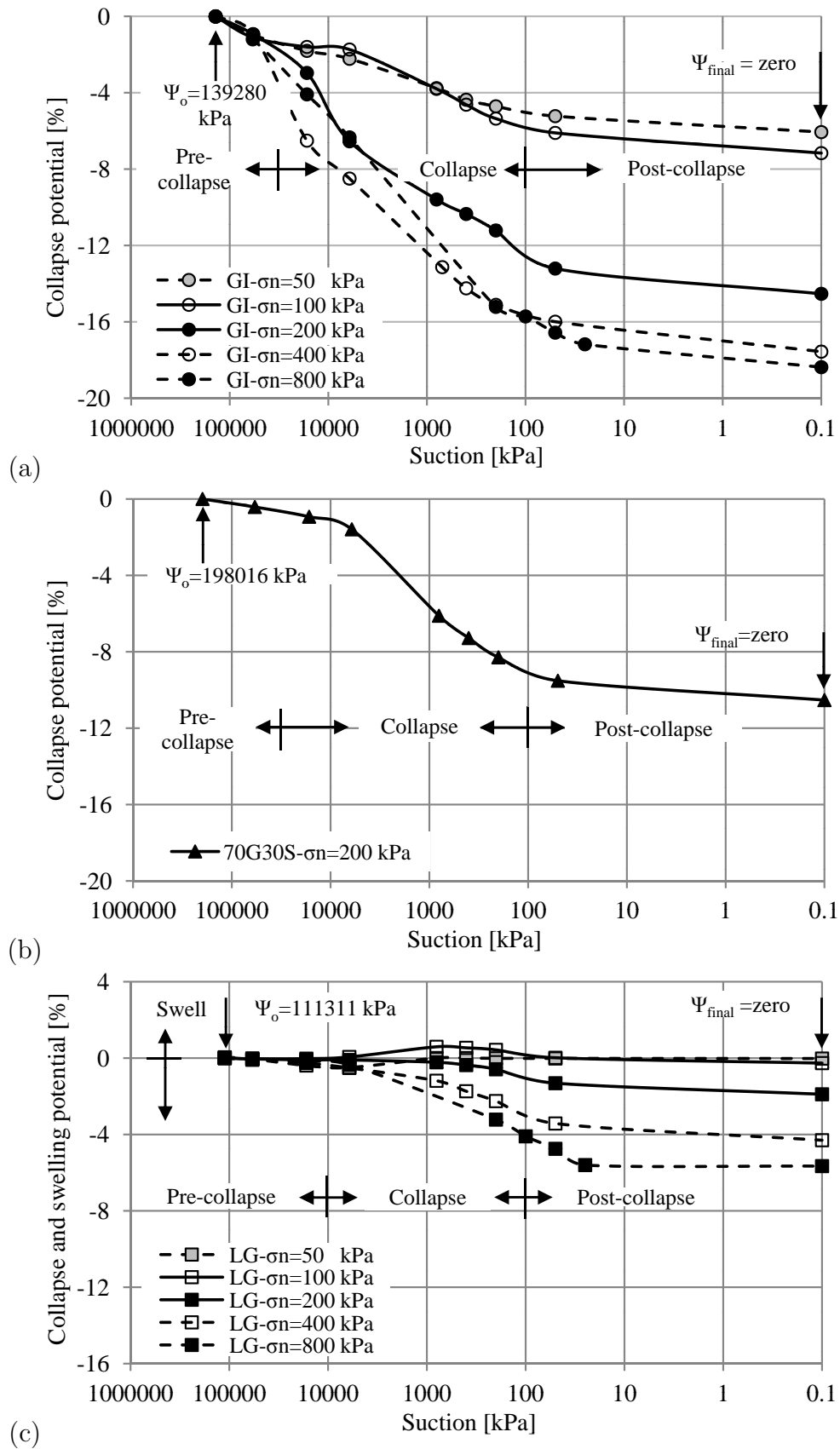
Figure 5.19.: Variation of collapse potential with suction of CNWT for: (a) GI, (b) 70G30S and (c) LG soils.

(a)

(b)

(c)
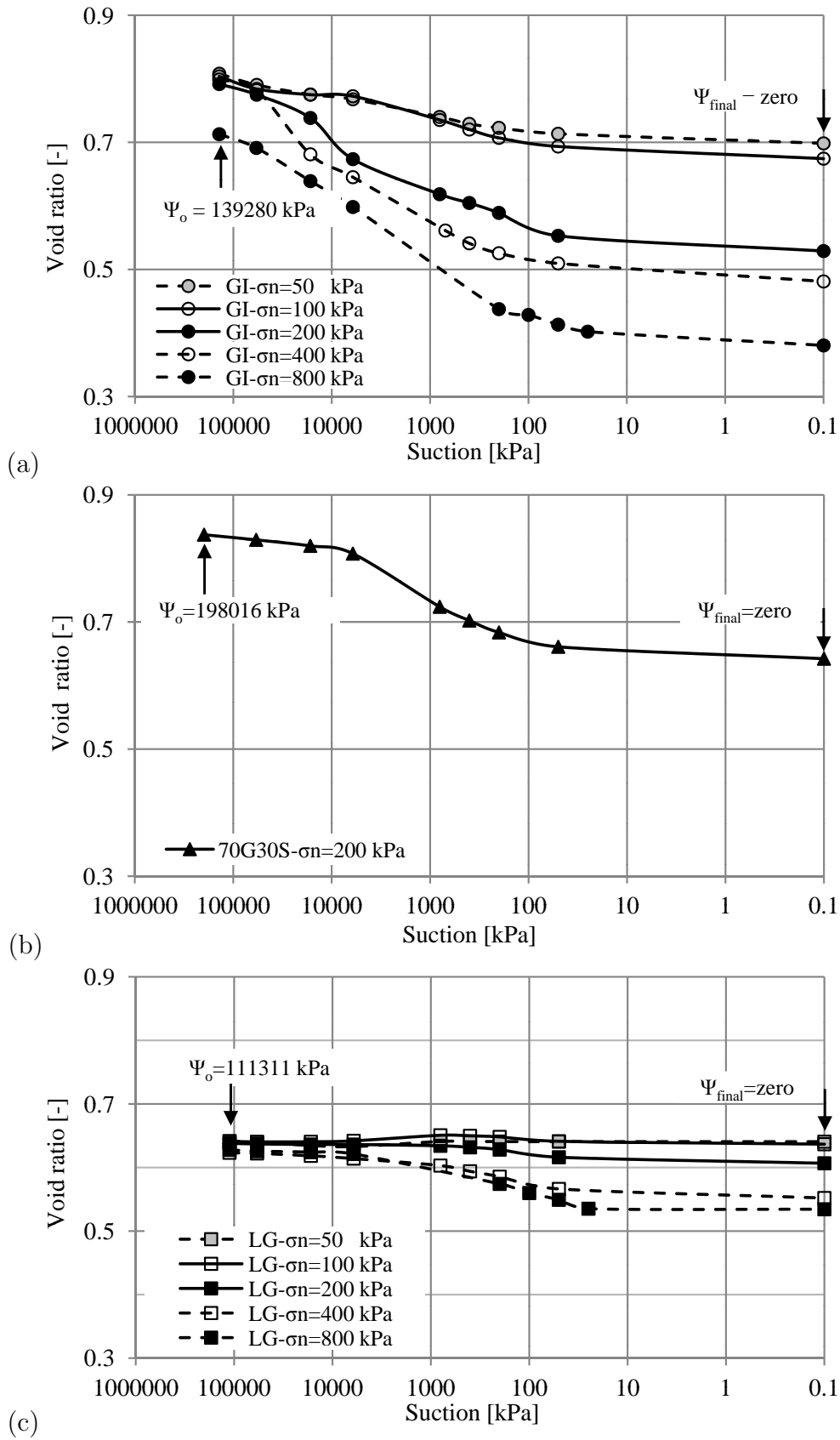
Figure 5.20.: Variation of void ratio with suction of CNWT for: (a) GI, (b) 70G30S and (c) LG soils.

This behaviour was the same for all the samples loaded under a range of net vertical stress equal to 50-800kPa (see Figures 5.19a, 5.21a and 5.22a). A similar behaviour was observed for 70G30S soil. The collapse percent was 58% of its final value at ψ=800kPa, w=0.3% and Sr=1%, and 90% of its final value at ψ=50kPa, w=6% and Sr=22% (see Figures 5.19b, 5.21b, and 5.22b).

For LG soil, the soil structure had insignificant potential to swell under a net vertical stress ranging between 50-100kPa and ψ=6100-50kPa, w=5-15% and Sr=19-61%. This swell could be attributed to the decrease in mean effective stress resulting from the reduction in matric suction, which in turn led to a relative increase in the void ratio. Moreover, the collapse potential reached over 12% of its final value when ψ=800kPa, w=4-5% and Sr=17-21%, and over 70% when ψ=50kPa, w=9-11% and Sr=39-49% (see Figures 5.19c, 5.21c, and 5.22c).

In other words, three main distinct phases are developed in the collapse mechanism of the tested soils: the pre-collapse phase, the collapse phase and the post-collapse phase. Such collapse mechanism is also observed and described by Pererira & Fredlund (2000) (subsection 2.8.4.2). In the pre-collapse phase, insignificant collapse deformation occurred with respect to a relatively large decrease in the value of imposed suction. This behaviour can be attributed to the action of cementing bonds between soil particles. The devaluation of the suction at that stage may stimulate gypsum-sand and clay-silt bonds, which start softening in place without any movement or deformation. Therefore, this action was insufficient to cause collapse deformation in the soil structure.

Pererira & Fredlund (2000) attributed this behaviour to the elastic compression of the soil structure without grain slippage. This phase of deformation arose at high suction ranges (i.e. $\psi\geq$ 50000 kPa for GI and 70G30S, $\psi\geq$ 10000 kPa for LG, see Figure 5.19). The collapse phase occurred at intermediate ranges of suction (i.e. ψ=100-50000 kPa for GI and 70G30S, ψ=100-10000 kPa for LG, see Figure 5.19) and could be recognized due to significant volume change and collapse deformation. This deformation was induced after only a few hours of the suction reduction, and it continued until the soil suction reached equilibrium at the microstructure level. However, this behaviour can be attributed to the collapse mechanism at both the microstructure and macrostructure level of analysis. At the microstructure level, the soil particles could not maintain their position during loading due to the open structure of the collapsing soil, the absence of strength and capillary forces between the particles, and weaknesses caused by a reduction in suction.

Moreover, for both GI and 70G30S soils, the gypsum bonds that connected the soil particles tended to be removed or softened after the disappearance of the suction, resulting in collapse.
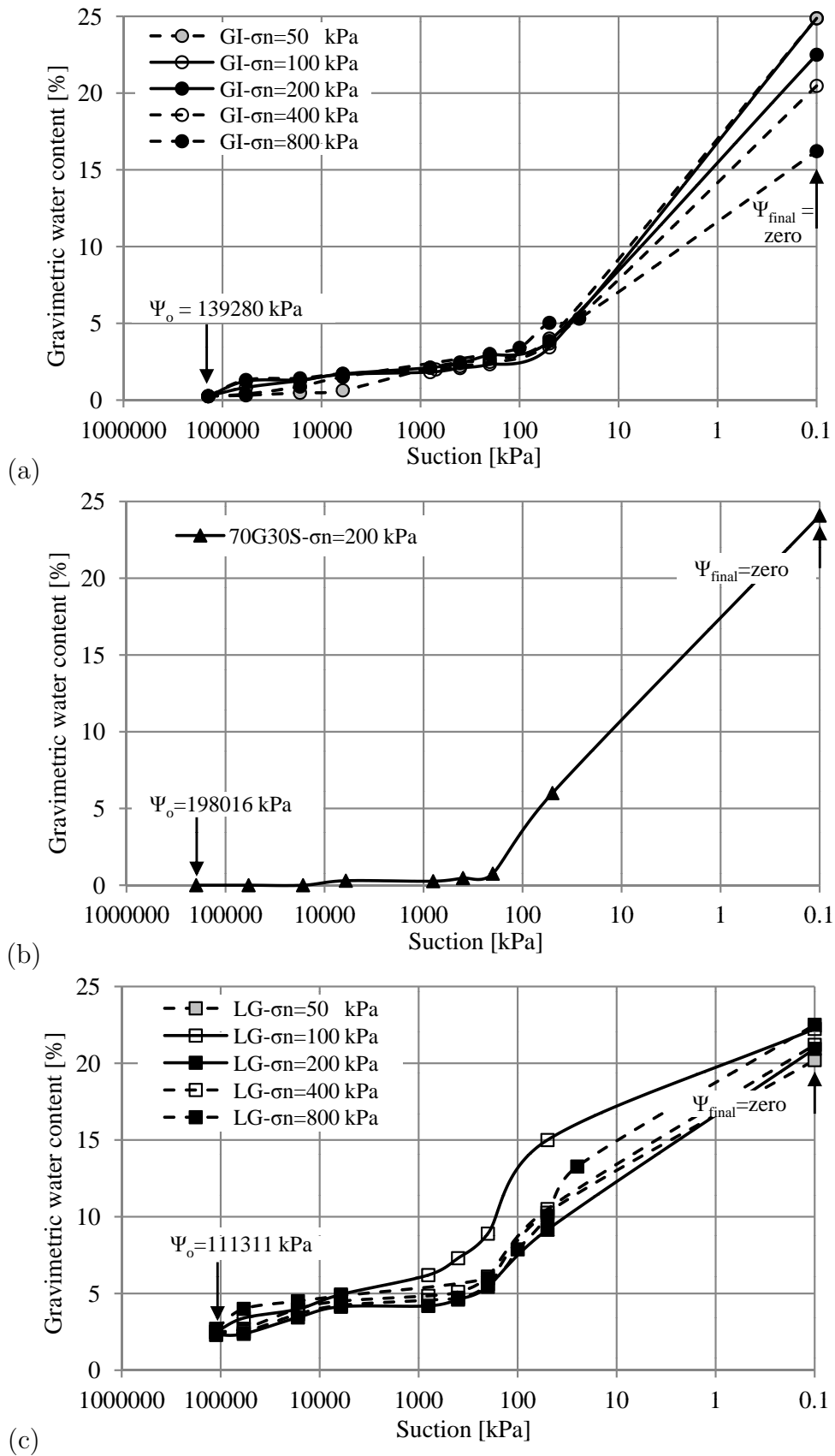
Figure 5.21.: Variation of gravimetric water content with suction of CNWT for: (a) GI, (b) 70G30S and (c) LG soils.
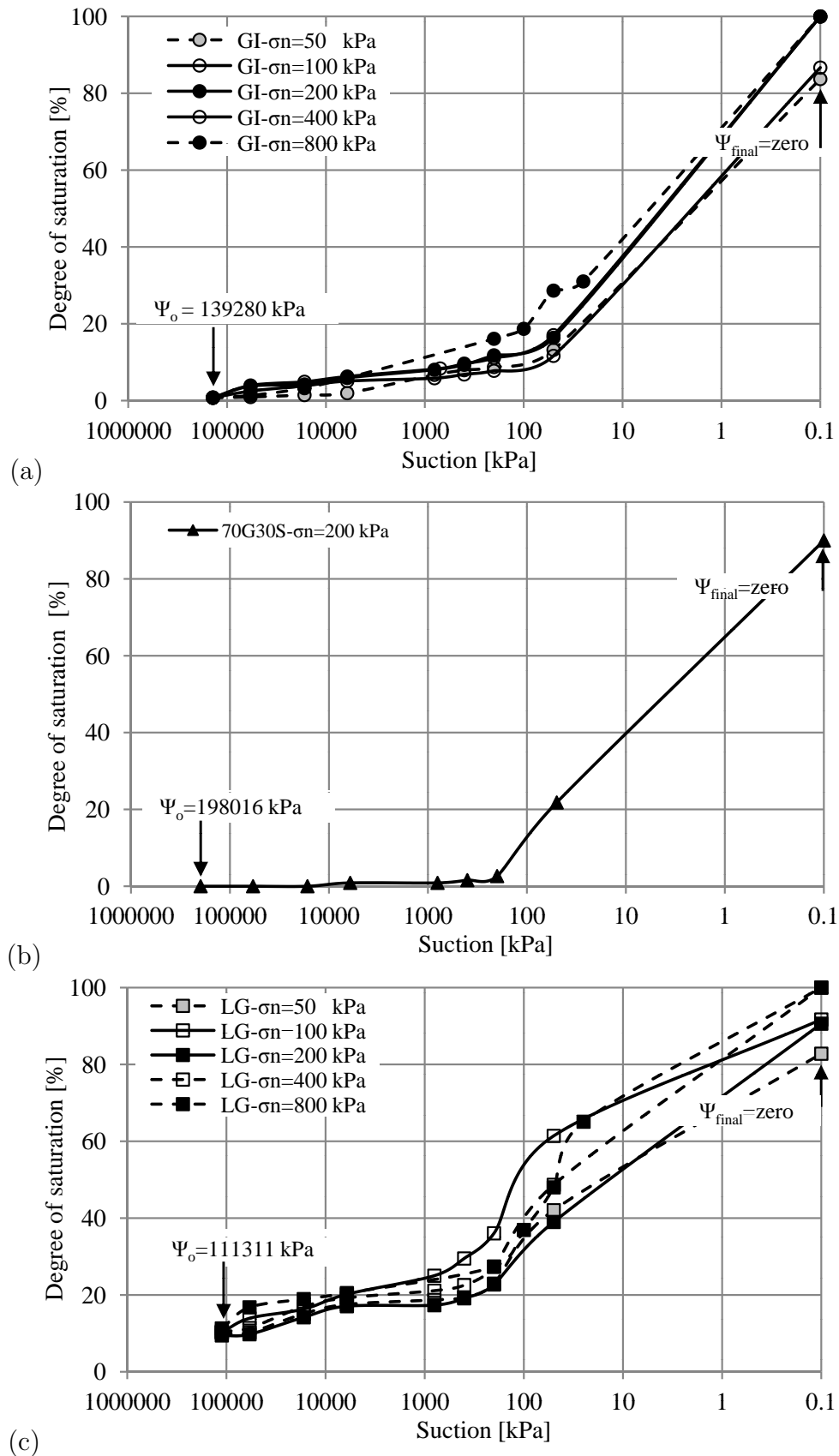
Figure 5.22.: Variation of degree of saturation with suction of CNWT for: (a) GI, (b) 70G30S and (c) LG soils.

For LG soil, collapse occurred as a result of the dispersion and disruption of silt-clay bridges or buttresses between loosely packed silt grains leading to initial rapid collapse of the interparticle matrix. At the macrostructure level, collapse deformation occurred as a result of the grains densifying and rearranging into a more closely packed structure after the cavities had crashed and had been destroyed by stress redistribution over time. In the third phase (i.e. post-collapse) the volume change commonly occurred at a low suction range (i.e. $\psi \leq 100$ kPa), and it was characterised by small volumetric deformations as a response to a further reduction in suction after reaching nearly full saturation. This deformation occurred because of secondary compression (i.e. creep) of the softened soil mass especially for GI and 70G30S soils. The test results also indicated that the gravimetric water content (Figure 5.21) and the degree of saturation (Figure 5.22) similarly increased as the suction of the soil was reduced from the initial value to zero irrespective of the differences in soil collapse caused by different net vertical stresses. In other words, when the amount of water in the soil sample increased at a low suction range (i.e. $\psi \leq 100$ kPa) the volume of air in the pore space decreased due to pore collapses. These results also showed that it was not possible to reach fully saturated soil sample at zero suction especially at low values of net vertical stress. This behaviour occurred because the soil structure still contained some air bubbles trapped between the soil particles.

In addition, the results indicated that the measured collapse potential (I_c) of GI soil obtained by multi-step wetting (i.e. CNWT) was relatively larger than those values obtained by single step wetting (i.e. SOT), see Figure 5.23.
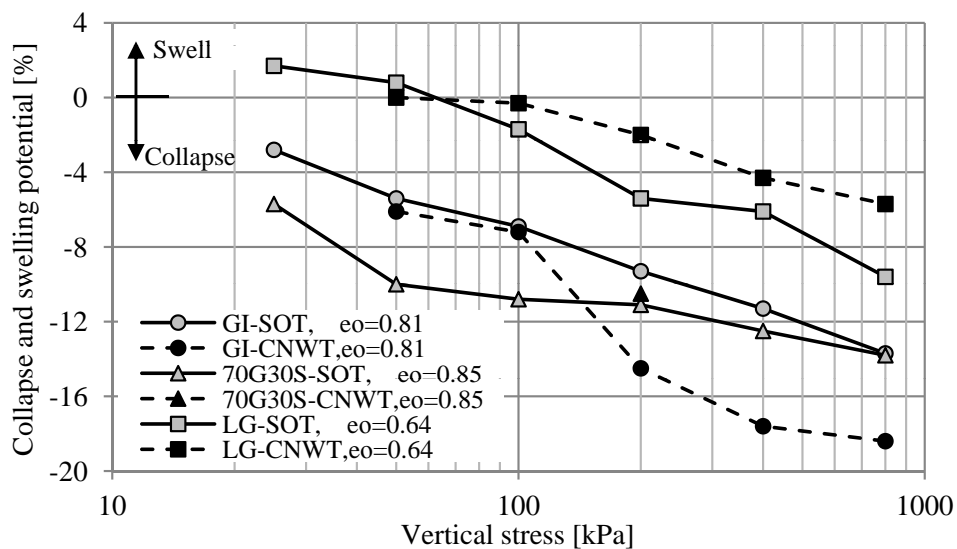
Figure 5.23.: Comparison of collapse and swelling potential obtained by SOT and CNWT.

For 70G30S soil, one test available for this comparison which indicated that both of the I_c values were nearly identical, while the opposite was observed for LG soil. This behaviour resulted from the dissolution of gypsum agents that induced the collapse deformation being comparable with the value of imposed suction (i.e. the degree of wetting) in the case of cementing bonds by gypsum particles. The new gypsum bonds rebuilt during the suction-equilibrium stage by non-dissolved gypsum particles could potentially collapse when the suction conditions approached the saturated state. Therefore the accumulative collapse potential rises with a successive reduction in suction values. This behaviour was not observed for the silty loess samples, where the amount of collapsed air voids in the pores seemed to rise when the suction dropped in single step (i.e. SOT) especially at a high stress level. The capillary forces and the silt-clay buttress bonds in the loess structure no longer have the ability to rebuild themselves after destruction.

From the foregoing discussion, it can be concluded that the collapse deformation of collapsible soils was considerably stress path dependent and was a function of net normal stress, suction and the degree of saturation. However, the changes in the volume of collapsible soils corresponded mostly to the changes in the degree of saturation and suction. Full saturation of the soil sample was not necessary to achieve final collapse as schown in Figure 5.24. In other words, partial saturation to a degree lower than 30% could introduce the final value of the collapse potential for naturally gypseous and artificially gypsified soils, particularly at low suction ranges regardless of net vertical stress.
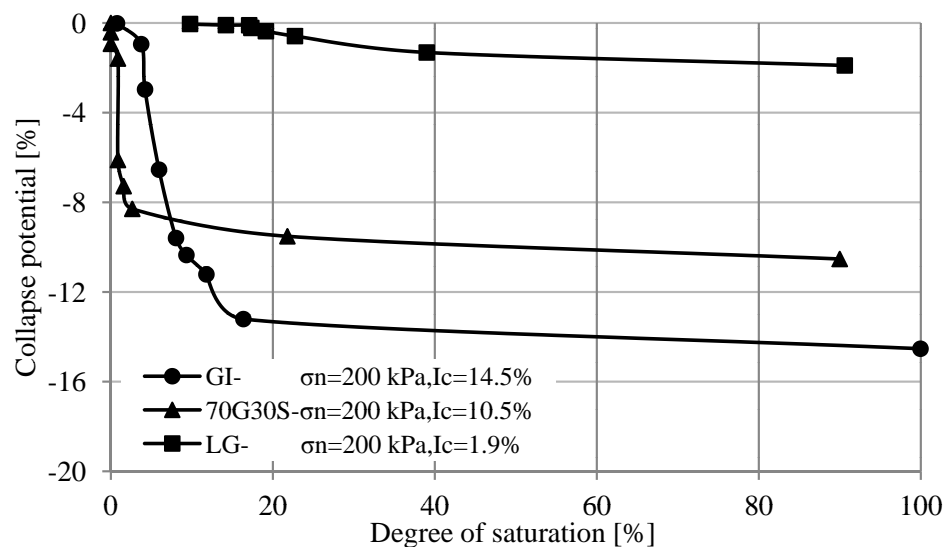
Figure 5.24.: Collapse potential versus degree of saturation of CNWT for: (a) GI, (b) 70G30S and (c) LG soils.

However, loess soils displayed the same behaviour with a degree of saturation near to 50% and under net normal stress greater than the maximum preconsolidation pressure. The estimated collapse potential obtained by utilising the constant net vertical stress-suction decreases method was more reliable and comparable to field conditions than the single Oedometer collapse method. The above-mentioned interpretations and discussion regarding CNWT were supported and confirmed by research conducted by Tadepalli & Fredlund (1991) (see Figure 2.10), Feda (1995), Habibagahi & Mokhberi (1998),Pererira & Fredlund (2000) (see Figure 2.11), Houston et al. (2001) (see Figure 2.13), Nelson et al. (2011); Vilar & Rodrigues (2011) and Haeri et al. (2013) (see Figure 5.25).
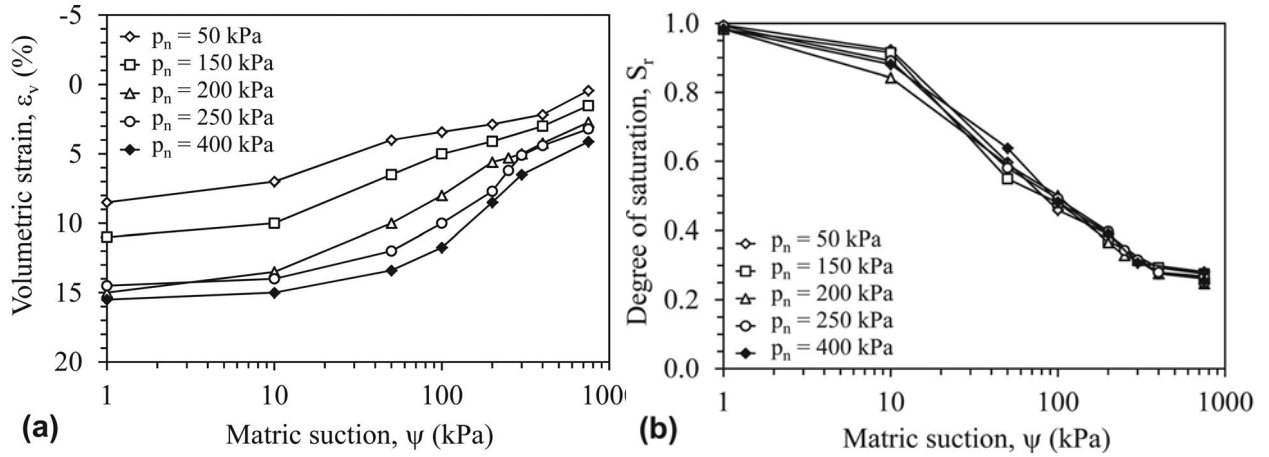
Figure 5.25.: The results of wetting-induced collapse tests of Aeolian loessial soil from northeast Iran using suction-controlled triaxial setup (Haeri et al., 2013).

Table 5.5.: Summary of the constant net stress-(wetting and drying) tests.

Soil type	$e_o[-]$	Test type	$w_o[\%]$	$Sr_o[\%]$	$\sigma_v[kPa]$				
					50	100	200	400	800
					Collapse potential,$I_c[\%]$				
GI	0.81	CNWT	0.25	0.7	6.1	7.2	14.5	17.6	18.4
		CNDT	34.5	100	-	-	3.0	-	-
70G30S	0.85	CNWT	0.25	0.7	-	-	10.5	-	-
		CNDT	35.4	100	-	-	3.3	-	-
LG	0.64	CNWT	2.5	10	0	0.3	1.9	4.3	5.7
		CNDT	42.6	100	-	-	2.3	-	-

5.3.2. Constant net stress-suction increases (drying) test (CNDT)

This test was carried out in order to investigate the behaviour of the saturated metastable structure after a substantial reduction in the degree of saturation as a result of successive increases in suction values. This investigation was the experimental keynote for simulating the behaviour of shallow collapsible deposits in the field when the temperature rises after a rainy season.

The test results for the three selected soils are shown in Figures 5.26 to 5.30. Figure 5.26 indicates the relationship of void ratio versus net vertical stress. Figure 5.27 to 5.30 demonstrate the variation in the collapse potential, the void ratio, the gravimetric water content and the degree of saturation with applied suction respectively. The summary of test results is given in Table 5.5.

In order to achieve a full saturated state, the soil sample was allowed to free access to water and to free swelling (when the soil structure has potential to swell) without any loading condition. The compression stage was started after saturation stage where ψ_o=zero by increasing the loading stepwise until the target constant net vertical stress was reached (i.e. σ_n =200 kPa, ψ_o=zero). Then, the sample followed the drying path (i.e. suction increases) until the final suction (ψ_{final}) was reached, which corresponded to the initial suction value of the soil under constant applied net vertical stress (i.e. σ_n=200 kPa, ψ_{final} =the value of initial suction). For naturally gypseous and artificially gypsified soils, no swell was recorded as expected. Loess soil presented considerable swell potential where the void ratio increased significantly from point a to point b in as shown in Figure 5.26.
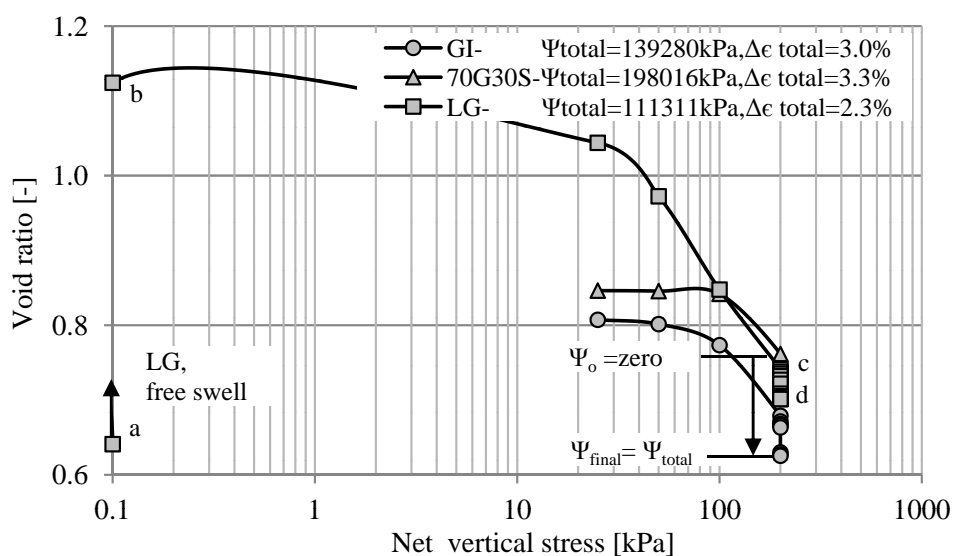
Figure 5.26.: Void ratio versus net vertical stress of CNDT for GI, 70G30S and LG soils.

The drying path for the three selected soils was started at full saturated state (i.e. ψ_o=zero; point c in Figure 5.26) when no further settlement was recorded under a constant net vertical stress of 200 kPa. After that, the applied suction was increased in a multi-step manner. The subsequent drying processes after initially fully saturated of the soil sample induced a significant volumetric strain, which was indicated by a settlement deformation and reduction in void ratio as shown in Figures 5.27 (points c-d) and 5.28. The fact signified that this deformation did not occur as a result of the collapse deformation,
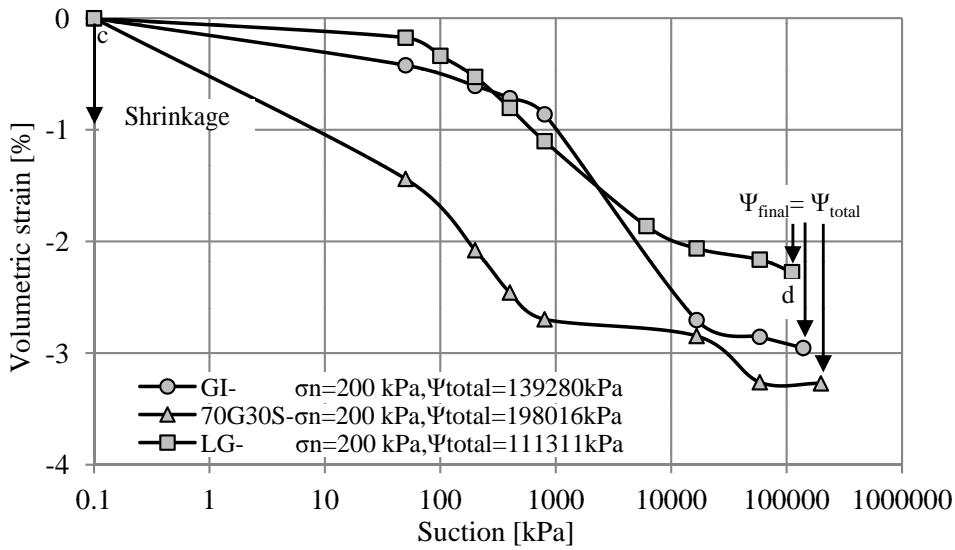
Figure 5.27.: Volumetric strain versus suction of CNDT for GI, 70G30S and LG soils.
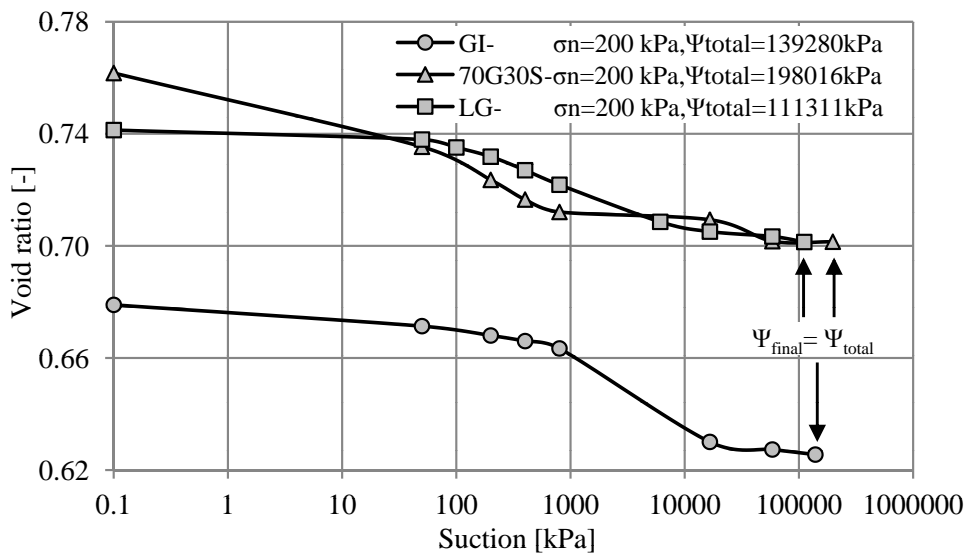
Figure 5.28.: Void ratio versus suction of CNDT for GI, 70G30S and LG soils.

but because of the shrinkage strain of the soil mass particularly at high net vertical stress, see Figure 5.28. This observation was in agreement with the experimental results of bentonite-sand mixture specimens presented by Alonso et al. (2001) and Agus (2005). This behaviour could be related to the fact that the entrapped air bubbles created by increasing the imposed suction replaced the water molecules in the pore space. Figures 5.29 and 5.30 demonstrate the great reduction that occurred in the values of gravimetric water content and the degree of saturation as a result of the increase in applied suction.
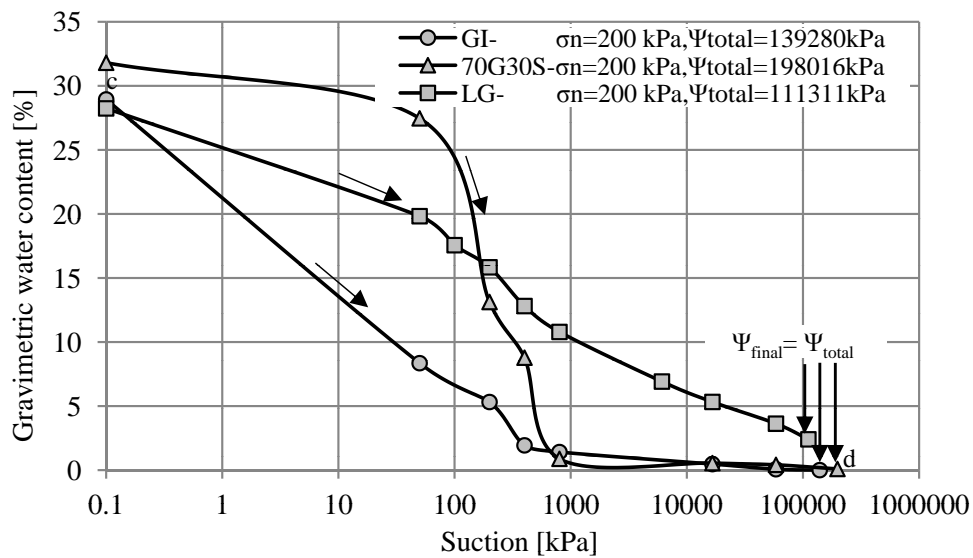
Figure 5.29.: Gravimetric water content versus suction of CNDT for GI, 70G30S, LG soils.
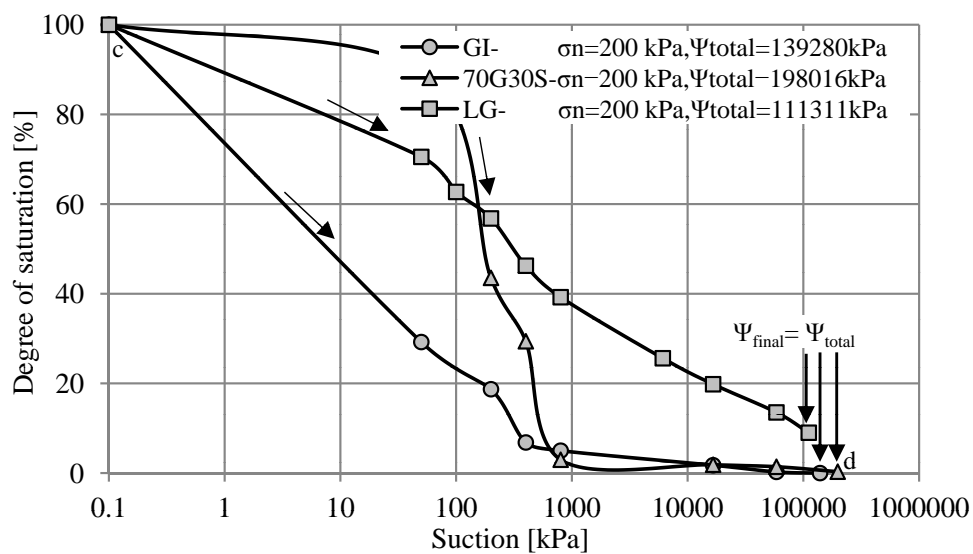
Figure 5.30.: Degree of saturation versus suction of CNDT for GI, 70G30S and LG soils.

5.4. Soil-water characteristics curve (SWCC) results

In this section, the results of drying and wetting processes over a wide range of imposed suction under unconfined conditions are presented for the three selected soils. The stress path of this test is shown in Figure 4.13.

In order to represent the SWCC and to verify the experimental data, several empirical equations or theoretical models were proposed in the literature to best-fit laboratory data for the SWCC. Such literatures include Fredlund & Rahardjo (1993); Fredlund et al. (2012).

In the present study, two of the most well known and most commonly used equations for representing the SWCC to best-fit laboratory data are the Van Genuchten (1980)-Mualem (1976) and Fredlund & Xing (1994) equation.

- **Van Genuchten (1980)-Mualem (1976) equation**

Van Genuchten (1980) proposed using a continuous function between soil suction and normalised water content as expressed in Equations 5.3 and 5.4. The Van Genuchten (1980) SWCC equation provided additional flexibility to obtain a best fit for the SWCC, since it depended on three fitting parameters a, n and m. In an attempt to obtain a closed-form expression for hydraulic conductivity, Van Genuchten (1980) used the Mualem (1976) relationship between n and m (Equation 5.5)in order to fix both parameters in a single variable.

$$\theta_n = \frac{1}{[1 + (a_m \psi)^n]^m} \tag{5.3}$$

or

$$\theta_n = \frac{w_{(\psi)} - w_r}{w_s - w_r} \tag{5.4}$$

and

$$m = 1 - \frac{1}{n} \tag{5.5}$$

where:

θ_n=normalized water content or the effective degree of saturation (Se).

ψ=applied suction (kPa).

a= the fitting parameter primarily related to inverse of air-entry value (unit equal to 1/kPa).

n= the fitting parameter primarily related to rate of water extraction from soil once air-entry value have been exceeded. Parameter (a) is also called the reference suction.

m= the fitting parameter that are primarily related to residual water content conditions.

$w_{(\psi)}$=gravimetric water content.

w_r=water content at residual conditions.

w_a=water content at saturated conditions.

• Fredlund and Xing (1994) equation

Fredlund & Xing (1994) further developed the best-fit SWCC equation in order to overcome the issue encountered with the other empirical SWCC equations. The common problem of other equations occurred at high soil-suction values beyond residual conditions where the results became asymptotic to a horizontal line as soil suction went to infinity (Fredlund & Rahardjo, 1993; Fredlund et al., 2012). The Fredlund & Xing (1994) SWCC equation expressed in Equations 5.6 or 5.10 used the correction factor in the equation to direct the SWCC to a soil suction of 10^6 kPa at zero water content. The correction factor $C(\psi)$ is as in Equation 5.9.

$$\theta = C(\psi)\frac{\theta_s}{\{\ln[e + (\psi/a)^n]\}^m} \tag{5.6}$$

or

$$w(\psi) = C(\psi)\frac{w_s}{\{\ln[e + (\psi/a)^n]\}^m} \tag{5.7}$$

where

$$\theta = \frac{w_{(\psi)}}{w_s} \tag{5.8}$$

$$C(\psi) = 1 - \frac{\ln(1 + \psi/\psi_r)}{\ln[1 + (10^6/\psi_r)]} \tag{5.9}$$

where:

θ=volumetric water content corresponding to the selected soil suction.

θ_s=saturated volumetric water content.

c= 2.71828; irrational constant.

ψ_r=soil suction corresponding to the residual volumetric water content θ_r.

If the SWCC is required to fit only between saturated conditions and residual conditions, another form of Equation 5.6 can be used to obtain best fit for the experimental data as follows:

$$\theta = \theta_r + C(\psi)\frac{\theta_s - \theta_r}{\{\ln[c + (\psi/a)^n]\}^m} \tag{5.10}$$

In this section, the results of SWCC test (i.e. drying and wetting paths) with best-fit using Equations 5.3 and 5.10 for the three selected soils are presented. Figure 5.31 and Figure 5.32 demonstrate the results of gravimetric water content versus suction and degree of saturation versus suction respectively, while Figure 5.33 indicates the verification of experimental data with predicted data.

From the SWCCs of both GI and 70G30S soils it can be observed that the air-entry value (AEV) and residual suction value (ψ_r) occurred in a relatively low range of suction values. Moreover, the AEV and ψ_r for GI soil obtained from the SWCC drying curve were 2 kPa and 60-70 kPa respectively (see Figures 5.31a and 5.32a), while the AEV and ψ_r for 70G30S soil were 3-4 kPa and 200-300 kPa respectively (see Figures 5.31b and 5.32b). From these results it can be concluded that the soil structure in the boundary effect zone could not hold the water molecules in the pore space due to its relatively coarse grain size distribution even with a low value of imposed suction. This behaviour can be attributed to the high permeability of the soil structure produced by the existence of the sand grains in addition to the weak interparticle tension forces of the metastable soil structure.

By comparing the SWCCs for both GI and 70G30S soils, the transition zone of 70G30S soil was greater and flatter than the transition zone of GI soil, where the residual suction of 70G30S soil exceeded the residual suction of GI soil by approximately five times. However, the gypsum cementing structure showed considerable hysteresis on its SWCC with a clear increase in the magnitude of hysteresis for 70G30S soil. This behaviour can be related to the type and the difference in geological formation and homogeneity of soil fabric and gypsum bonds.

For LG soil, the AEV and ψ_r were 14 kPa and 1800-2000 kPa respectively where the residual suction value occurred at a high suction range (see Figures 5.31c and 5.32c). Hysteresis between the drying and wetting curves was also recorded in the SWCC of LG soil but with a lower magnitude than for GI and 70G30S soils. The low permeability and the homogeneity of the silt fabric can explain this behaviour.

Figure 5.33 shows the verification results of experimental data with the predicted data of the SWCCs. Regression analysis for the experimental results using the Van Genuchten (1980)-Mualem (1976) and Fredlund & Xing (1994) equations reveal the high accuracy of these results in comparison with the predicted data of the SWCCs.

The Fredlund & Xing (1994) equation provided reliable closeness of fit with experimental data sets and more flexibility, particularly at the residual zone and at the inflection point of the wetting part of the SWCC. This assessment was also confirmed by many researchers such as (Leong & Rahardjo, 1997; Sillers, 1997; Fredlund et al., 2012).
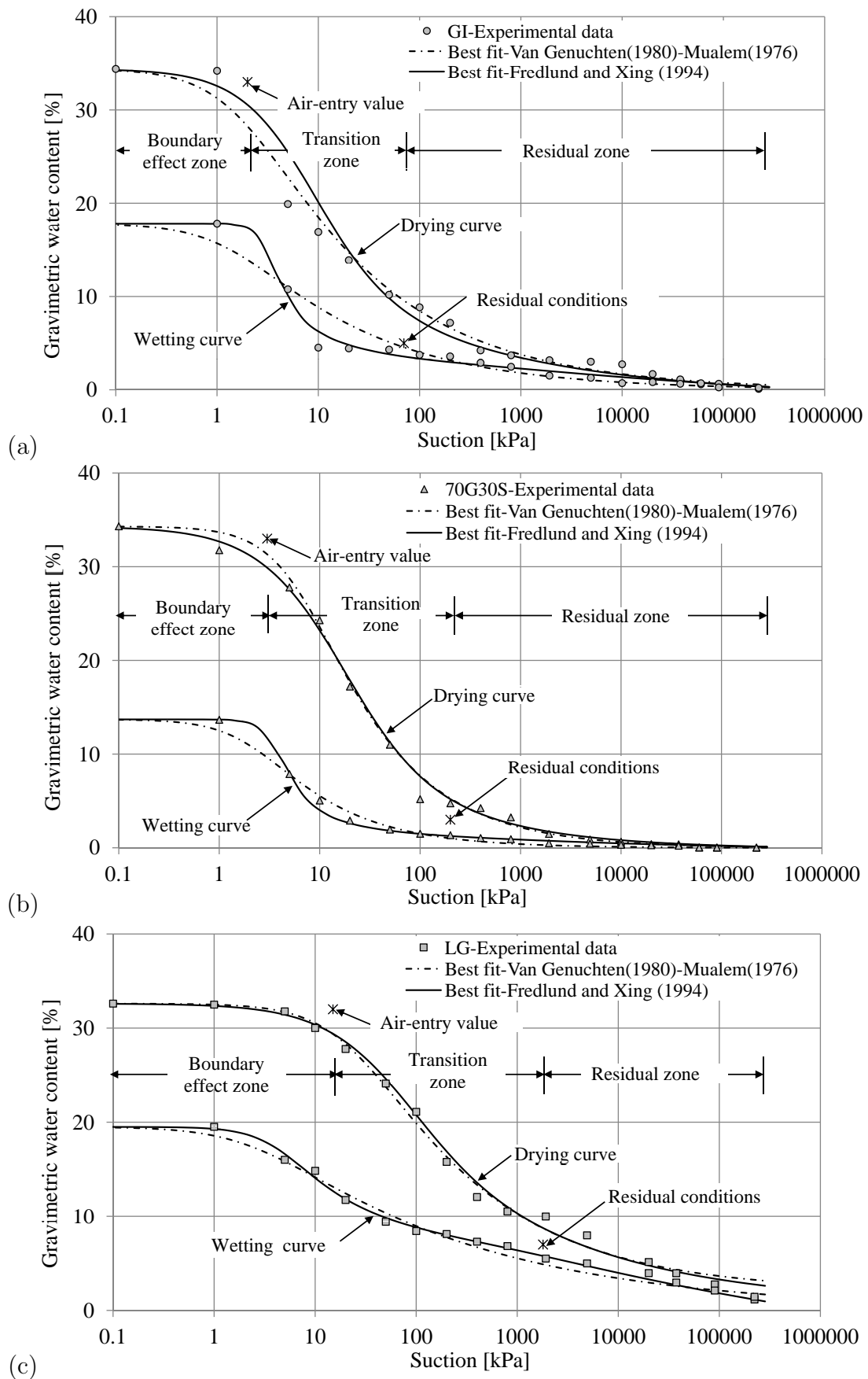
Figure 5.31.: Soil-water characteristics curve, $w - \psi$ relationship for: (a) GI, (b) 70G30S and (c) LG soils.
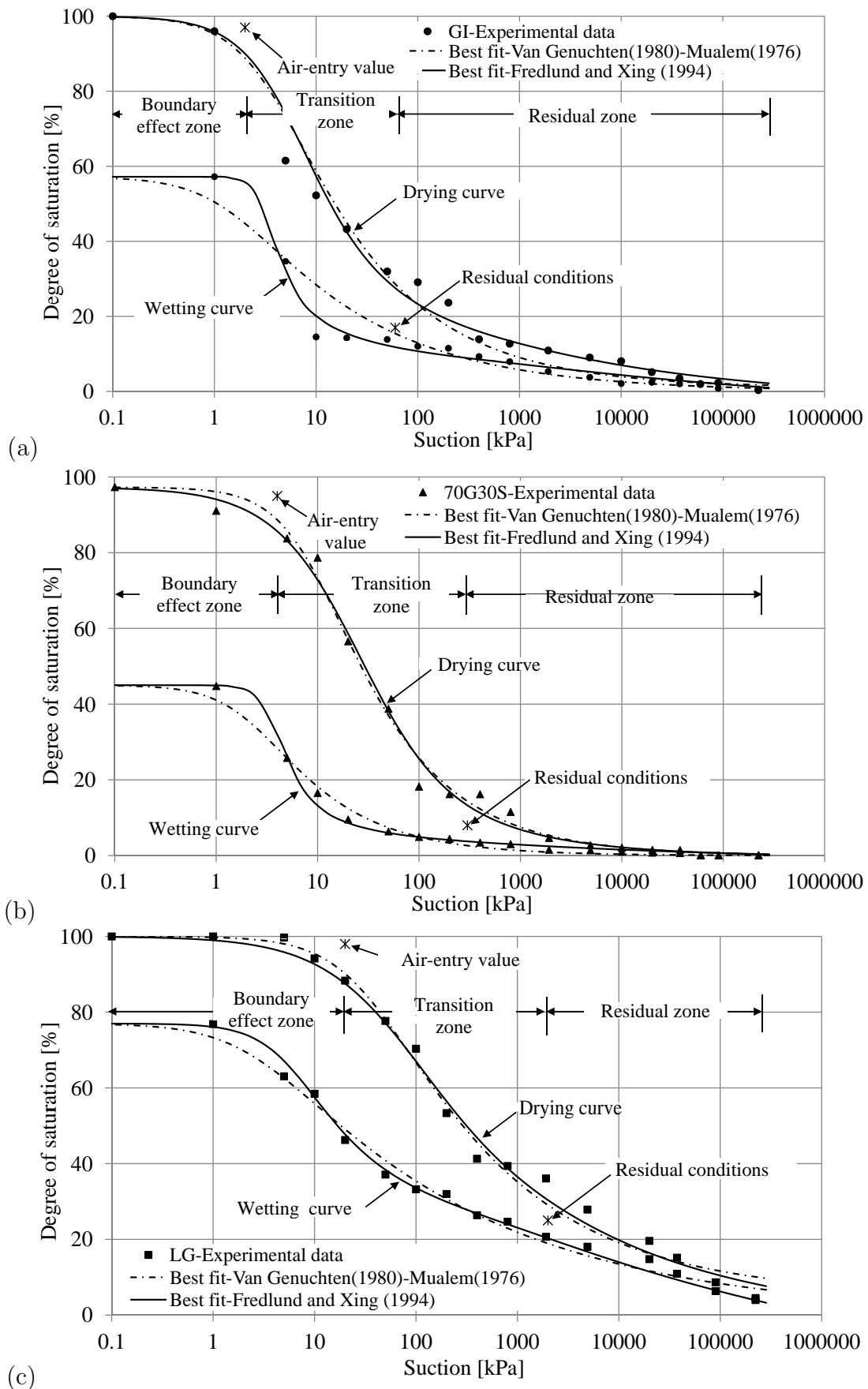
Figure 5.32.: Soil-water characteristics curve, $S_r - \psi$ relationship for: (a) GI, (b) 70G30S and (c) LG soils.
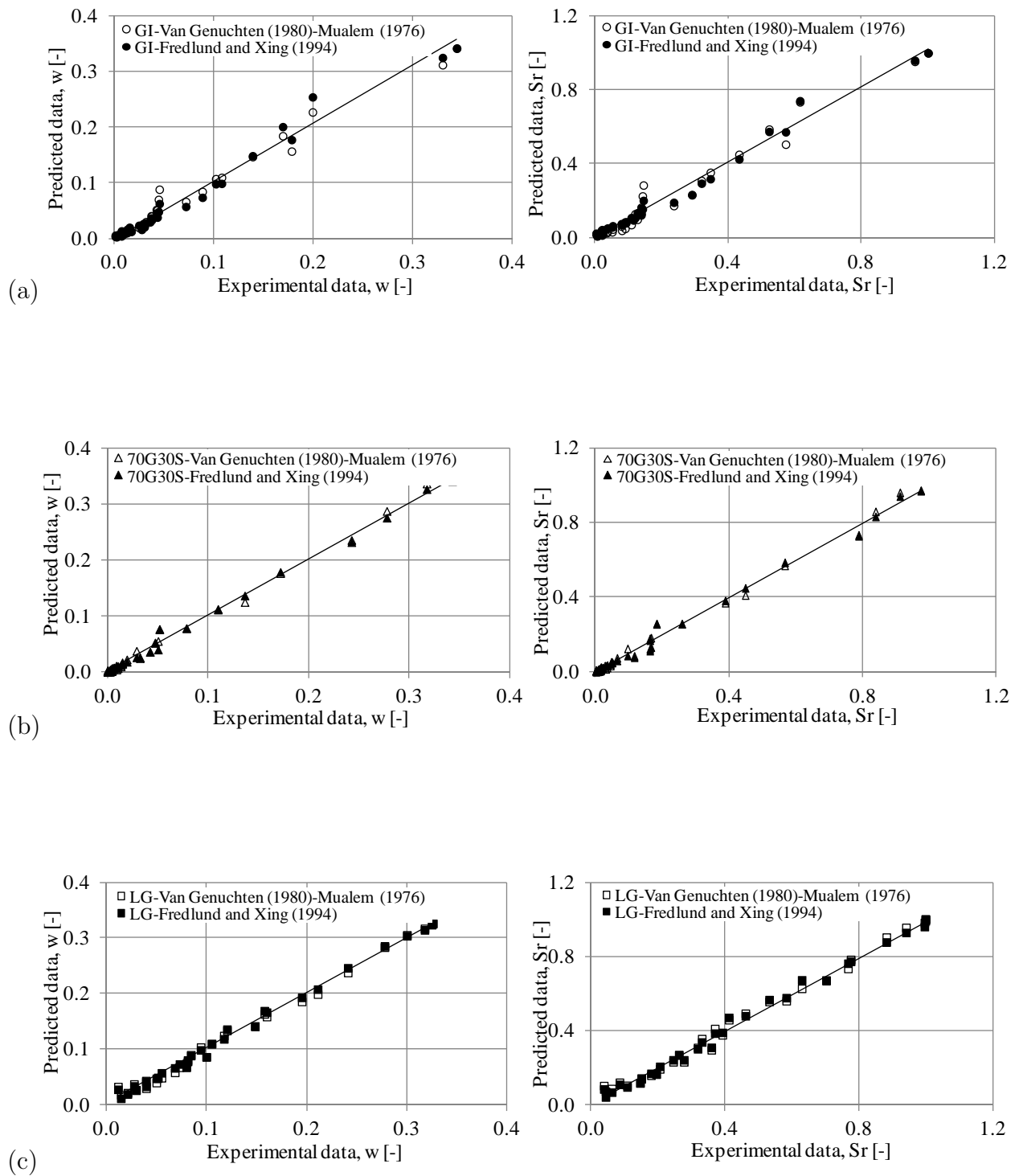
Figure 5.33.: Verification of experimental data with predicted data of SWCC test, (left) gravimetric water content (w) results and (right) degree of saturation (S_r) results for: (a) GI, (b) 70G30S and (c) LG soils.

In reference to the CNWT results (subsection 5.3.1), Figure 5.19 indicates that the main collapse phase for the three selected soil samples is occurred at low suction range, and it is completed once up to suction of 50-100 kPa. This means that the soil sample reached the final value of the collapse potential at the transition zone (i.e. not fully saturated condition of the wetting curve and before the air-entry value of the drying curve of SWCC), see Figure 5.31. In other words, even under partially saturated conditions (i.e. remaining air in the pore space), the final value of the collapse potential could be achieved.

5.5. Permeability-leaching test

5.5.1. Permeability-leaching test under saturated condition (PLT)

The permeability leaching test was performed on gypseous soil (GI) and loess soil (LG) at different vertical stress levels as shown in Table 3.9.

The permeability leaching stage followed the collapse stage of the constant net vertical stress-suction decreases (wetting-collapse) test.

The test results indicated that this test under such boundary conditions was not appropriate for the mixed soil (70G30S) due to the existence of opening channels in the soil mass that arose a few hours after starting the water flow. For the same reason, the GI sample test failed under a vertical stress of 50 kPa. However, the LG soil required a relatively high hydraulic gradient in order to induce the water flow through the soil mass because of its low permeability.

Figure 5.34 demonstrates the volume changes of GI and LG samples due to both saturation and leaching processes. For the GI sample, permeability-leaching results (Figure 5.34a) showed volume changes much greater than those resulting from the multi-step wetting fully saturation stage (i.e. ψ_{final}=zero) particularly under low vertical stress.

The leaching strain and the accumulative dissolved gypsum significantly increased as the water flow increased as depicted in Figures 5.35 and 5.36. This behaviour was due to the further dissolution of gypsum particles and the direct removal of these particles outside the soil mass. In addition, this behaviour occurred when the water flowed through an open structure of gypsum cementing bonds. This action also led to further development of the volumetric strain as shown in Figure 5.37.

Moreover, the soil fabric continuously attempted to adjust over time to maintain equilibrium with the externally applied load and the hydraulic gradient.

These results were supported and confirmed by the results of Nashat (1990); Al-Busoda (1999); Al-Neami (2000); Al-Obaidi (2003) (see Figure 2.2).

However, such behaviour was not observed for loess soil, in which no further volumetric strain or collapse deformation was recorded upon flowing water through the soil mass. The rearrangement of the loess fabric seemed to reach equilibrium after inundation under the same vertical load.

(a)

(b)
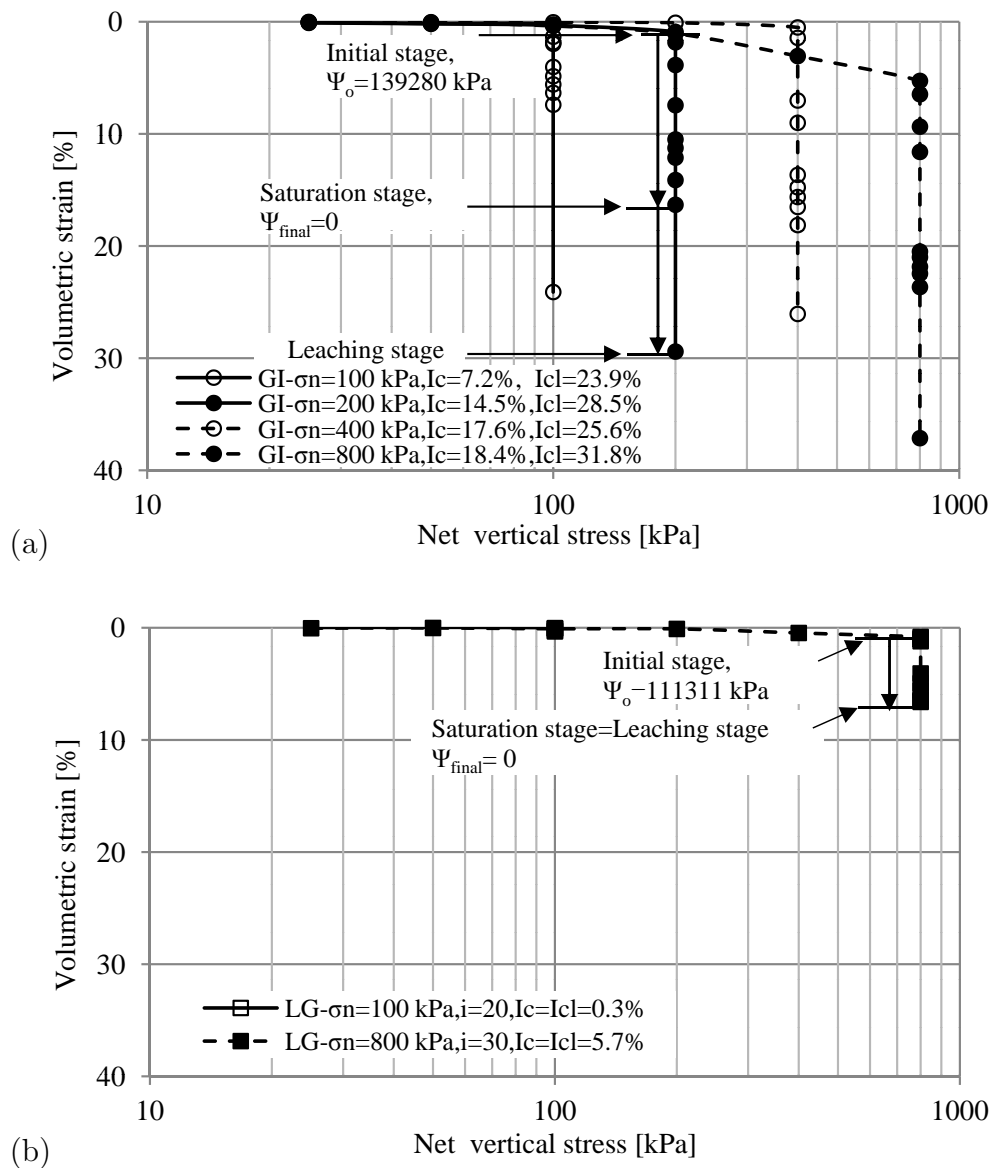
Figure 5.34.: Volumetric strain versus net vertical stress relationship of permeability-leaching test for: (a) GI and (b) LG soils.
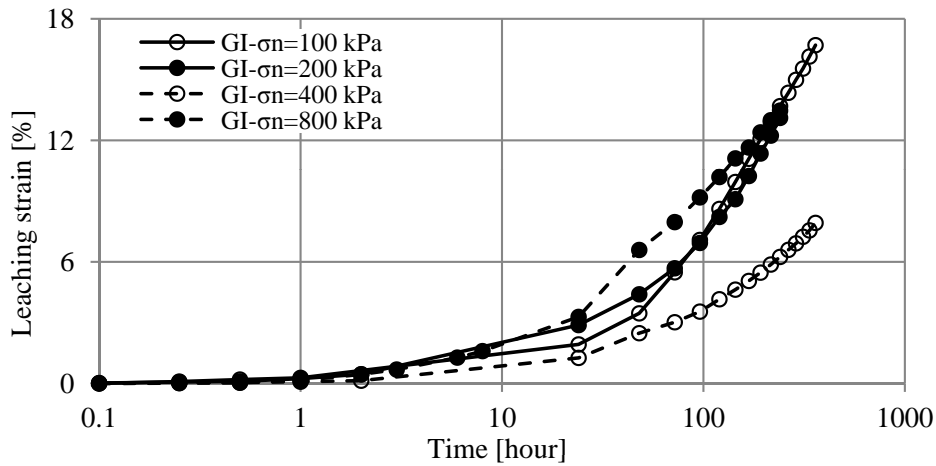
Figure 5.35.: Evolution of accumulative leaching strain over leaching time for GI soil.
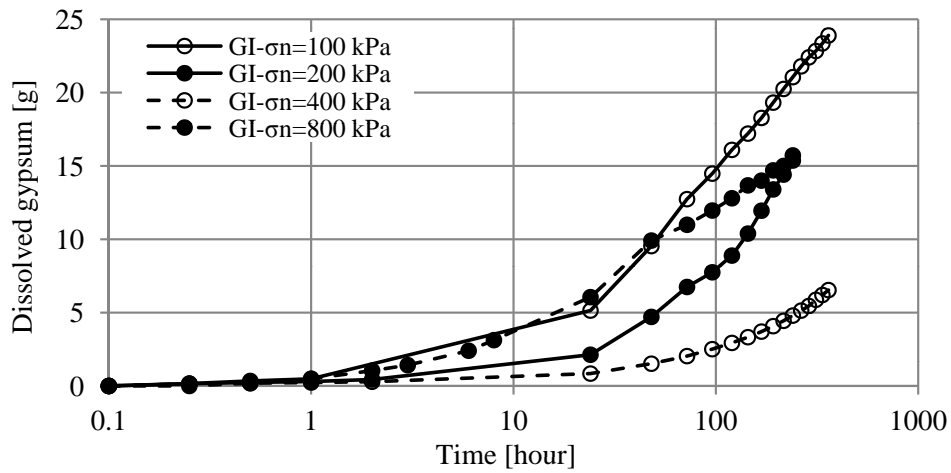
Figure 5.36.: Evolution of accumulative dissolved gypsum over leaching time for GI soil.
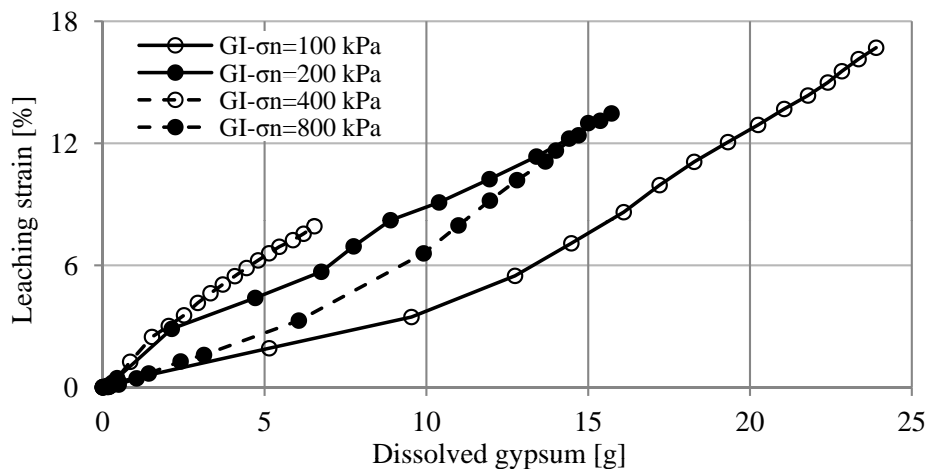
Figure 5.37.: Accumulative leaching strain versus accumulative dissolved gypsum for GI soil.

Figures 5.38 and 5.39 indicate that the permeability coefficient (k) significantly decreased with successive increases in the leaching period and dissolved gypsum. This behaviour can be attributed to the destruction most of the cavities and the large voids due to loading after the progressive removal of gypsum particles. In other words, the decrease in k could be related to the reduction in micro pore channels, which resulted from a drastic collapse of the metastable structure, and/or plugging of either these channels or the bottom pores stone by fine gypsum particles during their movement towards the outside of the soil mass. On the other hand, the reduction in the permeability coefficient did not necessarily result in an accompanying decrease in the void ratio during leaching processes.
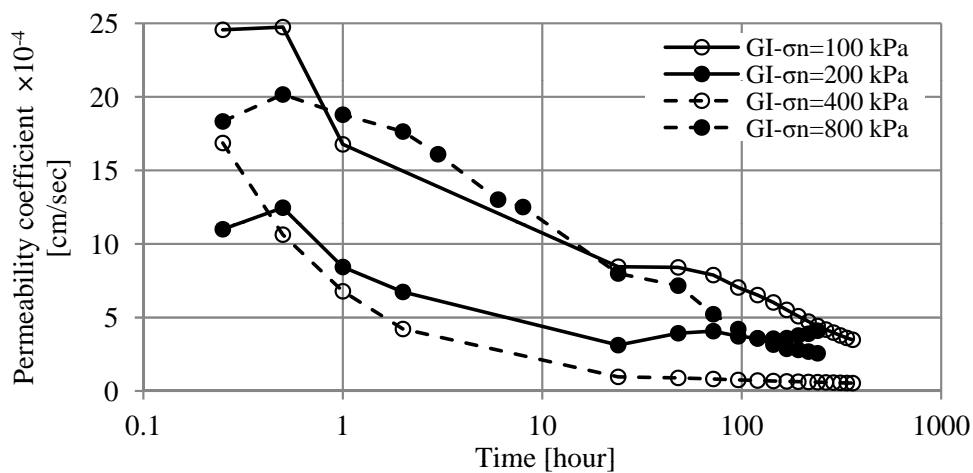
Figure 5.38.: Evolution of permeability coefficient over leaching time for GI soil.
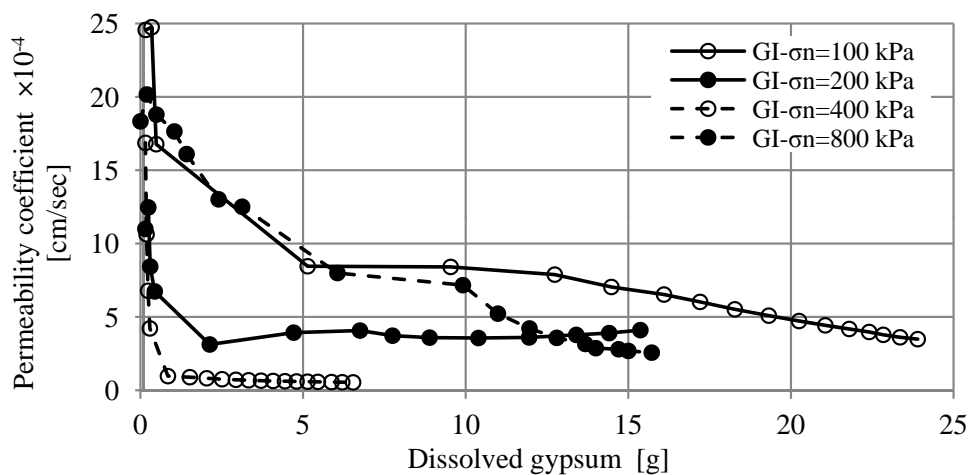
Figure 5.39.: Evolution of permeability coefficient with accumulative dissolved gypsum for GI soil.

On the contrary, Figures 5.40 and 5.41 indicate that the void ratio significantly increased as both the leaching strain and the dissolved gypsum developed especially when leaching was conducted at a low stress level (i.e. below or equal to the maximum preconsolidation pressure, σ_{vm}=176 kPa). However, relative increases in void ratio were observed when leaching was conducted greater than σ_{vm}. The reason behind this behaviour is related to the problem of a continuous loss of some soil particles during the leaching process at certain stress states. In other words, when the soil mass lost some of its solids under high stress level the soil structure rearranged itself at almost the same contact area as the previous amount of soil solids. However, when particles were lost at a low stress level, no dense state was created for the soil structure by the remaining soil solids, and/or the soil particles were redistributed in the same manner which provided a sufficient bearing capacity against the application of low stresses.
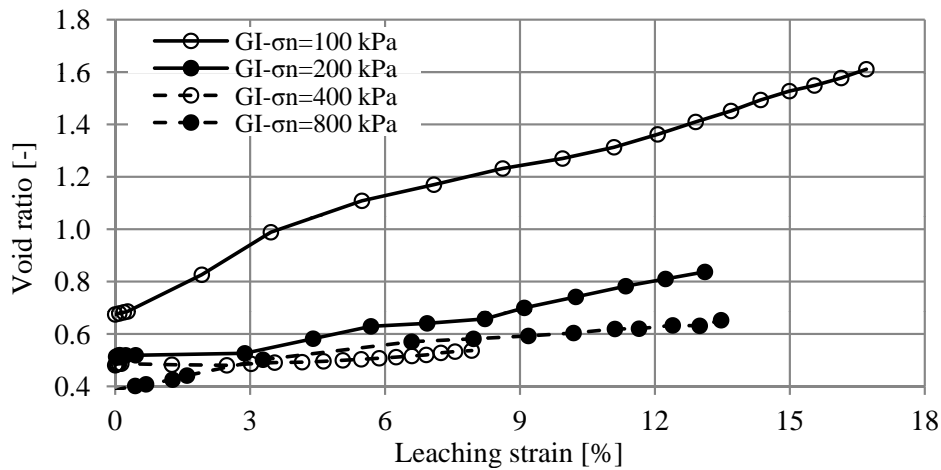
Figure 5.40.: Evolution of void ratio with accumulative leaching strain for GI soil.
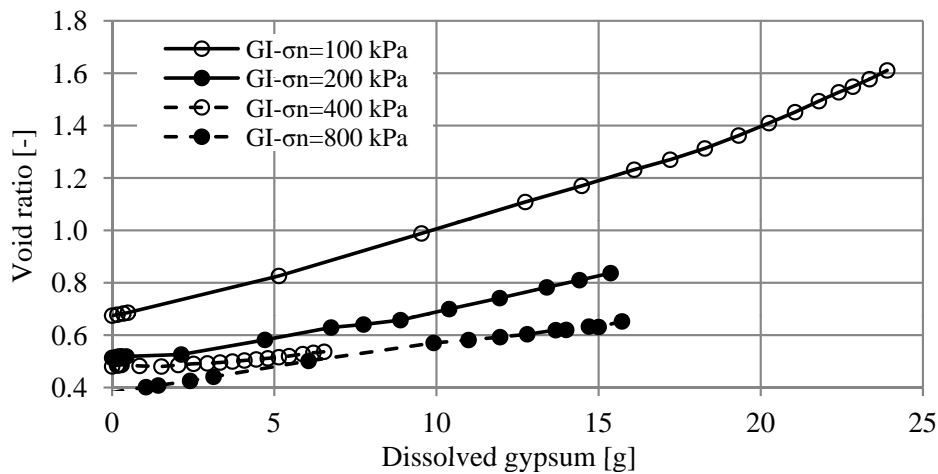
Figure 5.41.: Evolution of void ratio with accumulative dissolved gypsum for GI soil.

Hence, care must be taken when estimating the void ratio during or after leaching processes. Furthermore, the collapse potential due to the leaching phenomenon (I_{cl}) can be determined depending on the difference in volumetric strain before and after leaching to avoid any mistake that could be encountered when utilising the values of the void ratio in the calculations.

In conclusion, the change in the void ratio of gypseous soil during leaching is a function of stress level, hydraulic gradient, dissolved gypsum and leaching time. This interpretation corroborates the assumptions of the theoretical model proposed by Al-Mufty (1997). The obtained results are supported by many studies such as Nashat (1990); Al-Badran (2001) (see Figure 5.42) and Al-Obaidi (2003).

For LG soil, the behaviour during the permeability-leaching test was quite different from that of GI soil. No changes in volumetric strain or void ratio in the soil sample were observed during the leaching processes. The coefficient of permeability for σ_n=100kPa, i=20 progressively deceased as the leaching time increased. However, under σ_n=800kPa, i=30, it increased relatively until 48 hours of leaching time before it decreased. After this time, the k values under both stresses decreased linearly in a parallel trend as shown in Figure 5.43. This behaviour can be related to the fact that the loess fabric reached equilibrium more quickly after inundation under loading. The number of voids decreased and the contact area between the soil particles increased resulting in very low permeability particularly when the soil mass was confined at a high stress level.
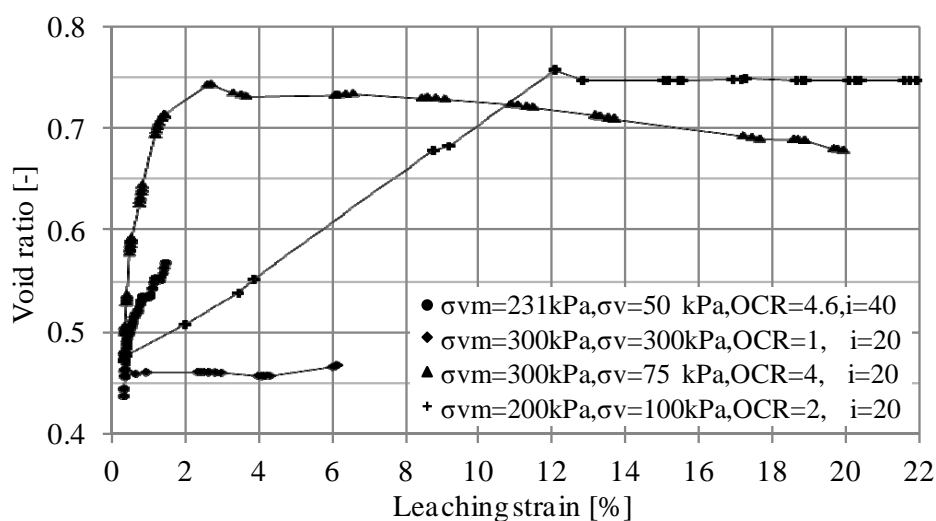
Figure 5.42.: Leaching test using Oedometer cell for sandy gypseous soil (e_o=0.54, Gs=2.36, χ'=74%), Al-Tharthar region, Iraq (Al-Badran, 2001).
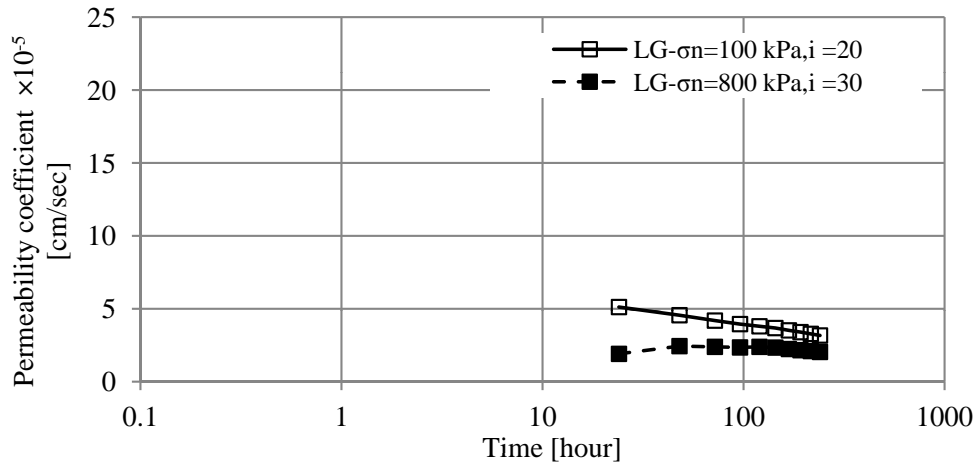
Figure 5.43.: Evolution of permeability coefficient over leaching time for LG soil.

5.5.2. Permeability coefficient under unsaturated condition

In this subsection, the results of the permeability coefficient estimation under unsaturated conditions for both GI and LG soils are presented. This estimation was based on the constant net vertical stress-suction decreases (wetting-collapse) test (Subsection 5.3.1).

The coefficient of permeability under unsaturated conditions (k_w) was determined using the empirical model proposed by Brooks & Corey (1964) (see Section 2.11).

The model parameters were estimated from the soil-water characteristics curve (drying curve) for both soils (i.e. GI soil of Figure 5.32a and LG soil of Figure 5.32c). The permeability coefficient under saturated conditions (k) was considered from permeability-leaching test results (Subsection 5.5.1).

For GI soil, the constant k value after one hour of leaching for each net vertical stress was used to avoid any variation in the k value resulting from gypsum dissolution, see Figures 5.38 and 5.39.

For LG soil, the constant k value after 24 hours of leaching was considered where the coefficient of permeability was relatively constant, see Figures 5.43.

Figure 5.44 shows the unsaturated coefficient of permeability versus suction for GI and LG soils respectively. In these figures it can be noticed that the k_w increased as the imposed suction decreased. This behaviour resembled the behaviour of the degree of saturation versus suction, see Figure 5.22a and c.

(a)

(b)
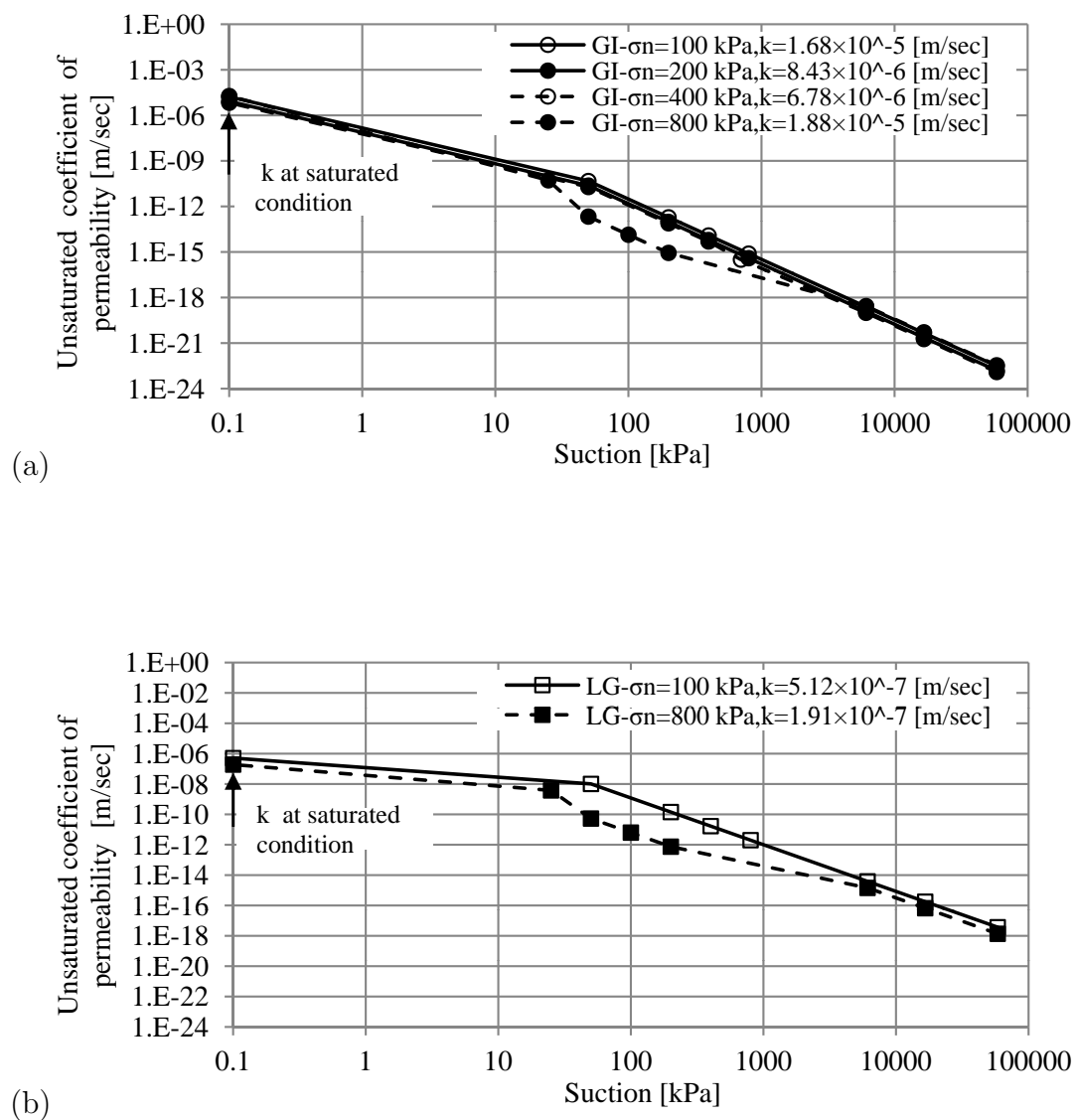
Figure 5.44.: Evolution of unsaturated permeability coefficient over suction for: (a) GI, (b) LG soils.

The relationship between the unsaturated coefficients of permeability and degree of saturation is shown in Figure 5.45. This figure indicated that the variation in the permeability coefficient with suction and/or with the degree of saturation under different net vertical stresses was congruent and in a band form. Moreover, no obvious effect was present on the value of the permeability coefficient for the collapse deformation of the soil sample at either the macrostructure or the microstructure level.

Nevertheless, the degree of saturation has significantly affected the value of the permeability coefficient at all suction ranges. This behaviour explained how the final collapse could be achieved even when the soil sample did not reach a fully saturated state.

(a)

(b)
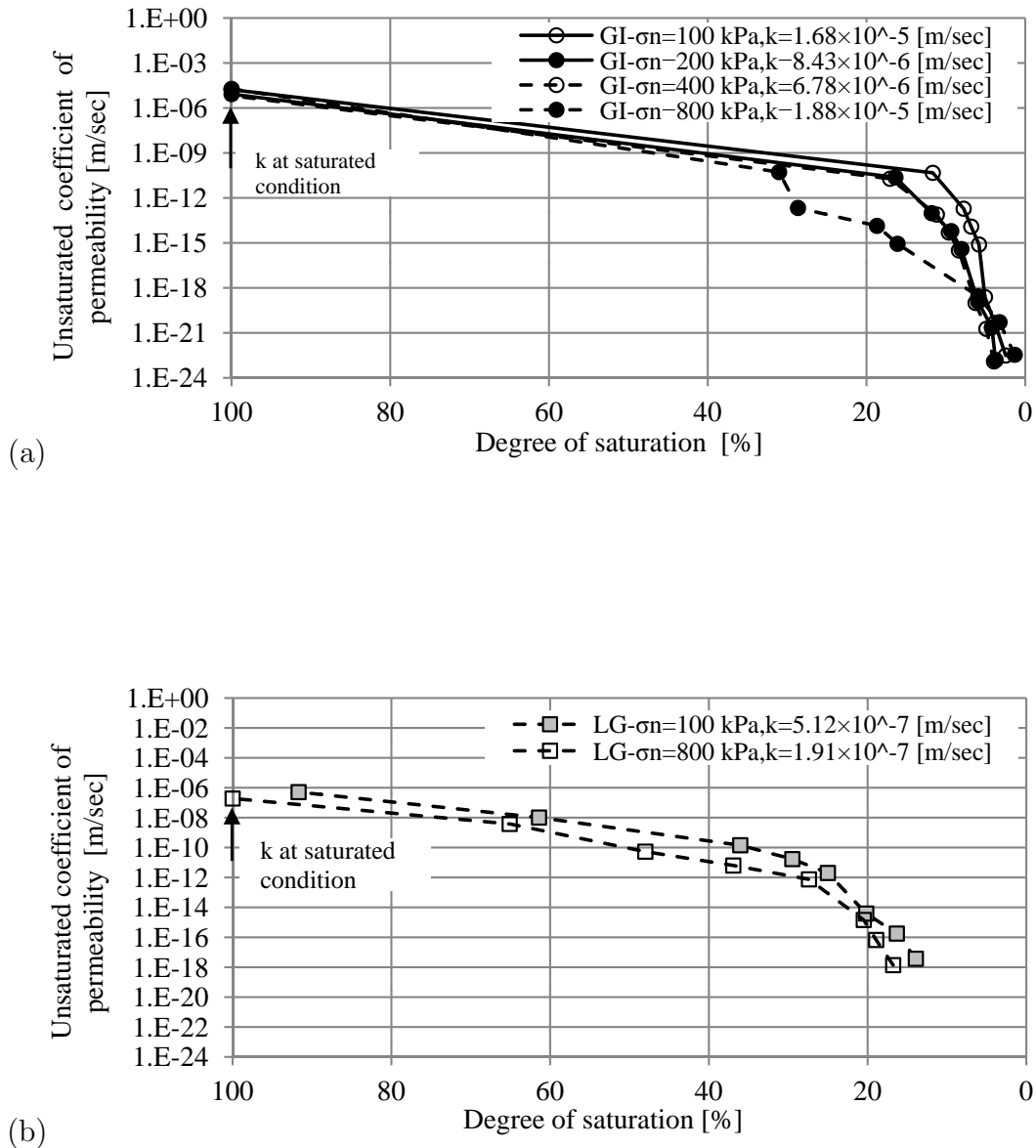
Figure 5.45.: Permeability coefficients versus degree of saturation at unsaturated condition for: (a) GI, (b) LG soils.

Pereira et al. (2005) presented similar results for the multi-step wetting test under constant confining vertical stress, see Figure 5.46. They added that, the soil collapse might have also generated internal hydraulic gradients that could alter the water flow paths through the soil structure. They also stated that, the unsaturated coefficient of permeability of the collapsible soil was primarily a function of the degree of saturation, while the saturated coefficient of permeability was a function of the void ratio.

(a)

(b)
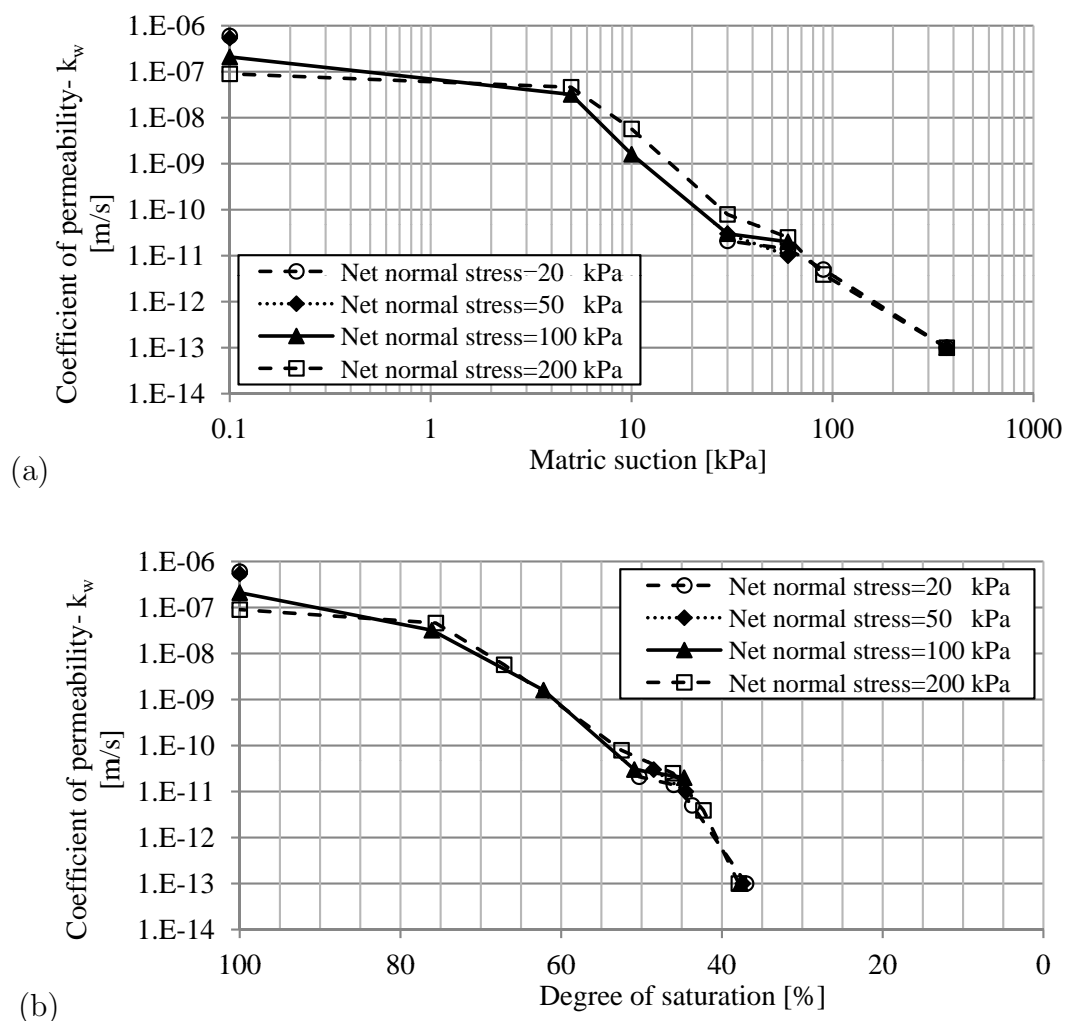
Figure 5.46.: Measurements of coefficient of permeability at unsaturated condition for "Alka-Seltzer dam" collapse soil of (SM-ML, e_o=0.754 and w_o=10.5%) from Brazil (Pereira et al., 2005).

5.6. Elementary characteristics (ESEM-EDX) analysis

In this study, ESEM-EDX analysis was carried out on the recompacted oven dried soil specimens after saturation and leaching processes under a vertical stress of 200 kPa for 24 hours. In addition to the initial unsaturated state. The ESEM measurements for all soil specimens are shown in Figure 5.47. Additional details about ESEM measurements with EDX analysis can be found in appendix C. Figures 5.47a, b and c show the ESEM measurements for gypseous soil (GI) under various initial conditions of the soil specimen.
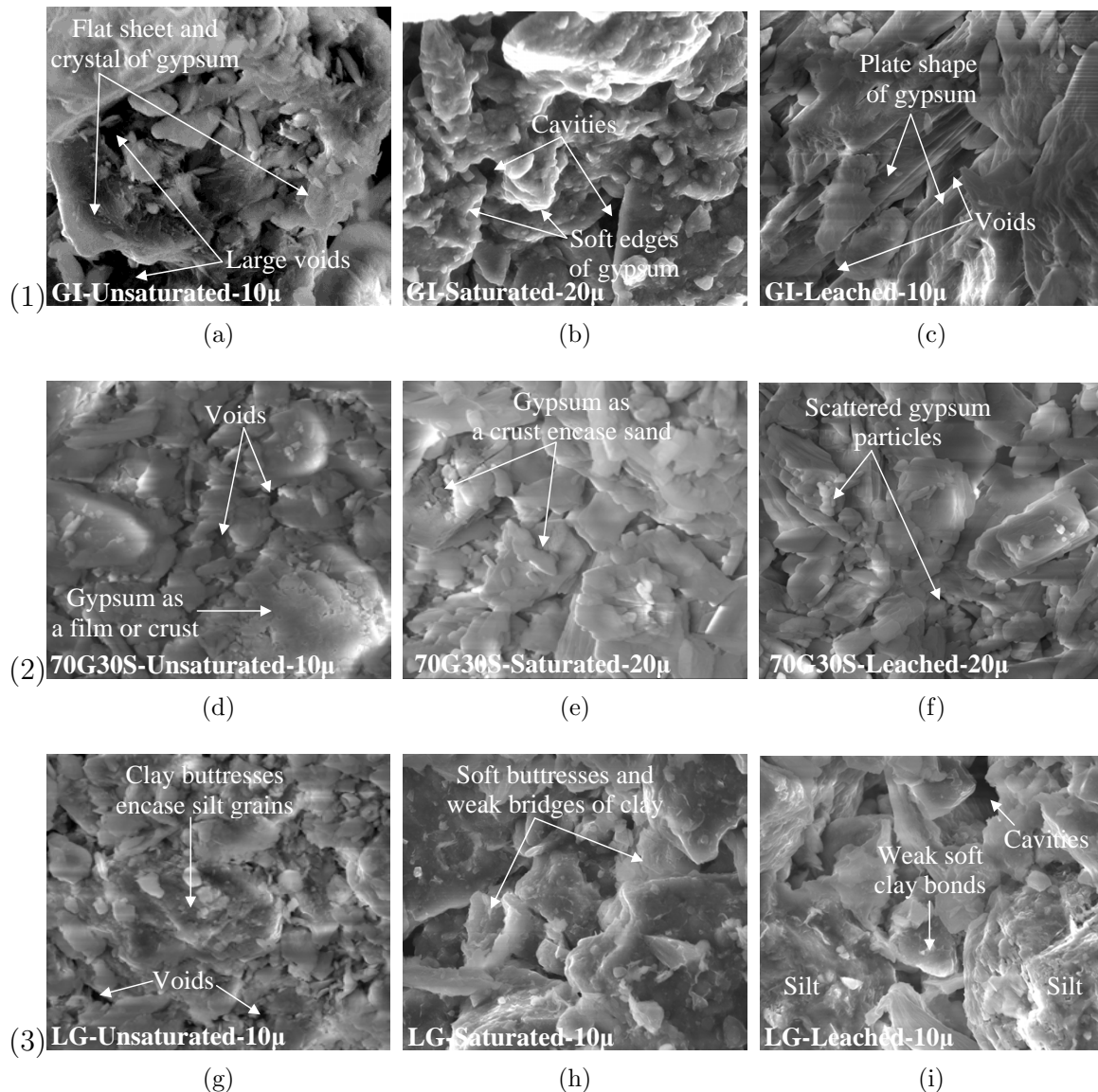
Figure 5.47.: ESEM measurements for: (1) GI, (2) 70G30S and (3) LG soils; (left) Unsaturated, (middle) Saturated and (right) leached soil states.

Figure 5.47a indicates that the natural formation of gypsum can be found in three phases: a phase of flat sheets or crusts, a phase of accumulative dense blocks or crystals and/or a phase of sand covered with silt particles. The recompacted specimen showed an absence or a rare presence of supporting cementing bonds between silt-silt particles in addition to the presence of cementing bonds type gypsum covered with silt-crystals gypsum with sharp edges particles (Figure 5.47a). The EDX analysis showed that the sulphate (S=19.6% per weight) and calcium (Ca=19.6% per weight) content formed the main parts of the chemical composition of the soil.

The effect of saturation and leaching processes on the microstructure of GI soil was quite clear as shown in Figures 5.47b and 5.47c respectively. The observed sharp edges of gypsum in unsaturated specimen were softened and nearly dissolved (Figure 5.47b). However, the previous shapes of gypsum (i.e. flat sheets or crusts) still existed. Such strong cementation of gypsum required substantial soaking or water flow under a hydraulic gradient in order to segregate it from other particles and complete the dissolution processes. The EDX analysis of normalised element of saturated GI specimen shows that the chemical composition particularly for S and Ca were almost unchanged after being fully saturated in comparison with the unsaturated GI specimen (see appendix C). This is because the dissolved gypsum at saturation condition still existed in the pore water and was not removed outside the soil mass. Subsequent re-precipitation of the gypsum from the soluble pore water occurred when oven drying of the soil mass. Nevertheless, upon leaching processes, the S and Ca contents were reduced to about 50% by weight in comparison with the unsaturated or saturated states after only 24 hours from the start of the leaching process. Moreover, Figure 5.47c shows that the water flow through the soil mass attempted to change the shape of the gypsum particles to a plate shape with smaller voids between particles. However, the crusts of gypsum still covered the sand or silt grains and required additional water action in order to destroy all those bonds.

The sequential changes or the transformation of the gypsum particles in the soil mass due to its sensitivity to water activity can explain the following: the creep phenomenon observed during the compression test of gypseous soil under saturated conditions (see Figure 5.14a) and the collapsibility characteristics observed when wetting under controlled suction (see Figure 5.19a). It can be concluded that this transformation is a function of vertical stress, suction and water activity through the soil mass.

A comparison between the natural and artificial occurrence of gypsum within soil structure (i.e. GI and 70G30S soils respectively) can be made considering the ESEM images in Figures 5.47a and 5.47d. From these figures, the differences in the gypsum formation and its distribution through the soil fabric can be recognised. In the case of natural formation of gypsum in GI soil fabric, three gypsum phases with a complex and relatively dense structure were observed. In the case of artificially occurring gypsum in 70G30S soil, the gypsum particles were uniformly distributed and coated the fine sand particles or appeared as a separate gypsum film or crusts. The cementing bonds between two coated sand particles were present (see Figure 5.47d). The soil fabric uniformity derived from the perfect mixing of the $CaSO_4.2H_2O$ powder characterised by a high specific area with Silber sand characterised by uniform grain size distribution.

Moreover, the EDX analysis of 70G30S soil shows more S and Ca minerals than in the

GI soil as well as the absence of some minerals such as Al, Mg and K.

Upon inundation and/or the leaching of 70G30S soil as shown in Figures 5.47e and 5.47f respectively, no substantial difference or transformation for the gypsum particles was observed as in the case of GI soil. In the case of saturated specimens, the particles maintained their formation and intensity but in a soft form and a closer voids. In the case of leaching process, the film or crusts formed by gypsum particles still existed but in a scattered form. This behaviour can be related to the genesis formation of the natural and artificial cementing bonds between soil particles in addition to the qualitative and quantitative gypsum material in the soil element. On the other hand, artificial gypsum $CaSO_4.2H_2O$ is very fine and compliant or ductile material, therefore the compaction method and the curing time for preparing the mixed soil have a great effect on the particle shape and bonding strength. However, all of the above-mentioned properties for 70G30S soil might explain the reason behind the sudden volume change in the soil specimen during the first ten minutes of the load application. In addition, it clarifies the substantial jump in the amount of water for both wetting and drying paths during the constant net stress-suction control tests (see Figures 5.21b and 5.29). On the other hand, such a weak fabric could not have maintained the bonds of a sand-gypsum form in position for a long time particularly when the water flowed under the hydraulic gradient. In other words, water activity in the soil mass led to the reseparation of the gypsum-sand mixture and the formation of piping or water channels through the soil skeleton. This behaviour explains the failure of permeability leaching test for 70G30S soil.

Figures 5.47g, h and i show the ESEM measurements for loess soil (LG) under different initial conditions in the soil specimen. Figure 5.47g indicates that the recompacted specimen of silt-sand fabric is connected togather through a superficial clay layer (i.e. clay bridges and buttresses) as well as presence of large voids. These observations corroborate the observations of Barden et al. (1973)and Klukanova & Frankovska (1995). The EDX analysis showed that the major elements of LG soil are Si and Al with 36.7% and 10.8% per weight respectively.

The effect of saturation and water flow (i.e. leaching) on the microstructure of LG soil is shown in Figures 5.47h and i respectively. When comparing the soil fabrics under different conditions (i.e. unsaturated, saturated and leaching) the silt-clay bonds with voids was presented under all conditions. Nevertheless, the saturated specimen showed scattered grain distribution, less homogeneity, soft bonds and large voids due to bioturbation (Figure 5.47h). In contrast, the leached specimen was characterised by more uniform grain distribution, smaller voids and softer clay buttresses and bridges. In addition, the silt grains lacked the support of clay buttresses and seemed to be shelled or segregated

from the clay bonds (and/or clay linings) and might have been trans-located into the surrounding voids by the water flow (Figure 5.47i). The foregoing discussion explains the absence of further volume change that might have resulted from the leaching of the soil mass (Figure 5.34b) and also explains the relative reduction in the value of permeability coefficients (k) at the time of leaching (Figure 5.43). However, the EDX analysis presented some changes in the mineral compositions of the silt soil which occurred as a result of inundation or leaching of the soil mass. For example, upon inundation, Mg is disappeared and new components such as C , Ti and V is appeared. Upon leaching, the previous components were replaced by Br (see appendix C). These observations agree with the finding of Derbyshire et al. (1995) and Muxart et al. (1995).

5.7. Soil-column test

In this section, the result of the soil-column test utilizing soil column device for compacted gypseous soil is presented. Figures 5.48, 5.49 and 5.51 show the evolution of pore-water pressure, volumetric water content and volumetric strain with time respectively. The initial condition of the soil sample and the stress path of the test are shown in Tables 3.8 and 5.6.

Corresponding to the tensiometer sensors measurements given in Figure 5.48, the soil sample under the initial conditions had negative pore-water pressure when compacted at an average initial volumetric water content of θ_o= 6.5%. Moreover, the pore-water pressure immediately rose from its initial value to around zero value simultaneously with increases in air pressure (u_a) from zero to 30 kPa. However, no change in volumetric water content was recorded. This behaviour indicates that sudden increases in the hydrostatic pore-water pressure occurred at the micro level of the soil structure. At the first stress path level of u_a=30 kPa, u_w=10 kPa, ψ=20 kPa, the hydrostatic pore water-pressure started sequentially dissipating until it reached equilibrium after 30 days from the beginning of the test. During this stage the deeper tensiometer (T3) showed lower matric suction than the upper one (T1). At the second stress path level of u_a=20 kPa, u_w=10 kPa, ψ=10 kPa, the pore water measurements of the three tensiometers coincided again but at approximately -20 kPa immediately following a decrement in the applied air pressure from 30 to 20 kPa. A similar trend for tensiometer measurements was observed and a similar time interval was required in order to reach equilibrium at this stage in comparison with the first stage. However, the development in measurements of the middle (T2) and deep (T3) tensiometers were too similar at this stage.
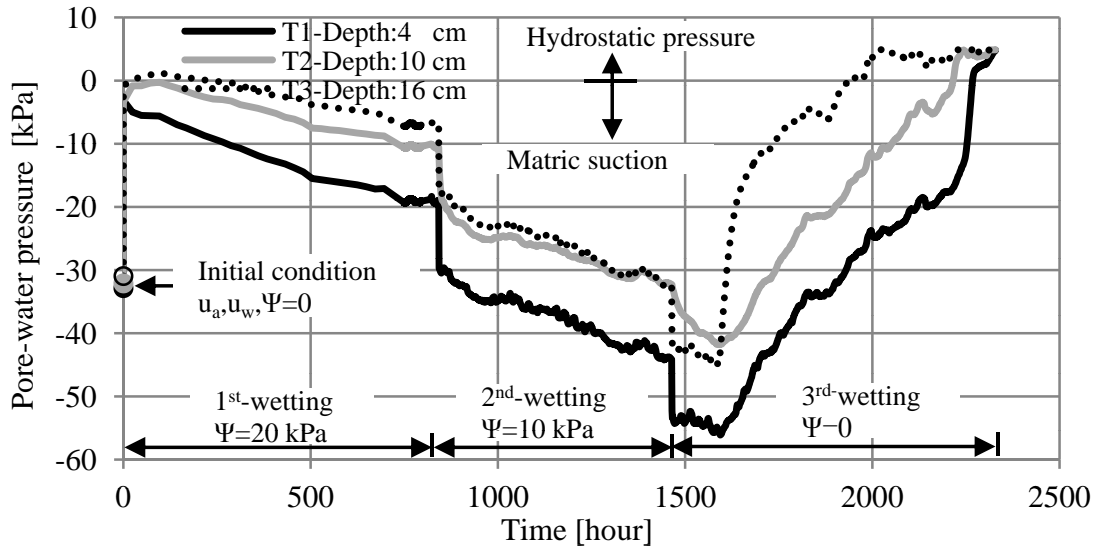
Figure 5.48.: Development of pore- water pressure with time under different stress condition in soil-column test for gypseous soil.

Nevertheless, no changes in the value of volumetric water content as well as in water level of the connected burette were observed during both stress path levels as shown in Figure 5.49. At the third stress path level of u_a=10 kPa, u_w=10 kPa, ψ=0 kPa when the air pressure was reduced from 20 to 10 kPa, a sudden increase was observed in the negative pore water-pressure without matching in the tensiometers measurements. After that, sharp increases in pore-water pressure towards positive values were recorded for three tensiometer measurements. Simultaneously a significant increase in the volumetric water content occurred as a result of water imbibitions processes.

The trend of pore water pressure evolutions for the third stress path level is completely opposite to the trends of both the first and second stress paths levels Furthermore, the deep tensiometer measurements showed a faster reduction in the negative pore water pressure (i.e. matric suction) than the middle and upper tensiometer. This is because the measuring zone of the deep tensiometer came into direct contact with the saturated ceramic base, which was directly connected to the water burette.

Therefore, the volume of the water surrounding the deep tensiometer at a specific time was higher than the others (Figure 5.49). At the equilibrium stage, the measurements of three tensiometers matched at a round positive pore water pressure of 4.8 kPa. The behaviour of gypseous soil during this test can be attributed to the effect of matric suction on the activity of the water in soil structure.
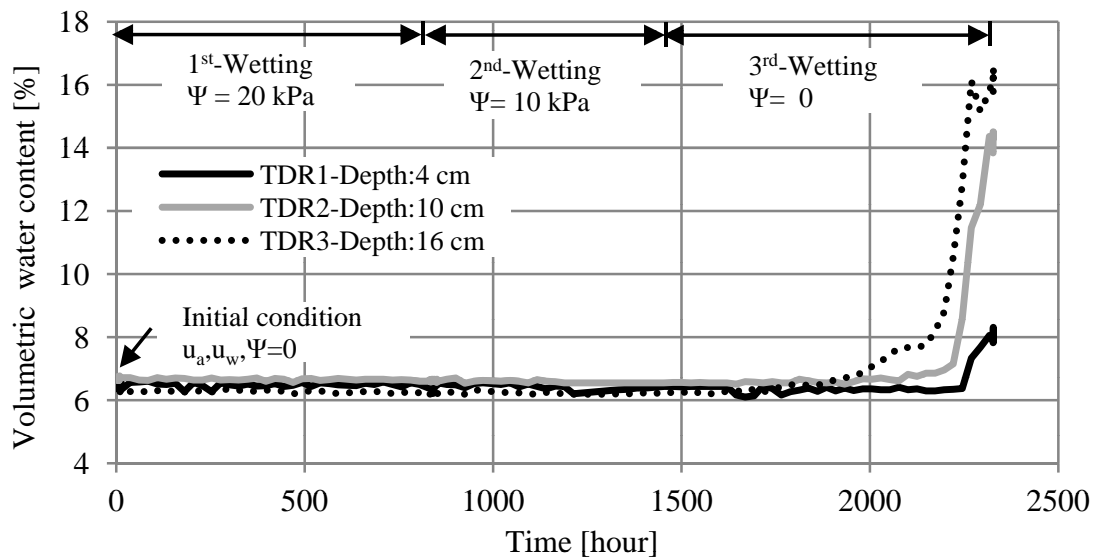
Figure 5.49.: Development of volumetric water content with time under different stress condition in soil-column test for gypseous soil.

In other words, the initial condition of the soil sample indicates that the soil with $\theta_o = 6.5\%$, $\psi=20$ kPa was located in transition zone and near the residual value of the wetting curve of the SWCC (see Figure 5.31a). Therefore, a reduction in the matric suction to $\psi=10$ kPa insignificantly affected the volumetric water content. Consequently, the presence of matric suction (even small values) at this stage forced the pore water to remain in place and reaching the equilibrium with externally applied pore water pressure. However, the absence of matric suction in third stress path level permitted the soil mass to have a full wetting and was transferred from the transition zone to the residual air content zone of higher water content on the SWCC.

Lins (2009) used the same technique with a different test procedure to investigate the effect of drainage/imbibitions cycles on the hydro-mechanical properties of partially saturated sand. She observed the same behaviour for the variation in pore-water pressure which was measured by several tensiometers installed at different depths of sand column sample, as shown in Figure 5.50.

Negligible volumetric strain or collapse deformation was recorded during the three stress paths levels as shown in Figure 5.51. This can be attributed to three reasons: low vertical stress (see Figure 5.10), relatively high initial moisture content (see Figure 5.16) and the effect of height to diameter H/D ratio of the soil sample. The higher the H/D ratio, the less collapse potential occurred for the soil mass as reported by Al-Obaidi (2003).
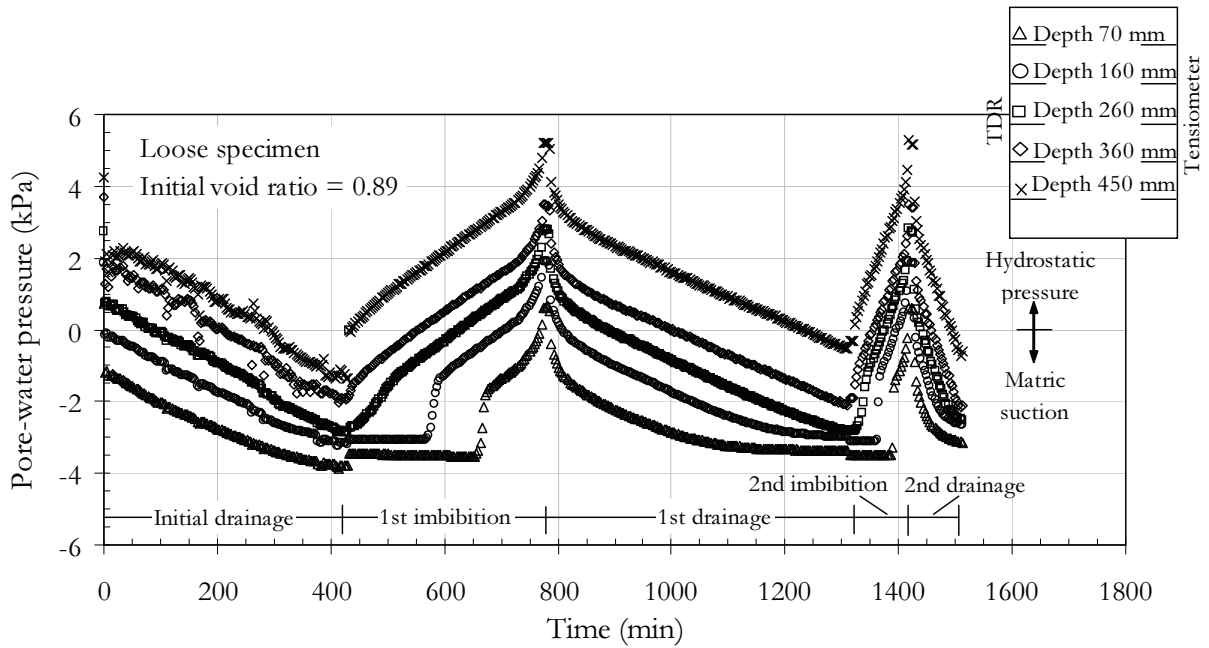
Figure 5.50.: Suction measurements for drainage and imbibitions processes using tensiometer technique in soil-column I device of loose Hostun sand (Lins, 2009).
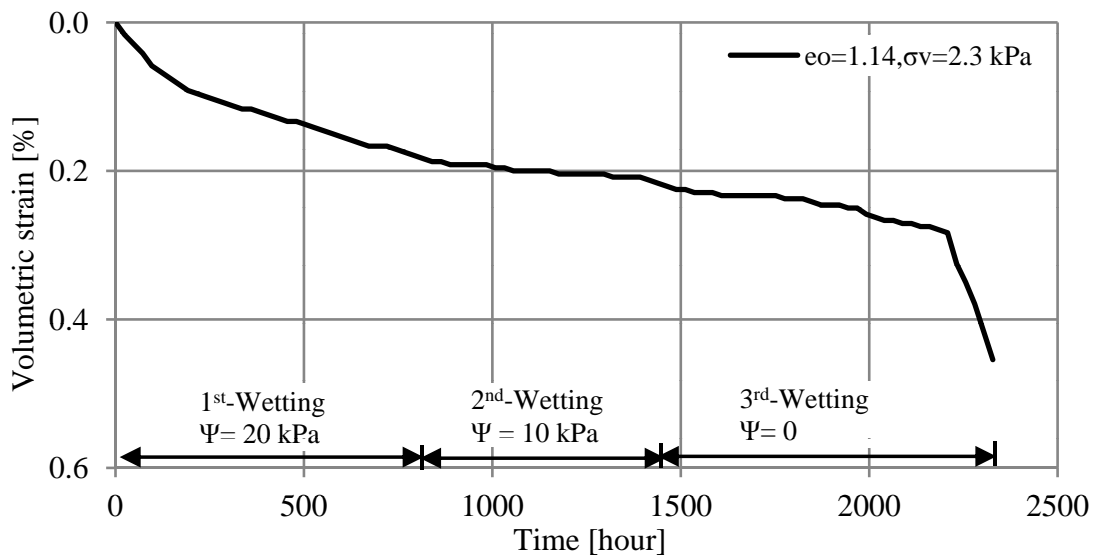
Figure 5.51.: Development of volumetric strain with time under different stress condition in soil-column test for gypseous soil.

Table 5.6.: The summary of soil-column test results at end of stress path level.

Stage	Stress path [kPa]			P.W.P [kPa]			θ [%]		
	u_a	u_w	ψ	T1	T2	T3	TDR1	TDR2	TDR3
Initial	0	0	0	-32.9	-32.1	-30.9	6.6	6.6	6.4
1 st	30	10	20	-19.1	-10.6	-7.1	6.4	6.6	6.3
2 nd	20	10	10	-44.1	-32.3	-32.5	6.4	6.6	6.2
3 rd	10	10	0	+4.8	+4.9	+4.8	8.2	14.5	16.6

As a conclusion, the soil column test results indicate that the shallow deposits of the collapsible soil were mostly influenced by matric suction, and it showed a considerable response to wetting processes. Therefore, critical collapse could be achieved in this zone particularly when shallow deposits were formed at low moisture content and low density. However, deeper deposits were affected by hydrostatic pressure which was greater than the matric suction, particularly when it was located near the ground water level. However, the danger of collapse deformation still existed due to the challenges of the leaching phenomenon in gypseous soil.

5.8. Soil improvement and foundation options

In order to minimise the effects of collapse deformation on engineering structures, a procedure for improving soil is suggested, and some foundation options are recommended. Nevertheless, it should be mentioned that the selection of any improvement techniques or foundation options is restricted by cost as well as the possibility and the efficiency of their application in the field. The suggestions are as follows:

-For shallow or undefined collapsible deposits level of relatively small constriction site:

1. Excavate and remove the soil layer to the elevation below the design foundation level.
2. Make a drainage system, such as pore holes or observation wells at sufficient depths.
3. Flood the construction site with water for a sufficient time period (considering the behaviour described in Subsections 5.2.2.3 and 5.3.1).
4. Preload the site area using a heavy vibratory compactor roller or any method of loading,

such as a dead load if it is available (considering the behaviour described in Subsections 5.2.2.1 and 5.2.2.2).

5. Cover the site area with a thin layer of water protection material, such as emulsified asphalt (considering the behaviour described in Subsection 5.5.1).

6. Cover the site area with a suitable geotextile grid such as a Geosynthetic Clay Liner (GCL) as additional water protection to avoid sudden collapse or snick holes (considering the behaviour described in Subsections 5.2.2.1 and 5.5.1).

7. Refill the site area with well-compacted sub-base soil.

8. Use a very stiff raft foundation.

-For deep collapsible deposits:

1. Take steps 1 to 7 as described above.

2. Use deep pile foundations to avoid collapsible soil and move toward a more stable underlying stratum.

This procedure is more suitable for gypseous soil where the main factors causing collapse behaviour are considered. For loess soil, the same procedure is proposed except that the excavated soil can be remixed with gravel and recompacted. In addition, the drainage system in point two can be skipped.

Many literatures include some of the above-mentioned procedures to improve the collapsibility characteristics of loess soil such as Bowles (1984); Lefebvre (1995); Terzaghi et al. (1996); Houston et al. (2001); Jefferson et al. (2005).

5.9. Summary

In this chapter, the experimental results, analysis and discussions of the test program for naturally gypseous, artificially gypsified and naturally loess soils are presented. The collapse characteristics and the factors affecting the estimation of the collapse potential are investigated, such as the inundation stress level, the initial dry density, the initial degree of saturation and the leaching phenomenon.

The collapse deformation is investigated utilising two procedures: single step wetting (i.e. the single and double Oedometer test) and stepwise wetting (i.e. suction decreases under constant net vertical stress). The results of the soil-water characteristics curve (SWCC), in addition to permeability coefficient determination under both unsaturated and saturated conditions are presented as well.

Moreover, elementary characteristics using ESEM-EDX analysis, soil column tests, soil improvement and foundation option procedures are also discussed. The summary of the experimental program results can be stated as follows:

Large volume changes and collapse deformation resulted upon single step or stepwise wetting (i.e. suction decrease) procedures. Gypseous soil suffered from very severe trouble deformations due to the leaching phenomenon, while no effect was observed in the case of loess soil (Figures 5.34a and 5.34b).

The collapse potential increased gradually with the increases in the vertical stress level, especially when it exceeded the maximum preconsolidation pressure. A decrease in matric suction also increased the collapse potential, especially at low suction ranges (Figure 5.23). However, it decreased significantly as the initial dry density and the initial degree of saturation increased (Figures 5.12c and 5.16).

ESEM-EDX measurements showed substantial effect for the inundation and leaching processes on the microstructure and the fabric of the collapse soils. According to the SWCC results, the hysteresis is present for all soil types. According to the SWCC results, hysteresis was present for all soil types. However, the AEV and the range of the transition zone were not the same for all soil samples because the geological formation and the homogeneity of soil fabric were different. At an unsaturated state, the coefficients of permeability increased as the applied suction and the degree of saturation decreased (Figures 5.37 to 5.45). For soil-column test, the deepest layer of collapsible deposits was influenced by hydrostatic pressure, while the shallow deposits were influenced by the matric suction (Figure 5.48).

6. Conclusions and Recommendations

6.1. Introduction

This chapter reviews the main conclusions regarding the behaviour of the naturally gypseous soil (GI), artificially gypsified soil (70G30S) and loess soil (LG) based on our analysis of the experimental test results. Recommendations and suggestions for further work are also outlined in this chapter.

6.2. Conclusions

6.2.1. Compressibility characteristics

1. The trend of compression and recompression consolidation curves for the three types of soils is approximately linear.

2. For the three collapsible soils, several hours are required to complete the primary consolidation stage. Secondary compression (i.e. creep) is recorded and continued for several days for GI and 70G30S, while no creep was observed for LG.

6.2.2. Collapsibility characteristics without suction control

1. The structures of the three selected soils generally exhibit unstable behaviour and "collapse" volume change in response to inundation under constant vertical stress.

2. The GI and 70G30S soils are susceptible to volume decreases (i.e. collapse) upon wetting irrespective of the value of the vertical stress applied. While the volume changes in LG soil is either increases (i.e. swelling) or decreases (i.e. collapse) upon wetting based on the stress level and the maximum preconsolidation pressure.

151

3. The collapse potential estimated from both single and double Oedometer tests increases linearly with incremental increases in inundation vertical stress. No critical vertical stress level is observed.

4. The collapse potential of both GI and 70G30S soils was uniformly increased with respect to the inundation vertical stress. However, three distinct regions of collapse deformation were noticed for LG soil.

5. The mechanism of collapse deformation and the action of the destruction of bonds upon inundation in both naturally gypseous and artificially gypsified soils is a function of the type and historical formation of these bonds, the heterogeneity of soil fabric and the degree of cementation.

6. After ten minutes of inundation, the degree of deformation of both GI and 70G30S soils reaches about 60% of its final value then creep is developed. However, the degree of deformation of LG soil reaches about 80% of its final value then negligible deformation is recorded.

7. The higher initial density and the higher initial volume of water in the soil mass, the lower the collapse deformation that occurs. Furthermore, insignificant deformation is recorded when inundation is induced at an initial critical degree of saturation of soil specimen.

6.2.3. Volume change under suction control (wetting path)

1. The final volume change of soil resulted from single or multi-step wetting is denoted as collapse deformation, which is a function of net vertical stress, initial void ratio, initial degree of saturation and range of applied suction.

2. Three main distinct phases for collapse mechanism over suction range are observed, namely: pre-collapse phase, main collapse phase and post-collapse phase.

3. Under a low range of applied suction, the final soil collapse is reached after few hours of wetting and at a degree of saturation of 30-50%. After final collapse, a creep deformation in gypseous soils is observed, while it was negligible in loess soil case.

4. The gravimetric water content as well as the degree of saturation experience similar increases in their values as the suction is reduced from the initial value to zero regardless the soil collapse which induced under different vertical stress. However,

fully saturation of soil specimen was not occurred even at zero suction due to the existent of entrapped air bubbles between the soil particles.

5. The estimation of final collapse potential obtained by utilizing multi-step suction decrease procedure is relatively larger, more reliable and comparable to field conditions than that values obtained by single step wetting procedure.

6.2.4. Volume change under suction control (drying path)

1. The subsequent drying processes by increasing the applied suction on the initial full saturated soil sample result a considerable settlement and volumetric strain. This behaviour was due to shrinkage of the soil mass.

2. The imposition of high suction value on the saturated soil mass leads to create the entrapped air bubbles which drive them to be replaced by the water molecules in the pore space. Hence, great reduction in gravimetric water content and degree of saturation is resulted.

6.2.5. Soil-water characteristics curve (SWCC)

1. The air-entry value for all soils occurs at very low suction range. The residual suction range for GI and 70G30S soils occurs at low suction range while for LG soil occurs at relatively high suction range.

2. At the boundary effect zone, the coarse grain size of the soil mass cannot hold the water molecules in the pore space, even with low value of imposed suction due to the high permeability and weak interparticle tension forces of the metastable soil.

3. The hysteresis in SWCC is presented for the three selected soils. The amount of the hysteresis was varied based on the geological formation and homogeneity of soil fabric.

6.2.6. Permeability-leaching investigation at saturated state

1. Leaching phenomenon causes a severe deformation in gypseous and mixed soils, but no such effect on loess soil.

2. Leaching process in GI soil caused volume decreases much greater than the volume decreases resulting from full saturation state especially under low vertical stress.

3. Accumulative leaching strain and accumulative dissolved gypsum significantly increases while the coefficient of permeability is decreased with the increases of leaching period.

4. The reduction in the permeability coefficient of gypseous soil does not necessary have to mean that accompanying decrease in the void ratio during leaching processes is occurred. Contrariwise the void ratio significantly increases with increases in both of the leaching strain and dissolved gypsum especially when leaching conducted under low stress level.

5. The collapse potential developed by leaching phenomenon can be calculated depending on the volumetric strain data to avoid any mistake when utilizing the values of void ratio.

6. For loess soil, no changes in volumetric strain or void ratio of the soil sample are observed during the leaching processes. The metastable structure of loess soil reached to equilibrium after achieved the final collapse.

6.2.7. Permeability coefficient investigation at unsaturated state

1. The coefficients of permeability at unsaturated state increase with the decrease of the imposed suction, gravimetric water content and the degree of saturation.

2. The variation of permeability coefficient with suction and/or with degree of saturation under different net vertical stresses is congruent and in band form.

6.2.8. Mineralogical characteristics and fabric studies

1. The natural formation of gypsum can be found in three phases as: a phase of flat sheet or crust, a phase of accumulative dense blocks or crystals and/or a phase of encase the sand or silt particles.

2. The artificially gypsified fabric consists of gypsum particles which are uniformly distributed and encase the fine sand particles, or may present as separately gypsum film or crusts.

3. Upon leaching processes for gypseous soil, the sulphate and calcium content have been reduced to about 50% of its initial values.

4. Loess structure is homogeneous with isotropic, non-oriented fabric. The fabric is connected with scarcely fine sand grains through clay bridges and buttresses with the existing of large voids.

5. A Sequential transformation on the particle shape of natural gypseous soil is observed due to its sensitivity against water activity, but this is not observed for artificially gypsified and loess soils.

6.2.9. Soil-column behaviour

1. According to the stress path and the elevation of soil element in regard to the water source, a soil element either lies under the influence of the hydrostatic pore-water pressure or lies under the influence of matric suction.

2. The relative reduction of matric suction has an insignificant effect on the volumetric water content of partial saturated soil. However, the absence of matric suction permits to start the imbibitions processes for the soil mass until it reaches to equilibrium when the full wetting state is achieved.

3. The critical collapse occurred mostly under the influence of matric suction, especially when the shallow deposits are formed at a low moisture content and density. Although, the risk of collapse deformation still exists in deeper deposit affected by the hydrostatic pressure and leaching phenomenon in gypseous soil.

6.2.10. Soil improvement and foundation options

1. For shallow or undefined collapsible deposits level, the use of drainage system and water proofing techniques is recommended to be performed before the prewetting and dynamic compaction processes.

2. After improvement processes, rigid raft foundation could be sufficient for shallow collapse deposits, while using deep pile foundations could be the suitable option to avoid the collapse of the soil to a more stable underlying stratum.

6.3. Recommendations

Based on the findings of the experimental work in this thesis, and the challenging arising from the collapsible soils in geotechnical engineering activities, the following further investigations are suggested:

1. Studying the effect of (wetting/drying) cycling under a range of constant net normal stress and a range of suction variation on the value collapse potential. This study will help to simulate the field conditions when the climate is changing.

2. Complementing the data that has been obtained in this study, through a series of collapse deformation (on the three type of soil used) induced by an increase in net normal stress under a range of constant suction conditions. Such conditions are similar to the construction of a new structure on the collapsible soil stratum.

3. Investigating the effect of gypsum content in the sand soil on the collapsibility characteristics. This can provide valuable geotechnical data when new structure is required to construct on such soil deposits. Such an investigation is based on performing of several constant net normal stress (one step and stepwise wetting) tests and several constant suction-net normal stress variations.

4. Complementing the data that has been obtained from sand-column test through measurements of pore-water pressure using high suction tensiometer probe and high sensitive of TDR probe are necessary to provide a better understanding to the behavior of collapsible soils.

5. Performing a series of soil-column tests under wide range of matric suction and volumetric water content measurements for different height to diameter ratio, in combination with leaching processes for the soil sample. These tests will help to investigate the critical collapse zone for foundation design.

6. Based on the obtained experimental data, a numerical simulation utilizing suitable software such as Code Bright to provide the required parameters for foundation design.

A. Techniques of Suction Application and Measurements

A.1. Techniques of suction application

A.1.1. Axis translation technique (ATT)

The concept of axis-translation technique (ATT) is based on imposing matric suction to a soil specimen through the use of high-air-entry ceramic disk. Hilf (1956) is the first researcher who proposed the ATT in order to develop matric suction in soil specimen as a differential air and water pressure (u_a-u_w), without creating cavitations in the water phase. In ATT technique, the difference between the pore-air pressure u_a and pore-water pressure u_w (i.e. matric suction) can be controlled by increasing or decreasing the applied pore-air pressure while keeping the pore-water pressure constant on the saturated ceramic disk. The ceramic disk is not an impermeable membrane to dissolve salts (or ions) in the soil. Therefore, water flow is bypassed due to osmotic effects since in this case; the water flow is an advective process (Agus, 2005). Fredlund et al. (2012) indicated that an over estimation of the measured matric suction may be occurred due to presence of occluded air bubbles in the soil specimen, while an underestimation of the measured matric suction may be occurred due to air diffusing through the high-air-entry disk. For this reason, flushing process of the ceramic disk is very important to remove the diffused air bubbles and to establish a continuous water phase between the soil and the water pressure through the ceramic disk. Several researchers used the concept of ATT with different types of equipment for applying matric suction on the soil specimens. Such researchers are: Romero (1999); Fredlund (2001); Lins & Schanz (2004); Agus (2005).

A.1.2. Vapour equilibrium technique (VET)

The vapour equilibrium technique (VET) was used for applying a high total suction range to soil specimens. The concept of VET is based on creating a constant-relative humidity chamber in the laboratory, through use of either saturated or unsaturated salt solutions. The ASTME104-02 (2003) standard and Fredlund et al. (2012) suggested a list of different types of salt solutions which can be used to create a range of relative humidity environments. Fredlund et al. (2012) outlined the main principle factors that affect the time required to establish vapour pressure equilibrium, and as follow: (1) the ratio of free surface area of the solution to the chamber volume, (2) the amount of air circulation, (3) the agitation of the salt solution, and (4) the absorbing properties of the sample; in addition to specimen size where the larger the specimen size, the longer the time required to attain equilibrium conditions. The total suction corresponding to a particular relative humidity value can be calculated using Kelvinâs law. Generally, the VET can be used to control almost the suction value of more than 2000 kPa because of its extreme sensitivity to temperature gradient that exists between the salt solution, the vapour space, and the soil specimen (Agus & Schanz, 2003; Agus, 2005).

A.2. Techniques of suction measurements

A.2.1. Time domain reflectometry (TDR)

This technique is commonly used for measuring volumetric water content of soils. The TDR sensors determine the dielectric constant by measuring the travel time of an electronic pulse when embedded in the soil layer. The dielectric constant can be converted into the volumetric water content by using different mathematical models. Hu et al. (2010) reported that for many types of soils, the same relationship between the volumetric water content and dielectric constant is observed. However, this relationship is not unique for all soils, therefore, before using the TDR, calibration is required. In order to achieve accurate matric suction measurement, the TDR requires very advance electronic data log device and high moisture sensitive TDR in addition to the precise determination of soil-water characteristic curve of the soil tested. More details about the TDR are given in: ASTMD6780 (2003); Agus (2005); Lins (2009); Schanz et al. (2010); Fredlund et al. (2012).

A.2.2. Tensiometer technique

Tensiometers are normally used for directly measuring the negative pore-water pressure of soil. A brief description of theory and the measuring method using tensiometers is given in Fredlund & Rahardjo (1993); Agus (2005); Fredlund et al. (2012).

The principle of suction measurement using tensiometer is reliant on achievement of pressure equilibrium between the soil and the tensiometer. The water in the tensiometer will be in tension of the same magnitude as the negative pore-water pressure in the soil.

At atmospheric pressure, the pore-air pressure (u_a) is equal to zero, then the measured negative pore-water pressure is numerically equal to the matric suction, while when the pore-air pressure is greater than atmospheric pressure (i.e., during axis translation), the summation of the tensiometer reading and the pore-air pressure reading equivalent to the value of matric suction. Because of cavitations phenomenon, measuring of pore-water pressure (i.e. matric suction) using the tensiometer is ranging to (-90 kPa) and must not exceed the air entry value of the ceramic cup. The measurement of suction using tensiometers is only provided matric suction value because the osmotic component of soil suction is not measured Fredlund et al. (2012).

A.2.3. Chilled-mirror hygrometer technique

The chilled-mirror hygrometer uses a dew-point measurement to determine the total suction in a soil. The measurement is performed under isothermal conditions in a sealed container. The chilled-mirror technique allows the total suction to be measured in the mid-to high-suction range (i.e. from 3000 kPa to 300,000 kPa) (Gee et al., 1992).

Total suction, or the free energy of soil-water, is the equivalent suction derived from the measurement of the partial pressure of water vapour in equilibrium with the soil water, which is relative to the partial pressure of water vapour in equilibrium with free pure water (Aitchison, 1964; Fredlund & Rahardjo, 1993).

Several geotechnical researchers have used the chilled-mirror hygrometer device for total suction measurement of the soil such as: Leong et al. (2003); Schanz et al. (2004); Agus & Schanz (2005); Campbell et al. (2007); Schanz et al. (2010); Al-Obaidi & Schanz (2013). The testing procedure was introduced in the (ASTMD6836, 2008) standard.

The chilled-mirror hygrometer device used in this study is a water activity meter (Type 3TE, Decagon Devices, Inc., Pullman, WA). The device is shown in Figure A.1.

The total suction is calculated using the thermodynamic relationship between soil suction,

or the free energy of the soil-water, and the partial pressure of the pore water vapour as follow:

$$\psi = -\frac{RT}{\upsilon_{wo}\omega_V}\ln(\frac{\overline{u}_v}{\overline{u}_{vo}}) \tag{A.1}$$

where: ψ=soil suction or total suction (kPa), R= universal (molar) gas constant (i.e., 8.31432 J/(mol K)), T_K= absolute temperature (i.e., $T_K = (273.15+T$ (K)), T= temperature, ^oC,υ_{wo}=specific volume of water or the inverse of the density of water (i.e., $1/\rho_w$ (m^3/kg)), ρ_w= density of water (i.e. 998 (kg/m^3) at temperature T=200 ^oC), ω_V= molecular mass of water vapour (i.e., 18.016 kg/kmol), $\overline{u}_v$= partial pressure of pore water vapour (kPa), and $\overline{u}_{vo}$=saturation pressure of water vapour over a flat surface of pure water at the same temperature (kPa). The term ($\frac{\overline{u}_v}{\overline{u}_{vo}}$) is called the relative humidity (RH) and is entered as a fraction (i.e. water activity) in equation A.1.

(a)   (b)

Figure A.1.: Chilled-mirror hygrometer device: (a) Device set up and (b) Schematic plot.

B. Calibration of the Equipments

B.1. UPC-Barcelona cell

The calibration of UPC-Barcelona cell against pressure-deformability during loading and unloading was verified using dummy stainless steel specimen, under two conditions of filter paper; dry and wet. The stainless steel dummy disk was placed in the cell ring instead of the soil specimen with two filter papers (i.e. one on the top and the other on the bottom of the dummy disk). The stainless steel dummy disk was subjected to loading condition by stepwise increasing of the applied vertical stress. Then it was subjected to unloading condition by stepwise decreasing of the applied vertical stress. The deformations of the loading and unloading steps are recorded and plotted in Figure B.1, for both versions of the Barcelona cells (i.e. one and two). The deformability calibration of the cells was considered during the volume change calculations of the real soil specimens.

Based on the function of this cell, the soil sample can follow the wetting or drying stress paths by decreasing or increasing the applied matric suction under the effect of the single dimensional net vertical stress.
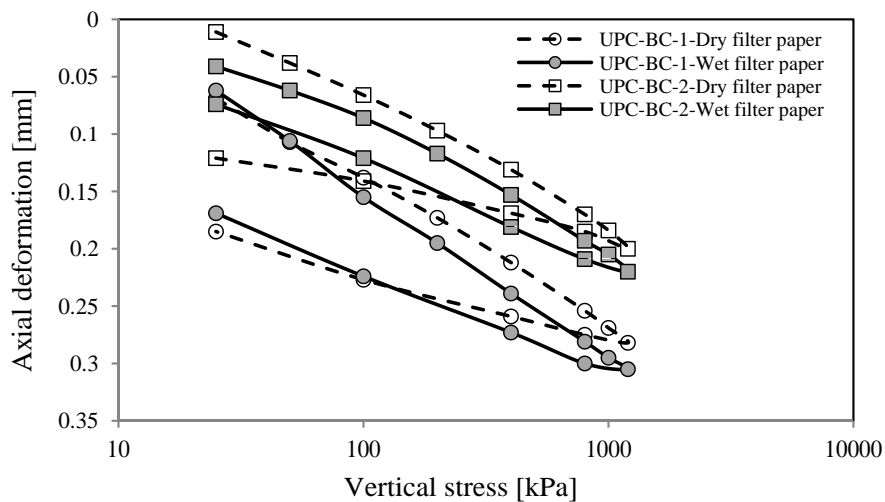
Figure B.1.: Pressure-deformability calibrations of the two UPC-Barcelona cells.

B.2. UPC-Isochoric cell

Two types of calibration are performed for the modified UPC-Isochoric-Oedometer cell. The first calibration was to define the exact surcharge weight, which is required for each stress value. This calibration was performed on the two of the modified UPC-Isochoric-Oedometer cell using a special load cell. The second calibration was against pressure-deformability of UPC-Isochoric cell during loading and unloading using a dummy stainless steel specimen under two conditions of filter paper, dry and wet. The procedure of the pressure-deformability calibration is exactly the same procedure followed for calibration the UPC-Barcelona cell in B.1 and as shown in Figure B.2.

B.3. Soil-column device

B.3.1. Time domain reflectometry (TDR) sensors

Two types of calibrations are carried out on the three TDRs sensors used in this study. The first calibration is to check the reasonability of the TDRs sensors measurements in different media such as air, water and dry sandy gypseous soil. The measurements were obtained for 30 minutes with time interval of 1 minute between each two successive measurements. The results of this calibration are presented in Table B.1, which are the average value of 30 measurements for each media. The results seem to be reasonable and as expected.
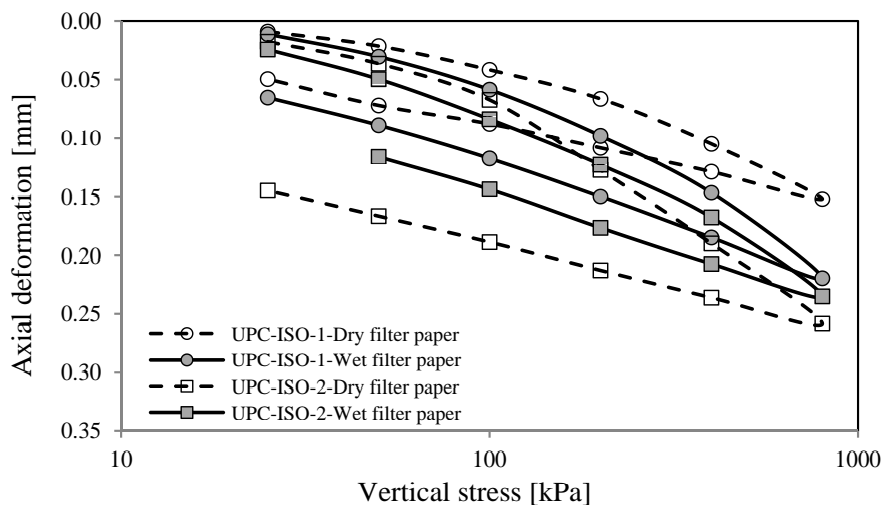

Figure B.2.: Pressure-deformability calibrations of the two UPC-Isochoric cells.

Table B.1.: Average measurements of TDRs sensors in different media.

	Average volumetric water content [%]		
Media	TDR1-32157	TDR1-32158	TDR1-32159
Air	0	0	0
water	99.99	94.1	99.99
Dry sandy gypseous soil (GI)	0.91	0.79	0.92

The second calibration for the three TDR sensors is to check the accuracy of the TDRs measurements, corresponding to the actual range values of the volumetric water content of the soil sample. The calibration is conducted in similar condition of the soil-column test. The sandy gypseous soil (GI) is compacted to the initial void ratio of e_o=1.14 and wide range of predefined volumetric water contents. The calibration cylinder used in this study (Figure B.3) considered the influence zone of measurements given by Cabral et al. (1999), and the suitable distances between the TDRs probe given by Suwansawat & Benson (1999).Cabral et al. (1999) examined the influence zone of measurements around TDR probes and found an influence zone of 90 mm in length, 15 mm in height and 35 mm in depth for the TDR probes types (Mini Buribale Waveguides) used by Lins (2009). Sizing of a calibration cell that can be used for the determination of the volumetric water content was studied by Suwansawat & Benson (1999). The authors found that a distance of 36 mm between the cell and the probe as well as a distance of 30 mm between the probes is required to determine the calibration function between dielectric constant and volumetric water content.

In this study, the soil sample was prepared in a plastic container of 160 mm height and 195 mm diameter, see Figure B.3. Three TDR probes were horizontally placed in a cylindrical plastic container with a distance of 40 mm between the adjacent TDR probes and 40 mm between the cell wall and the TDR probes. The cylindrical plastic container was closed by the nylon folia and the top cover during the calibration processes to keep the moisture content of the soil sample constant over the calibration time.

Moreover, during the calibration time of 30 minutes, 30 TDRs measurements were obtained for each predefined volumetric water contents. The results of this calibration (shown in Figure B.4) are considered in the calculations of soil-column test results. Furthermore, Figure B.5 shows the verification of the TDR sensors with time for different water contents. It can be seen that, the response of the TDR sensors is constant and react immediately with the changes in the water contents. Therefore, the TDR sensors are suitable for use in soil-column test.
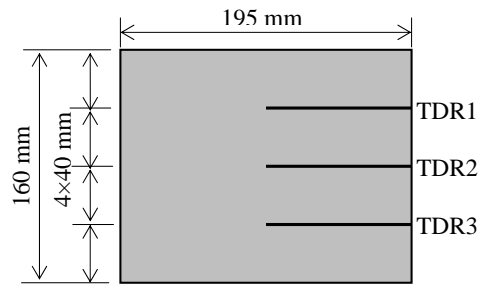
Figure B.3.: Schematic of the TDRs calibration container.
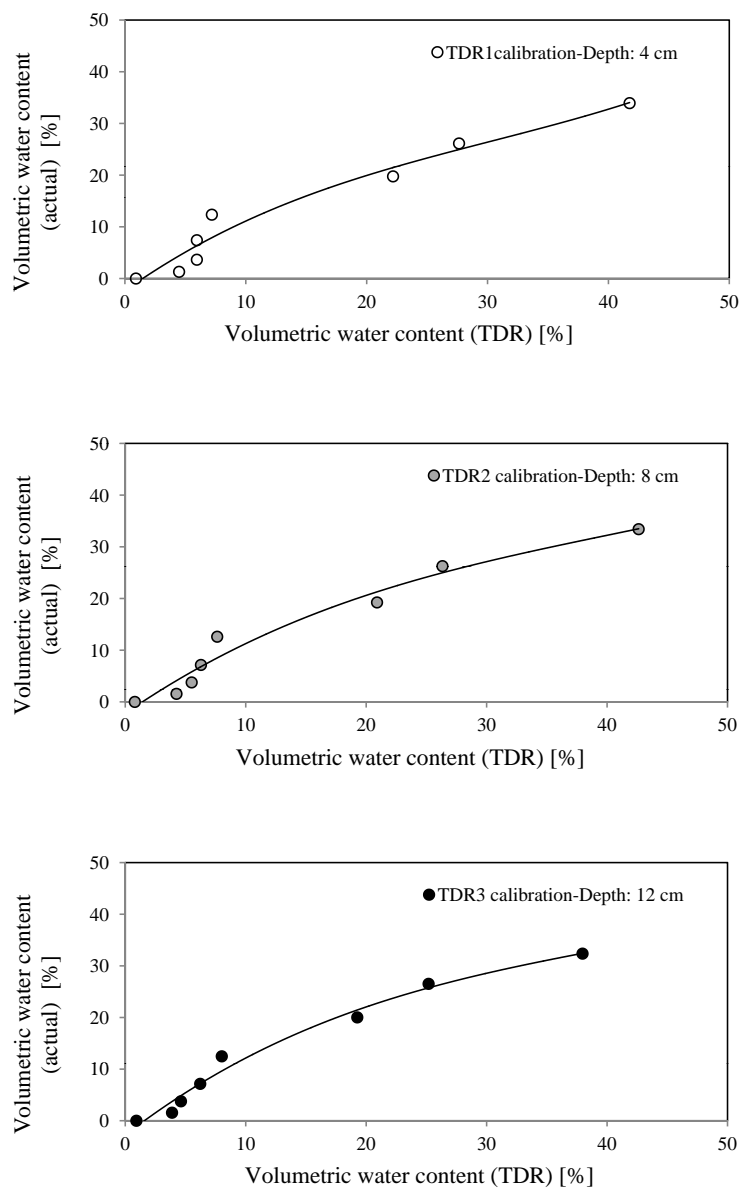
Figure B.4.: Calibration of TDR sensors with sandy gypseous soil (GI).
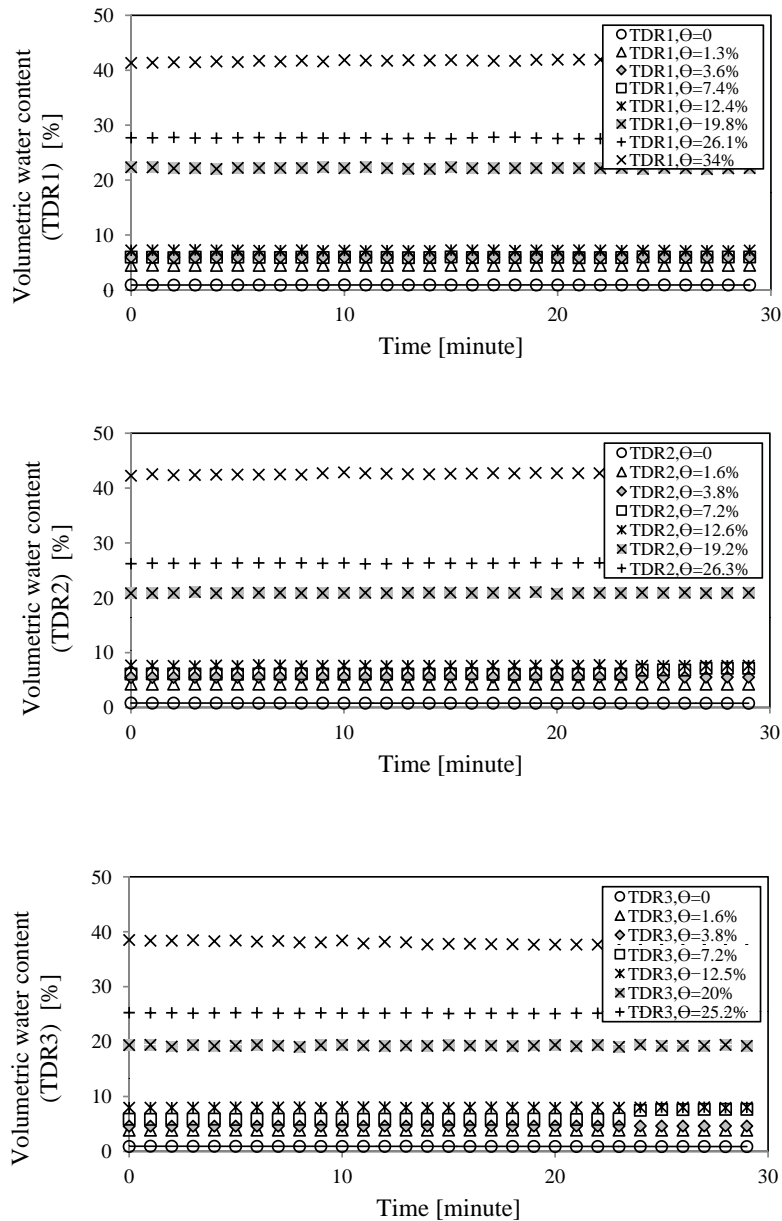
Figure B.5.: Verification of response time of TDR sensors.

B.3.2. Tensiometer Sensors

The calibration was done to check the accuracy of the tensiometer measurements and the efficiency of water refill and removal of the air bubbles processes. It was performed through applying a predefined negative and positive pore-water pressure (i.e. matric suction and hydrostatic pressure respectively) on the three tensiometers used in this study,

after checking the zero offset of each tensiometer. The predefined negative pore-water pressure domain is -20, -15, -10, -8, -6, -4, -2 and -1 kPa, while the predefined positive pore-water pressure domain is 1, 2, 4 and 5 kPa. The calibration was carried out using the high accuracy burette, as shown in the Figure B.6. The calibration results are given in Figure B.7. These results indicate that, the three tensiometers have a high accuracy of measurements, a very sensitive and a fast response to any change in the applied pore-water pressure. Therefore these tensiometers are suitable for use in soil-column test.
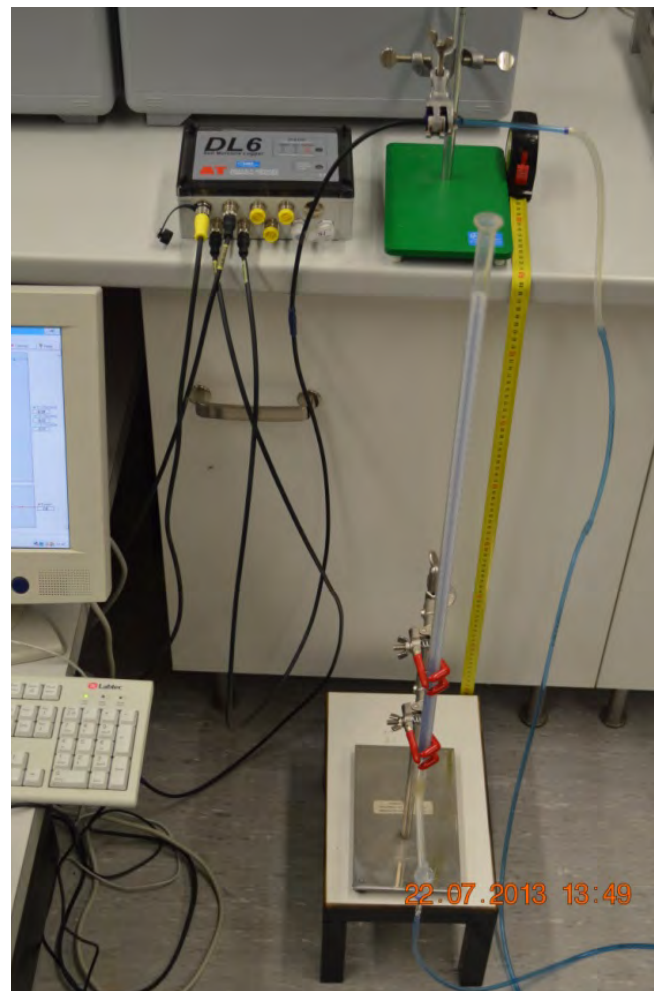
Figure B.6.: Calibration procedure of tensiometer sensor.
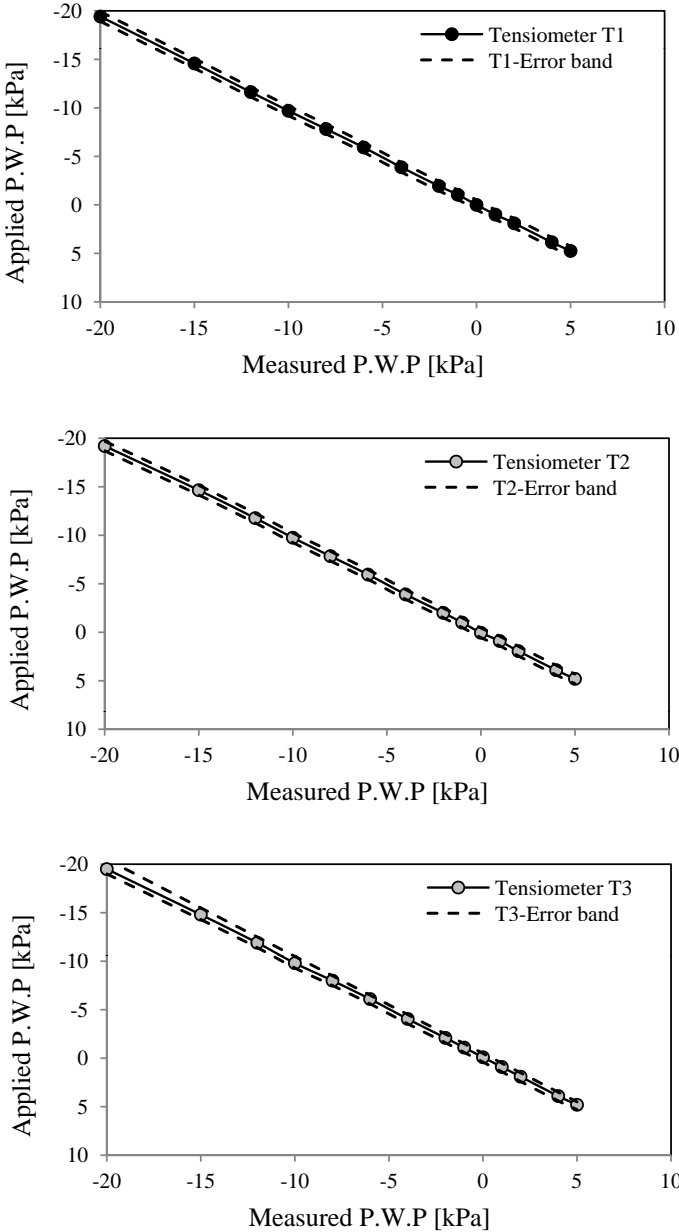
Figure B.7.: Calibration results of tensiometer sensors.

C. Elementary characteristics (ESEM-EDX) analysis

C.1. ESEM-EDX analysis for gypseous soil (GI)

Element	C	O	Mg	Al	Si	S	K	Ca	Total
(%) Per weight	5.3	34.7	2.1	2.2	7.2	19.6	0.6	28.3	100

Figure C.1.: ESEM-EDX measurements for GI soil at unsaturated state; (a) ESEM $40\mu_m$ image, (b) ESEM $10\mu_m$ image and (c) EDX analysis with element quantification.

Element	C	O	Mg	Al	Si	S	Ca	Fe	Total
(%) Per weight	-	45.4	1.9	1.9	5.4	19.1	25.1	1.2	100
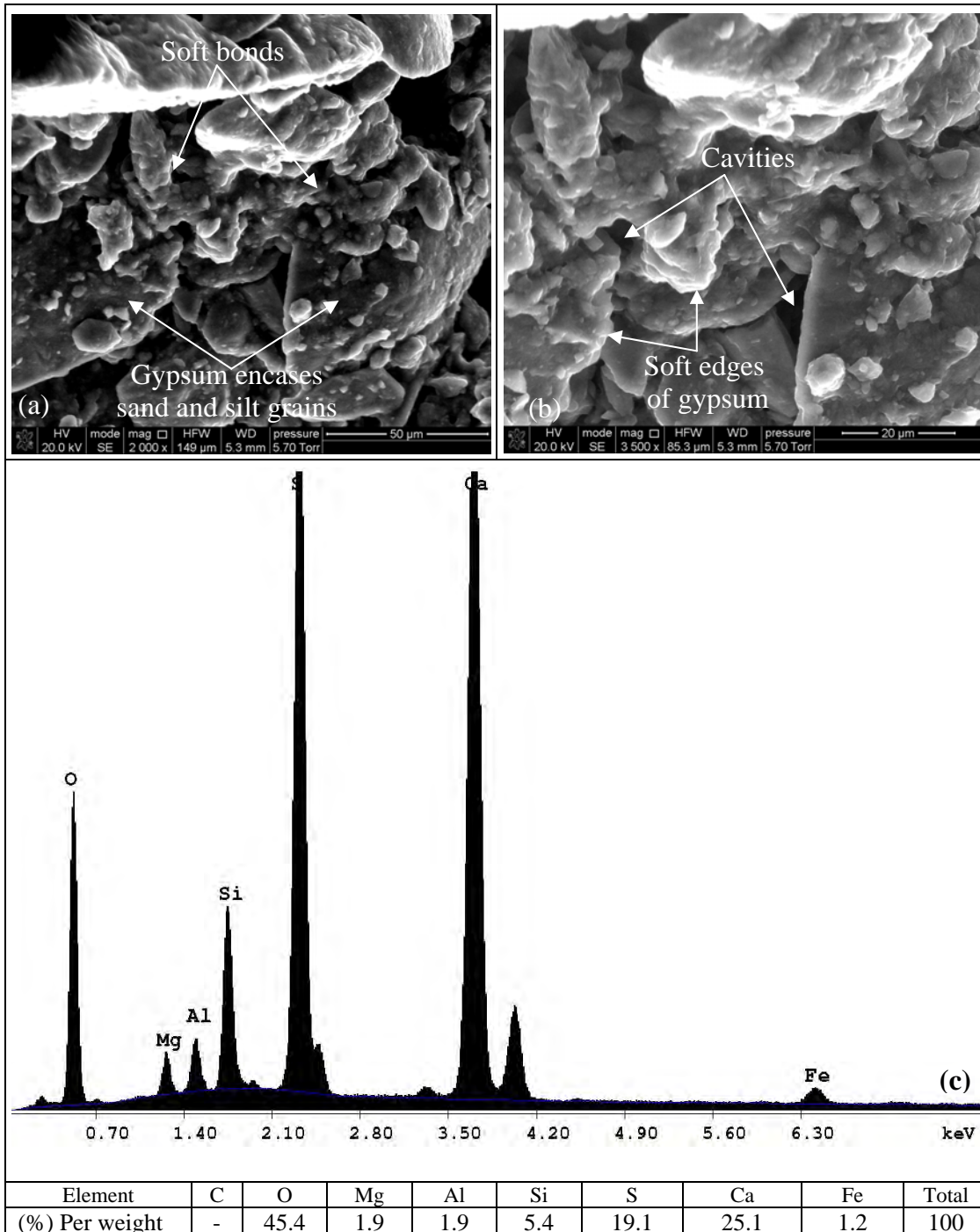
Figure C.2.: ESEM-EDX measurements for GI soil at saturated state; (a) ESEM $50\mu_m$ image, (b) ESEM $20\mu_m$ image and (c) EDX analysis with element quantification.

Element	C	O	Mg	Al	Si	S	K	Ca	Fe	Total
(%) Per weight	24.8	39.3	2.3	2.3	7.9	8.4	0.6	12.4	2.0	100
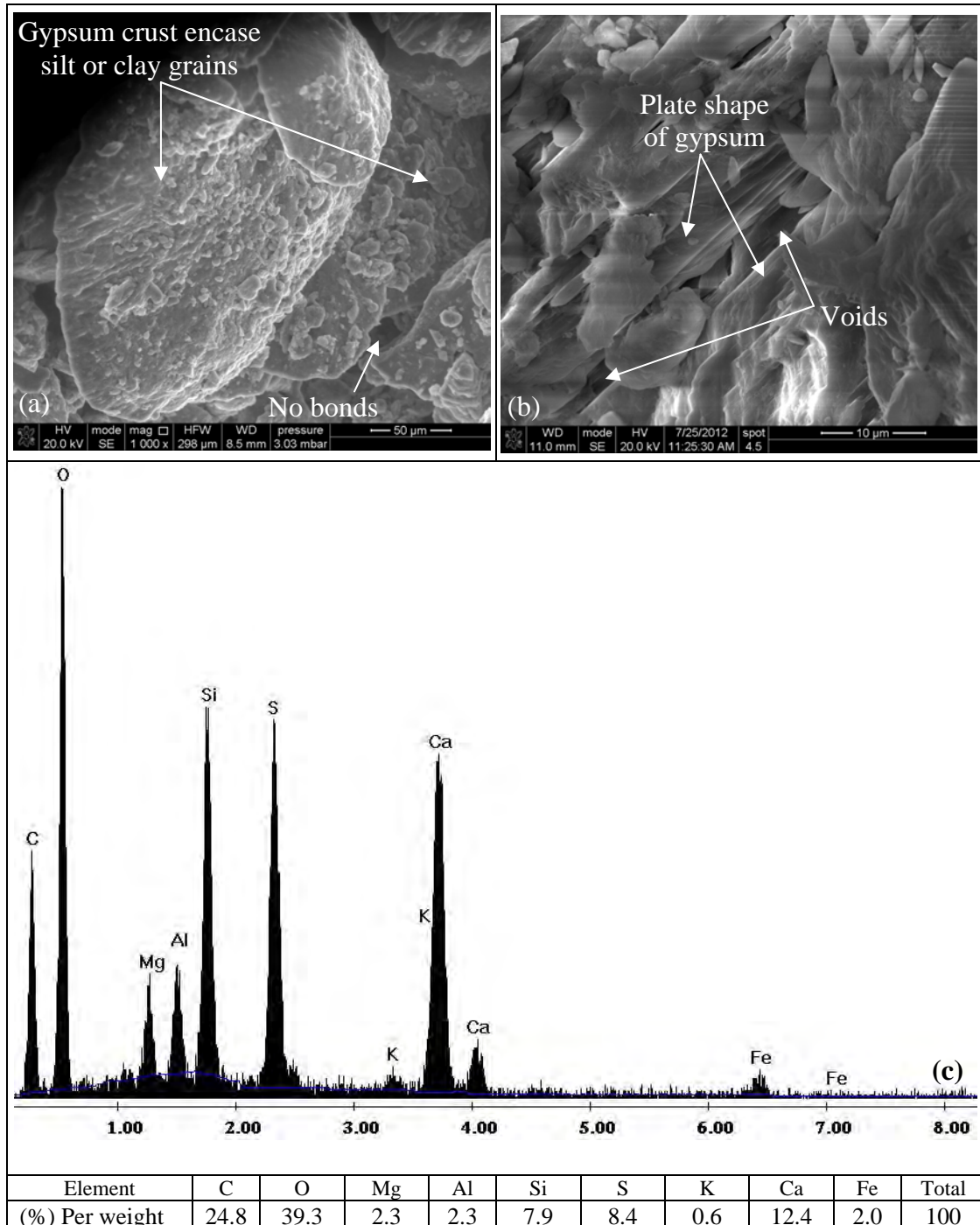
Figure C.3.: ESEM-EDX measurements for GI soil at leached state; (a) ESEM $50\mu_m$ image, (b) ESEM $10\mu_m$ image and (c) EDX analysis with element quantification.

C.2. ESEM-EDX analysis for mixed soil (70G30S)

Element	O	Si	S	Ca	Total
(%) Per weight	28.8	0.6	29.3	41.3	100
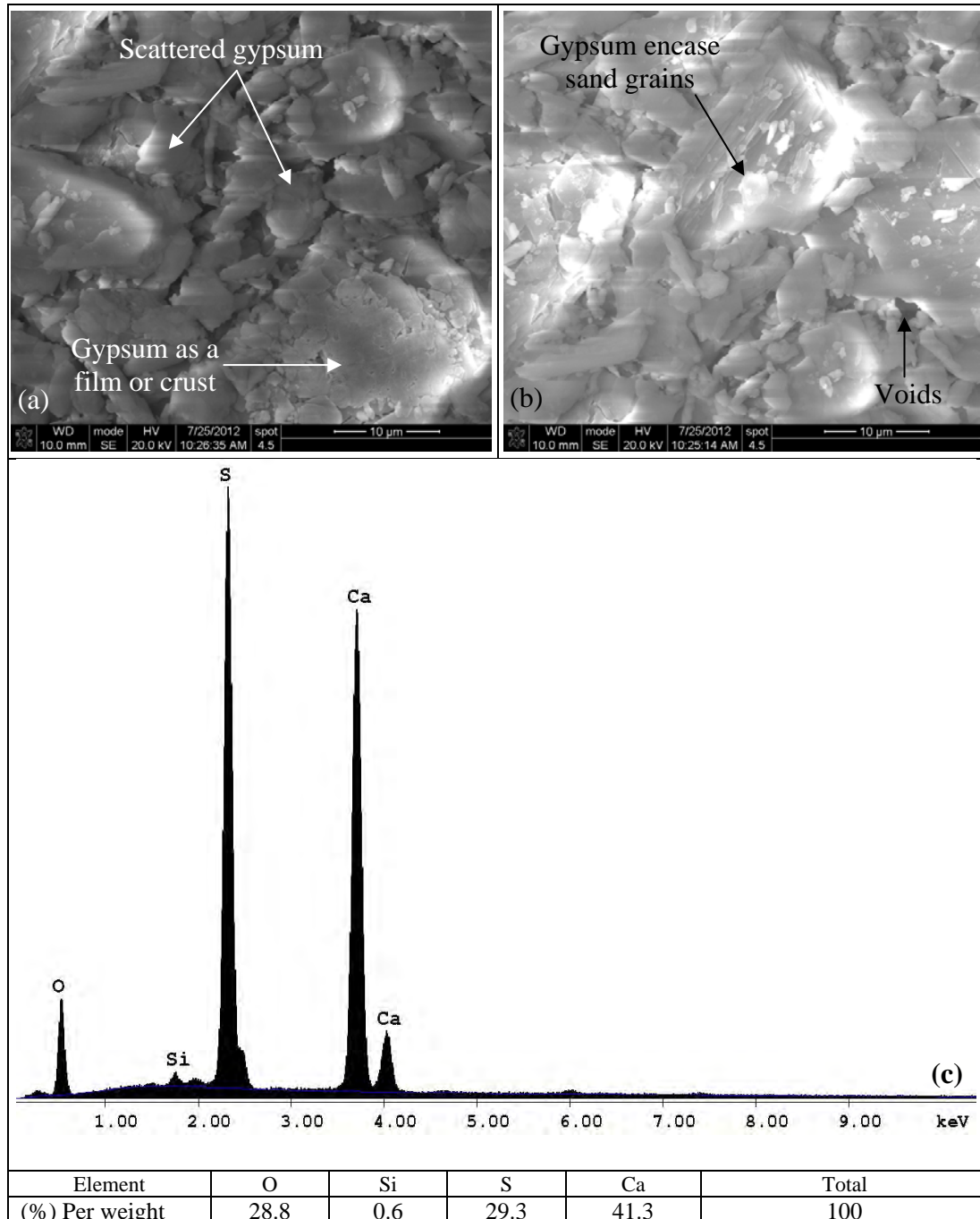
Figure C.4.: ESEM-EDX measurements for 70G30S soil at unsaturated state; (a) ESEM $10\mu_m$ image, (b) ESEM $10\mu_m$ image and (c) EDX analysis with element quantification.
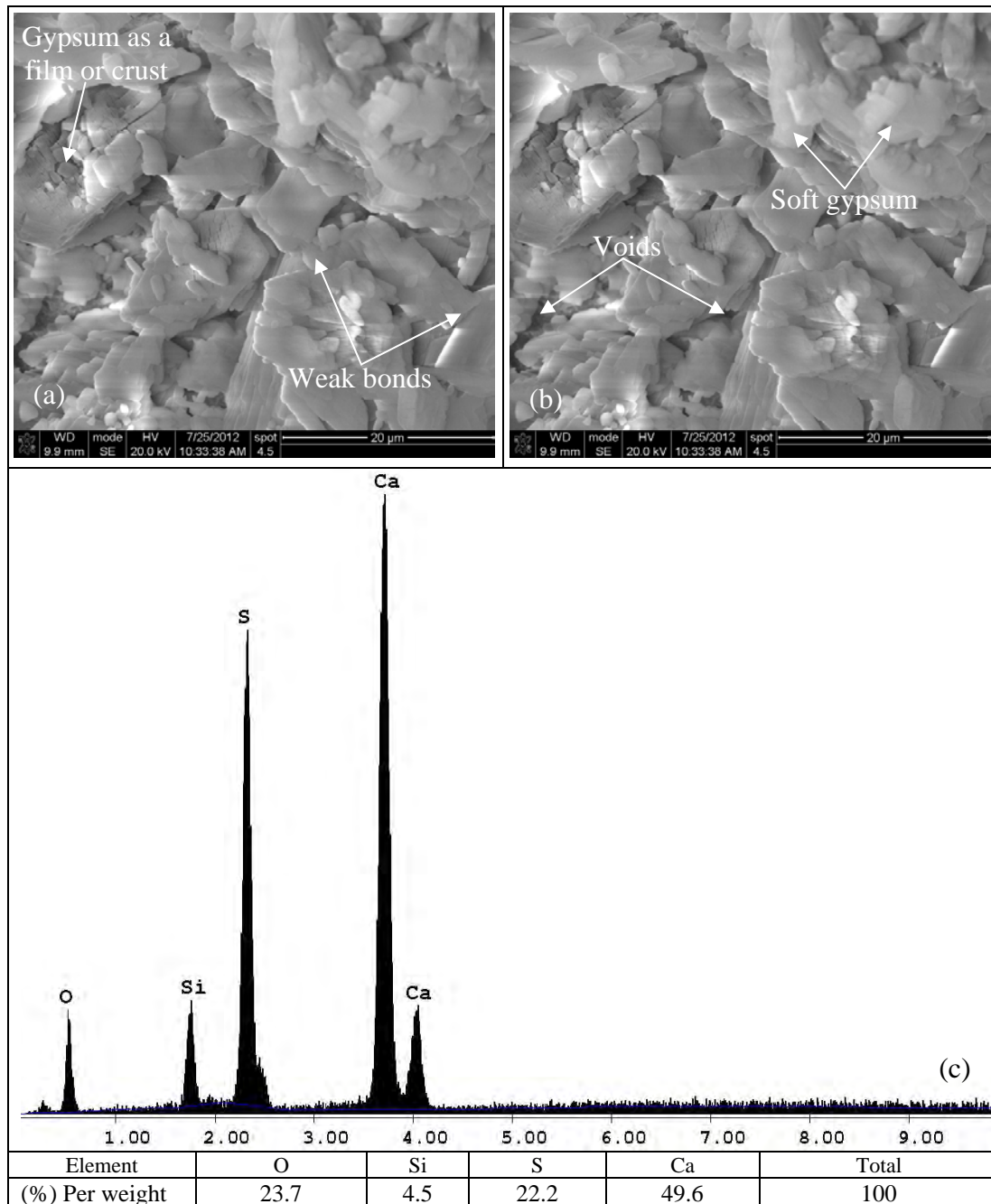
Figure C.5.: ESEM-EDX measurements for 70G30S soil at saturated state; (a) ESEM $20\mu_m$ image, (b) ESEM $20\mu_m$ image and (c) EDX analysis with element quantification.

Element	O	Si	S	Ca	Total
(%) Per weight	41	1.7	24.1	33.2	100
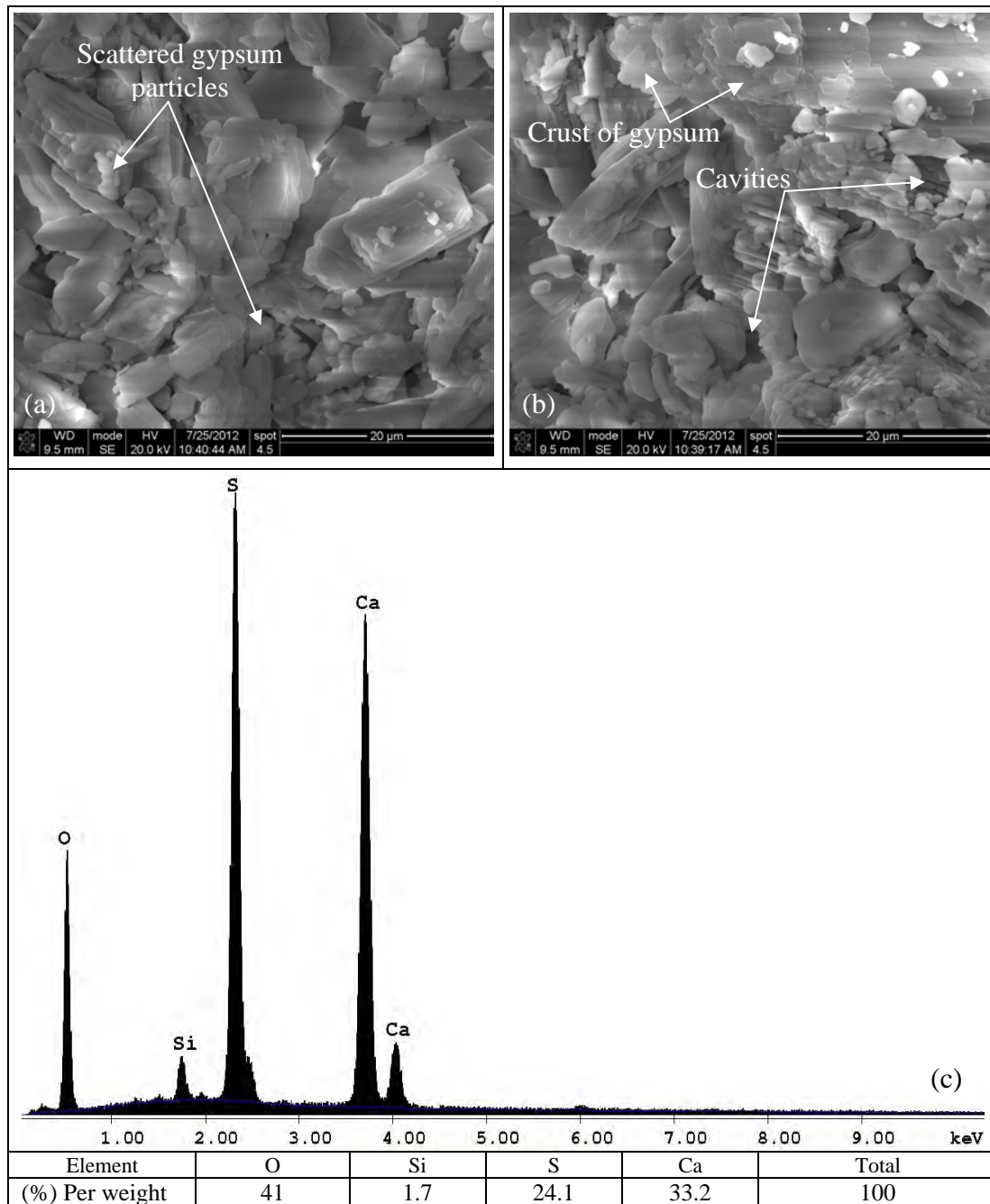
Figure C.6.: ESEM-EDX measurements for 70G30S soil at leached state; (a) ESEM $20\mu_m$ image, (b) ESEM $20\mu_m$ image and (c) EDX analysis with element quantification.

C.3. ESEM-EDX analysis for loess soil (LG)

Element	O	Mg	Al	Si	K	Fe	Total
(%) Per weight	41.8	1.1	10.8	36.7	4.2	5.4	100

Figure C.7.: ESEM-EDX measurements for LG soil at unsaturated state; (a) ESEM $100\mu_m$ image, (b) ESEM $10\mu_m$ image and (c) EDX analysis with element quantification.
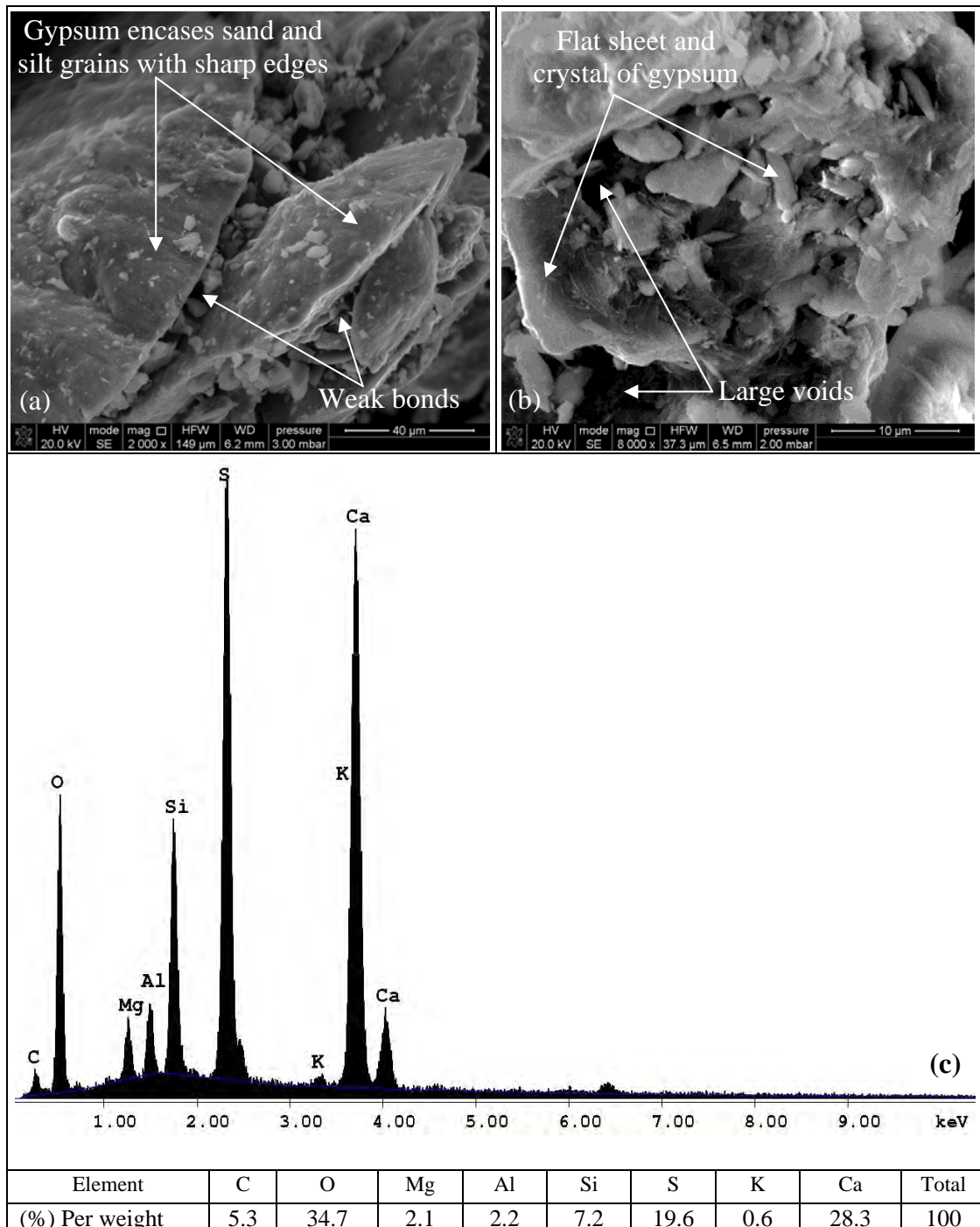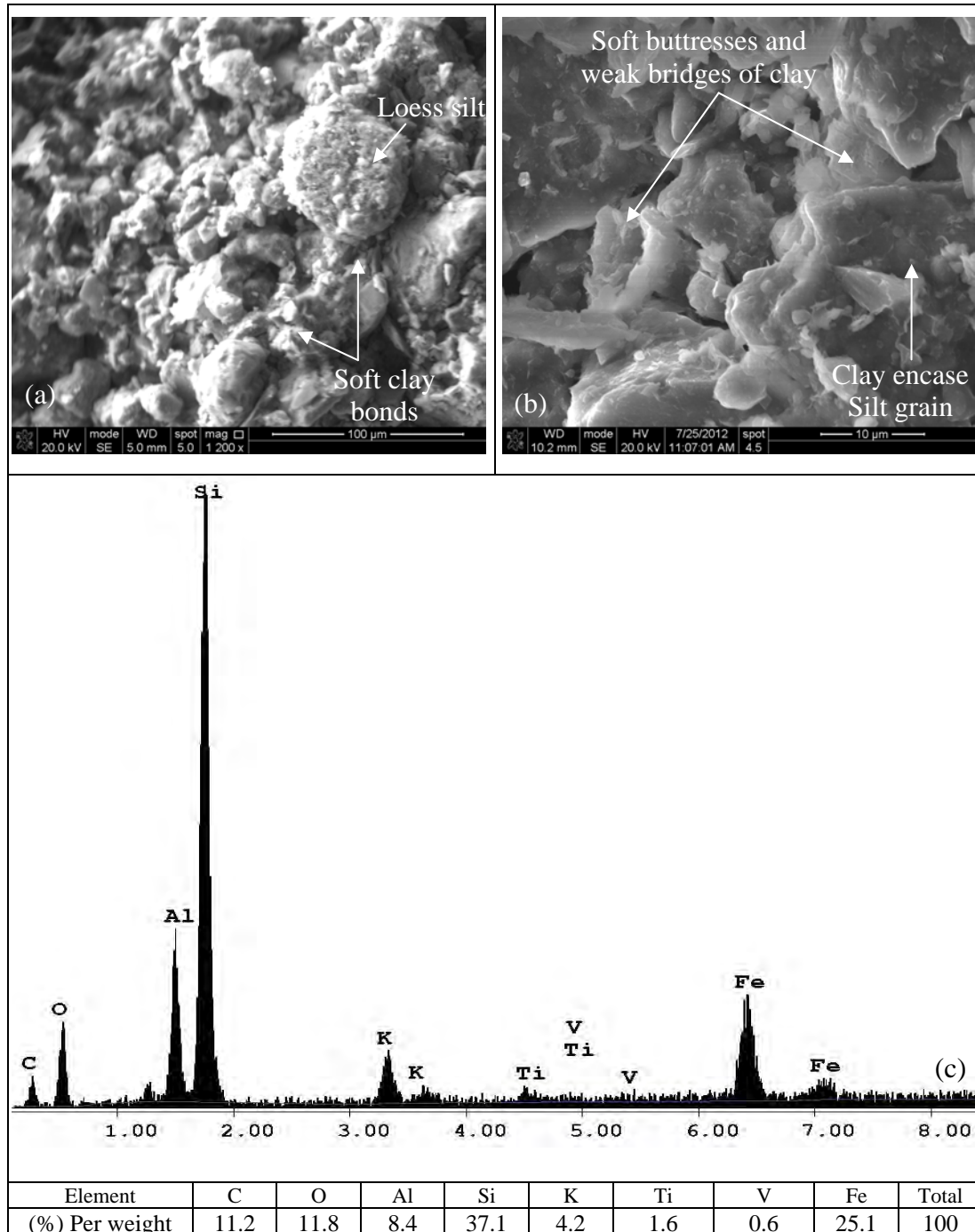
Figure C.8.: ESEM-EDX measurements for LG soil at saturated state; (a) ESEM $100\mu_m$ image, (b) ESEM $10\mu_m$ image and (c) EDX analysis with element quantification.

Element	C	O	Al	Si	K	Ti	V	Fe	Total
(%) Per weight	11.2	11.8	8.4	37.1	4.2	1.6	0.6	25.1	100

Element	O	Br	Si	K	Fe	Total
(%) Per weight	19	17	40	3	21	100
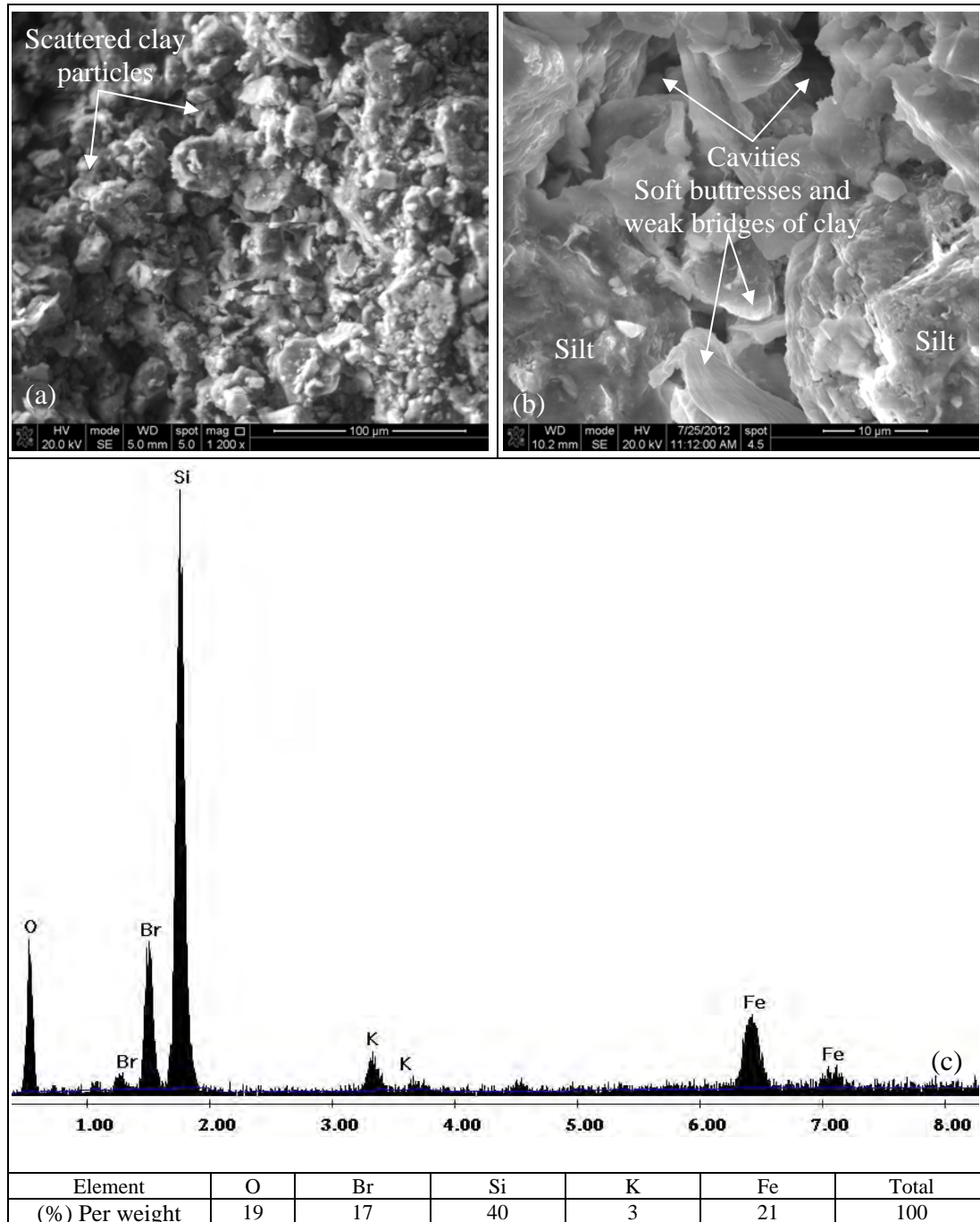
Figure C.9.: ESEM-EDX measurements for LG soil at leached state; (a) ESEM $100\mu_m$ image, (b) ESEM $10\mu_m$ image and (c) EDX analysis with element quantification.
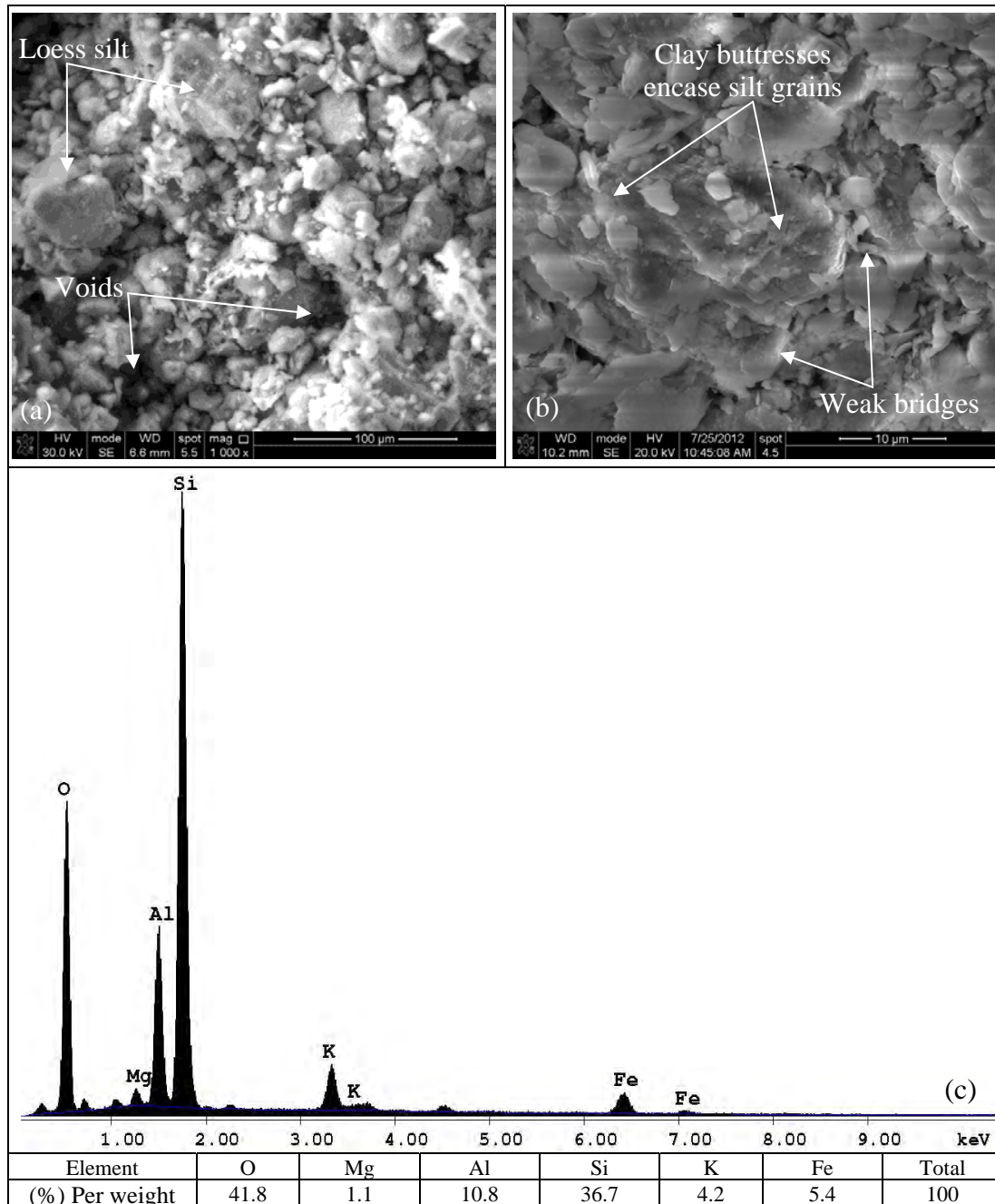
Bibliography

Abbas, H. (1995), Effect of gypsum on the engineering soil properties, M.sc. thesis, Dep. of CIvil Eng., University of Baghdad, Baghdad, Iraq.

Agus, S. (2005), An experimental study on hydro-mechanical characteristics of compacted bentonitesand mixtures, PhD thesis, Faculty of Civil Eng., Bauhaus-Universitaet Weimar, Germany.

Agus, S. & Schanz, T. (2003), Vapour equilibrium technique for tests on a highly compacted bentonite-sand mixture, *in* 'In Proceedings of the International Conference on Problematic Soils', Nottingham, United Kingdom, pp. 467–474.

Agus, S. & Schanz, T. (2005), 'Comparsion of four methods for measuring total suction', *Vadose Zone Journal* **4**, 1087–1095.

Aitchison, G. D. (1964), Engineering concepts of moisture equilibria and moisture changes in soils, *in* S. of the Review Panel, ed., 'Published in Moisture Equilibria and Moisture Changes in Soils Beneath Covered Areas, A Symp,-in-print', Butterworths, Australia, pp. 7–21.

Al-Abdullah, S. (1995), The Upper limits of Gypseous Salts in the Clay Core of Al-Adhaim Dam, PhD thesis, Department of civil Engineering, University of Baghdad, Iraq.

Al-Abdullah, S., Dalaly, N. & Seleam, S. N. (2000), 'A proposed approach on improvement of gypseous soils', *Journal of Engineering and Broughting, Al- Mustansyria University* .

Al-Ani, M. & Seleam, S. (1993), 'Effect of initial water content and soaking pressure on the geotechnical properties of gypseous soil', *Journal of Al-Muhandis* **116**(2), 3–12.

Al-Badran, Y. (2001), Collapse behavior of al-tharthar gypseous soil, M.sc. thesis, Civil Engineering Department, University of Baghdad, Iraq.

Al-Badran, Y. (2011), Volumetric Yielding Behavior of Unsaturated Fine-Grained Soils, Phd dissertation, Faculty of Civil and Environmental Engineering, Ruhr-Universitaet Bochum, Germany.

Al-Busoda, B. (1999), Studies on the behavior of gypseous soil and its treatment during loading, Master's thesis, Civil Engineering Department, University of Baghdad, Iraq.

Al-Farouk, O., Al-Damluji, S., Al-Obaidi, A., Al-Omari, R., Al-Ani, M. & Fattah, M. (2009), Experimental and numerical investigations of dissolution of gypsum in gypsifer-rous iraqi soils, *in* M. H. et al., ed., 'Proceedings of the 17th International Conference on Soil Mechanics and Geotechnical Engineering', number doi:10.3233/978-1-60750-031-5-820, © 2009 IOS Press., pp. 820–824.

Al-Jumaily, F. (1994), 'Gypsum and its mechanical effect on engineering properties of soils', *Journal of Arabic Universities Union* **19**. (in Arabic).

Al-Kaabi, F. (2007), Distribution of the gypsiferous soil in iraq, Technical Report 3044, State Company of Geological Survey and Mining, Baghdad, Iraq. (in Arabic).

Al-Kashab, M. (1981), Investigation of foundation soil and behaviour of qadisiyah site-mosul, Master's thesis, Civil Eng. Dep., University. of Mosul, Mosul, Iraq.

Al-Khuzaie, H. (1985), The effect of leaching on the engineering properties of al-jazirah soil, Master's thesis, Civil Eng. Dep., University of Mosul, Mosul, Iraq.

Al-Mufty, A. (1997), Effect of Gypsum Dissolution on the Mechanical Behaviour of Gypseous Soils, PhD thesis, Department of civil Engineering, University of Baghdad.

Al-Mufty, A. (2004), Determination of collapse potential of gypseous soils, *in* 'International Conference on Geotechnical Engineering - Beirut 2004'.

Al-Mufty, A. & Nashat, I. (2000), Gypsum content determination in gypseous soils and rocks, *in* 'Third International Jordanian Conference on Mining', Vol. 2, Amman, Jordan, pp. 485–492.

Al-Neami, M. (2000), Effect of kaolin mechanical properties of gypseous soils, Master's thesis, Civil Eng Dep., Military College of Engineering, Iraq.

Al-Obaidi, Q. (2003), Studies in geotechnical and collapsible characteristics of gypseous soil, Master's thesis, Civil Engineering Department,College of Engineering,Al-Mustansiriyah University, Baghdad, Iraq.

Al-Obaidi, Q. & Schanz, T. (2013), 'Total suction measurement of unsaturated artificial gypsified soil using the chilled-mirror hygrometer technique', *Engineering and Technology Journal* **31**(20), 359–374.

Al-Sharrad, M. (2003), Behavior of the gypseous soil during field loading, Master's thesis, Civil Engineering Department, Al- Anbar University, Iraq.

Al-Sharrad, M. (2007), 'Leaching effects on some propeties of sandy gypseous soils', *IJCE-ISSUE* **8th**, 70–89.

Al-Zgry, E. (1993), The effect of leaching on lime stabilized gypseous soil, Master's thesis, Department of Civil Engineering, University of Mousl, Iraq.

Alonso, E., Gens, A. & Josa, A. (1990), 'A constitutive model for partially saturated soils', *Geotechnique* **40/3**, 405430.

Alonso, E., Romero, E., Hoffmann, C. & Garcia-Escudero, E. (2001), Expansive bentonite/sand mixtures in cyclic controlled-suction drying and wetting, *in* 'In Proceeding of the 6th International Workshop on Key Issues in Waste Isolation Research (KIWIR 2001)', Paris, France, pp. 513–541.

Alonso, E., Vaunat, J. & Gens, A. (1999), 'Modelling the mechanical behaviour of expansive clays', *Engineering Geology* **54**, 173–183.

Arfin, Y. & Schanz, T. (2009), 'Osmotic suction of highly plastic clays', *Acta Geotechnica* (DOI 10.1007/s11440-009-0097-0).

Arifin, Y. (2008), Thermo-Hydro-Mechanical behavior of compacted bentonite-sand mixtures: An experimental study, PhD thesis, Faculty of Civil Eng., Bauhaus-Universitaet Weimar, Germany.

ASTMD1557 (2012), 'Standard test methods for laboratory compaction characteristics of soil using modified effort (56,000 ft-lbf/ft3 (2,700 kn-m/m3))', Annual Book of ASTM Standards,Vol.04.08, Philadelphia,PA, ASTM,USA. Copyright , ASTM International, 100 Barr Harbor Drive, PO Box C700, West Conshohocken, PA 19428-2959, United States.

ASTMD2216 (2010), 'Standard test methods for laboratory determination of water (moisture) content of soil and rock by mass', Annual Book of ASTM Standards,Vol.04.08, Philadelphia,PA, ASTM,USA. Copyright , ASTM International, 100 Barr Harbor Drive, PO Box C700, West Conshohocken, PA 19428-2959, United States.

ASTMD2435 (1996), 'Standard test method for one-dimensional consolidation properties of soils', Annual Book of ASTM Standards,Vol.04.08, Philadelphia,PA, ASTM,USA. Copyright , ASTM International, 100 Barr Harbor Drive, PO Box C700, West Conshohocken, PA 19428-2959, United States.

ASTMD2937 (2000), 'Standard test method for density of soil in place by the drive-cylinder method', Annual Book of ASTM Standards,Vol.04.08, Philadelphia,PA, ASTM,USA. Copyright , ASTM International, 100 Barr Harbor Drive, PO Box C700, West Conshohocken, PA 19428-2959, United States.

ASTMD422 (1963), 'Standard test method for particle-size analysis of soils', Annual Book of ASTM Standards,Vol.04.08, Philadelphia,PA, ASTM,USA. Copyright , ASTM International, 100 Barr Harbor Drive, PO Box C700, West Conshohocken, PA 19428-2959, United States.

ASTMD4318 (2010), 'Standard test methods for liquid limit, plastic limit, and plasticity index of soils', Annual Book of ASTM Standards,Vol.04.08, Philadelphia,PA, ASTM,USA. Copyright , ASTM International, 100 Barr Harbor Drive, PO Box C700, West Conshohocken, PA 19428-2959, United States.

ASTMD5333 (2003), 'Standard test method for measurement of collapse potential of soils', Annual Book of ASTM Standards,Vol.04.08, Philadelphia,PA, ASTM,USA. Copyright , ASTM International, 100 Barr Harbor Drive, PO Box C700, West Conshohocken, PA 19428-2959, United States.

ASTMD6780 (2003), 'Standard test method for water content and density of soil in situ by time domain reflectometry (tdr)', Annual Book of ASTM Standards,Vol.04.08, Philadelphia,PA, ASTM,USA. Copyright , ASTM International, 100 Barr Harbor Drive, PO Box C700, West Conshohocken, PA 19428-2959, United States.

ASTMD6836 (2008), 'Standard test methods for determination of the soil water characteristic curve for desorption using a hanging column, pressure extractor, chilled mirror hygrometer, and/or centrifuge', Annual Book of ASTM Standards,Vol.04.08, Philadelphia,PA, ASTM,USA. Copyright , ASTM International, 100 Barr Harbor Drive, PO Box C700, West Conshohocken, PA 19428-2959, United States.

ASTMD854 (2010), 'Standard test methods for specific gravity of soil solids by water pycnometer1', Annual Book of ASTM Standards,Vol.04.08, Philadelphia,PA, ASTM,USA. Copyright , ASTM International, 100 Barr Harbor Drive, PO Box C700, West Conshohocken, PA 19428-2959, United States.

ASTME104-02 (2003), 'Standard practice for maintaining constant relative humidity by means of aqueous solutions'. Vol.11.03, pp.1133-1137.

Aziz, A., Ali, F., Heng, C., Mohammed, T. & Huat, B. (2006), 'Collapsibility and volume change behavior of unsaturated residual soil', *American Journal of Environmental Sciences* **2(4)**, 161–166.

Bally, R. (1988), 'Some specific problems of wetted loessial soils in civil engineering', *Engineering Geology* **25**, 303–324.

Barden, L., Madedor, A. & Sides, G. (1969), 'Volume change calculations of unsaturated clay', *ASCE, Journal of Soil Mechanics and Foundations Engineering Division* **95**, 33–51.

Barden, L., McGown, A. & Collins, K. (1973), 'The collapse mechanism in partly saturated soil', *Engineering Geology* **7**, 49–60. Elseier Scientific Publishing Company, Amsterdam, The Netherlands.

Barzanji, A. (1973), Gypsiferous Soils in Iraq, PhD thesis, University of Ghent, Belgium.

Barzanji, A. (1986), Distribution of gypsiferous soils in iraq, *in* M. of Irrigation, ed., 'Symposium on gypsiferous soils and their effects on the structure', The Institute of Water and Soil Research, Iraq. (in Arabic).

Bell, F. & Culshaw, M. (2001), Problem soils: a review from a british perspective, *in* 'Proc. Symp. on Problematic Soils, Nottingham Trent University, Jefferson I., Murray E.J., Faragher E. and Fleming P.R., Thomas Telford eds, London', pp. 1–35.

Berner, R. (1980), 'Early diagenesis:a theoretical approach', Princeton University Press, Princeton, New Jersey.

Bishop, A. (1959), 'The principle of effective stress', *Lecture delivered in Oslo, Norway, 1955,Technisk Ukeblad* **106(39)**, 859–863.

Bishop, A. & Blight, G. (1963), 'Some aspects of effective stress in saturated and partly saturated soils', *Geotechnique* **13**, 177–197.

Bishop, A. W. & Henkel, D. J. (1962), *The Measurement of Soil Properties in the Triaxial Test*, 2nd edn, London, England.

Bower, C. & Huss, R. (1948), 'Rapid conductimetric method for estimating gypsum in soils', *Soil Scince* **66**, 199–204.

Bowles, J. (1984), *Foundation Analysis and Design*, 3rd edn, Mc Graw-Hill Book Co., New York.

Brenner, R., Nutalaya, P., Chilingraian, G. & Robertston, J. (1981), *Engineering Geology of Soft Clay in (Soft Clay Engineering)*, Elsevier Scientific Publishing Company.

Brooks, R. & Corey, A. (1964), 'Hydraulic properties of porous media', *Colorado State Univ. Hydrol. Paper* (3), 27.

Buringh, P. (1960), *Soils and Soil Conditions In Iraq*, Ministry of Agricultural, Baghdad,Iraq.

Cabral, A. R., Burnotte, F. & Lefebvre, G. (1999), 'Application of tdr technology to water content monitoring of capillary barriers made of pulp and paper residues', *Geotechnical Testing Journal* **22**, 39–43.

Campbell, G., Smith, D. & Teare, B. (2007), Application of a dew point method to obtain the soil-water characteristic, *in* 'Proceedings of the Second International Conference on Mechanics of Unsaturated Soils', Bauhaus-Universitaet Weimar, Weimar, Germany, pp. 71–77.

Charles, J. & Skinner, H. (2001), Compressibility of foundation fill, *in* 'Geotechnical Engineering', Vol. 149 of *Proceedings of the ICE*, pp. 145–157.

Charles, J. & Watts, K. (2001), *Building on Fill: Geotechnical Aspects*, 2nd edn, London.

Chen, Z., Huang, X., Qin, B., Fang, X. & Guo, J. (2008), Negative skin friction for cast-in-place piles in thick collapsible loess, *in* D. Toll, C. Augarde, D. Gallipoli & S. Wheeler, eds, 'Unsaturated Soils: Advances in Geo-Engineering', CRC Press, London, pp. 979–985.

Chiu, C. & Ng, C. (2003), 'A state-dependent elasto-plastic model for saturated and unsaturated soils', *Geotechnique* **53/9**, 809829.

Clemence, S. & Finbarr, A. (1981), 'Design consideration for collapsible soils', *ournal of Geotechnical Engineering, Division proc. ASCE* **107**(GT3), 305–317.

Clevenger, W. A. (1958), 'Experience with loess as foundation material', *ASCE, J. Soil Mech. Found. Div.* **85**, 151–180.

Coleman, J. (1962), 'Stress-strain relations for partly saturated soils', *Geotechnique* **12(4)**, 348–350.

Croney, D. & Coleman, J. (1961), Pore pressure and suction in soils., *in* 'Proc.Conf. on Pore Pressure and Suction in Soils', Butterworths, London, pp. 31–37.

Cui, Y., Yahia-Aissa, M. & Delage, P. (2002), 'A model for the volume change behavior of heavily compacted swelling clays', *Engineering Geology* **64**, 233–250.

Das, B. (1984), *Principles of Foundation Engineering*, PWS-KENT publishing Company, Boston.

Das, B. (1990), *Principles of Geotechnical Engineering*, PWS- KENT publishing Company, Boston.

Delage, P., Cui, Y. & Antoine, P. (2005), Geotechnical problems related with loess deposits in northern france, *in* 'Proceedings of International Conference on Problematic Soils', pp. 517–540.

Derbyshire, E., Dijkstra, T. & Smalley, I. (1995), Genesis and properties of collapsible soils, *in* E. Derbyshire, T. Dijkstra & I. Smalley, eds, 'Genesis and properties of collapsible soils', number ISBN0-7923-3587-2 *in* 'NATO ASI Series C: Mathematical and Physical Sciences', Kluwer Academic Publishers, The Netherlands, Loughborough,UK, p. 468.

DIN18123 (1996), 'Bestimmung der korngroessenverteilung (determination of grain-size distribution)'.

DIN18126 (1996), 'Bestimmung der dichte nichtbindiger boeden bei lockerster und dichtester lagerung'.

Dudly, J. (1970), 'Review of collapsing soils', *Journal of soil Mechanics and Foundation Division proc. ASCE* **96**(SM3), 925–947.

Eissmann, L. (2002), 'Quaternary geology of eastern germany (saxony,saxon-anhalt, south brandenburg, thüringia), type area of the elsterian and saalian stages in europe', *Quaternary Science Reviews* **21**, 1275–1346.

FAO (1990), Management of gypsiferous soils, Technical report, Food and Agricultural Organization of the United Nations, Rome.

Fattah, M., Al-Musawi, H. & Salman, F. (2012), 'Treatment of collapsibility of gypseous soils by dynamic compaction', *Geotech. Geol. Eng.* **30**, 1369–1387. Springerlink.com.

Fattah, M., Al-Shakarchi, Y. & Al-Numani, H. (2008), 'Long -term deformation of some gypseous soils', *Engineering and Technology* **26**(12), 1461–1485.

Feda, J. (1988), 'Collapse of loess upon wetting', *Engineering Geology* **25**, 263–269.

Feda, J. (1995), Mechanisms of collapse of soil structure, *in* E. Derbyshire, T. Dijkstra & I. Smalley, eds, 'Genesis and Properties of Collapsible Soils', number ISBN0-7923-3587-2 *in* 'NATO ASI Series', NATO, Kluwer Academic Publishers, The Netherlands, Loughborough,UK, pp. 149–172.

Feng, M. & Fredlund, D. (1999), Hysteretic influence associated with thermal conductivity sensor measurements, *in* 'In Proc. from Theory to the Practice of Unsat. Soil Mech- in Association with the 52nd Canadian Geotechnical Conf- and the Unsat- Soil Group', Vol. 14:2, Regina, Sask., pp. 14–20.

Fleureau, J. M., Kheirbek-Saoud, S., Soemitro, R. & Taibi, S. (1993), 'Behaviour of clayey soils on drying-wetting paths', *Canadian Geotechnical Journal* **30**, 287–296.

Fookes, P. & Parry, R. (1994), Engineering characteristics of arid soils, *in* 'Proc. of the 1st Int. Symp. on Engrg Chars of Arid Soils', London.

Frechen, M., Oches, E. & Kohfeld, K. (2003), 'Loess in europe- mass accumulation rates during the last glacial period', *Quaternary Science Reviews* **22**, 1835–1857.

Fredlund, D. (1996), The emergence of unsaturated soil mechanics, The fourth spencer j. buchanan lecture.p.39, College Station, Texas, A & M University Press.

Fredlund, D. (2000), 'The implementation of unsaturated soil mechanics into geotechnical engineering', *Canadian Geotechnical Journal* **37**(5), 963–986.

Fredlund, D. (2001), Ensuring a sound scientific basis for geotechnical engineering in developed countries, *in* 'Proceedings of the International Conference on Management of the Land and Water Resources', Hanoi, pp. 3–20.

Fredlund, D. & Gan, J. (1995), The collapse mechanism of a soil subjected to one-dimensional loading and wetting, *in* E. Derbyshire, T. Dijkstra & I. Smalley, eds, 'Genesis and properties of collapsible soils', NATO ASI Series C: Mathematical and Physical Sciences, Kluwer Academic Publishers, The Netherlands, Loughborough,UK, pp. 173–205.

Fredlund, D. & Morgenstern, N. (1977), 'Stress state variables for unsaturated soils', *J. Geotech. Engrg. Div., ASCE, GT5* **103**, 447–466.

Fredlund, D. & Rahardjo, H. (1993), *Soil Mechanics for Unsaturated Soils*, John Wiley & Sons Inc., New York.

Fredlund, D., Rahardjo, H. & Fredlund, M. (2012), *Unsaturated Soil Mechanics in Engineering Practice*, number ISBN-978-1-118-13359-0, John Wiley & Sons, Inc.,Hoboken, New Jersey, Hoboken, New Jersey.

Fredlund, D. & Xing, A. (1994), 'Equations for the soilwater characteristic curve', *Canadian Geotechnical Journal* **31(3)**, 521–532.

Freeze, R. & Cherry, J. (1979), *Ground Water*, Prentice Hall, Inc., Englewood Cliffs, New Jersey.

Gee, G., Campbell, M., Campbell, G. & Campbell, J. (1992), 'Rapid measurement of low soil potentials using a water activity meter', *Soil Science Society of America Journal* **56**, 1068–1070.

Grabowska-Olszewska, B. (1988), 'Problems of loess in poland', *Engineering Geology* **25**, 177–199.

Grahmann, R. (1932), 'Der loess in europa', *Mitteilungen der Gesellschaft fuer Erkunde Leipzig* **51**, 5–24.

Grigoryan, A. (1997), 'Pile foundations for buildings and structures in collapsible soils', A.A.Balkema, Brookfield,USA.

Haase, D., Fink, J., Haase, G., Ruske, R., Pecsi, M., Richter, H., Altermann, M. & Jaeger, K.-D. (2007), 'Loess in europe- its spatial distribution based on a european loess map, scale 1:2,500,000', *Quaternary Science Reviews* **26**, 1301–1312.

Habibagahi, G. & Mokhberi, M. (1998), 'A hyperbolic model for volume change behavior of collapsible soils', *Ca* **35**, 264–272. NRC Canada.

Haeri, S., Garakani, A., Khosravi, A. & Meehan, C. (2013), 'Assessing the hydromechanical behavior of collapsible soils using a modified triaxial test device', *Geotechnical Testing Journal* **37**(2), 1–15.

Hassan, H. (2000), Effect of emulsified asphalt on some properties of gypseous soil, Master's thesis, Civil Eng. Dep., College of Eng., Al-Mustansiriya University, Baghdad, Iraq.

Head, K. (1980), *Manual of Soil laboratory Testing*, London. Vol. 1, Published by:Prentch, press.

Head, K. & Epps, R. (2011), *Manual of Soil Laboratory Testing*, 3rd edn. Vol.(II), (ISBN:978-1904445-69-2),Published by whittles Publishing, Scotland, UK.

Herrero, J. (1987), Suelos sobre los yesos Paleogenos Barbastro-Balaguer-Tora, Phd thesis, Unversity of Zaragoza. pp.468, In Spanish.

Hesse, P. (1976), 'Particle size distribution in gypsic soils', *Plant and Soil* **44**, 241–247.

Hilf, J. (1956), An Investigation of Pore-Water Pressure in Compacted Cohesive Soils, Phd dissertation, Tech. Memo. No. 654, U.S. Dept. of the Interior, Bureau of Reclamation, Design and Construction Div., Denver, CO, p. 654., USA.

Hobbs, N. (1986), 'Mirw morphology and the properties and behaviour of some british and foreign peats.', *Quarterly Journal of Engineering Geology* **19**(1). London, UK.

Horta, J. (1980), 'Calcrete, gypcrete and soil classification in algeria', *Engineering Geology* **15**, 15–52.

Houston, S. (1995), Foundations and pavements on unsaturated soilspart one:collapsible soils, unsaturated soils, *in* P. D. P. e. B. Alonso, E.E., ed., 'Proc. 1st Int. Conf. on Unsaturated Soils', Presses des Ponts et Chaussees, Paris, p. 14211439.

Houston, S. & EI-Ehwany, M. (1991), 'Sample disturbance of cemented collapsible soils', *J. Geotech. Engrg. Div., ASCE* **117/5**, 731752.

Houston, S., Houston, W., Chen, C. & Febres, E. (1998), Site characterization for collapsible soil deposits, *in* I. Academic, ed., 'Proc., 2nd Int. Conf. on Unsaturated Soils', Vol. 1, Beijing, China, p. 6671.

Houston, S., Houston, W., Zapata, C. & Lawrence, C. (2001), 'Geotechnical engineering practice for collapsible soils', *Geotechnical and Geological Engineering* **19**, 333–355.

Hu, Y., Vu, H. & Hubble, D. (2010), 'Evaluation of dielectric-based bubbles for expansive soils: Application to regina soils', *Ca* **47**(34), 346–358.

ISRIC (1987), Procedures for soils analysis, Technical report, International Soil Reference and Information Center, Wageningen.

Jackson, J., Mehl, J. & Neuendorf, K. (2005), 'Glossary of geology', *American Geological Institute,Alexandria, Virginia.* (ISBN 0-922152-76-4), 800 pp.

James, A. & Kirkpatrick, I. (1980), 'Design of foundations of dams containing soluble rocks and soils', *Q.J.Engineering Geology* **13**, 189–198.

James, A. & Lupton, A. (1978), 'Gypsum and anhydrite in foundation hydraulic structures', *Geotechnique* **28**(3).

Jefferson, I. & Rogers, C. (2012), *ICE manual of geotechnical engineering*, Vol. 1 of *ICE manuals*, ICE Publishing, London, UK.

Jefferson, i., Rogers, C., Evstatiev, D. & Karastanev, D. (2005), *Treatment of metastable loess soils: lessons from eastern Europe. In ground improvements-Case Histories*, Vol. 3 of *Elsevier Geo-Engineering Book series*, Elsevier, Amsterdam.

Jefferson, I. & Smalley, I. (1995), Six definable particle types in engineering soils and their participation in collapse events:proposals and discussions, *in* E. Derbyshire, T. Dijkstra & I. Smalley, eds, 'Genesis and Properties of Collapsible Soils', number ISBN0-7923-3587-2 *in* 'NATO ASI Series C: Mathematical and Physical Sciences', Kluwer Academic Publishers, The Netherlands, pp. 19–31.

Jennings, J. & Burland, J. (1962), 'Limitations to the use of effective stresses in partly saturated soils', *Geotechnique* **12(2)**, 125–144.

Jennings, J. & Knight, K. (1957), The addition settlement of foundation sandy subsoil on wetting, *in* 'Proceeding of 4th International Conference on Soil Mechanics and foundations Engineering', Vol. 1, pp. 316–319.

Jennings, J. & Knight, K. (1975), A guide to construction on or with materials exhibiting additional settlement due to collapse of grain structure, *in* 'Proceeding of 6th Regional Conference for Africa on soil mechanics and Foundation Engineering, Durban, South Africa', pp. 99–105.

Jotisankasa, A. (2005), Collapse behaviour of compacted silty clay, Ph.d. thesis, Imperial College of Science, Technology and Medicine, University of London, London, UK.

Kakoli, S. (2011), Negative skin friction induced on piles in collapsible soils due to inundation, PhD thesis, Concordia University, Canada. Unpublished PhD thesis.

Karim, H., Schanz, T. & Nasif, M. (2012), 'Improving collapsibility and compressibility of gypseous sandy soil using bentonite and kaolinite', *Engineering and Technology Journal* **30**(18), 3141–3153.

Khalili, N., Geiser, F. & Blight, G. (2004), 'Effective stress in unsaturated soils: review with new evidence', *International Journal of Geomechanics* **4(2)**, 115–126.

Khalili, N. & Khabbaz, M. (1998), 'A unique relationship for the determination of the shear strength of unsaturated soils', *Geotechnique* **48(5)**, 681–688.

Khan, S. & Webster, G. (1968), 'Determination of gypsum in solonetzic soils by an x-ray technique', *Analyst* **93**, 400–402.

Klausner, Y. (1991), *Fundamentals of continuum mechanics of soils*, Springer-Verlag., New York.

Klein, C. & Hurlbut, C. (1985), *Manual of Mineralogy, after J.D.Dana*, John Wiley & Sons Inc. New York., New York.

Klukanova, A. & Frankovska, J. (1995), The slovak carpathians loess sediments, their fabric and properties., *in* E. Derbyshire, T. Dijkstra & I. Smalley, eds, 'Genesis and properties of collapsible soils', number ISBN0-7923-3587-2 *in* 'NATO ASI Series C: Mathematical and Physical Sciences', Kluwer Academic Publishers, The Netherlands, Loughborough,UK, pp. 129–147.

Knight, K. (1960), The Collapse of Structures of Sandy Subsoils on Wetting, PhD thesis, University of Witwatersrand.

Larionov, A. (1965), Structural characteristics of loess soils for evaluating their constructional properties, *in* '6th Proc.Int.Conf.Soil Mechanic Foundation Engineering', Vol. 1, Montreal, pp. 64–68.

Lawton, E., Fragaszy, R. & Hardcastle, J. (1989), 'Collapse of compacted clayey sand', *Jouranal of Geotechnical Engineering* **115(9)**, 1252–1267. ASCE.

Lawton, E., Fragaszy, R. & Hardcastle, J. (1991), 'Stress ratio effects on collapse of compacted clayey sand', *Journal of geotechnical engineering* **5/117**, 714–730.

Lawton, E., Fragaszy, R. & Hetherington, M. (1992), 'Review of wetting induced collapse in compacted soils', *Jouranal of Geotechnical Engineering* **118/9**, 1376–1392.

Lefebvre, G. (1995), Collapse mechanisms and design considerations for some partly saturated and saturated soils, *in* D. E. et al., ed., 'Genesis and Properties of Collapsible Soils', number ISBN0-7923-3587-2 *in* 'NATO ASI Series', NATO, Kluwer Academic Publishers, The Netherlands, Loughborough,UK, pp. 361–374.

Leong, E. & Rahardjo, H. (1997), 'Review of soil-water characteristics curve equations', *Jouranal of Geotechnical and Geoenvironmental Engineering* **123**(12), 1106–1117. ASCE,ISSN 1090-0241/97/0012-1106-1117.

Leong, E., Tripathy, S. & Rahardjo, H. (2004), 'A modified pressure plate apparatus', *Geotechnical Testing Journal, ASTM* **27**(3), 322–331.

Leong, E., Tripathy, S. & Rahardjo, R. (2003), 'Total suction measurement of unsaturated soils with a device using the chilled-mirror dew-point technique', *Geotechnique* **53/2**, 173–182.

Lin, Z. (1995), Variation in collapsibility and strenth of loess with age, *in* E. Derbyshire, T. Dijkstra & I. Smalley, eds, 'Genesis and Properties of Collapsible Soils', number ISBN0-7923-3587-2 *in* 'NATO ASI Series', NATO, Kluwer Academic Publishers, The Netherlands, pp. 247–265.

Lin, Z. & Wang, S. (1988), 'Collapsibility and deformation characteristics of deep-seated loess in china', *Engineering Geology* **25**, 271–282.

Lins, Y. (2009), Hydro-mechanical properties of partially saturated sand, Phd. thesis, Ruhr-Universitaet Bochum, Germany.

Lins, Y. & Schanz, T. (2004), Determination of hydro-mechanical properties of sand, *in* 'From Experimental Evidence towords Numerical Modeling of Unsaturated Soil', Weimar, Germany, pp. 11–29.

Loret, B. & Khalili, N. (2000), 'A three phase model for unsaturated soils', *Int. J. Numer. Analyt. Meth. Geomech.* **24(11)**, 893–927.

Lu, N. & Likos, W. (2004), *Unsaturated Soil Mechanics*, John Wiley & Sons, Inc., Hoboken, New Jersey.

Lu, N. & Likos, W. (2006), 'Suction stress characterstic curve for unsaturated soil', *Jouranal of Geotechnical and Geoenvironmental Engineering* **132(2)**, 131–142.

Lutenegger, A. & Saber, R. (1988), 'Determination of collapse potential of soils', *Geotechnical Testing Journal,ASTM* **11/3**, 173–178.

Madhyannapu, R., Madhav, M., Puppala, A. & Ghosh, A. (2006), 'Compressibility and collapsibility characteristics of sedimented fly ash beds', *Jouranal of Material in Civil Engineering* **20/6**, 401–409.

Matyas, E. & Radhakrishna, H. (1968), 'Volume change characteristic of partially saturated soils', *Geotechnique* **18**, 432–448.

Mikheav, V. & Petrukhin, V. (1973), 'Construction properties of saline soils used as foundation beds in industrial and civil construction', *Soil Mechanics and Foundation Engineering* **9**(3), 30–36.

Mikheev, V., Petrukhin, V. & Boldirev, G. (1977), Deformability of gypseous soils, *in* 'Proc. of 9th Int. Conf. on Soil Mechanics and Foundation Engineering,ICSMFE', Vol. 1, pp. 211–214.

Milodowski, A., Northmore, K. & Kemp, S. (2012), 'The mineralogy and fabric of "brick-earths" and their relationship to engineering properties', *Engineering Geology* . In press.

Morgenstern, N. (1979), Properties of compacted soils, *in* 'Proc. 6th Pan-Am. Conf.on Soil Mech. & Fdn. Engrg', Vol. 3 of *Contribution to panel discussion Session IV*, Lima, Peru, pp. 349–354.

Mualem, Y. (1976), 'A new model for predicting the hydraulic conductivity of unsaturated porous media', *Water Resources Research* **12**, 513–522.

Munoz-Casteblanco, J., Delage, P., Pereira, J. & Y.J., C. (2011*a*), 'Hydromechanical behaviour of a natural unsaturated loess', *Geotechnique* pp. 174–224. Ecole des Ponts ParisTech, Laboratoire Navier CERMES, Universite Paris-Est, France.

Munoz-Casteblanco, J., Delage, P., Pereira, J. & Y.J., C. (2011*b*), 'The water retention properties of a natural unsaturated loess from northern france', *Geotechnique* pp. 54–83. Ecole des Ponts ParisTech, Laboratoire Navier CERMES, Universite Paris-Est, France.

Muxart, T., Billard, A., Andrieu, A., Derbyshire, E. & Meng, X. (1995), Changes in water chemistry and loess porosity with leaching: Implications for collapsibility in the loess of north china, *in* E. Derbyshire, T. Dijkstra & I. Smalley, eds, 'Genesis and properties of collapsible soils', number ISBN0-7923-3587-2 *in* 'NATO ASI Series C: Mathematical and Physical Sciences', Kluwer Academic Publishers, The Netherlands, Loughborough,UK.

Nafie, F. (1989), The properties of High Gypsiferous Soils and their significance for land Management, PhD thesis, University of London.

Namiq, L. & Nashat, I. (2011), Influence of leaching on volume change of a gypseous soil, *in* J. Han & D. A. Alzamora, eds, 'Geo-Frontiers 2011: Advances in Geotechnical Engineering', number 978-0-7844-1165-0 *in* 'GSP 211', American Society of Civil Engineers (ASCE), Dallas, Texas, United States, pp. 2611–2620.

Nashat, I. (1990), Engineering Characteristiec of some Gypseous Soils in Iraq, PhD thesis, Civil Engineering Department, University of Baghdad.

Nelson, J., Hatton, C. & Chao, K. (2011), A constitutive relationship for collapsible doild in terms of stress state variables, *in* Alonso & Gens, eds, 'Unsaturated Soils', Vol. 1, Taylor and Francis Group, London, pp. 317–322.

Ng, C., Chiu, C. & Shen, C. (1998), Effects of wetting history on the volumetric deformations of an unsaturated loose fill, *in* 'Proc. 13th Southeast Asian Geotech. Conf.', Vol. ROC, 1, Taipei, Taiwan, pp. 141–146.

Ng, C. & Menzies, B. (2007), *Advanced Unsaturated Soil Mechanics and Engineering*, number ISBN 978-0-415-43679-3, Taylor and Francis,London and New York.

Nouaouria, M., Guenfoud, M. & Lafifi, B. (2008), 'Engineering properties of loess in algeria', *Engineering Geology* **99**, 85–90. Published by ELSEVIER.

Osopov, V. & Sokolov, V. (1995), Factors and mechanism of loess collapsibility, *in* E. Derbyshire, T. Dijkstra & I. Smalley, eds, 'Genesis and properties of collapsible soils', number ISBN0-7923-3587-2 *in* 'NATO ASI Series C: Mathematical and Physical Sciences', Kluwer Academic Publishers, The Netherlands, Loughborough,UK, pp. 49–63.

Pecsi, M. (1990), 'Loess is not just the accumulation of dust', *Quaternary International* **7/8**, 1–21.

Pecsi, M. (1995), 'The role of principles and methods in loess-paleosol investigations', *GeoJournal* **36**, 117–131.

Pengelly, A., Boehm, D., Rector, E. & Welsh, J. (1997), 'Engineering experience with in situ modification of collapsible and expansive soils', *Unsaturated Soil Engineering, ASCE Special Geotechnical Publication* **68**, 277–298.

Pereira, J. & Fredlund, D. (1997), 'Constitutive modeling of metastable-structured compacted soil', *Recent Developments in Soil and Pavement Mechanics* (ISBN-905-410-885-1), 317–326. Reproduced with permission from the (Recent Developments in Soil and Pavement Mechanics),Edited by Marcio Almeida,Balkema, Rotterdam (Proof).

Pereira, J., Fredlund, D., Neto, M. & M.ASCE, G. (2005), 'Hydraulic behavior of collapsible compacted gneiss soil', *Jouranal of Geotechnical and Geoenvironmental Engineering, ASCE* **131**(10), 1264–1273. ISSN 1090-0241/2005/10-12641273.

Pererira, J. & Fredlund, D. (2000), 'Volume change behaviour of collapsible compacted gneiss soil', *Journal of Geotechnical and Geoenvironmental Engineering* **126/10**, 907–916.

Petrukhin, V. & Boldyrev, C. (1978), 'Investigation of the deformability of gypsified soils by a static load', *Soil Mechanics and Foundation Engineering* **15**(3), 178–182.

Pham, H., Fredlund, D. & Barbour, S. (2002), A simple soil-water hysteresis model for predicting the boundary wetting curve, *in* 'Proceedings of the Fifty-Fifth canadian Geotechnical Conference: Ground and Water-Theory to Practice', Niagara Falls, ON, pp. 1261–1267.

Pham, H., Fredlund, D. & Barbour, S. (2003), 'A practical hysteresis model for the soil-water characteristic curve for soils with negligible volume change', *Geotechnique* **53(2)**, 293–298.

Pham, Q., Fredlund, D. & Barbour, S. (2005), 'A study of hysteresis models for soil-water characteristic curves', *Canadian Geotechnical Journal* **42**, 1548–1568.

Phien-wej, N., Pientong, T. & Balasubramaniam, A. (1992), 'Collapse and strength characteristics of thailand loess', *Engineering Geology* **32**, 59–72.

Pirsson, L. & Knopf, A. (1958), *Rocks and Rock Minerals*, John Wiley & Sons Inc. New York., New York.

Poch, R. (1992), Fabric and physical properties of soils with gysic and hypergypsic horizons of the Ebro Valley, PhD thesis, Universiteit of Gent.

Popescu, M. (1992), Engineering problems associated with expansive and collapsible soil behaviour, *in* 'In proceedings of the 7th International Conference on Expansive Soils', Vol. 2, Dallas, Texas,USA, pp. 25–46.

Porta, J. (1975), Redistribuciones ionicas en suelos salinos,Influencia sobre la vegetacion halofilay las posibilidades de recuperacion de los suelos con horizonte gypsico y otros suelo shalomorfos de las margenes del r?o Giguela, Phd thesis, ETSIA, Madrid. pp.261, In Spanish.

Porta, J. (1998), 'Methodologies for the analysis and characterization of gypsum in soils: A review', *Geoderma* **87**(PII: S0016-706198.00067-6), 31–46. Copy Right: Elsevier Science B.V. All rights reserved.

Porta, J. & Herrero, J. (1990), Micromorphology and genesis of soils enriched with gypsum, *in* L. Douglas, ed., 'Soil Micromorphology', Elsevier, Amsterdam, pp. 321–339.

Porta, J., Lopez Acevedo, M. & Rodriguez, R. (1986), 'Tecnicas y experimentos en edafolog?a', *AEAC, Barcelona* . In Spanish.

Rahardjo, H. & Fredlund, D. G. (1992), Mechanics of soil with matric suction, *in* 'In Proc. Int. Con8 Geotech. Eng. (GEO7ROPIM -92)', Univetsiti Teknologi Malaysia, Johor Bahm, Malaysia.

Rao, S. & Revanasiddappa, K. (2000), 'Role of matric suction in collapse of compacted clay soil', *Jouranal of Geotechnical and Geoenvironmental Engineering* **126**(1), 85–90.

Rao, S. & Revanasiddappa, K. (2003), 'Role of soil structure and matric suction in collapse of a compacted clay soil', *Geotechnical Testing Journal* **26**(1), 1–9. Copyright by ASTM.

Razouki, S., Al-Omari, R., Nashat, I., H.F., R. & Khalid, S. (1994), The problems of gypsiferous soils in iraq, *in* 'Proc. Symposium on Gypseous Soils and their effects on structures', NCCL, Baghdad, Iraq.

Reid, J. (2012), *ICE manual of geotechnical engineering*, Vol. 1 of *ICE manuals*, ICE Publishing, London, UK.

Rivers, D., Hallmark, C., West, L. & Dress, R. (1982), 'A technique for rapid removal of gypsum from soil samples', *Soil Sci. Soc. Am. J.* **46**, 1338–1340.

Rogers, C. (1995), Types and distribution of collapsible soils, *in* E. Derbyshire, T. Dijkstra & I. Smalley, eds, 'Genesis and Properties of Collapsible Soils', number ISBN0-7923-3587-2 *in* 'NATO ASI Series', NATO, Kluwer Academic Publishers, The Netherlands, pp. 1–17.

Rogers, C., Djikstra, T. & Smalley, I. (1994), 'Hydro-consolidation and subsidence of loess:studies from china, russia, north america and europe', *Engineering* **37**, 83–113.

Rogers, C. & Smalley, I. (1993), 'The shape of loess particles', *Naturwissenschaften* **80**, 461–462.

Rollings, K. & Kim, J. (2011), 'Dynamic compaction of collapsible soils based on us case histories', *Jouranal of Geotechnical and Geoenvironmental Engineering* **136/9**, 1178–1186.

Rollins, K. & Rogers, G. (1994), 'Mitigation measures for small structures on collapsible alluvial soils', *J. Geotech. Engrg. Div., ASCE* **120/9**, 1533–1553.

Romero, E. (1999), Characterisation and T-H-M behavior of unsaturated Boom clay: an experimental study, PhD thesis, Uni. Polytecnica de Catalunya.

Rousseau, D., Gerasimenko, N., Maatvishina, Z. & Kukla, G. (2001), 'Late pleistocene environments of central ukraine', *Quaternary Research* **56**, 349–356.

Saaed, S. A. & Khorshid, N. N. (1989), Some essential characteristics of the gypseous soils of al-dour area, *in* 'Proc. of the 5th Scientific Conference, Vol. 4, Part2, Scientific Research Council', Vol. 2, Baghdad, Iraq. (in Arabic).

Schanz, T., Agus, S. & Tscheschlok, G. (2004), Determination of hydro-mechanical properties of trisoplast, Research Report Bo-015/03, Laboratory of Soil Mechanics, Bauhaus-University Weimar, Weimar, Germany.

Schanz, T., Baille, W. & Tuan, L. (2010), 'Effects of temperature on measurements of soil water content with time domain reflectometry', *Geotechnical Testing Journal* **34**(1), 1–8. Copyright by ASTM Int'l (all rights reserved).

Seleam, S. (1988), Geotechnical characteristics of a gypseous sandy soil including the effect of contamination with some oil products, Master's thesis, Building and Construction Department, University of Technology Baghdad, Iraq.

Seleam, S. (2006), 'Evaluation of collapsibility of gypseous soils in iraq', *Journal of Engineering* **13**(3), 712–726.

Sillers, W. S. (1997), The mathmetical representation of the soil-water characteristic curve, Phd thesis, University of Saskatchewan.

Skarie, R., Arndt, J. & Richardson, J. (1987), 'Sulfate and gypsum determinations in saline soils', *Soil Sci. Soc. Am. J.* **51**, 901–903.

Smalley, I., Markovic, S. & Svircev, Z. (2011), 'Loess is almost totally formed by the accumulation of dust', *Quaternary International* **240**, 4–11.

Smalley, I., OHara-Dhand, K., Wint, J., Machalett, B., Jary, Z. & Jefferson, I. (2007), 'Rivers and loess: the significance of long river transportation in the complex event-sequence approch to loess deposit formation', *Qua* **198**, 7–18.

Smith, R. & Robertson, V. (1962), 'Soil and irrigation classification of shallow soils overlying gypsum bed,northern iraq', *Journal of Science* **13**(1), 106–115.

Stern, R., Alperovitch, N. & Levy, G. (1989), 'Rapid removal of gypsum by resin prior to particle size distribution analysis in soils', *Soil Scince* **148(6)**, 448–451.

Sun, D., Sheng, D. & Xu, Y. (2007), 'Collapse behavior of unsaturated compacted soil with different initial densities', *Canadian Geotechnical Journal* **44(6)**, 673–686.

Suwansawat, S. & Benson, C. H. (1999), 'Cell size for water content-dielectric constant calibratios for time domain reflectometry', *Geotechnical Testing Journal* **22**, 3–12.

Tadepalli, R. (1990), The study of collapse behavior of soils during inundation, Master thesis, University of Saskatchewan, Saskatoon, Saskatchewan, Canada.

Tadepalli, R. & Fredlund, D. (1991), 'The collapse behaviour of a compacted soil during inundation', *Canadian Geotechnical Journal* **28**, 477–488.

Tadepalli, R., Rahardjo, H. & Fredlund, D. (1992*a*), 'Measurements of matric suction and volume changes during inundation of collapsible soils', *Geotech. Test. J., ASTM, GTJODJ* **15**(2), 115–122.

Tadepalli, R., Rahardjo, H. & Fredlund, D. (1992*b*), Soil collapse and matric suction change, *in* 'Proc. of the 7th Int. Conf. on Expansive Soils', Vol. 1, Dallas, Texas, pp. 286–291.

Taha, S. (1979), The effects of leaching on the engineering properties of qayiara soil, M. sc. thesis, Civil Eng. Dep., Univ. of Mosul, Iraq.

Tami, D., Rahardjo, H. & Leong, E. (2004), 'Effects of hysteresis on steady-state infiltration in unsaturated slopes', *Jouranal of Geotechnical and Geoenvironmental Engineering,ASCE* **130**(9), 956–967.

Taylor, R. & Cripps, J. C. (1984), *(Mineralogical Controls on Volume change) From Ground Movements and their effects on structures*, Surrey university press.

Terzaghi, K. (1936), The shear resistance of saturated soils, *in* 'Proc. 1st Int.Conf. Soil Mech. & Fdn. Engrg.', Vol. 1, Cambridge, Mass., Harvard University, pp. 54–56.

Terzaghi, K., Peck, R. & Mesri, G. (1996), *Soil Mechanics in Engineering Practice*, number ISBN 978-0-471-08658-1, 3rd edn, John Wiley & Sons,Inc., United States of America.

Torrance, J. (1974), 'A laboratory investigation of the effect of leaching on the compressibility and shear strength of norwegian marine clay', *Geotechnique* **24**(2), 155–173.

Van Alphen, J. & Romero, F. (1971), Gypsiferous soils:notes on their characteristics and management, Technical report, Int.Inst. for Land and Improvement, Bulletin 12, Wageningen, Netherlands.

Van Genuchten, M. (1980), 'A closed-form equation for predicting the hydraulic conductivity of unsaturated soils', *Jouranal of Soil Science Society of America* **44**, 892–898.

Vanapalli, S., Nicotera, M. & Sharma, R. (2008), 'Axis translation and negative water column techniques for suction control', *Geotechnical and Geological Engineering* **26(6)**, 645–660.

Vieillefon, J. (1979), 'Contribution a l ame lioration de l e tude des sols gypseux', *Cah. ORSTOM, ser. Pedol* **XVII(3)**, 195–223.

Vilar, O. & Rodrigues, R. (2011), 'Collapse behavior of soil in a brazilian region affected by a rising water table', *Canadian Geotechnical Journal* **48**, 226–233. Published by NRC Research Press.

Villar, M., Rivas, P., Campos, R., Lloret, A., Romero, E. & Mariano, A. (2001), First report on thermohydro-mechanical laboratory tests., Technical Report 70-IMA-L-0-86.

Wagner, B. (2011), 'Spatial analysis of loess and loess-like sediments in the weser- aller catchment (lower saxony and northern hesse, nw germany)', *Quaternary Science Journal* **60**(1), 27–46. GEOZON SCIENCE MEDIA, ISSN 0424-7116.

Waltham, A. (1988), 'Hydrocompaction of collapsing soils', *Ground subsidence, Blackie, Glasgow* p. 202.

Schriftenreihe des Lehrstuhls für Grundbau, Boden- und Felsmechanik der Ruhr-Universität Bochum

Herausgeber: H.L. Jessberger

1 (1979) **Hans Ludwig Jessberger**
Grundbau und Bodenmechanik an der Ruhr-Universität Bochum

2 (1978) **Joachim Klein**
Nichtlineares Kriechen von künstlich gefrorenem Emschermergel

3 (1979) **Heinz-Joachim Gödecke**
Die Dynamische Intensivverdichtung wenig wasserdurchlässiger Böden

4 (1979) **Poul V. Lade**
Three Dimensional Stress-Strain Behaviour and Modeling of Soils

5 (1979) **Roland Pusch**
Creep of soils

6 (1979) **Norbert Diekmann**
Zeitabhängiges, nichtlineares Spannungs-Verformungsverhalten von gefrorenem Schluff
unter triaxialer Belastung

7 (1979) **Rudolf Dörr**
Zeitabhängiges Setzungsverhalten von Gründungen in Schnee, Firn und Eis
der Antarktis am Beispiel der deutschen Georg-von-Neumayer- und Filchner-Station

8 (1984) **Ulrich Güttler**
Beurteilung des Steifigkeits- und Nachverdichtungsverhaltens von
ungebundenen Mineralstoffen

9 (1986) **Peter Jordan**
Einfluss der Belastungsfrequenz und der partiellen Entwässerungs-
möglichkeiten auf die Verflüssigung von Feinsand

10 (1986) **Eugen Makowski**
Modellierung der künstlichen Bodenvereisung im grundwasserdurchströmten
Untergrund mit der Methode der finiten Elemente

11 (1986) **Reinhard A. Beine**
Verdichtungswirkung der Fallmasse auf Lastausbreitung in nichtbindigem
Boden bei der Dynamischen Intensivverdichtung

12 (1986) **Wolfgang Ebel**
Einfluss des Spannungspfades auf das Spannungs-Verformungsverhalten
von gefrorenem Schluff im Hinblick auf die Berechnung von Gefrierschächten

13 (1987) **Uwe Stoffers**
Berechnungen und Zentrifugen-Modellversuche zur Verformungsabhängigkeit
der Ausbaubeanspruchung von Tunnelausbauten in Lockergestein

14 (1988) **Gerhard Thiel**
Steifigkeit und Dämpfung von wassergesättigtem Feinsand unter Erdbebenbelastung

15 (1991) **Mahmud Thaher**
Tragverhalten von Pfahl-Platten-Gründungen im bindigen Baugrund,
Berechnungsmodelle und Zentrifugen-Modellversuche

16 (1992) **Rainer Scherbeck**
Geotechnisches Verhalten mineralischer Deponieabdichtungsschichten
bei ungleichförmiger Verformungswirkung

17 (1992) **Martin M. Bizialiele**
Torsional Cyclic Loading Response of a Single Pile in Sand

18 (1993) **Michael Kotthaus**
Zum Tragverhalten von horizontal belasteten Pfahlreihen aus langen Pfählen in Sand

19 (1993) **Ulrich Mann**
Stofftransport durch mineralische Deponieabdichtungen:
Versuchsmethodik und Berechnungsverfahren

20 (1992) **Festschrift anlässlich des 60. Geburtstages von**
Prof. Dr.-Ing. H. L. Jessberger
20 Jahre Grundbau und Bodenmechanik an der Ruhr-Universität Bochum

21 (1993) **Stephan Demmert**
Analyse des Emissionsverhaltens einer Kombinationsabdichtung im Rahmen der
Risikobetrachtung von Abfalldeponien

22 (1994) **Diethard König**
Beanspruchung von Tunnel- und Schachtausbauten in kohäsionslosem Lockergestein
unter Berücksichtigung der Verformung im Boden

23 (1995) **Thomas Neteler**
Bewertungsmodell für die nutzungsbezogene Auswahl von Verfahren zur Altlastensanierung

24 (1995) **Ralph Kockel**
Scherfestigkeit von Mischabfall im Hinblick auf die Standsicherheit von Deponien

25 (1996) **Jan Laue**
Zur Setzung von Flachfundamenten auf Sand unter wiederholten Lastereignissen

26 (1996) **Gunnar Heibrock**
Zur Rissbildung durch Austrocknung in mineralischen Abdichtungsschichten
an der Basis von Deponien

27 (1996) **Thomas Siemer**
Zentrifugen-Modellversuche zur dynamischen Wechselwirkung zwischen Bauwerken
und Baugrund infolge stoßartiger Belastung

28 (1996) **Viswanadham V. S. Bhamidipati**
Geosynthetic Reinforced Mineral Sealing Layers of Landfills

29 (1997) **Frank Trappmann**
Abschätzung von technischem Risiko und Energiebedarf bei Sanierungsmaßnahmen
für Altlasten

30 (1997) **André Schürmann**
Zum Erddruck auf unverankerte flexible Verbauwände

31 (1997) **Jessberger, H. L. (Herausgeber)**
Environment Geotechnics, Report of ISSMGE Technical Committee TC 5
on Environmental Geotechnics